UNIVERSITÀ DEGLI STUDI DELL'AQUILA
DIPARTIMENTO DI SCIENZE CLINICHE APPLICATE E BIOTECNOLOGICHE

Dottorato di Ricerca in MEDICINA SPERIMENTALE

Curriculum Biotecnologie Mediche

XXXII ciclo

MicroRNA expression analysis, target genes and pathways induced by NGF in corneal epithelial cells: comparison among different bioformulations.

SSD MED/46

Dottoranda

Chiara Compagnoni

Coordinatore del corso

Prof.ssa Mariagrazia Perilli

Tutor

Prof.ssa Alessandra Tessitore

A.A. 2018/2019

INDEX

ABSTRACT

Background. Nerve Growth Factor (NGF) is a member of the neurotrophins family that plays a key role in the maintenance and functions of both the central and peripheral nervous systems, as well as in non-neuronal cells. It exerts its action through two classes of transmembrane receptors, one high affinity, TrkA, and one low affinity, p75^{NTR}, regulating different and important biological functions such as cell differentiation, survival, proliferation, apoptosis. Besides several neuropathies, some studies showed that NGF revealed translational clinical application for ulcers of the eye's anterior segment, and a NGF bioformulation (Cenegermin) has been EMA and FDA approved as first-in-class treatment for neurotrophic keratitis (NK), a rare degenerative corneal disease due to corneal trigeminal innervation defects causing spontaneous injuries and wounds. However, NGF-induced biomolecular mechanisms in corneal cells are still unknown.

MicroRNAs (or miRNAs) are a novel class of endogenous, small non-coding RNAs (~22 nucleotides), able to regulate target genes, at the post-transcriptional level, in plants and animals. MiRNAs are involved in maintaining cell homeostasis and tuning fundamental biological processes, such as growth, proliferation, apoptosis, cell metabolism; dysregulated expression of miRNAs' is observed and strictly linked to relevant human diseases (e.g. viral, immune, neurodegenerative and cardiovascular diseases, cancer). MiRNAs are found not only in cells, but also in body fluids, such as blood, saliva, urine and tears, where they can be released by active (i.e. exosomes or vesicles) or passive (i.e. cell death) mechanisms.

In this study we evaluated miRNAs' expression modulation in corneal cells after treatment with different NGF bioformulations, by focusing the analysis on target genes and pathways as well.

Methods. The modulation of microRNAs (miRNAs) expression in human epithelial corneal cells (HCECs) after treatment with three different NGF bioformulations (NGF1, NGF2, NGF3) was studied. Nearly 700 miRNAs were analysed by qRT-PCR at three different time points. Those showing significant expression differences were examined by DIANA tools (miRpath v3.0, based on Tarbase and microT database) to identify target genes and pathways. Furthermore, Genemania gene and functional enrichment analysis was performed as well to strengthen *in silico* study. *In silico* data were organized in a first, second and third-level analysis, by considering global data or by restricting them to neurotrophin signalling pathway or to specific miRNAs' subgroups.

Results. Tens of miRNAs were significantly dysregulated, mainly hypo-expressed, after treatment. Among those, 3 were shared by all the bioformulations, 37 by 2 of them, whereas 12, 16 and 20 were correlated to each single bioformulation. A total number of 91 unique pathways were identified by DIANA experimentally-supported Tarbase analysis: 46, including the neurotrophin signalling

pathway, were shared by all three bioformulations, 28 by 2 of them, whereas 9, 2 and 6 were related to each single bioformulation. More than 2.000 experimentally supported target genes were identified. After focusing the analysis on the neurotrophin signalling pathway, no relevant differences were globally detected among the NGF bioformulations, all appearing to drive through proliferative and survival signals. However, one of the three bioformulations here used appeared to be more specific than the remaining two, as, when proportionally compared to them, it involved less significant miRNAs which, however, can target higher numbers of genes involved in this pathway. The same result was achieved when analysis was restricted to miRNAs' sub-groups specifically related to each single bioformulation. Genemania gene and functional enrichment analysis further confirmed data. Futhermore, the gene list can be in depth analysed in order to identify targets suitable for further molecular analyses and validations, especially for each single bioformulation, with the aim to possibly identify target genes and functions specifically related to them. For this reason, more experiments by immunoblotting to evaluate expression levels of interesting target genes are ongoing.

Conclusion. We examined the effects induced by different NGF bioformulations on epithelial corneal cells, by focusing the attention on miRNAs expression levels, and *in silico* target genes and pathways analysis. Although further functional studies to validate results are needed, original and novel insights about genes and epigenetics mechanisms induced by NGFs were provided. Our data may leave to hypothesize that NGF1 might be more specific and effective in inducing neurotrophin signalling pathway compared with NGF2 and NGF3. Importantly, given the putative role of miRNAs as biomarkers or therapeutic targets, this study makes available data potentially exploitable in clinical practice.

INTRODUCTION

1. miRNAs

MicroRNAs (or miRNAs) are a novel class of endogenous, small non-coding RNAs (~22 nucleotides), with negative role in gene expression, at the post-transcriptional level, in plants and animals (Bartel, 2004). In particular, miRNAs control the target gene expression by base pairing to sequence motifs in the 3' UTR of mRNAs with perfect or near perfect complementarities, inducing the breakdown of the targeted mRNAs or inhibition of translation from the mRNA.

MiRNAs are involved in maintaining cell homeostasis and tuning fundamental biological processes, such as growth, proliferation, apoptosis, cell metabolism; dysregulated expression of miRNAs is observed and strictly linked to relevant human diseases (e.g. viral, immune, neurodegenerative diseases, cancer) (Li and Kowdley, 2012). MiRNAs are found not only in cells, but also in body fluids, such as blood, saliva, urine and tears, where they can be released by active (i.e. secretion by exosomes or vesicles) or passive (i.e.cell death) mechanisms.

1.1. The discovery of miRNAs

The first miRs were discovered in *Caenorhabditis elegans* in 1993, lin-4 and lin-14, by Gary Ruvkun group through genetic screening. Lee's study (1993) shows that the lin-4 gene did not encode for a protein, but instead produced two small RNA molecules, about 22 and 61 nucleotides long respectively. The longest of which assumes a phylogenetically preserved secondary stem-loop structure, in nematodes, and acts as the shortest precursor. The shorter RNA molecule regulates the lin-14 gene, by matching bases not perfectly complementary to the 3' non-coding ends of the lin-14 mRNA (Wightman et al.,1991). This form of post-transcriptional gene silencing by a small regulatory RNA was initially considered a rare and specific phenomenon of nematodes.

The big role miRNA had been understood after the second miRNA, identified again in the nematode, let-7, the sequence of which was highly conserved (Pasquinelli et al., 2000); hence definitely suggesting the existence of a large group of gene regulatory networks. The identification of let-7 not only provided another vivid example of developmental regulation by small RNAs, but also raised the possibility that such miRNAs might be present in species other than nematodes.

In fact, both let-7 and lin-41 are evolutionarily preserved among a wide variety of multicellular organisms and in addition, let-7 was differentially expressed during the development of animals with bilateral symmetry (Pasquinelli et al., 2000). This allowed to understand that the regulation of

expression gene by these small RNAs is actually a general mechanism present in many multicellular organisms, among them the *Drosophila* and the human (Lau et al., 2001).

The high conservation of these organ-specific microRNAs among the various animal species suggests that they could play an accurate and phylogenetically preserved role in the formation and/or maintenance of a cell or tissue type of a specific organ.

The miRNAs are present also in multicellular organisms, but not in unicellular organisms, and are phylogenetically preserved in many of the bilateral animals; ~55% of the mRNAs in *C. elegans* are homologous to miRNAs of the human and this indicates that miRNAs has played an important role in animal evolution. (Ibanez-Ventoso et al., 2008). The miRNAs present in the animals seem to have evolved separately from the miRNAs present in the plants, since their sequences, precursors and biogenetic mechanisms are distinct from the latter. Computational analysis indicates that the genes coding for microRNAs represent approximately 1% of the genome of different species and that each of them has preserved sequences and not in hundreds of different target genes: it is estimated in fact that approximately 30% of the genes are regulated by at least one microRNA (Bartel, 2004). An increasing number of miRNAs had been identified in mammals and it is estimated that humans have approximately 2000 known miRNA. (Kozomara et al.,2011).

In the last few years the importance of microRNAs in the human development, physiology and pathology is becoming increasingly important. The identification and characterization of targets and molecular pathways regulated by miRNA represents an essential step to clarify biological actions applied by microRNAs. In addition to genetic analysis, it is necessary to perform an accurate computational analysis and a subsequent *in vitro* functional analysis to show the real regulation of target genes by miRs. The *in silico* analysis involves the use of bioinformatic algorithms that are used to predict the biological targets of microRNAs.

MiRNAs, with the development of next-generation sequencing technologies, could be future candidates for new generation biomarker, due to their position in regulation cascades and their high or specific expression in various tissue during different conditions such as neurodegenerative diseases, various forms of cancer and eye diseases.

1.2. Biogenesis of miRNAs

In order to carry out their function, miRNAs must undergo a process of maturation that starts within the nucleus and ends in the cytoplasm. First miRNAs genes, often located in the introns of protein-coding genes, are transcribed by RNA polymerase II (Pol II), and sometimes by RNA polymerase III (Pol III). The microRNAs are transcribed as long primary transcript, called pri-miRNA, with the

length of several hundred nucleotides, that in the nucleus folds to form a double filament hairpin structure, often containing the sequence for different mature miRNAs. Pri-miRNA have a stem-loop structure with a 5' 7-methylguanosine cap and a poly(A) tail, and also contains sequences of uridine residues, which would be expected to prematurely terminate pol III transcription.

The nuclear cleavage of the pri-miRNA is carried out by Drosha RNase III endonuclease, protein of ~ 160kDa, and begins in the nucleus. Drosha in cooperation with protein DiGeorge syndrome critical region gene 8 (DGCR8), known also Pasha in flies and nematodes, cleaves both strands of the stem at sites near the base of primary stem loop, releasing 60-70 nucleotides stem loop intermediate known as pre-miRNAs (miRNA precursor), with 5' phosphate and 2-nucleotide 3′-overhang. This phase is called cropping (Lee et al., 2002).

Pre-miRNAs are then exported from the nucleus to the cytoplasm by the RanGTP binding nuclear transporter exportin-5 (Exp5) (Yi et al., 2003). Once inside the cytoplasm, these hairpin precursors are cleaved by RNaseIII endonuclease Dicer into a small, imperfect dsRNA duplex (miRNA: miRNA*), about 25 bases in length. MiRNA is a mature miRNA whereas miRNA* is the opposing arm of the miRNA. The Dicer contains helicase domain, a DUF283 domain, a PAZ (Piwi–Argonaute-Zwille) domain, two tandem RNase-III domains and a dsRNA-binding domain (dsRBD). The Paz domain identifies the 3' overhang. The helicase domain identifies the loop region and the two RNase-III domain cleaves both the strands. The procedure takes place only when the miRNA complex is loaded in the Dicer (He and Hannon, 2004).

Dicer interacts with Argonaute family proteins (Ago1-Ago4 in the mammals) to assemble RNA-induced silencing complex (RISC), for target recognition, in which the mature miRNA is incorporated. The other strand is either degraded to Ago2 or can act as a template for synthesis of new dsRNA by the presence of RNA-dependent RNA polymerase, which again forms more miRNA. The Ago2 is an Argonaute protein that has endonuclease activity and cleaves the 3' arm of the miRNA before being processed by Dicer. Within the RISC protein complex, mature miRNAs are usually capable of matching by 2-8 nucleotides present at the 5'end, known as *seed* sequence, to complementary sequences present in the 3'UTR region of messenger RNA (mRNA) and to regulate gene expression at the post-transcriptional level (Diederichs and Haber, 2007). According as how Dicer processes the pre-miRNA into the miRNA:miRNA* duplex, the stability of the 5′ ends of the two arms of the miRNA:miRNA* duplex is usually different. The relative instability (lower thermodynamic energy) at the 5' end of the mature miRNA facilitates its preferential incorporation into the RISC becoming the active miRNA (Schwarz et al., 2003).

Mature miRNAs control the target expression by base pairing to the sequence motif in the 3'UTR of mRNA: perfect or near perfect complementarity between miRNA and target produces the cleavage

of the mRNA by Ago2, whereas imperfect base pairing lets the mRNA's destabilization by miRNA/RISC complex through deadenylation and subsequent decapping (Figure 1). In this manner, translation prematurely terminates (Xie et al., 2005).

One miRNA can have a multiple target sites in the mRNA transcript of downstream gene, while one mRNA can be targeted by multiple miRNAs. Therefore, miRNAs contribute a newly recognized level of regulation of gene expression, playing important roles in the development and normal function of almost all tissues and organ systems.
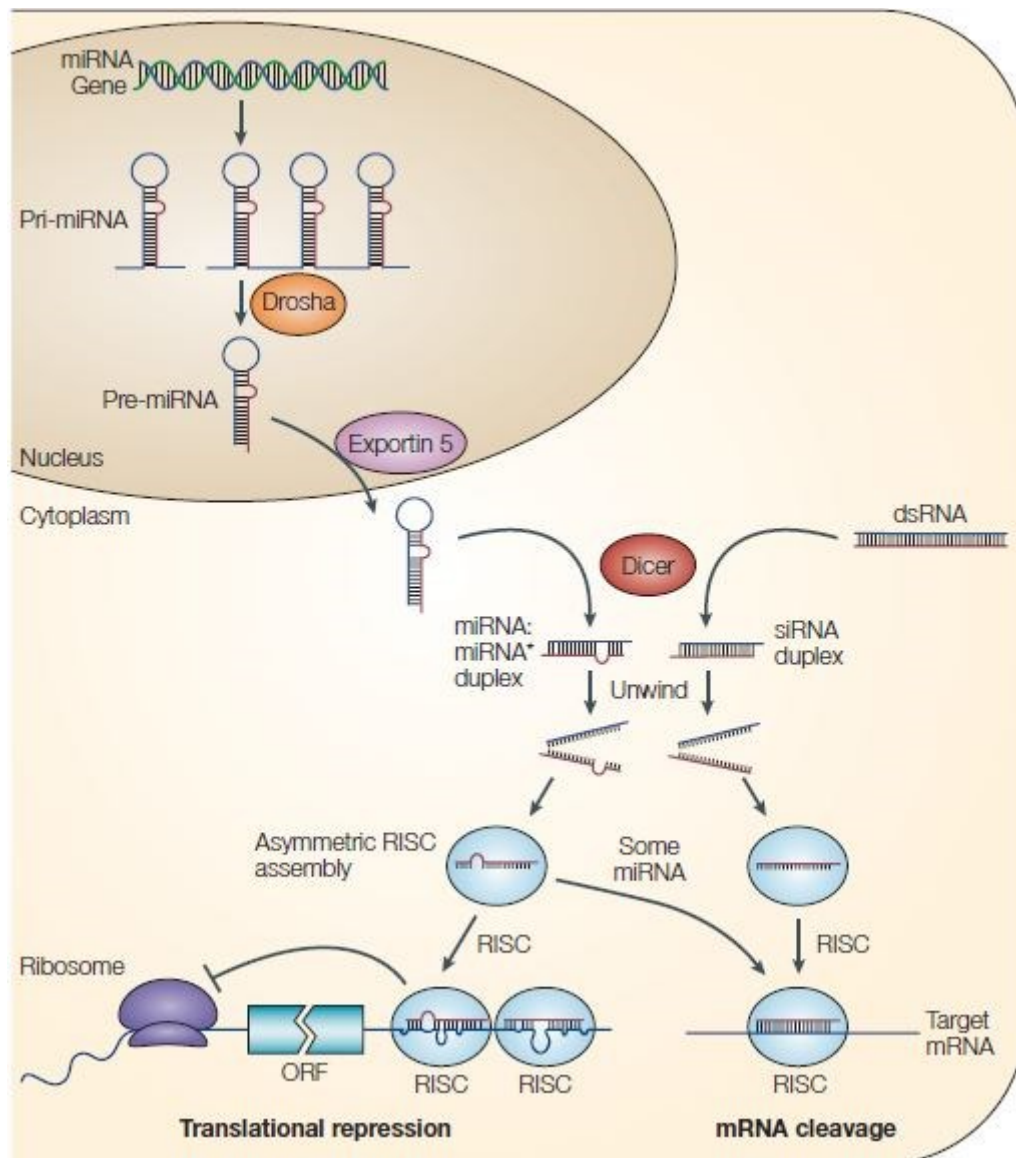
***Figure 1-* Biogenesis and post-transcriptional suppression of microRNAs.** pri-miRNAs are transformed into pre-miRNA by Drosha and DGCR8 within the nucleus. Then, they are exported from the cytoplasm nucleus by Exp 5 and Ran-GTP. Later, the pre-miRNAs are processed by Dicer in mature double-stranded microRNA (dsRNA, Mirna:Mirna*). Dicer also processes long dsRNA molecules in small interferent RNA (siRNA) duplex. These dsRNAs are subsequently bound by AGO2 and incorporated by RISC that allows the degradation of the previously unused complementary filament, while the filament remained associated with AGO2 constitutes the mature miRNA. Once incorporated by RISC, the miRNA induces the mRNA cleavage if there is sufficient complementarity between the two, while it represses the translation, if the mRNA has a partial complementarity. The degradation of the mRNA occurs after recognition of the ORF (open reading frame) by the miRNA (He and Hannon, 2004).

1.3. The Eye

Basic eye anatomy helps to understand the possible miR's role in the physiology and eye diseases. The eye allows to capture the stimuli coming from the external environment and transforming them into information that stimulate responses from the nervous system.

The eyeball is a spheroidal organ, located in the front of the orbital cavity, equipped with a nervous peduncle, optic nerve, which places it in continuity with the formation of the diencephalon (chiasma and optical traits) necessary for visual perception. This structure makes the sense of vision available since it activates photoreceptors and transmits nerve impulses to the visual cortex of the occipital lobes where interpretation occurs.

In ophthalmology it is important to divide the bulb in two segments: anterior and posterior. The first one is made up of conjunctiva, cornea, iris, pupil, crystalline lens and ciliary body whereas the posterior is made up of vitreous, sclera, retina, optic nerve and macula (Figure 2).
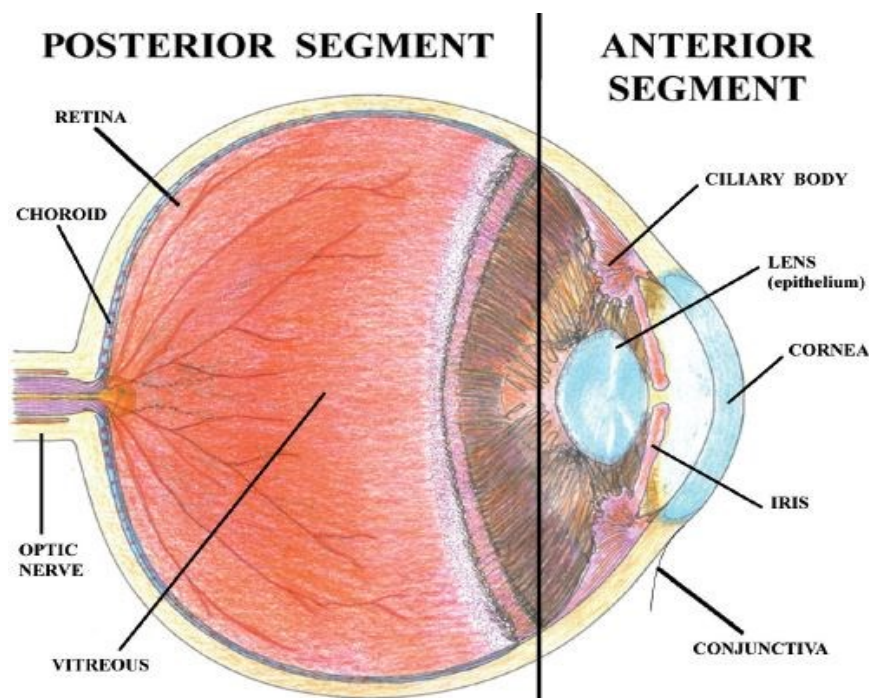
Figure 2- **Drawing of the human eye.** The eyeball is divided into anterior segment (conjunctiva, iris, cornea, lens, ciliary body) and posterior segment (vitreous, optic nerve, choroid, retina) (Lambiase et al., 2011a)

The wall of the eye consists of three main layers, overlapped each other:

- the outer layer (fibrous) that protects the most internal structures and it includes the sclera, behind, and the cornea, in the front.

  The sclera covers the ocular surface and it is formed by dense and opaque fibrous connective tissue, rich in collagen and elastic fibers.

The cornea is a transparent avascular tissue that refracts or bends light entering the eye toward the lens of the eye which then focuses on the retina. The cornea acts as a protection against foreign substances and is one of the most nervous tissues. The cornea is made up of cellular components (epithelial, keratocytes and endothelial cells) and the acellular component includes collagen and glycosaminoglycans. The corneal layers include:

- epithelium, nonkeratinized stratified squamous;

- Bowman's layer is composed of collagen and proteoglycans and helps to maintain the shape of the cornea;

- stroma makes up 90% of the corneal thickness. It's mainly composed of layers of collagen fibers regularly oriented;

- Descemet's membrane is elastic. It consists of an anterior zone with vertical bands, which is formed in the foetal period and of a posterior zone without bands, synthesized by the endothelium during the life.

- endothelium is a single layer of hexagonal cells. It plays a vital role in maintaining corneal transparency, but has no regenerative capacity (Sridhar, 2018).

Being an avascularised tissue, the cornea receives blood from the loops of the anterior ciliary vessels, found in the subcongiuntival tissue (Figure 3).
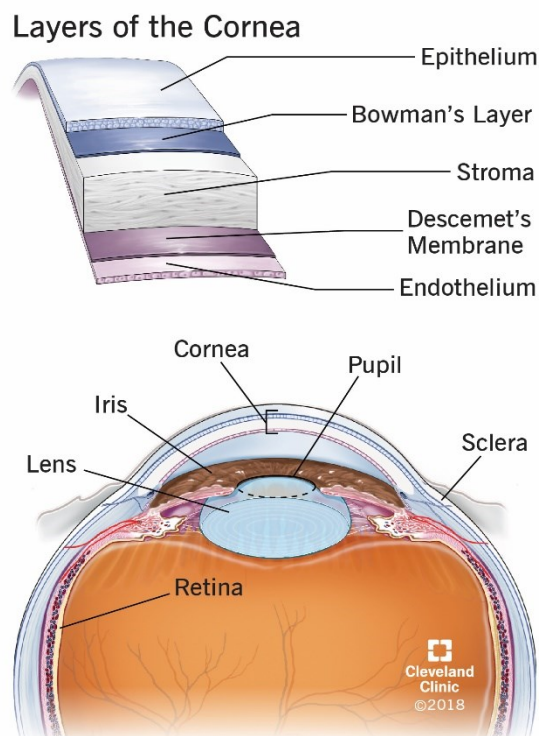
Figure 3- **Anatomy of the eye and layers of the cornea**.
(https://my.clevelandclinic.org/health/treatments/17714-cornea-transplant)

- the middle layer (vascular) or uvea, situated between the sclera and the retina, is very rich in blood vessels and strongly pigmented. It represents the nutritious membrane of the eye and has the task of absorbing the light rays preventing their reflection. The iris, anterior part of the choroid, contains the papillary muscles which, contracting, control the size of the pupil. The pupil regulates the amount of light beams that will then hit the retina. The choroid membrane constitutes the posterior segment of the tonac vascular and is an easily lacerable foil having a thickness that varies from 0.4 to 0.2 mm. It is highly vascularized and provides a blood supply to the eyeball. The ciliary body is a muscle that sits behind the iris, with its outer face it adheres to the sclera, while on the inner face, it is coated by the ciliary portion of the retina. This muscle is attached to the lens of the eye by many zonules fibers. When the ciliary body contracts, tension is taken off the zonules tying to the lens and the lens is allowed to change its shape. The backside of the ciliary body has cells that secrete the aqueous fluid that fills up the anterior chamber of the eye where it is drained out through the trabecular meshwork.

- The inner layer is the retina which lines the back two-thirds of the eyeball. The retina is a multi-layered sensory organ responsible for translating light into a pattern of electrophysiological signals, finally interpreted as vision by the brain. There are five types of neurons in the retina: photoreceptors, bipolar cells, ganglion cells, horizontal cells and amacrine cells. The retina is composed of many overlapping layers. The outer nuclear layer (ONP) contains rods and cones. When light photons arrive in the retina, they are first captured by these two photoreceptors, that have the function of detecting the intensity and frequency of the incoming light. The cones cells are assembled in the central retina (macula) whereas the rods are more in the peripheral parts of the retina. The rods and cones send nerve impulses to the brain, which travel through a network of nerve cells. There are also retinal interneurons in the retina that encode light energy in optic nerve impulses before passing them back to brain. The synapses between axons of photoreceptors and the dendrites of horizontal and bipolar cells are in the outer plexiform layer. The retinal pigment epithelium (RPE) contains numerous melanosomes and pigment granules. This structure plays a critical role in the conservation of photoreceptors, renewing photopigments and phagocytosing the photoreceptor disks and reduces backscattering of the light that enters the eye. In the inner nuclear layer (INL) horizontal cells, amacrine cells and bipolar cells are contained. The latter provides a link for visual information, between the terminals of the photoreceptors and the dendrites of the ganglion cells, while horizontal cells and amacrine cells are responsible for lateral interactions in the retina. In the plexiform inner layer synaptic contacts are created between the ganglion cells (RGC), contained in the ganglion layer, and bipolar cells. Axons

of ganglion cells form the nerve fiber layer, forming the optic nerve. In addition, RGCs bring information about retinal stimulation to the central nervous system (Purves et al., 2001). Other cells are present in the retina: astrocytes and Müller cells, which belong to microglia and are arranged radially by filling all the volume not occupied by nerve cells (Figure 4).
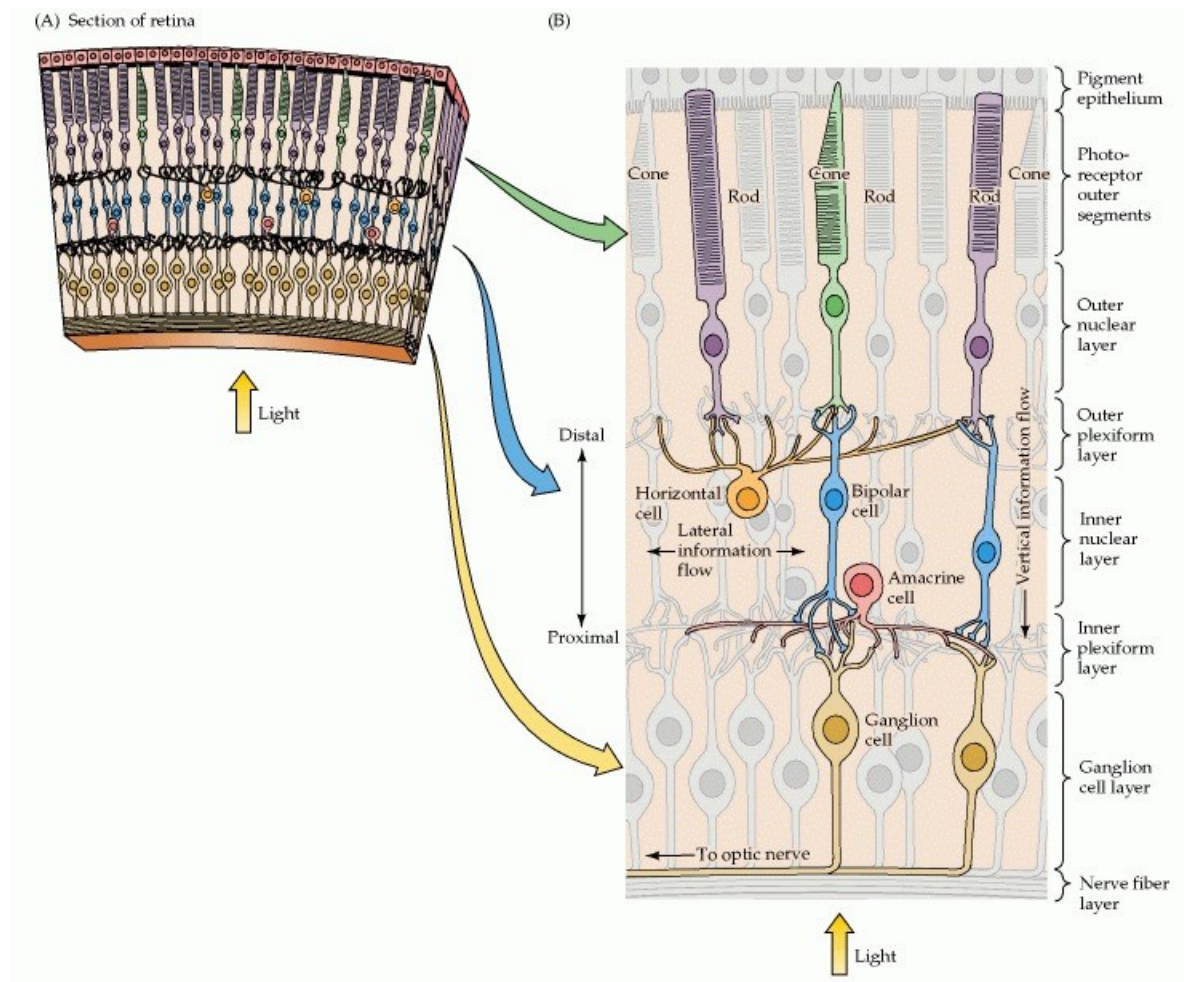
Figure 4 - **Structure of the retina.** (A) Section of the retina showing overall retinal layers, shown in detail in the next figure. (B) Diagram of the basic circuitry of the retina. Photoreceptor, bipolar cell, and ganglion cell provide the most direct route for transmitting visual information to the brain. Horizontal cells and amacrine cells mediate lateral interactions in the outer and inner plexiform layers, respectively (inner, near the centre of the eye; outer, away from the centre, or toward the pigment epithelium) (Purves et al., 2001).

The inner part of the eye is divided into three sections called chambers: anterior chamber between the posterior surface of the cornea and the iris and posterior chamber between the iris and lens. In the anterior and posterior chamber circulates a watery fluid called aqueous humor. Whereas, in the vitreal, the vitreous body chamber is contained; both these materials act, together with the cornea and the crystalline lens, to help the eyeball keep its shape.

1.4. Eye and miRNAs

Many miRNAs show unique tissue-specific and developmental stage-specific expression patterns, suggesting potential unique functions in the cornea and other ocular tissues. The apparent miRs abundance in the eye suggests that they may be responsible for the strict gene regulation necessary to maintain visual health, even under pathological conditions. MiRNAs have been found to play essential roles not only in eye development and survival, but also in their normal functioning, even if their key roles are still largely unknown.

Among some of the first reports on the tissue-specific expression of miRNA in the eye, one was carried out by Lagos-Quintana et al. (2003) who described 21 new miRs in different mouse tissues. Among these, it was noted that some miRNAs were more expressed in specific tissues, such as miR-124, which was present in both the eyes and the spinal cord, probably because neuronal cells are in both. Subsequent studies about miR-124a have shown that this miR persisted in the neural retina from the development to adulthood. In the latter, it was strongly expressed in all cell layers, in photoreceptor, neurons within the inner nuclear layer and the ganglion cell layer (Karali et al., 2007). MiR-124 targets different developmental genes (Rdh10) proving that this miR has a role in retinal development (Arora et al., 2007). Another target is Mitf, a highly expressed transcription factor in RPE, essential in maintaining neuroretinal identity (Adijanto et al., 2012). Subsequently, through a profiling of 78 miRNAs in the mouse retina, heart and brain, Xu (2009) confirmed that 19 of the 21 miRNAs emerged in the Lagos-Quintana's study, were expressed in the adult mouse retina: in particular, six of these were expressed exclusively in the retina (mir-96, mir-182, mir-183, mir-184, mir-210, mir-140AS). These miRs may play an important role in normal retinal functions. MiRNA expression has been analyzed both in the different embryonic stages and at the post-natal level showing that specific miRNAs can be expressed in several stages of retinal development to regulate both proliferation and sequential differentiation of retinal progenitor cells (RPCs) (Xu, 2009).

For example, miR-204 is highly expressed in RPE, in the ganglion cell layer, lens epithelial cells, in the ciliary body as well as in the retina of the mouse embryo. This suggests that miR-204 can contribute to the differentiation of RPE and neuronal cells from their common precursors as well as in the development of the retina (Karali et al., 2007). Conte et al. (2010) showed, using medaka fish as experimental model, that the dysregulation of the transcription factor Meis caused the loss of mir-204 function, which led to macroscopic abnormalities in eye's development. Also, this miRNA indirectly fed back Pax6 through targeting Meis (Shaham et al., 2013).

Besides miR-204, miR-211 is also widely expressed in RPEs. These two miRNAs share the same *seed*-region sequence and are classified as a family with the same targets. Wang et al. (2010) revealed

that high expression of miRs-204/211 can preserve epithelial phenotype, while maintaining high expression levels of tight junction proteins and membrane channels, which helped to preserve the interaction between retinal photoreceptors and RPE, physiology and epithelial barrier function. To prove the miR-211 protective role on the RGC, *in vivo* experiments were carried out on rats, and they showed that the up-regulation of this miR down-regulated Frs2 expression, decreasing cell death (Yang et al., 2018).

Karali's study (2007) also showed that miR-182, miR-183 and miR-96 are grouped in the same genomic region. The deletion target of one of these three caused visible alterations in the retina and this explained the overlap in functions, as they have shared targets and sometimes the one can replace the other. These miRs were highly expressed in all retinal layers (miR-182), ganglion cell, inner plexiform, and inner nuclear layer (miR-181), while miR-183 was found only in outer nuclear layer. The neurogenic effects of this miRNA's overexpression in different cell types and, its relationship with neurotransmitter transporter, pro-apoptotic genes (Casp2) and genes important for survival (Rac1), have explained their role in photoreceptor homeostasis and as a pro-survival factor under stressful conditions (Zuzic et al., 2019). It has been shown that the cluster miR-183 has as target Casp2 given that an increase of both was detected in wild-type mice in response to light stimuli. In transgenic mice, a pharmacological inhibition of Casp2 saved the light-induced degeneration of the retina. Therefore, this study demonstrated the role of the miR-183 cluster in the protection and photoreceptors survival (Zhu et al., 2011). In addition, to demonstrate that miRNAs play a key role in maintaining homeostasis and retinal functions, mice Dicer CKO (conditional knockout) models were created, which allow to detect the phenotypic consequences of the loss of miRNA gene regulation in the visual system. Depending on when Dicer's deletion occurred, Dicer excision in retinal progenitors led to different severity of phenotypes, including: retinal degeneration, progressive disorganization of retinal morphology, abnormalities in electroretinogram responses, abnormal retinal cell types differentiation and diffuse apoptosis. (Damiani et al., 2008; Sundermeier and Palczewski, 2016).

Furthermore, it has been seen that let-7, miR-9 and miR-125 were cell-type specification regulators as they regulated the transition from early to late progenitor differentiation and they were involved in Müller glia differentiation (La Torre et al., 2013). MiR-125b was able to regulate dendritic growth in bipolar rod cells and its functions as a result of retinal degeneration (Fu et al., 2017).

Ryan et al. (2006) showed that miR-184 was more abundant in both lens epithelium and corneal epithelium and did not suffer alterations from the proliferative state of the corneal epithelium during wound healing after a trauma to the corneal epithelium. MiR-184 expression in corneal epithelium and lens suggested that it plays a key role in corneal epithelial differentiation as well as in extracellular

matrix synthesis, transparency maintenance and avascularity. In the same study the expression of miR-205 was detected in all layers of the corneal, limbal and conjunctival epithelium. This miR is involved in the healing process in human corneal epithelial cells (HCEC) because it was demonstrated that it acted at every stage of the healing process of injured corneal cells, from migration to proliferation, through the inhibition of KCNJ10 (Lin et al., 2013). MiR-205 and miR-184 also play a role in the migration of keratinocytes. It was shown that miR-205 repressed SH2-containing phosphoinositide 5'-phosphatase 2 (SHIP2) that dephosphorylated phosphatidyinositol 3,4,5-triphosphate (PIP3), which was involved in many signalling pathways, including Akt. MiR-205 improved cell survival by suppressing SHIP2 and, thus improving the signalling pathway of Akt. Yu et al. (2010) demonstrated that suppression of miR-205 with antago-miR increased to SHIP2 levels, decreasing the migration of keratinocytes. It also caused cytoskeleton rearrangement events, such as a decrease in the actin cytoskeleton, as the down-regulation of miR-205 led to an increase in Rho-ROCKI activity. They also demonstrated that the suppression of mir-184 in human corneal epithelial keratinocytes (HCEK) improved Akt signalling and that wounds were sealed faster, as its suppression allowed miR-205 to inhibit SHIP2.

To confirm the role that the lens plays in the anterior segment of the eye, it has been seen that miR-26a, miR-31, miR-125b, miR-181 and miR-204, highly expressed on corneal epithelial, are also expressed in lens epithelium. One might also think that the transcriptional regulation of these miRs may be directed by eye specific transcription factors such as Pax6 (Collinson et al., 2003). This confirms that, as miRNAs are specific tissue, they can play a role in maintaining tissue identity. The link with Pax6, whose abnormal expression is related to ocular pathologies, was also confirmed by Shalom-Feuerstein (2012) through a miRNA profiling using pluripotent stem cells as model of corneal epithelial embryogenesis. It was found that miR-450-5p plays a role as a Pax6 molecular switch. Reprising Pax6, miR-450-5p acted on the fate of corneal epithelial cells, while it has been shown that its knockout permitted the expression of Pax6 in the ocular surface, allowing the corneal epithelium development. Moreover, in this study, it was shown that the knockdown of miR-184 led to a decrease in Pax6 and K3, which play a role in corneal integrity, probably through indirect action as the 3'UTRs of Pax6 and K3 have no binding sites to miR-184.

Lee et al. (2011) have shown that miR-143 and miR-145 are expressed in limbal and corneal epithelium. In particular, miR-145 is involved in the cells development and differentiation of the corneal epithelium given that it regulated formation and integrity maintenance of the epithelium, through the regulation of integrinβ8 (ITG8B). ITG8B was expressed in epithelial and neuronal cells *in vivo* and regulated the activation of transforming growth factor β (TGFβ) in matrix modeling, cell growth, epithelial homeostasis and vasculogenesis (Cambier et al., 2005). Moreover, studying human

corneal epithelium cells (HCE) transfected with miR-145 it has been seen an up regulation of IFNB1, which has anti-inflammatory activity, that could contribute to the improvement of anti-inflammatory activity of corneal cells.

MiR-122 has been shown to block apoptosis in corneal keratinocytes by down-regulation of cytoplasmic polyadenylation element-binding protein-1 (CPEB1). In this way it prevented the expression of inflammatory cytokines induced by apoptosis also reducing the risk of immune rejection after corneal transplantation (Wang et al., 2017).

Li et al. (2015) showed that miR-206, miRNA normally poorly expressed in the mouse cornea, was significantly up-regulated in the alkali-burned cornea models and promoted inflammation by regulating the Connexina 43 (Cx43), that is associated with inflammatory responses in the injured cornea.

1.5. MiRNAs and their role in human diseases

MiRNA functions are based on the regulation of gene expression to maintain homeostasis, depending on the cellular requirements, and on the control of cellular responses during differentiation through negative-feedback loops (Bartel, 2004). In fact, miRs play a key role in physiological and pathological processes such as cell differentiation, proliferation and apoptosis, immunity, neuronal and hematopoietic lineage differentiation, stem cell division and maintenance. Furthermore, they are deregulated in human diseases and involved in tumorigenesis. Since miRNA expression patterns are tissue-specific and in many cases define the physiological nature of the cell, it has been hypothesized that mutations of miRNA function may have a role in human diseases.

The expression level of miRNAs can vary as a result of mutations in their sequence and alterations in their production phase, thus causing distorted regulation of the target gene. Indeed, this situation can lead to an increase in the expression of the mature miRNA, with consequent reduction in target gene expression, or decrease of the expression of the mature miRNA, with consequent over-expression of the target. Moreover, translocations may also result in the relocation of miRNAs under the control of a new promoter, resulting in expression in a new tissue.

In particular, miRNA genes are located in genomic regions that are frequently reordered in the tumors as minimal region of loss of heterozigosity (LOH) or minimal amplicons and common regions of breakpoints, to support the hypothesis of the involvement of miRNAs in tumors (Calin et al., 2004). MiRNAs' dysregulation is displayed by overexpression of oncomiRs, which target transcripts of genes with tumor-suppressor activity, or hypo-expression of tumor suppressor miRs, which regulate mRNAs encoded by oncogenes. The abnormal miRs' activity can be attributed to epigenetic

mechanisms, to the location of microRNAs' coding genes, and to malfunctions of miR-processing machinery. Therefore, an increased level of a miRNA, which could be produced inappropriately or in incorrect tissue, would inhibit the expression of a miRNA-target oncosuppressor and lead to tumor progression. Thus, the alterations of miRNA expression can involve increased proliferation, invasiveness or angiogenesis, decreased levels of apoptosis or tissue differentiation, ultimately resulting in tumorigenesis.

Calin and colleagues first reported the role of miRNAs in human diseases in 2002. Notably, down-regulation of miR-15 and miR-16 expression was observed among B-cell chronic lymphocytic leukemia (B-CLL) patients without deletion, suggesting that pathogenesis of B-CLL may be attributed to intracellular abundance of these two miRs (Calin et al., 2002).

Furthermore, the correlation between aberrant miRNA expression patterns and an increased development of different types of cancer was demonstrated by expression profiling studies. For instance, the deregulation of miR-155, miR-21, miR-125b and miR-145 expression was linked to an increased risk of breast cancer and increased expression of miR-210 was observed during the invasive transition of the same cancer. Meanwhile the up-regulation of miR-155 and down-regulation of let-7 were associated with poor survival of lung cancer patients (Li and Kowdley, 2012).

Numerous studies corroborated the role of miRNAs in various human pathologies, not only cancer, but also, nervous system, inflammatory, cardiovascular diseases, and others.

Altered expression of miRNAs could be also associated with central nervous system diseases. For example, high expression of target BACE1, protein that plays an important role in Alzheimer's disease pathogenesis, is linked to decreased expression of miR-29a, miR-29b-1 and miR-9 in Alzheimer's disease patients (Hébert et al., 2008). Analysis of miRNA and mRNA expression in Alzheimer's disease patients demonstrated a correlation between the expression levels of miRNAs and predicted mRNA targets, involving functional relevance of microRNA-mediated regulation in Alzheimer's disease pathogenesis.

Many immune-related diseases such as systemic lupus erythematosus, nonalcoholic fatty liver disease, multiple sclerosis, a type I/II diabetes have shown correlations with cellular microRNAs. Some miRNAs, as miR-155, regulate key signalling pathways (Jak/Stat, NF-κB, Akt, etc.) and target negative regulators of the immune response to promote inflammation. In fact, miRs play critical roles in inflammation primarily by regulating the pathways associated with nuclear factor kappa beta (NF-κB), the central mediator of inflammatory response. In a negative feedback loop in which NF-κB activation up-regulates miR-146 expression, miR-146 subsequently down-regulates the expression of IRAK1 and TRAF6, two up-stream activators of NF-κB (Taganov et al., 2006). Similarly, increased

expression of miR-155 by NF-κB could repress both IKK-b and IKK-e and prevent NF-κB from being constitutively activated (Xiao et al., 2009).

MiRNAs were found to be extremely stable in body fluids (as blood, saliva, urine and tears) and their expression profile was modified under pathological conditions. In this setting, several publications identified circulating miRNAs as reliable biomarkers in several human diseases ranging from cancer to cardiovascular diseases (Creemers et al., 2012). It was studied that circulating levels of miR-126-3p were reduced in patients with type 2 diabetes, underling the potential effects of this miRNA on vascular biology and angiogenic proprieties that are affected in diabetic patients (Zampetaki et al., 2010). Besides, dysregulated circulating levels of miRNAs, such as miR-144, miR-375, and members of let-7 family, were involved in glucose homeostasis and in insulin resistance (Santovito et al., 2014).

1.6. MiRNAs and eyes disease

The dysregulation of miRNA expression has been reported in many studies to be involved in the regulation of pathological processes, in common eye disorders, such as age related macular degeneration, retinoblastoma, diabetic retinopathy, glaucoma, that are diseases that affect the posterior segment and pterygium, cataract, keratoconus, dry eye, uveitis, uveal melanoma that affect the anterior segment.

1.6.1. Age related macular degeneration (AMD)

Age related macular degeneration (AMD) is an age-related, multifactorial disease of central retina and the primary cause of blindness in developed countries. The AMD can be divided in dry and wet forms. Dry AMD is characterized by abnormal RPE pigment distribution in the macula and the formation of yellowish cellular debris, identified as drusen bodies, that accumulate between choroid and retina, in Bruch's membrane. Dry ADM is often asymptomatic but leads to decline in visual acuity and function resulting in delayed dark adaptation. The wet form is defined by abnormal growth of choroidal blood vessels, through cracks in the pathologically changed Bruch's membrane, to invade the retina with a destructive effect on its cellular elements. This leads to detachment of retina along with vascular leakage and related retinal edema (Velez-Montoya et al., 2014). Ertekin et al. (2014) have been conducted a study to investigate the differential expression of miRNA in patients with wet ADM and healthy control. They examined the expression profiles of 384 miRNAs, in plasma of 33 patients. Among these, 11 miRNAs were significantly down-regulated in the patient group (miR-21, miR-25-3p, miR-140, miR-146b-5p, miR-192, miR-335, miR-342, miR-374a, miR-410, miR-574-3p and miR-660-5p) and 5 were found to be significantly up-regulated (miR-17-5p, miR-

20a, miR-24, miR-106a and miR-223). The most significant outcome from the study was that 10 miRs (miR-26b-5p, miR-27b-3p, miR-29a-3p, miR-130-3p, miR-212-3p, miR-324-3p, miR-324-5p, miR-532-3p, miR-744-5p and let-7c) were specifically expressed in AMD patients. These miRs may be potential biomarker for early detection of AMD.

MiR-146a was found to be up-regulated in both forms of AMD and in different tissue. It is under transcriptional control by nuclear factor-kappa B (NF-κB) and has been shown to be up-regulated by reactive oxygen species, pro-inflammatory cytokines, and amyloid peptides. Studies have demonstrated that up-regulation of miR-146a in stressed human neural cells such as astroglia and microglia, led to the down-regulation of complement factor H (CFH) that is a repressor of the inflammatory and innate-immune response (Pogue et al., 2009). CFH also plays a key role in AMD pathogenesis and it has been hypothesized that the up-regulation of miR-146a promoted the pathogenesis of AMD (Beber et al., 2016). MiR-146a was associated with two modulators of the NF-κB, pathway interleukin-1-receptor-associated kinase-1 (IRAK1) and TNF receptor-associated factor 6 (TRAF6) as well as directly down-regulating interleukin (Taganov et al., 2006). Their repression inhibited pro-inflammatory cytokine signalling. Since IL-6 is associated with progression of AMD, miR-146a may be a protective regulator of inflammation in wet AMD (Ménard et al., 2016). Other miRs such as, miR-9, miR-125b and miR-155, are involved in a progressive complement factor H (CFH)-mediated inflammatory degeneration characteristic of AMD (Lukiw et al., 2012). MiR-9 played an important role in maintaining RPE cell function and also has been found to be regulated by retinoic acid, reactive oxygen species (ROS) and pro-inflammatory cytokines such as tumor necrosis factor-alpha (TNF-α) and interleukin-1 (IL-1), that were found abundantly in retina diseases (Askou et al., 2018). It was found that miR-184 was down-regulated in primary culture of human RPE cells isolated from eyes of AMD donors and in oxygen-induced retinopathy (OIR) mouse retinae (Murad et al., 2014; Shen et al., 2008). This miR negatively regulated Wnt signalling in OIR retinae. The Wnt signalling is a conserved intracellular signalling pathway also involved in regulating angiogenesis and inflammation. Murad et al. (2014) demonstrated that the inhibition of miR-184 significantly reduced phagocytosis, important for maintenance of photoreceptors efficiency in adult RPE cells. They also hypothesized that age-related decline in phagocytosis contributed to AMD. Another miRNA which may regulated neurovascolarization and apoptosis is miR-106b, that was down-regulated in AMD plasma and vitreous humor and in RPE after oxidative stress (Ménard et al., 2016). The identification of miRNAs in AMD patients might have a relationship with inflammation, angiogenesis and oxidative stress and therefore being not only potential candidates for novel biomarkers of ADM but they could also be important as therapeutic target.

1.6.2. Retinoblastoma

Retinoblastoma is the most common paediatric cancer of the eye. Molecular characteristic of this disease is alteration or loss of the RB1 gene and is thought to be the tumor-initiating event. There are other genomic alterations and changes in oncogenes and tumor suppressor genes that have been identified in retinoblastoma (RB), such as inactivation of the p53 pathway due to amplification of MDMX, a p53 inhibitor, causing tumor progression. Studies have demonstrated that p53 transcriptionally activated the miR-34 family that contributes in p53-dependent tumor suppression through cell cycle arrest and activation of apoptosis (He et al., 2007). Interestingly, MDMX has been identified as an mRNA target of miR-34a. Thus, expression of miR-34a in MDMX-overamplified RB may outcome in tumor growth inhibition. It has also been shown to be able to inhibit silent information regulator 1 (Sirt1) expression, a NAD+-dependent deacetylase that negatively regulates p53 transcriptional activity. By taking into consideration that the regulation of microRNA functions plays a role in cancer and p53 pathway inactivation, it may be essential for tumor progression in RB tumors. Dalgard et al. (2009) examined, in RB cell lines, the expression of miR-34 after activation of p53 pathway and demonstrated that miR-34a should have played a role in RB tumor. Other miRs, from human retinoblastoma tissues, were identified to be essential in the progression of retinoblastoma tumorigenesis: miR-494, let-7e, miR-513-1, miR-513-2, miR-518c*, miR-129-1, miR-129-2, miR-198, miR-492, miR-498, miR-320, miR-503 and miR-373* were found up-regulated in RB in comparison with normal retina (Zhao et al., 2009). MiR-365b-3p played a role in progression and development of RB and worked as tumor suppressor. It was found that this miR was down-regulated in human RB tissues and it reduced cell growth and induced cell cycle arrest in G1 phase and cell apoptosis by inhibiting PAX6. PAX6 played a role in eye development and in the development and progression of RB. The cell cycle arrest was due to the increased levels of P21 and P27 proteins and the decrease levels of cyclin D1 and cdc2, by targeting PAX6, in response to expression of miR-365b-3p (Wang et al., 2013a).

1.6.3. Diabetic retinopathy

Diabetic retinopathy (DR) is a late complication of diabetes. This progressive disease displays microvascular alteration that lead to retinal permeability, retinal ischemia, retinal neovascularization and macula edema. Structural and functional changes in the retina of diabetic patients are triggered by altered expression of growth factor and vasoactive factors, such as VEGF. In fact, VEGF is an important stimulator of neovascularization (NV) in several tissue type including ocular NV. Moreover, recent studies have indicated that miRs were involved in retinal and choroidal neovascularization. Thus, it was demonstrated that VEGF can be reduced after injection of precursor

of some miRs, such as miRNA-31, miR-150, and miR-184 that were involved in retinal and choroidal neovascularization (NV). In Shen's study (2008) it was shown that intraocular injection of pre-miR-31 into retina of postnatal mice with ischemic retinopathy caused significant reductions in PDGF-B, HIF-1a, and VEGF. Injection of premiR-150 also resulted in reduction in PDGF-B and VEGF, suggesting that down-regulation of these miRNAs should have contributed, along with transcriptional regulation mechanisms, to the disease phenotype. As mentioned before, both the miR-184 that miR-31 are highly expressed in lens, cornea and retina (Ryan et al.,2006; Xu,2009) and their constitutive expression could prevent vascular invasion of these tissues. Instead, their hypo-expression contributed a permissive environment for NV when the retina is ischemic. The role of miRs in the pathogenesis of diabetic retinopathy was provided by studying of altered miRNA expression in the retina and retinal endothelial cells (RECs) of streptozotocin (STZ)-induced diabetic rats 3 months after diabetic onset. The numbers of miRNAs in the total retina was much higher than the ones in RECs and although, fewer miRNAs were detected in RECs, the number of differentially expressed miRNAs in RECs was higher than in total retina. Thus, this proved that RECs are one of the first cell types affected in the pathogenesis of DR. Moreover, most of the miRNAs altered were up-regulated in the total retina but down-regulated in RECs (Kovacs et al., 2011). In this study it was also found that NF-κB-responsive miRNAs (miR-146a, miR-146b, miR-155, miR-132, and miR-21) were up-regulated in the RECs of diabetic rats. In addition, VEGF-inducible miRNAs (miR-17-5p, miR-18a, miR-20a, miR-21, miR-31, and miR-155), up-regulated in both retinas and RECs of the diabetic rats, played a roles in pathogenesis of DR through their modulation on both leukostasis and angiogenesis (miR-17-1-92 and miR-17-2-363). They also helped angiogenesis by targeting angiogenic inhibitors, thrombospondin, and connective tissue growth factor (miR-18a and miR-19b). Furthermore, it was shown that, following p53 activation in the diabetic retina, p53-responsive miR-34 family was increased in the retina and RECs isolated from diabetic rats, suggesting that members of miR-34 family could participate to the development of DR and intercede p53-induced apoptosis of neuroretinal and endothelial cells.

In another study (Platania et al., 2019) several dysregulated miRs were found in the retina and in serum of 5 and 10 weeks diabetic C57BL/6J mice. miR-20a-5p, miR-20a-3p, miR-20b and miR-106-5p were found to be down-regulated, whereas miR-27a-5p, mir-27b-3p, miR-206-3p and miR-381-3p up-regulated. This confirms the Nunes'study (2015) in which was shown that the early diabetes led to down-regulation of miR-20a-5p, miR-20a-3p, miR-20b and miR-106-5p, that triggered retinal neovascularization *in vivo*, and then an angiogenic switch in the retina. Moreover, these miRs target VEGF and HIF: when up-regulated, they promote degradation of VEGF and HIF mRNA. Also, the dysregulated miRNA targets, brain-derived neurotrophic factor (BDNF) and cAMP response

element-binding protein 1 (CREB1), modulate protein expression in diabetic retina. It was shown that protein levels of VEGF and CREB1 were up-regulated, while BDNF and PPAR-α were down-regulated in diabetic retinas. In particular, miR-206-3p and miR-381-3p modulated BDNF that is currently considered as a pathogenic hallmark of DR. BDNF was decreased in inner plexiform layer and this could be negative to the neuronal retina in the early phases of DR (Platania et al.,2019) Mortuza et al. (2014) described the role of miR-195, up-regulated in human retinal microvascular endothelial cells exposed to high glucose levels, in causing silent information regulator protein 1 (SIRT1) down-regulation, which also intervenes ageing-like changes, vascular permeability and fibronectin increase in diabetes. In fact, SIRT1 played a key role in regulating cell cycle, survival, metabolism and development in mammals. In this study, glucose-induced increased oxidative stress and was shown to cause fast ageing in endothelial cells and retinas in diabetes, because increased production of extracellular matrix (ECM) proteins and these processes were mediated through alteration of SIRTs.

1.6.4. Glaucoma

Glaucoma is a neurodegenerative disease characterized by the progressive death of retinal ganglion cells (RGCs) and optic nerve axons, and it is accompanied with a progressive and consequent deficit of the peripheral and central visual field. The main risk factor developing this disease is an elevated intraocular pressure (IOP). MiRs have been found to play a role in glaucoma pathogenesis either directly or indirectly because are linked with maintaining the balance of the aqueous humor (AH), the variation in the trabecular meshwork, and the apoptosis of RGCs. In fact, one of the main treatments to glaucoma consists in the decrease of aqueous humor production and the promotion of aqueous humor drainage, thus relieving the intraocular pressure. The balance of the aqueous humor can be modified by the deposition of the extracellular matrix in the trabecular meshwork, the contraction of trabecular meshwork cells (TM) and the anomalies in the trabecular meshwork structure and miRNAs can impact these changes. It was demonstrated that miR-183 was up-regulated after the induction of cellular senescence by exposure to H_2O_2 in human trabecular meshwork cells and human diploid fibroblast cell, in which is expressed usually at low levels. This miR post-transcriptionally regulates two targets genes: ITGB1 and KIF2A. MiR-183 mediated ITGB1 alterations in senescent cells influenced trabecular meshwork cells functionality during glaucoma and aging (Li et al., 2009). The changes of the extracellular matrix in the trabecular network are affected by many growth factors, such as the transformation growth factor (TGF-β). In the Fuchshofer 's study (2012), it was shown that TGF-β, secreted and synthesized by trabecular meshwork cells, influenced the synthesis of the extracellular matrix in patients with primary open-angle glaucoma through

regulating connective tissue growth factor. The role of miRNAs in the molecular mechanisms of ECM synthesis offers potentiality for therapies of glaucoma. It was been shown that miR-29 family regulated the ECM synthesis in trabecular meshwork since this miR negatively regulated ECM proteins, leading to changes in intraocular pressure. In fact, the increased levels of the miRNA-29 family inhibited extracellular matrix protein synthesis (SPARC, collagen I, collagen IV, and laminin) (Villarreal et al, 2011). MiR-29b was down-regulated under chronic oxidative stress causing up-regulation of ECM genes, resulting in increased ECM deposition and loss of cells (Luna et al., 2009). Other researches have shown that miR-24 negatively regulated the expression of the anthropogenic protease transformation (FURIN) that activated TGF-β by targeting FURIN and, consequently, the overexpression of miRNA-24 could reduce the expression of TGF-β. The up-regulated level of miR-24 by TGF-β is crucial to contain the TGF-β levels during cyclic mechanical stress led to by the targeting of FURIN by miR-24 (Luna et al., 2011). MiR-200c is highly expressed in TM cells and inhibits the expression of genes (ZEB1, ZEB2, FHOD1, LPAR1/EDG2, ETAR, and RHOA) linked to the contraction of trabecular meshwork cells and collagen. It was demonstrated that after intraocular injection of miRNA-200c, the intraocular pressure is reduced. For this reason, it might be a novel target for the treatment of glaucoma (Luna et al., 2012). Jayaram et al. (2015) observed several microRNAs to be down-regulated in glaucomatous retinae influencing TGF-β signalling, with repression of miR-204, miR-106b and miR-25, that stimulated downstream components of this pathway. Only miR-27a was observed up-regulated and functional analysis of its altered gene targets displayed repression of genes linked to the mTORC-1 signalling, lipid biosynthesis, and axonal development. Moreover, the activity RGCs, is decreased by the increase of miRNA-96 and this effect was realised through the activation of caspase. MiRNA-96 was able to affect the survival and apoptosis of RGCs by interaction with caspase-2 since, the role of miRNA-96 in RGCs disappeared when the caspase-2 gene was silenced (Wang et al., 2014).

1.6.5. Pterygium

Pterygium is an ocular surface disease that is associated with chronic UV exposure and is characterized by proliferation, inflammatory infiltrates, fibrosis, angiogenesis and extracellular matrix breakdown in conjunctiva and progressively invaded the cornea. Many miRNAs have been reported to play key role in the manifestation and development of pterygium.

A list of 35 differentially expressed miRNAs and 301 genes and their possible interaction in pterygium was identified by He et al. (2019). They showed that miR-29b-3p could be associated with pterygium development and that the collagen family (COL3A1 and COL4A1), regulated by miR-29-3p and associated with the PI3K-Akt signalling pathway, could be involved in pterygium

pathogenesis. Among the found miRs, both miR-215 and miR-221 by target genes functioning cell cycling, had some effects on fibroblast proliferation. The down-regulated miR-215 targeted Cdc25A and Mcm10 and helped fibroblast proliferation (Lan et al., 2015) while the up-regulated miRNA-221 targeted p27Kip1 gene. Wu et al. (2014) found a negative association between miR-221 and p27Kip1 in pterygium group. MiR-221 could down-regulate p27kip1 gene expression following activation by the β-catechin protein nuclear/cytoplasmic expression, thus promoting cell proliferation. In addition, activation of cyclin D1 by the β-catenin nuclear/cytoplasmic expression appeared to be involved in the pathogenesis of pterygium, leading to cellular proliferation and division. In the Cui's study (2016) it was shown that miR-122 was down-regulated in pterygium compared with normal conjunctiva with an inverse correlation with the expression of Bcl-w, and miR-122 regulated pterygium epithelial cells apoptosis via targeting Bcl-w. A family of miRs, the miR-200 family, has been considered as an important regulator of EMT and have an important role in wound healing and tissue remodelling during pterygium event. Indeed, the miR-200 family promotes the epithelial phenotype through post-transcriptional repression of ZEB1/ZEB2 and TGFβ2, thereby enabling the expression of E-cadherin and polarity factors that are important to the formation of cell-cell junctions. Engelsvold et al. (2013) had found seventy miRNAs to be differentially expressed in human pterygium samples when compared with the normal conjunctiva. 25 miRNAs were significantly differentially expressed by more than two-fold compared to normal conjunctiva. 14 miRNAs were up-regulated, whereas 11 were down-regulated. Among them miR-200a, miR-200b and miR-141, from the miR-200 family, were down-regulated in pterygium.

1.6.6. Cataract

Cataract is the clouding of the eye's natural crystalline lens that become hard, opaque and yellow. The optimal transformation growth factor β (TGF-β) maintains the central lens epithelium at mitotic dormancy state. However, when this exceeds the optimal level, the lens epithelial cells (LECs) head towards to the epithelial-to-mesenchymal transition (EMT), differentiating into fibroblastic/myofibroblastic cells that lead to the pathology of the lens. TGF-β promotes deviation in the differentiation pathway on LECs to progress into cataract. Thus, miRNAs in the lens may be involved in the pathogenesis of cataracts. Dunmire at al. (2012) studied aqueous humor (AH) from human subjects undergoing cataract surgery to find the presence and relative quantities of known miRNAs. Of the 264 miRs tested, 110 were present in the AH. MiR-202, miR-193b, miR-135a, miR-365, and miR-376a were the most abundant. The miRNAs present in the AH showed more than one target, suggesting that they may have multiple roles in regulating target genes in anterior chamber tissues and in several pathways. Deficiency of peroxiredoxin (PRDX6) is a multifunctional protein

essential for cell proliferation, differentiation and protection that causes cataractogenesis and is the target for miR-551b. This miR down-regulated PRDX6 led activation of TGF-β which in turn caused the extracellular matrix protein up-regulation ultimately resulting in cataract (Raghunath et al., 2015). The posterior capsular opacification (PCO) is the most common complication of cataract surgery. After surgery, it is possible that the residual lens epithelial cells (LECs) lose their differentiated phenotype and change their morphology, becoming a mesenchymal myofibroblast cells with epithelial-to-mesenchymal transition (EMT) that can migrate and expand from anterior to the posterior area of the lens capsule. The lens opacity is the result from up-regulation of cytoskeletal proteins such as α-smooth muscle actin, fibrotic extracellular matrix remodelling and EMT-associated changes in crystallin proteins. During surgery, exogenous TGF-β_2 activates the signal, binding its receptor triggers the Smad proteins through its transmembrane kinases. Following TGF-β ligand stimulation, SMAD4 forms a heteromeric complex with SMAD2 and SMAD3 (R-Smads), which are phosphorylated by an activated TGF-β receptor complex. It was identified a molecular mechanism involving miR-204-5p and SMAD4 in the EMT during the development of secondary cataracts. SMAD4 expression was shown significantly suppressed when miR-204-5p was overexpressed, thus it was possible to assume that the regulation of miR-204-5p should be SMAD4-dependent. In fact, up-regulated miR-204-5p enhanced the repression of TGF-β2–induced EMT in the presence of SMAD4 small interfering RNA. Furthermore, up-regulation of miR-204-5p in primary LECs increased E-cadherin expression and decreased the expression of vimentin and alpha smooth muscle actin. (Wang et al., 2013b).

1.6.7. Keratoconus

Keratoconus (KC) is an eye condition that affects the shape of the cornea that, normally round, thins and begins to vary its curvature towards the outside, becoming cone-shaped. These corneal changes can lead to myopia, blurred vision that cannot be improved with corrective lenses and vision loss. The aetiology and pathogenesis of KC are poorly understood. As mentioned above, miR-184 is abundantly expressed in the lens epithelium and in the corneal epithelial basal and suprabasal cells. Studies have reported that miR-184 seems to be a potential candidate for various ocular defects. In fact, it was studied by Hughes at al. (2011) a heterozygous C-to-T transition (r.57c>T) in the seed region of miR-184 in 18 individuals, from Northern Irish family, affected with Keratoconus associated with cataract. Individuals with c.57C>T mutation miR-184 showed different corneal abnormalities such as congenital cataract with keratoconus or corneal thinning but no keratoconus. MiR-184 has a competitive inhibition on the binding of miR-205 to its mRNA target that encodes inositol polyphosphate-like 1 (INPPL1) and integrin, beta 4 (ITGB4), which regulate the corneal

healing. (Hughes et al., 2011). A study was carried out on patients from Saudi Arabia where was examined not only mutations in the miR-184, but also the expression of miR-184 versus miR-205 in post-mortem unaffected ocular tissues. No mutation was detected in KC cases and this proposed that mutation in miR-184 was a rare cause of keratoconus alone and should be more relevant to KC associated with other ocular defects (Abu-Amero et al., 2015). Altered expression of six miRNAs in corneal epithelia from surgery (miR-151a-3p, miR-138-5p, miR-146b-5p, miR-194-5p, miR-28-5p, and miR-181a-2-3p) and four miRNAs in squamous corneal epithelial samples (miR-151a-3p, miR-195-5p, miR-185-5p, and miR-194-5p) were described in thinner keratoconic corneal epithelia by Wang et al. (2018).

1.6.8. Dry eye

Dry eye is a multifactorial disease of the ocular surface and tears condition characterized by an impairment of tear film quantity and/or quality resulting in visual troubles, symptoms of discomfort and tear film instability with probable damage to the ocular surface. This disease is consistent with increased osmolarity of the tear film and inflammation of the eye surface and can lead to corneal blindness for corneal opacity and/ or keratinization Dry eye is often linked to Sjögren's syndrome (SS), that is an autoimmune disease characterized by lymphocytic infiltration of salivary and lacrimal glands, which results in dry mouth and dry eyes, respectively. To investigate the correlations between expression level of miRs and clinical feature of SS, Shi et al. (2014) have been studied 27 patients with SS and 22 normal control to explore the miR-146a and miR-155 expression levels in peripheral blood mononuclear cells (PBMCs) from patients with SS. It's useful to know that miR-146a played a significant role in autoimmune disease by repressing the expression of interleukin-1 (IL-1) receptor-associated kinase 1 (IRAK-1) and TNF receptor-associated factor 6 (TRAF-6), thus impairing NF-κB activity and suppressing the expression of its target genes, such as IL-6, IL-8, IL-1b, and TNF-α. MiR-155 carried out influential regulatory functions in immune cells by targeting several specific mRNAs, such as SOCS1, TAB-2, and c-Maf and miR-155 deficiency led to reduced IgG1 production. It was observed that miR-146a was up-regulated while the miR-155 was down-regulated in PBMCs from the patients with SS and both were correlated with visual analog score (VAS) for dry eye. Moreover, almost nothing is known regarding the influence of miRNAs on dry eye and corneal pathology in SS.

1.6.9. Uveitis

Uveitis is an inflammation of the uveal tract which involves the iris, ciliary body and choroid and is the most common cause of blindness. It can affect surrounding tissues and carry out to inflammation

of the retina (retinitis), optic disc (papillitis) and vitreous (vitritis). Moreover, the uveitis can occur due to an infection or an autoimmune or autoinflammatory aetiology such as in Behcet's disease (BD) and Vogt-Koyanagi-Harada disease (VKH). Differentially expressed extracellular miRNAs in uveitis, either in serum or easily accessible intraocular fluid, such as aqueous humour, could lead to the discovery of disease biomarkers. In a study in which was investigated the intracellular miRNA expression of retina and choroid cells from patients with sympathetic ophthalmia, twenty-seven miRs were significantly down-regulated when compared to controls. Among them, four down-regulated miRs (miR-1, miR-9, let-7e and miR-182) were associated with inflammatory signalling pathway (Kaneko et al., 2012). But only miR-9, at the moment, had validates targets previously shown to be connected to inflammation in sympthatetic ophthalmia such as, TNF-α and NF-κB (Bazzoni et al., 2009). On the other hand, the others miRs were involved in a lot of different pathway for instance miR-182 was linked to Fas/Fas ligang system apoptotic pathway (O'Neil, 2010), let-7e to IL6 signalling pathway (Iliopoulos et al., 2009) and miR-9 to CD4+T cell regulation (Lindberg et al, 2010). Zhou et al. (2012) had investigated the role of miRNAs in the pathogenesis of uveitis and studied the expression of 5 immunologically relevant miRs in peripheral blood mononuclear cells (PBMCs), monocyte derived dendritic cells (mo-DCs), and CD4+T cells from patients with Behcet's disease (BD) with active and inactive uveitis, VKH patients with active uveitis and healthy controls. Among them, it was revealed that miR-155 expressed less in PBMCs cells and dendritic cells of BD, but not in VKH disease, compared to healthy controls, confirming its role in the pathogenesis intraocular inflammation. As shown above, this miR can negatively regulate the production of proinflammatory cytokines (IL-6 and IL1β) and the production of an anti-inflammatory cytokine, IL10, through the TRL/IL1 signalling cascade by targeting TGF-β activated kinase (MAP3K7) binding protein 2 (TAB2) protein, which has been tested as target for miR-155. Also, the abnormal production of proinflammatory cytokines by dendritic cells and CD4+T, caused by the down-regulation of miR-155, were involved in pathogenesis of BD. It was investigated the decrease expression of miR-20a-5p in CD4+T cells from patients with VKH disease compared to control group. This miR targets the oncostatin M (OSM) and C-C motif chemokine ligand 1 (CCL1) gene, which could prevent the inhibitory effects of miR-20a-5p on the production of IL-17 in patients with VKH disease. It has been seen that phosphoinositide-3-kinase–protein kinase B (PI3K-AKT) can contribute to the production of IL-17 and could control the effect of miR-20a-5p on the pathogenesis of VKH disease. OMS is also involved in regulating the activity of the PI3K-AKT pathway as its over-expression rescues the decreased activities of the PI3K-AKT pathway caused by miR-20a-5p mimic. (Chang et al., 2018).

1.6.10. Uveal melanoma

Uveal melanoma is the most common primary intraocular malignancy, which develops from the choroid in 90% of cases and from the iris and ciliary body in 10%. It begins with visual symptoms (blurring of vision, photopsyche, myodesopsia and reduction of the visual field), the presence of a visible mass and pain. In about half of patients, lethal metastases are observed, usually at liver level. MiRNAs was found in retinal cells or serum and, by Ragusa et al. (2013), their expression were compared in 18 vitrous humor samples from different ocular pathologies (from patients with choroidal melanomas, retinal detachment, or macular hole) to serum from healthy donors normal retina cells, and epithelioid uveal melanoma cells. Some miRNAs were detected significantly overexpressed in eyes with uveal melanoma compared to the two other groups. Among them, miR-146a and miR-26a were up-regulated about threefold. The up-regulation of miR-146a induced the overexpression of VEGF that was elevated in ocular fluids of eyes with uveal melanoma (Boyd et al., 2002). Also, this miR regulated extracellular matrix in retinal microvessels and it was involved in retinal neovascularization. On the other hand, miR-26a helped vascular proliferation inhibiting cellular differentiation, apoptosis and inducing VEGF expression (Liu et al., 2012).

Dysregulated miRNAs have been studied in uveal melanocytes and melanoma cell lines. Microphthalmia-associated transcription factor (MITF) plays an essential role in the homeostatic up-regulation of c-Met expression by direct binding to the c-Met promoter in melanoma cells and primary melanocytes. MITF is a regulator of melanocyte cell growth, maturation, apoptosis, and pigmentation. c-Met, which is highly expressed in melanomas, is thought to justify the metastatic potential of melanomas. Furthermore, c-Met mediated inhibition of the Akt and ERK1/2 pathways can lead to cell cycle arrest. Another mechanism of MITF in cell cycle regulation could be attributed to its modulation of CDKs (McGill et al., 2006). There are several miRs linked to MITF and its networks. MiR-137, contained in the chromosome 1, has been shown to regulate MITF. This miR, overexpressed, acted as a tumor suppressor in uveal melanoma cell proliferation by down-regulation of its targets MITF and CDK6 (Chen et al., 2011). Furthermore, it was validated that miR-34a is a proapoptotic transcriptional target of the p53 tumor-suppressor gene and, in uveal melanoma cells, acted as tumor suppressor leading to cells inhibition of growth and migration. c-Met, down-regulated by mir-34a, inhibited cell proliferation and migration via Akt signalling pathway in an HGF dependent mode (Yan et al., 2009). Yan et al. (2012) have demonstrated the down-regulation of miR-182 in uveal melanoma, suggesting that this miR should be responsible for the development of uveal melanoma. This miR decreased the expression levels of c-Met that inhibited uveal melanoma proliferation, apoptosis, invasion and migration. It was also found that miR-182 can inhibit BCL2, influenced by the presence of MITF, and cyclin D2, target of miR-182, directly. Both *in vitro* and *in*

vivo experiments demonstrated that the growth of uveal melanoma was suppressed by the overexpression of miR-182.

MiR-20a, miR-125b, miR-146a, miR-155, miR-181a, miR-223 and miR-17-92 complexes, immunoregulatory miRs in circulation, were found to be higher in the plasma of uveal melanoma patients. The levels of these miRs, except miR-181a, were elevated in metastasis compared to primarily diagnosed uveal melanoma. Instead the miR-181a level was lower. The difference of the immunoregulatory miR expression, at various stages of uveal melanoma, could be important to develop a potential blood biomarker (Achberger et al., 2014).

This overview of ocular pathologies sheds light about the fact that there is much more data in the literature on the relationship between the miRNA and pathologies that affect the posterior segment than on the anterior segment, of which little is known yet.

1.7. Therapeutic application of microRNAs

The value of miRNAs as therapeutic agents is broadly recognized. The knowledge of the mechanisms of miRs regulation suggests that they can become therapeutic targets or can themselves become drugs for a wide range of pathologies. Studies have highlighted the strong potentiality of miRNA to define diagnosis, prognosis and therapeutic application in human diseases (Li and Kowdley, 2012; Rupaimoole and Slack, 2017). In fact, a relevant concept in the therapeutic field is that a microRNA can regulate the expression of multiple target proteins, interacting with multiple target mRNAs. The use of microRNAs could be considered as a new way of epigenetic therapy and could be applied to multigenic pathologies caused, at least in part, by the altered regulation of miRs. It was demonstrated the possibility of restoring the normal or inhibiting the aberrant activity of dysregulated miRNAs in pathology. Dysregulated miRNAs could potentially be treatment's option themselves by using miRNA mimics or antagomirs, short synthetic molecules, specifically modified to modulate miRNA levels in the cell and to increase stability, specificity and binding affinity to target. The development of molecules similar to miRNAs but with a higher half-life and increased *in vivo* efficacy, such as locked nucleic acid (LNA) often referred to as inaccessible RNAs or modified ribonucleotides, in which the ribose ring contains an extra bridge connecting the 2' and 4'carbons, anti-miR oligonucleotides (AMO) and antagomirs' conjugated to cholesterol molecules (Li and Rana, 2014), was the first step in the translation of scientific progresses within clinical practice in the last decade. In addition, software has been developed able to draw miRNAs artificial that bind and inhibit different targets at the same time, allowing a contemporary regulation of many mRNA. Although their therapeutic role is under evaluation in several clinical trials for more in-depth-studied and high-impact

diseases, such as those on the cardiovascular system and cancer, miRNAs are not included now in any clinical trials about the treatment of eye disorders. Most probably, this can be attributable to the lack of knowledge about their specific role in this organ and related diseases. Therefore, by improving the knowledge in this field, in the future miRNAs would also represent a suitable method in the treatment of ocular disorders.

2. NERVE GROWTH FACTOR

The nerve growth factor (NGF), discovered by Rita Levi-Montalcini in the 1950s, is the best-characterized member of the neurotrophin family, which includes also brain derived neurotrophic factor (BDNF), neurotrophins 3 (NT-3), 4/5 (NT-4/5) and 6 (NT-6). The discovery took place after the transplantation of a malignant mouse sarcoma into the body wall of a 3-day-old chick embryo where the tumour seemed to be able to release a chemical factor capable of inducing ganglion growth, production and atypical ramification of nerve fibres, acting via humoral. Subsequently studies revealed that mouse submandibular salivary glands were an excellent source of NGF purification, greater than what was found within the snake venom. (Levi-Montalcini, 1987; Cohen et al., 1954; Cohen et al., 1959). NGF plays a key role in the maturation and development of the central nervous system and peripheral. It acts directly on peripheral sensory and sympathetic neurons promoting survival, differentiation, functional activity and maintaining their phenotype. Moreover, NGF regulates neuronal gene expression by interaction with specific cellular receptors.

The NGF's structure is formed by two pairs of twisted, antiparallel β-strands of amino acids. To support the fold on one end there are three hairpin loops, and the other end carries a cysteine-knot motif, formed by three disulphide bonds. In the mature form, two monomers are organized in a parallel manner to form a close-packed homodimer (Figure 5). In tissues, NGF is initially synthesized as a precursor (pro-NGF) in the reticulum of Golgi, and after cleavage by intracellular convertases and metal protein matrix extracellular, becomes the mature form (NGF) (Wiesmann C et al., 2001).
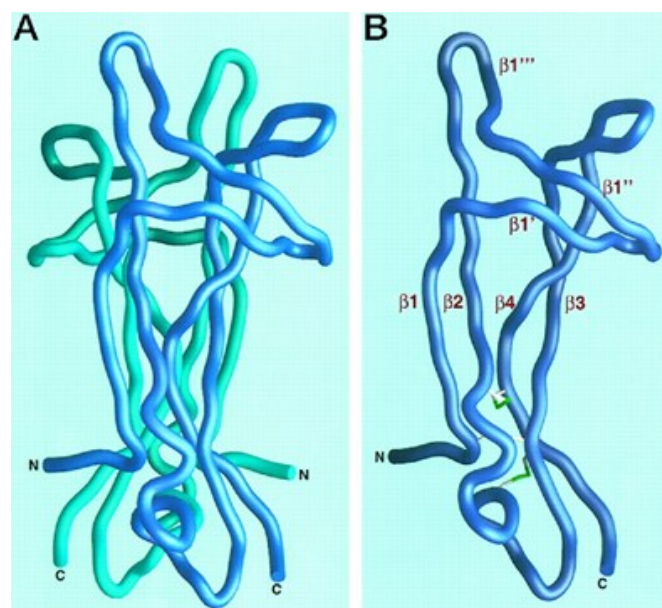
Figure 5-**NGF structure**. *(A*) NGF dimer with each subunit colored differently. (*B*) the tertiary fold for the NGF subunit with β-Strands labelled. The three disulfide bridges are drawn as *whitesticks* with *green* indicating the sulfur atom (McDonald and Chao, 1995)

NGF exerts its action through two classes of trans-membrane receptors, the high-affinity tropomyosin tyrosine kinase receptor TrkA and the low-affinity p75^{NTR}.

Trk receptors are able to stimulate neuronal survival, differentiation, neuritic growth, myelination and synaptic plasticity while p75 ^{NTR} may induce survival or apoptosis, depending on the cell type in which it is expressed, the functional state of the cell, presence or absence and the type of ligand.

The TrkA receptor is a transmembrane glycoprotein with a molecular weight of 140 kDa, encoded by a gene located on chromosome 1 and belonging to the family of tyrosine kinase receptors (Trks). TrkA, expressed in both central and peripheral nervous systems but also in non-neuronal cells, has a series of repeated segments in its extracellular domain, rich in leucine (domain 2), linked to two clusters of cysteine residues (domain 1 and domain3) and two immunoglobulin (Ig)-like domains (domain 4 and domain 5) allowing the interaction of the receptor with superficial proteins (Pattarawarapan and Burgess, 2003).

Like other tyrosine-kinase receptors, the receptor-ligand binding induces a dimerization of the receptor and subsequent triggers intracellular signals through kinase phosphorylation. In addition, in the nucleus, it activates transcription factors that induce the expression of specific genes.

NGF binding with TrkA determines phosphorylation of two tyrosine sites: Y758 and Y490 which interact with the phospholipase Cγ (PLCγ) and the adaptor protein Src homology 2-containing protein (Shc) respectively. PLCγ catalyses the hydrolysis of phosphatidyl inositol 4,5-bisphosphate in diacylglycerol (DAG) and inositol(1,4,5)triphosphate (IP3). DAG activates a series of kinases, while IP3, promotes the calcium release from intracellular reserves which enhances the release of neurotransmitters. In this fashion, this pathway modulates plasticity and synaptic function. Whereas Shc, once phosphorylated by TrkA, binds to an adaptor protein, growth factor receptor bound protein-2 (Grb-2). Subsequently, this protein actives several reactions by Ras/MAPK cascade which plays an essential role in axonal growth, then it can transmit signals from the cytoplasm to the nucleus and can also act at the cytoplasmic level, phosphorylating proteins of the cytoskeleton. This pathway, as a finale effect, induces to the activation of transcription factors involved in survival and cell proliferation. Shc also promotes PI3K/AKT: PI3K stimulates Akt, a protein with serine-threonine kinase activity, which induces cell survival (Figure 6). This protein is able to suppress apoptotic signals thanks to the inactivation of pro-apoptotic proteins, such as Bad, thus preventing the association of Bad with Bcl2 and favouring the survival of the cell (Freund and Frossard, 2008; Chao, 2003).

The p75^{NTR} receptor is a transmembrane glycoprotein, with a molecular weight of 75 kDa, that belongs to the family of death receptors, characterized by domain death, a specific intracellular sequence. The activation of this receptor leads to apoptosis or survival cell in neuronal and structural

cells, depending on signalling pathways and on adaptor proteins or co-receptors recruited in the p75^{NTR} receptor. The p75^{NTR} receptor binds all neurotropins with a nanomolar affinity and binds also the pro-neurotropins (Chao, 2003). The p75 receptor is made up of four negatively charged cysteine-rich extracellular repeats, all required for full-affinity NGF binding, and a unique cytoplasmic domain which is highly conserved among species. Thus, the 4 cysteine-rich domains (CRD-1/-4), contained in the extracellular domain of p75, are negatively charged and responsible for binding neurotrophins to the p75^{NTR} receptor. The NGF binds to the p75^{NTR} receptor in two specific points: the site I composed of the CRD1-CRD2 junction and the CRD2 domain and the site II composed of the CRD3-CRD4 junction. Conversaly, the juxtamembran or Chopper domain and the death domain help recruit adaptor proteins. Crystallographic studies show an asymmetrical complex containing a dimer of NGF bound to a single monomer of the p75^{NTR} receptor, thus also able to bind a TrkA monomer and lead to the formation of a heterodimer (He and Garcia, 2004). The biological effect mediated by p75^{NTR} depends on the cellular context in which it is expressed. In the presence of TrkA, p75^{NTR} increases the NGF-binding affinity of TrkA, creating high-affinity binding sites, and promoting survival. On the contrary, in the absence of the TrkA, it is responsible for the apoptosis processes involving the activation of the kinase Jun amino-terminal kinase (JNK). This leads to the phosphorylation of c-jun and, through the activation of proteins p53, Bad and Bim, to the mitochondrial translocation of Bax, with release of cytochrome c, and subsequent activation of caspase 3, 6 and 9. The activation of p75^{NTR} can also produce an increase in ceramide levels and activate the cell death pathway, consisting of JNK-p53-Bax proteins, and the small G proteins of the Rho family resulting in activation of MKKK and MKK 4 and 7. In addition, there are other pathways that can interact simultaneously. NF-κB activation, mediated by factor associated with the TNF-receptor complex (TRAF6), one of the many JNK activators, leads to the induction of cell survival (Figure 6). This is due to the recruitment of TRAF6 and the activation of kinase associated with the receptor for IL-1 (IRAK1) and atypical PKC kinase, the activation of PI3K and AKT and the involvement of RIP-2 (receptor interacting protein-2). The transcription of peptides with antiapoptotic activity (AIP or BCL-2 family) or molecules that block or apoptotic pathways (Gadd45β) is induced by the activation of NF-κB (Nykjaer et al., 2005; Papa et al., 2004).
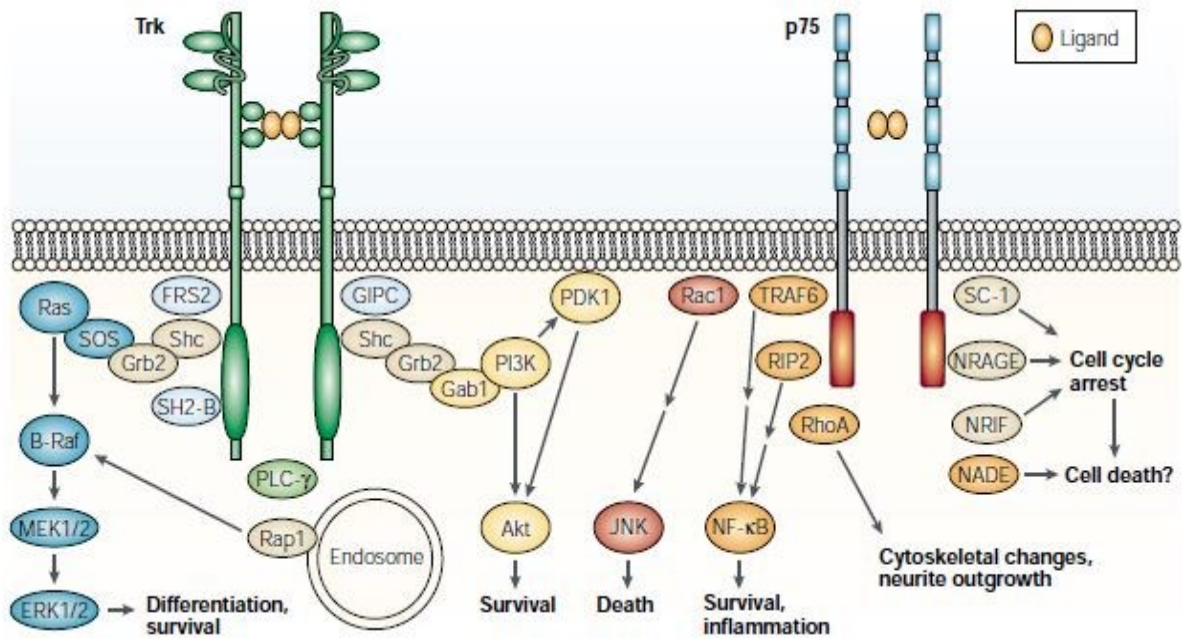
Figure 6- **Neurotrophin receptor signalling.** The NGF binds to the Trk receptor by inducing its dimerization promoting its auto-phosphorylation and the activation of several signalling pathways. Trk signalling regulates differentiation, survival, plasticity and synaptic function. p75NTR binds interacting proteins, regulates apoptosis or survival in neuronal and structural cells (Chao, 2003).

2.1. NGF in the eye

The nerve growth factor and its receptors play an important role in the eye both in physiological and pathological states. NGF plays a role in trophism and in maintaining the integrity of the corneal epithelium in basal conditions, while its coexpression with the TrkA receptor on the same cells suggests the presence of a mechanism of action autocrine and/or paracrine. This mechanism supports the survival and function of epithelial cells. The corneal tissue, when damaged, reacts to the mechanical insult with an increase in NGF levels, synthesized by the cornea itself (Lambiase et al., 2000). The potential role of NGF has also been demonstrated in conjunctival cells, where it is produced, stored, released and used. NGF is normally released also in aqueo humor and is has a role in maintaining the homeostasis of the tear film as it is basally released from the lacrimal gland (Lee et al., 2005). NGF is also expressed by the iris and ciliary body, which overexpress and release NGF after an eye injury (Lambiase et al., 2002). However, molecular mechanisms inducing biological response to NGF at the corneal level are still unknown.

NGF is also expressed in posterior segment tissues, including vitreous, choroid, optic nerve and retina (Micera et al., 2004). NGF is able to control the development and differentiation of the retina and optic nerve well as promote survival and recovery of retinal ganglion cells (RGC). The latter also plays a protective role, since injected intravenously protects the degeneration of retinal cells; this has

been demonstrated in retinal detachment experiments (Bai et al., 2010). NGF promotes several effects in the retina on different cell types (Figure 7) including proliferation, plasticity, transmitter synthesis, reorganization, cytoskeleton changes and synaptic transmission. Studies have demonstrated the ability of NGF to inhibit the degeneration of ganglion cells and nerve fibers of the optic nerve (Carmignoto et al., 1989).
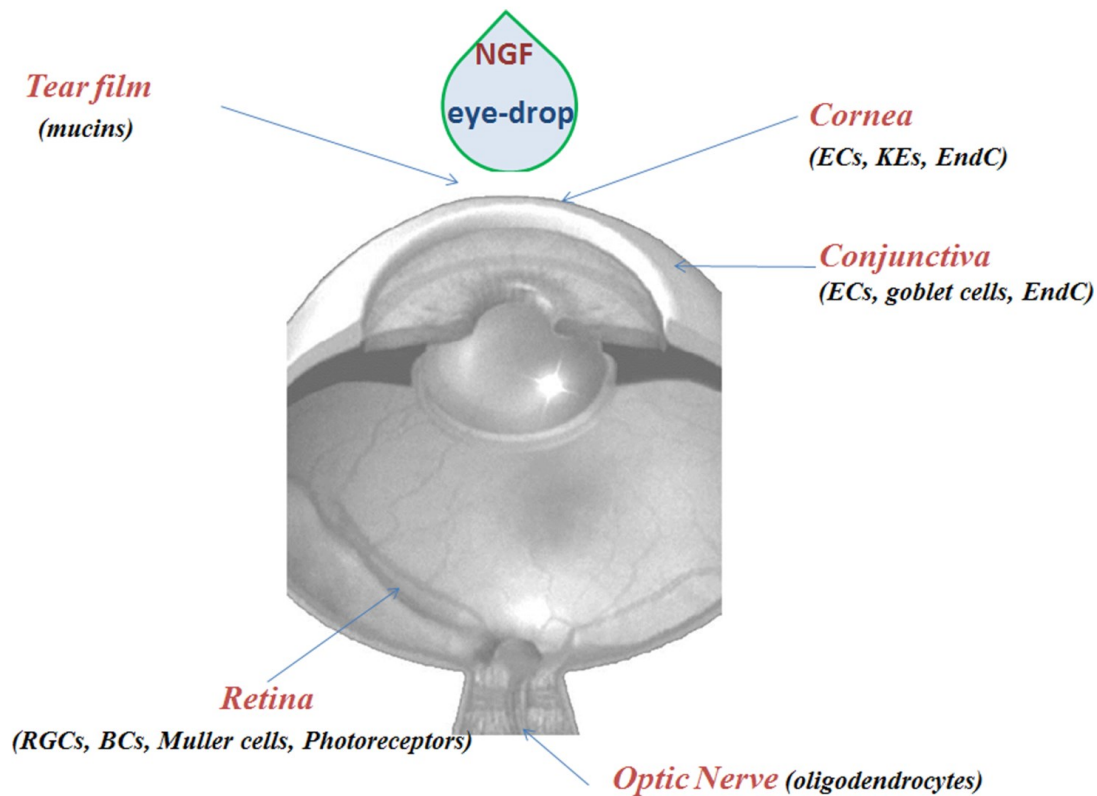
Figure 7- **NGF and eye.** Eye cell types responsive to NGF. ECs: epithelial cells, KEs: keratocytes, EndC: endothelial cells, RGCs: retinal ganglion cells, BCs: bipolar cells. (Aloe et al., 2015).

2.2. NGF and its role in human diseases

The biological role of NGF is crucial not only for central and peripheral nervous system's functions and maintenance, but it is also relevant for non-neuronal cells, such as immune-hematopoietic cells or epithelia. In the central nervous system (CNS), NGF is produced in the hippocampus, cortex and pituitary gland as well as in the thalamus, basal ganglia, spinal cord and retina. NGF regulates the autonomic response and the modulation of the stress axis activity since it regulates the phenotypic characteristics in noradrenergic nuclei of the hypothalamus and the brainstem. Also, the cells of the immune system- hematopoietic (lymphocytes, granulocytes, antigen presenting cells, hematopoietic stem cells, mast cells and eosinophils) produce and use NGF which plays a role in survival, in cell differentiation and in immune response (Aloe et al., 2012). *In vivo* experiments have shown that some

autoimmune inflammatory diseases, (i.e. systemic lupus erythematosus, psoriasis, Kawasaki syndrome, scleroderma and rheumatoid arthritis), and allergic diseases (i.e. asthma, urticaria-angioedema, rhinoconjunctivitis and spring keratoconjunctivitis), are characterized by an activation of immunocytes and a significant alteration in basal levels of NGF (Aloe et al., 1997).

NGF plays a key role in the survival and function of cholinergic neurons of the basal forebrain complex (BFC), such functions include attention, excitement, motivation, memory and consciousness. NGF has been shown as a potential protective and/or healing factor for neurodegenerative disorders associated with BFC neurons, such as, when this last are affected by Alzheimer's disease (AD). NGF has been displayed to play an important role in aging and, consequently, age-related diseases. The aging, indeed, can act with pre-existing abnormalities in trophic signalling and activate cholinergic and cognitive decline as observed in age-related diseases, such as AD. Studies in AD patients demonstrated lower levels of amyloid β in their cerebrospinal fluid after treatment with NGF for 12 months, achieving an improvement in cognitive function, although this treatment showed the onset of side effects. A correct strategy could be to allow the release of NGF in the proximity of cholinergic cell bodies, where NGF deficits have been detected, so as to improve the survival or neurotransmission of cholinergic neurons (Budni et al., 2016).

Moreover, it was also demonstrated that the constitutive synthesis of NGF in adult tissues is linked with several Peripheral Nervous System (PNS) neurons phenotypic features (Aloe et al., 2015). In addition to supporting the survival and regeneration of peripheral axons during nerve repair, studies have shown that NGF is involved in both to phenotypic regulation and to the elimination of dedifferentiated Schwann cells. Such cells express p75^{NTR} on two cases: during peripheral nerve development and in nerve regeneration or repair. In response to local IL-1, the macrophages recruited to the damaged site release NGF while, Schwann cells increase NGF receptors after nerve injury, which is induced by interleukin-1 (IL-1). NGF signalling through p75^{NTR} plays an important role in regulating Schwann cellular events during peripheral repair or nerve regeneration by intracellular ceramide elevation, which generates apoptosis, and NF-κB activation (Hirata et al., 2001; Taniuchi et al., 1986). Patients with diabetic neuropathy have a high risk of chronic ulcers and compromised wound healing. The application of NGF aimed to the treatment of diabetic neuropathy has been studied, so much that it has arrived to phase III of the experimentation, in which however some problems have been found. However, NGF accelerates the rate of healing of skin wounds and prevents both programmed neuroretinal cell death and capillary pathology in experimental diabetes (Apfel, 2002).

As mentioned above, NGF also has wide biological activities on non-neuronal cells, as well as inflammatory cells (neutrophils, macrophages and mast cells), but also keratinocytes, fibroblasts and

endothelial cells that are significant cellular components in the wound healing process. Furthermore, NGF has a pivot role in tissue repair and wound healing, proving to have a powerful pharmacological effect in treating human skin and corneal ulcer. Wound healing is a complex process, regulated by cytokines, which includes induction of acute inflammation following the lesion, followed by proliferation of parenchymal and mesenchymal cells, migration and activation with extracellular matrix production and deposition. Effects of NGF on healthy and diseased skin could be exerted directly through NGF receptors expressed on epidermal and skin cells or by the influence of NGF on skin innervation of PNS. NGF exerts a powerful chemotactic activity to polymorphonuclear cells, whose recruitment is an important early event in the wound healing process, and to cutaneous fibroblasts by stimulating their migration into the wound healing development. Micera et al. (2001) demonstrated that an *in vitro* culture of skin fibroblasts, treated with NGF, has begun to express p75^{NTR} after a long exposure, suggesting that apoptosis triggered by NGF in fibroblasts during the last stages of repair, as in the remodelling of the wound healing process and tissue repair. NGF also changes the phenotype of skin fibroblasts in myofibroblasts as it induces the expression of alphasmooth muscle actin (α-SMA) in cutaneous fibrobalsts. NGF can also act on endothelial cells by playing a role in angiogenic activity. In fact, it has been shown that NGF stimulates the production of vascular endothelial growth factor (VEGF), the most powerful mitogen for endothelial cells that promotes angiogenesis and blood permeability, in peripheral sensory neurons (Calza et al., 2001). To confirm this and the role of NGF in neo-vascularisation, a treatment was performed on a child with severe left limb crushing syndrome with subcutaneous mNGF (Chiaretti et al., 2002). The gradual improvement of the ischemic treated area has been observed leading to a reduction in the size of the general ischemia that finally underwent calcaneal escharotomy.

Tuveri et al. (2000) conducted a clinical trial on patients with rheumatoid arthritis (RA) with chronic skin ulcer, treated with topical application of NGF, purified from submaxillary glands of mice. They showed that, with continuous application of NGF, the size of the lesion was gradually decreased. NGF is also competent for patients with pressure ulcers (Bernabei et al., 1999). The healing effect of NGF on vascular ulcers can be explained by its angiogenic activity and the its effects on keratinocytes and fibroblasts.

Several therapeutic strategies for the administration of NGF in animal models and human diseases have been explored and many studies are currently under way to assess whether NGF can prevent or protect against cellular degeneration in the nervous system, visual system and skin tissue.

2.3. NGF and eye diseases

As mentioned above, NGF and its receptors are expressed in the anterior and posterior segments of the eye, both in physiological and pathological states, where they exercise different specific tissue functions. Changes in the NGF expression and its receptors in these segments of the eye are correlated with the onset or severity of ocular pathologies in both animal models and patients. The potential therapeutic efficacy of NGF has been shown in several studies, which have shown that the local administration of NGF on the eye affects not only the ocular surface, but it is also able to reach the optic nerve, retina and brain. In this way it can oppose tissue damage and loss of visual functions.

2.3.1. Neurotrophic Keratitis

To note that there are studies on neurotrophic keratitis (NK), a rare degenerative corneal condition caused by impairment of the trigeminal innervation, after corneal surgery or complications of diabetes mellitus and multiple sclerosis. Such pathology leads to deterioration of corneal sensitivity and consequent degenerative changes of the corneal epithelium. To date, neurotrophic keratitis is considered an orphan disease of treatment. A molecule structurally identical to the human NGF, produced in *Escherichia coli*, has been approved by the EMA (European Medical Agency) and, recently, by the FDA as a first-class treatment for NK. This drug, administered as eye drops, acts directly on the corneal epithelium stimulating its survival and growth. Furthermore, it promotes also tears' production by lacrimal glands, thus providing lubrication and natural protection from pathogens and injury, and supports corneal innervation, usually lost in neurotrophic keratitis (Versura et al., 2018; Bonini et al., 2018; Bonini et al., 2018).

2.3.2. Dry Eye

NGF and its p75 receptor have been in the human lacrimal gland tissue as well as being quantified in human tears, thus indicating that it can be basally released by the lacrimal gland (Lee et al., 2005). Therefore, it is possible that NGF can play an important role in the pathology of the dry eye and that it can be used as a therapeutic treatment, as it regulates the lacrimal production and the homeostasis of the lacrimal film. In fact, one of the characteristics of the dry eye is an increase in lacrimal osmorality that can cause damage and apoptosis of the cornea epithelial cells. *In vivo* studies have shown that topical administration of NGF in a dog model of dry eye improves tear production and conjunctival goblet cells density (Coassin et al., 2005). Although there is no specific therapy, currently the treatments for the dry eye aim to the lubrication with tear substitutes or to control the

ocular superficial inflammation with immunosuppressive drugs and steroids (Lambiase et al., 2011b; Lee et al., 2005).

2.3.3. Glaucoma

RGCs express TrkA to which NGF binds, leading to up-regulation of Bcl-2 that protects cells from apoptosis by preventing caspase activation. In pathological conditions, such as glaucoma, the increase in intraocular pressure alters the NGF expression level and its receptors. Experiments on rodent models in which glaucoma was induced showed that NGF levels and NGF receptors in the retina are significantly down-regulated, while NGF administration in the eyes promoted damaged RGC recovery (Morrison et al., 1997). Subsequently experiments on patients with glaucoma, who presented progressive visual field defects, showed that patients treated with NGF presented a lower reduction of RGC, associated with inhibition of cell death by apoptosis, in comparison with the untreated (Sposato et al., 2009). In addition, patients treated with NGF presented improvements in optic nerve function, contrast sensitivity and visual acuity (Lambiase et al., 2009).

2.3.4. Retinitis Pigmentosa

One of the first experiments in which the role of photoreceptors' protection by NGF, in retinitis pigmentosa, was demonstrated, was done using a strain mouse C3H, which are characterized by the progressive photoreceptor degeneration during the first postnatal phase. NGF, administered intravenously, is able to delay photoreceptor degeneration (Lambiase et al., 1996). Subsequent studies were carried out on patients with retinitis pigmentosa treated with NGF murine eye-drops. Some patients reported a feeling of improved visual performance, associated with a temporary amplification of the visual field (Falsini et al., 2016).

2.3.5. Corneal Ulcer

NGF plays a pivotal role in maintaining corneal trophism and restorative mechanisms. A clear evidence was given by Lambiase et al. (1998) since they demonstrated that NGF topical administration in the eyes of corneal ulcer patients stimulates corneal healing. Both improved corneal transparency and the production of tear films following treatment with NGF were observed, thereby improving visual function. These results support the role of topical NGF in the eye since it acts on the ocular surface by stimulating innervation of damaged cornea, improving both stroma and endothelial cells, and modulating corneal stem cells (Lambiase et al., 2000; Micera et al., 2006).

2.4. NGF and miRNAs

At present few studies described the relationship between NGF and microRNAs. It has been shown that NGF-modulated miRs regulate several protein components of signalling pathways involved in neuronal development and diseases. Studies on pheochromocytoma cell line (PC12) showed that miR-21 improves NGF signalling and controls neuron differentiation induced by NGF. This miR also prevents neurodegeneration, preserving the neuronal network and supporting the viability of neurons in an NGF removal situation (Montalban et al, 2014). Another study on PC12 showed an up regulation of 8 miRs and a down-regulation of 12 miR were modulated by NGF. Among them was emerged miR-221, whose expression is greatly increased. In addition, miR-221 plays a protective role against apoptosis in PC12 cells since it is able to decrease the expression of Foxo3 and Apaf-1. MiR-221 is assumed to compensate for defective NGF signalling in pathological conditions, such as in AD, as miR-221 seems to have improved neuronal differentiation induced by low doses of NGF (Hamada et al., 2012)

In particular, there is only one study about the involvement of miRs in the eye after treatment with NGF. Wu et al. (2017) studied the microRNA response following the treatment of human corneal epithelial cell (HCEC) with NGF. This altered the expression of some miRNAs present in HCEC, especially miR-494. The down-regulation of miR-494 led to a decrease in the expression of the cyclin D1, its target, causing G1 arrest.

AIM OF THE STUDY

The study was aimed at analysing and comparing the effects of three NGF bioformulations, at different time points, on miRNAs' expression levels modulation in human corneal epithelial cells, in order to shed light on some of the molecular mechanisms, still unknown, at the base of NGF biological activity. To this purpose, the analysis was focused on significantly dysregulated miRNAs, target genes and pathways of interest by using in silico tools. Original and novel insights about genes and epigenetics mechanisms induced by the different NGF bioformulations were provided.

In agreement with Dompé S.p.A., the company partner of the PhD programme, the NGFs here used were codified as NGF1, NGF2 and NGF3.

MATERIALS AND METHODS

4.1. In vitro corneal model and treatments

The Human Corneal Epithelial Cells (HCEpiC) (Innoprot) (positive for CK18 and CK19 epithelial markers) were cultured in Corneal Epithelial Cell Medium (Innoprot) supplemented with 5% fetal bovine serum (Gibco), 1% Corneal Epithelial Cell Growth Supplement (CEpiCGS) (Innoprot) and 1% penicillin/streptomycin solution (Innoprot). Cells were cultured on T75 flasks precoated with Collagen I (Corning® BioCoat™ Collagen I Cultureware) and maintained in humidified atmosphere at 37°C with 5% CO2. The medium was changed every 3 days, until the culture reached approximately 70% confluency, and subsequently every day, until the culture was approximately 80-90% confluent.

Cells were treated with three different NGF bioformulations (here codified as NGF1, NGF2 and NGF3, in agreement with Dompé, the company partner of the PhD programme) at 200 ng/ml (You et al., 2000; Blanco-Mezquita et al., 2013, Li et al., 2010), which were added to the medium when cells were 80-90% confluent. Then, cells were incubated at 37°C for three time points: 30 min, 12h and 48h. Untreated control cells were cultured as well.

4.2. RNA extraction

Total RNA, including the fraction less than 200 nucleotides in length, was isolated from HCECs using the mirVana isolation kit (Ambion Biosystems), according to the manufacturer's procedure. The concentration of RNAs was assessed by Nanodrop (Thermo Fisher Scientific) and RNA samples were stored at -80°C.

4.3. MiRNAs' expression analysis

Total RNAs from treated samples and control were reverse-transcribed using the Megaplex RT primer Human Pool A and Pool B set v3.0 (Applied Biosystem) and the TaqMan miRNA RT kit (Applied Biosystem). Subsequently, for every NGF bioformulation, three replicated samples from each time point,plus unstimulated control, were run on microfluidic TaqMan Array Human MicroRNA cards v3.0 (set A and B) (Applied Biosystems), according to manufacturer's instructions. These cards are preconfigured for 384 wells for a total of 754 unique assays specific to human miRNAs. Samples were analysed on a ViiA7 instrument (Applied Biosystems) and data processed by ViiA7 software (Thermo Fisher). MicroRNA's expression levels (RQ relative quantification) were evaluated by comparative assay ($2^{-\Delta\Delta Ct}$). In order to avoid interferences due to variations with respect to basal qRT-

PCR set-up conditions, all flagged wells were removed and not considered for the analysis, aware that this is a sort of compromise: if, on the hand, some flagged wells with putative relevance could be eliminated, on the other hand, the analysis, focused at the same way on a high number of targets, was easier and cleaner.

4.4. Statistics and target genes/pathways analysis.

Comparative data analysis was carried out by Expression Suite v1.1 (Thermo Fisher). Among the differentially expressed miRNAs (Relative Quantification -RQ- fold change ≤0.5 or ≥2), those showing significant P value (P<0.05) were analysed by Diana tools (Diana-miRpath v.3, -microT-CDS,-TarBase v7.0, Vlachos et al., 2015) to identify predicted (microT-CDS database, Paraskevopoulou et al, 2013) and/or experimentally supported (Tarbase database, Karagkouni et al., 2018) target genes and pathways. We used KEGG database annotation with standard statistics and genes union settings for an exploratory functional analysis.

4.5. Enrichment annotation analysis and network construction

For the network construction and the enrichment annotation step, it was taken also advantage of Genemania (Warde-Farley et al., 2010), which operated a functional clusterization of a query gene list, based on predicted, physical interactions, co-expression, pathway, shared protein domains, co-localization, genetic Interactions, also reporting FDR (False Discovery Rate) and gene coverage for each cluster.

4.6. Western Blot analysis

Immunoblotting experiments were performed to assess protein expression levels related to some of the miRNAS' target genes. Protein lysates from HCECs, treated as described, were prepared in 50 μl modified RIPA Buffer (PBS 1X, NP40 1%, sodium deoxycholate 0.5%, SDS 1%, water and Complete-Mini protease inhibitor cocktail tablet (Roche Diagnostics), PMSF 10 mg/ml, Aprotinin 10 mg/ml e sodium orthovanadate 0.1 M (Sigma-Aldrich). The lysates were incubated in ice for 30 minutes and then centrifuged at 14000 rpm for 15 minutes at 4°C. At this point, the supernatant was collected and stored at -80 ° C.

Protein concentration was determined using the standard BCA control with the Pierce BCA Protein assay kit (Thermo Scientific) and spectrophotometric reading at wavelength of 562 nm, according to the manufacturer's instructions.

A total of 20μg of protein extracts were separated on a precast Bolt 4-12% Bis Tris Plus gel (Invitrogen) by SDS-PAGE. Electrophoresed proteins were transferred overnight onto nitrocellulose membrane by using Mini Trans-Blot transfer system (Bio-Rad Laboratories). Membranes were stained with Ponceau (EuroClone) washed twice in TBS-T (Tris-HCl 1M pH 8, NaCl 5M and 0.2% Tween-20,) for 10 min, and blocked in TBS-T containing 5% BSA (Sigma-Aldrich) for one hour at room temperature. Subsequently, the membrane was incubated overnight at 4° C with anti-AKT (#9272, Cell Signalling Technology), recognizing AKT1, 2 and 3 isoforms. The next day, the membrane was washed in TBS-T and incubated one hour at room temperature with the goat anti-rabbit IgG-HRP sc-2030 secondary antibody (Santa Cruz Biotechnology). The Super Signal West Pico Chemiluminescent Substrate Kit (Thermo Scientific) and the ChemiDoc XR + (Bio-Rad) system were used to visualize and determine the proteins by means of a chemiluminescent signal. Actin (C-11 sc-1615 Santa Cruz Biotechnology) was used as endogenous control.

4.7. Scratch wound healing assay

The effects of NGF1 on corneal epithelial migration were measured over HCEC seeded into 6-well tissue culture plates precoated with Collagen I (Corning® BioCoat™ Collagen I Multiwell Plate). When cells reached approximately 90-100% confluency, forming a monolayer, a 200μl pipette tip was used to create a perpendicular scratch. To remove cell debris, medium was aspirated, replaced with fresh Corneal Epithelial Cell Medium with NGF1 (200ng/ml) and incubated for 24h. The control group was performed in the same manner, without NGF's treatment. An inverted microscope was used to observe the migratory response of cells to NGF. The images were taken at time point 0 and 24h. The quantification of scratch closure was evaluated by residual open area using the MRI-Wound Healing Measurement, tool of ImageJ. The experiment, consisting of two plates, was performed in 3 replicates.

4.8. Scratch analysis statistics

Statistical analysis was carried out by *t-test* to compare the two different group by using GraphPad Prism software. Statistical significance was set at $p < 0.05$.

RESULTS

5.1. MicroRNA Expression in HCEC in response to NGF bioformulations

5.1.1. NGF 1

Expression levels of approximately 700 human miRNAs were evaluated in HCECs after NGF1 incubation for 30 minutes, 12 hours and 48 hours. Dysregulated miRNAs, detected by comparing samples from different NGF1 time points and unstimulated control cells, are represented by volcano plots in Figure 8 (A-B). Among them, a total of significant 21 microRNAs were differentially expressed and reported above the represented $P < 0.05$ threshold (horizontal blue line) in at least 1 of the comparisons. As shown, the most of microRNAs were down-regulated after 12 and 48 hours compared with unstimulated cells, whereas up-regulation was observed for several miRNAs in 48 hrs-treated cells compared with 12 hrs. Global dynamic expression levels of the above-mentioned miRNAs are reported in Table 1. By comparing each NGF-treated sample with untreated cells, no relevant expression level's dysregulation was observed after 30 min; miR-362-5p was significantly hypo-expressed after 12 hours; miR-26a-1-3p and miR-146a-5p after 12 and 48 hours; whereas 8 miRNAs (miR-30d-3p, miR-27b-5p, miR-550a-5p, miR-34a-3p, miR-1227-3p, miR-27a-5p, miR-222-5p, miR-151a-5p) were significantly hypo-expressed after 48 hours (Table 1). On the other hand, by considering the sequential miRNAs' expression, based on the temporal progression of treatments, miR-146a-5p, miR-449a, let7c-5p, miR-337-5p, miR-29b-3p, miR-200b-3p, miR-141-3p were significantly hypo-expressed after 12 hours with respect to 30 minutes, whereas 6 miRNAs showed significant differences after 48 with respect to 12 hours (miR-222-5p, miR-411-3p, miR-425-3p, hypo-expressed; miR200b-3p, miR-671-3p, miR-324-5p, hyper-expressed) (Table 1).

A
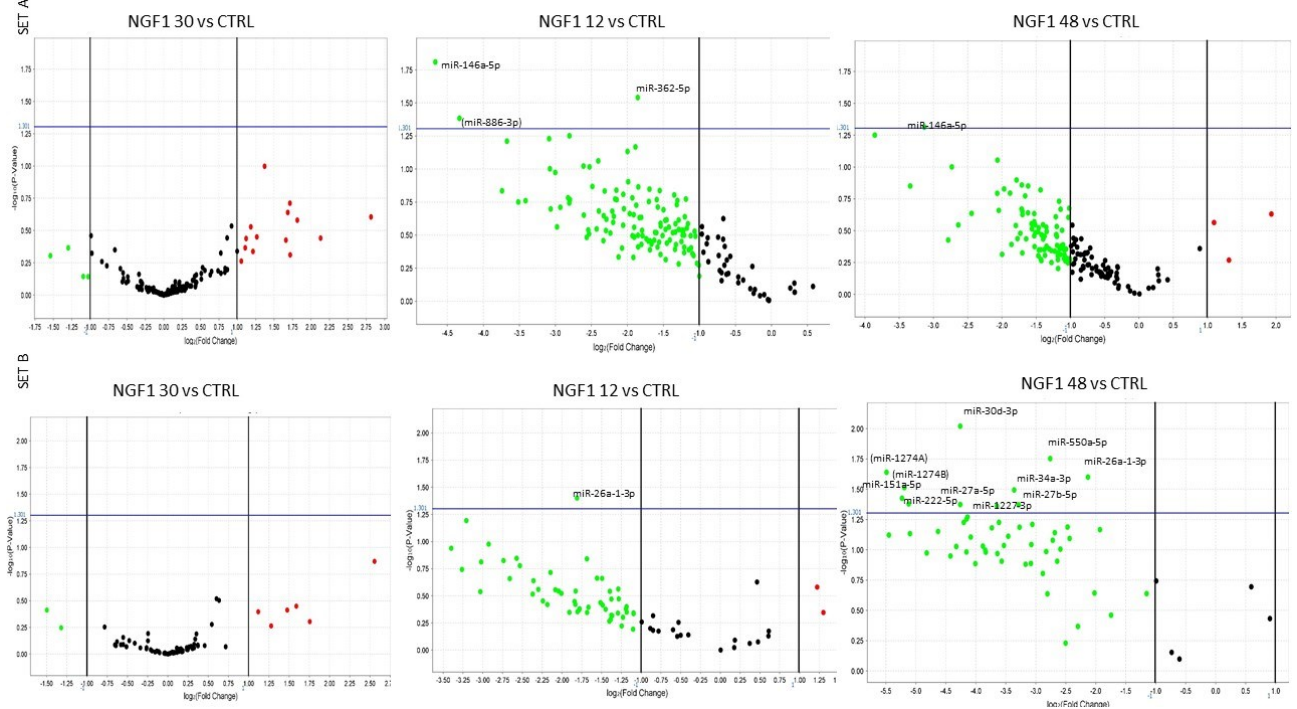
B
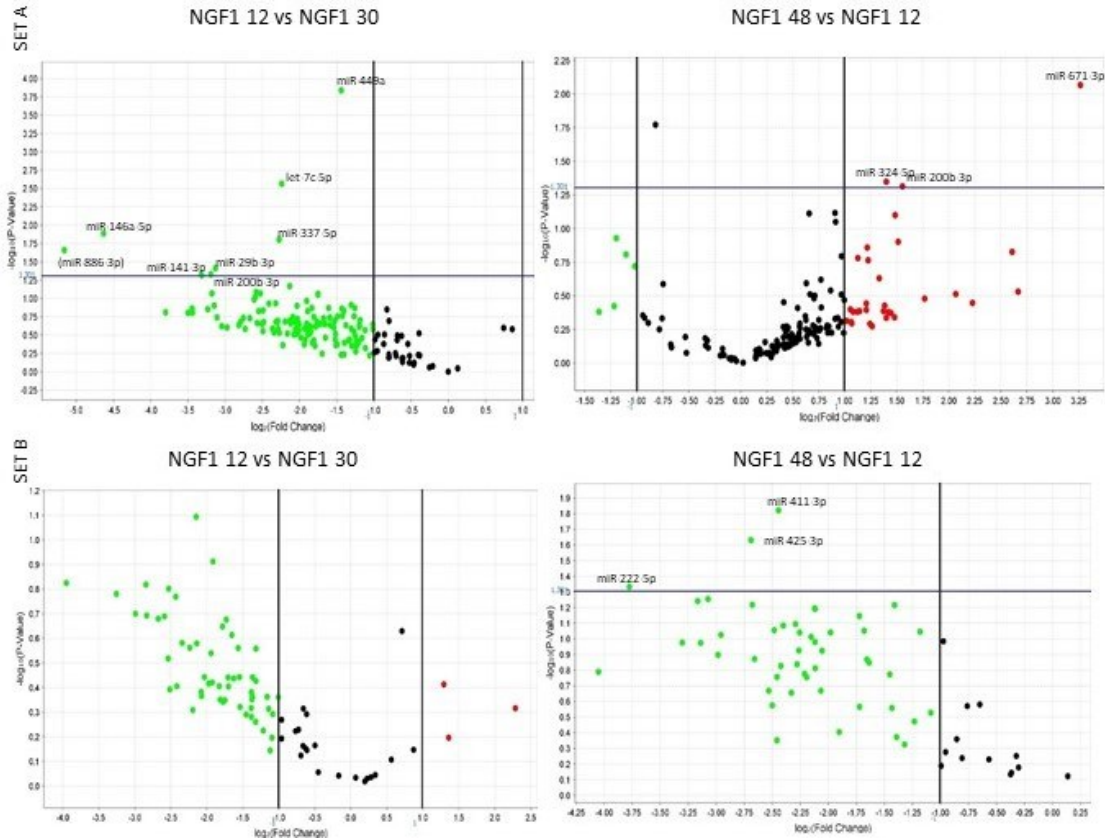
Figure 8 (A-B)-**NGF1 volcano plots.** NGF1 volcano plots from human microRNA array cards Set A (top) and Set B (bottom) analysis, representing miRNAs' levels compared to unstimulated cells (CTRL) (A) and, dynamically, through experimental time points (B). Significant miRNAs IDs are reported close to the corresponding plot. X axis: fold change (RQ, relative quantification, log scale); Y axis: P value (log scale). Horizontal blue line: P=0.05 threshold.

miRNA miRbase ID	NGF30	p-value	NGF12	p-value	NGF48	p-value	NGF12vs30	p-value	NGF48vs12	p-value
hsa-miR-26a-1-3p	1.264	n.s.	0.285	0.04	0.228	0.025	0.226	n.s.	0.799	n.s.
hsa-miR-30d-3p	0.682	n.s.	0.194	n.s.	0.052	0.01	0.285	n.s.	0.268	n.s.
hsa-miR-27b-5p	1.175	n.s.	0.34	n.s.	0.102	0.043	0.291	n.s.	0.303	n.s.
hsa-miR-146a-5p	0.973	n.s.	0.039	0.015	0.114	0.049	0.04	0.013	2.854	n.s.
hsa-miR-362-5p	0.504	n.s.	0.276	0.029	0.271	n.s.	0.548	n.s.	0.939	n.s.
hsa-mir-550a-5p	1.038	n.s.	0.311	n.s.	0.147	0.018	0.301	n.s.	0.471	n.s.
hsa-mir-34a-3p	0.974	n.s.	0.168	n.s.	0.097	0.032	0.173	n.s.	0.572	n.s.
hsa-mir-1227-3p	1.292	n.s.	0.44	n.s.	0.08	0.044	0.343	n.s.	0.179	n.s.
hsa-mir-27a-5p	0.863	n.s.	0.226	n.s.	0.052	0.042	0.261	n.s.	0.23	n.s.
hsa-mir-222-5p	1.013	n.s.	0,388	n.s.	0.029	0.042	0.384	n.s.	0.073	0.046
hsa-mir-151a-5p	0.968	n.s.	0.236	n.s.	0.027	0.038	0.244	n.s.	0.111	n.s.
hsa-miR-449a	3.279	n.s.	1.199	n.s.	1.85	n.s.	0.368	0.000	1.548	n.s.
hsa-let7c-5p	7.035	n.s.	1.491	n.s.	2.485	n.s.	0.212	0.003	1.629	n.s.
hsa-miR-337-5p	3.215	n.s.	0.661	n.s.	2.105	n.s.	0.207	0.016	3.414	n.s.
hsa-mir-29b-3p	4.379	n.s.	0.5	n.s.	0.955	n.s.	0.114	0.038	1.917	n.s.
hsa-miR-200b-3p	1.252	n.s.	0.125	n.s.	0.373	n.s.	0.109	0.047	2.936	0.049
hsa-miR-141-3p	1.18	n.s.	0.118	n.s.(0.059)	0.514	n.s.	0.101	0.048	4.192	n.s.
hsa-miR-671-3p	1.819	n.s.	0.399	n.s.	3.819	n.s.	0.219	n.s.	9.616	0.009
hsa-miR-324-5p	0,712	n.s.	0.173	n.s.	0.446	n.s.	0.245	n.s.	2.639	0.045
hsa-mir-411-3p	0.725	n.s.	1.391	n.s.	0.203	n.s.	1.927	n.s.	0.184	0.015
hsa-mir-425-3p	1.043	n.s.	0.661	n.s.	0.104	n.s.	0.631	n.s.	0.155	0.023

Table 1- **Dynamic expression of miRNAs significantly dysregulated (n=21) at least in 1 comparison after NGF1 treatment.** Relative quantification (RQ) data obtained by comparing 30 min, 12 and 48 hours NGF-treated vs untreated cells (NGF30, NGF12, NGF48), NGF 12 hours vs 30 min (NGF12vs30) and NGF 48 vs 12 hours (NGF 48vs12). Green: RQ values expressing significant down-regulation, red: RQ values expressing significant up-regulation. n.s.: not significant.

5.1.2. NGF 2

Dysregulated miRNAs, detected by comparing samples from different time points and unstimulated control cells, are represented by volcano plots in Figure 9 (A-B). As shown, the most of microRNAs were down-regulated compared with the unstimulated cells. In this case, as many microRNAs were down-regulated after 30 minutes, the cell response seems to be earlier than that observed after treatment with NGF1. Among the dysregulated miRNAs, a total number of 52, more than two-fold compared to NGF1, were differentially expressed and reported above the represented P<0.05 significant threshold in at least one of the comparisons. Global dynamic expression levels of the above-mentioned significant miRNAs are reported in Table 2. By comparing each NGF2-treated samples with untreated cells, significant hypo-expression of 6, 20 and 42 miRs was observed after 30 min, 12 and 48 hrs, respectively. Among them, 4 miRs (miR-146a-5p, miR-200c-3p, miR-126-3p, miR-197-3p), showed significant down-regulation in all the time points; 8 miRNAs (miR-26a-1-3p, miR-224-5p, miR-422a, miR-370-3p, miR-328-3p, miR-28-3p, let-7e-5p, miR-95-3p) in 2 out of 3; 40 in 1 out 3 time points (1 miR after 30 min, 9 miRs after 12 hsr, 30 miRs after 48 hrs). By considering the sequential miRNAs' expression, based on temporal progression of treatments, just miR-212-3p showed significant hypo-expression in the comparison 12 vs 48 hrs.

A

B

Figure 9 (A-B)- **NGF2 volcano plots.** NGF2 volcano plots from human microRNA array cards Set A (top) and Set B (bottom) analysis, representing miRNAs' levels with respect to unstimulated cells (CTRL) (A) and, dynamically, through experimental time points (B). Significant miRNAs IDs are reported close to the corresponding plot. X axis: fold change (RQ, relative quantification, log scale); Y axis: P value (log scale). Horizontal blue line: P=0.05 threshold.

miRNA miRbase ID	NGF30	p-value	NGF12	p-value	NGF48	p-value	NGF12vs30	p-value	NGF48vs12	p-value
miR-146a-5p	0,037	0,024	0,016	0,008	0,032	0,016	0,426	n.s.	1,982	n.s.
hsa-miR-98-5p	0,115	0,024	0,279	n.s.	0,06	n.s.	2,86	n.s.	0,211	n.s.
hsa-miR-200c-3p	0,128	0,033	0,143	0,033	0,146	0,044	1,102	n.s.	1,014	n.s.
hsa-miR-126-3p	0,149	0,039	0,099	0,016	0,147	0,033	0,67	n.s.	1,48	n.s.
hsa-miR-197-3p	0,136	0,042	0,094	0,006	0,158	0,005	0,693	n.s.	1,681	n.s.
hsa-miR-26a-1-3p	0,063	0,015	0,109	n.s.	0,157	0,031	1,891	n.s.	1,355	n.s.
hsa-miR-224-5p	0,52	n.s.	0,056	0,021	0,045	0,007	0,108	n.s.	0,799	n.s.
hsa-miR-422a	0,202	n.s	0,097	0,027	0,126	0,039	0,48	n.s.	1,309	n.s.
hsa-miR-370-3p	0,154	n.s	0,121	0,028	0,158	0,02	0,788	n.s.	1,311	n.s.
hsa-miR-15b-5p	0,153	n.s	0,038	0,034	0,117	n.s (0,056)	0,249	n.s.	3,086	n.s.
hsa-miR-182-5p	0,294	n.s	0,151	0,038	0,184	n.s	0,515	n.s.	1,222	n.s.
hsa-miR-328-3p	0,123	n.s	0,04	0,042	0,056	0,051	0,322	n.s.	1,402	n.s.
hsa-miR-99b-5p	0,164	n.s	0,088	0,048	0,097	n.s (0,055)	0,537	n.s.	1,107	n.s.
hsa-miR-31-5p	0,151	n.s	0,095	0,048	0,135	n.s	0,632	n.s.	1,432	n.s.
hsa-miR-28-3p	0,252	n.s	0,138	0,046	0,118	0,027	0,55	n.s.	0,857	n.s.
hsa-miR-210-3p	0,175	n.s	0,122	0,044	0,202	n.s	0,701	n.s.	1,671	n.s.
hsa-miR-103a-3p	0,348	n.s	0,138	0,046	0,216	n.s	0,391	n.s.	1,654	n.s.
hsa-let-7e-5p	0,156	n.s	0,15	0,046	0,128	0,014	0,963	n.s.	0,853	n.s.
hsa-miR-95-3p	0,27	n.s	0,182	0,046	0,725	n.s	0,686	n.s.	3,917	n.s. (0,053)
hsa-miR-106b-3p	0,058	n.s	0,018	0,034	0,081	n.s	0,339	n.s.	4,167	n.s
hsa-miR-1225-3p	0,049	n.s	0,035	0,036	0,149	n.s	0,759	n.s.	4,851	n.s
hsa-miR-18a-3p	0,182	n.s	0,041	0,011	0,108	n.s	0,242	n.s.	2,499	n.s
hsa-miR-148b-3p	0,599	n.s	n.a.	n.s.	0,026	0,004	n.a.	n.s.	n.a.	n.s.
hsa-miR-362-5p	0,183	n.s	0,105	n.s (0,054)	0,088	0,011	0,586	n.s	0,787	n.s.
hsa-miR-137-3p	0,204	n.s	0,289	n.s	0,045	0,013	1,415	n.s	0,155	n.s.
hsa-miR-324-5p	0,441	n.s	0,033	n.s	0,035	0,016	0,074	n.s	1,074	n.s.
hsa-miR-636	0,28	n.s	0,266	n.s	0,109	0,015	0,914	n.s	0,411	n.s.
hsa-miR-212-3p	0,683	n.s	0,852	n.s	0,382	0,02	1,238	n.s	0,382	0,015
hsa-miR-491-5p	0,306	n.s	0,242	n.s	0,105	0,024	0,809	n.s	0,433	n.s.
hsa-miR-489-3p	0,225	n.s	0,215	n.s	0,044	0,03	1,007	n.s	0,204	n.s.
hsa-miR-758-3p	0,335	n.s	n.a.	n.s.	0,058	0,029	n.a.	n.s	n.a.	n.s.
hsa-miR-539-5p	0,237	n.s	0,221	n.s	0,059	0,027	0,928	n.s	0,268	n.s.
hsa-miR-141-3p	0,134	n.s	0,039	n.s	0,062	0,031	0,291	n.s	1,6	n.s.
hsa-miR-379-5p	0,202	n.s	0,139	n.s	0,076	0,032	0,657	n.s	0,558	n.s.
hsa-miR-339-5p	0,222	p-value	0,257	n.s	0,079	0,031	1,119	n.s	0,311	n.s.
hsa-miR-28-5p	0,363	n.s	0,154	n.s	0,079	0,028	0,55	n.s	0,514	n.s.
hsa-miR-301b-3p	0,271	n.s	n.a.	n.s	0,082	0,031	n.a.	n.s	n.a.	n.s.
hsa-let-7d-5p	0,184	n.s	0,185	n.s	0,11	0,029	1,007	n.s	0,592	n.s.
hsa-miR-708-5p	0,114	n.s	0,036	n.s	0,031	0,045	0,314	n.s	0,87	n.s.
hsa-miR-185-5p	0,27	n.s	0,213	n.s	0,063	0,042	0,768	n.s	0,298	n.s.
hsa-miR-9-5p	0,163	n.s	0,094	n.s (0,054)	0,076	0,04	0,572	n.s	0,813	n.s.
hsa-miR-192-5p	0,086	n.s	0,09	n.s	0,084	0,041	1,046	n.s	0,936	n.s.
hsa-miR-139-5p	0,159	n.s	0,15	n.s	0,101	0,041	0,945	n.s	0,659	n.s.
hsa-miR-218-5p	0,247	n.s	0,084	n.s	0,109	0,036	0,341	n.s	1,304	n.s.
hsa-let-7f-5p	0,274	n.s	0,491	n.s	0,15	0,044	1,765	n.s	0,318	n.s.
hsa-miR-335-5p	0,111	n.s	0,322	n.s	0,101	0,048	2,918	n.s	0,309	n.s.
hsa-miR-92a-3p	0,157	n.s	0,107	n.s	0,078	0,051	0,685	n.s	0,729	n.s.
hsa-miR-204-5p	0,208	n.s	0,258	n.s	0,119	0,05	1,255	n.s	0,453	n.s.
hsa-miR-125a-3p	0,766	n.s	n.a.	n.s	0,124	0,052	n.a.	n.s	n.a.	n.s.
hsa-miR-493-3p	0,172	n.s	0,3	n.s	0,143	0,051	1,729	n.s	0,475	n.s.
hsa-miR-382-5p	n.a.	n.s	n.a.	n.s	0,125	0,042	n.a.	n.s	n.a.	n.s.
hsa-miR-378a-5p	0,103	n.s	n.a.	n.s	0,029	0,016	n.a.	n.s	n.a.	n.s.

Table 2- **Dynamic expression of miRNAs significantly dysregulated (n=52) at least in 1 comparison after NGF2 treatment.** Relative quantification (RQ) data obtained by comparing 30 min, 12 and 48 hours NGF-treated vs untreated cells (NGF30, NGF12, NGF48), NGF 12 hours vs 30 min (NGF12vs30) and NGF 48 vs 12 hours (NGF 48vs12). Green: RQ values expressing significant down-regulation, red: RQ values expressing significant up-regulation. n.s.: not significant, n.a.: not available.

5.1.3. NGF 3

Dysregulated miRNAs, detected by comparing samples from different time points and unstimulated control cells, are represented by volcano plots in Figure 10 (A-B). As shown, after 12 and 48 hrs, the most of microRNAs were down-regulated with respect to unstimulated cells with slight difference of significant miRNAs (above the blue threshold) with respect to that observed after NGF2 stimulus. Furthermore, overexpression of several miRs was identifiable after 48 hrs. Overall, 58 microRNAs were differentially expressed and reported above the represented $P<0.05$ significant threshold in at least one of the comparisons. Global dynamic expression levels of the above-mentioned significant miRNAs are reported in Table 3. By comparing each NGF3-treated sample with untreated cells, significant deregulation of 35 (hypo-expressed), 37 (hypo-expressed) and 2 (hyper-expressed) miRs was observed after 30 min, 12 and 48 hrs, respectively. Among them, 22 miRNAs showed significant deregulation in 2 out of 3 and 30 in 1 out 3 time points (13 miR after 30 min, 16 miRs after 12 hsr, 1 miRs after 48 hrs). By taking into consideration dynamic expression, miR-487b-3p and miR-486-5p were significantly down-regulated and up-regulated, respectively, in the 30min vs 12hrs comparison, whereas 7 miRNAs (miR-485-3p, miR-495-3p, miR-139-5p, miR-452-5p, miR-138-5p, miR-125a-3p, miR-449a) showed significant hyper-expression in the 12 vs 48 hrs comparison.

A

B
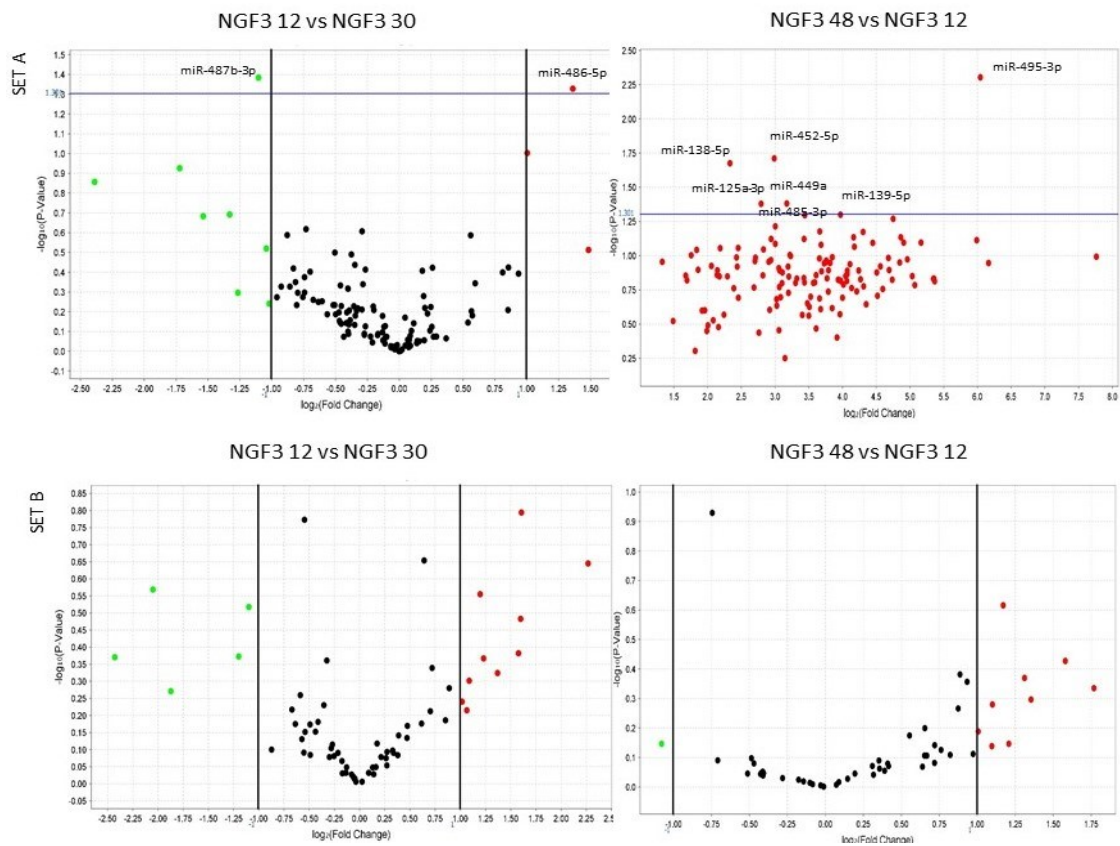
Figure 10 (A-B)- NGF3 volcano plots. NGF3 volcano plots from human microRNA array cards Set A (top) and Set B (bottom) analysis, representing miRNAs' levels with respect to unstimulated cells (CTRL) (A) and, dynamically, through experimental time points (B). Significant miRNAs IDs are reported close to the corresponding plot. X axis: fold change (RQ, relative quantification, log scale); Y axis: P value (log scale). Horizontal blue line: P=0.05 threshold
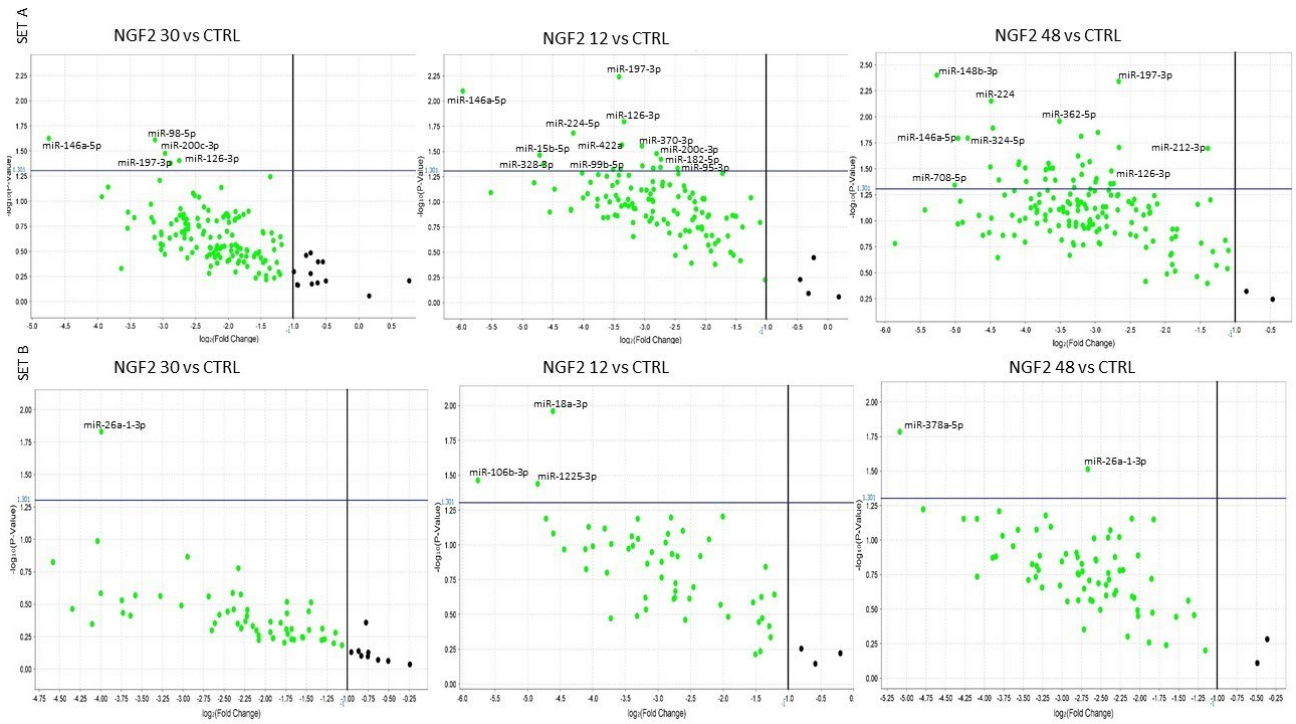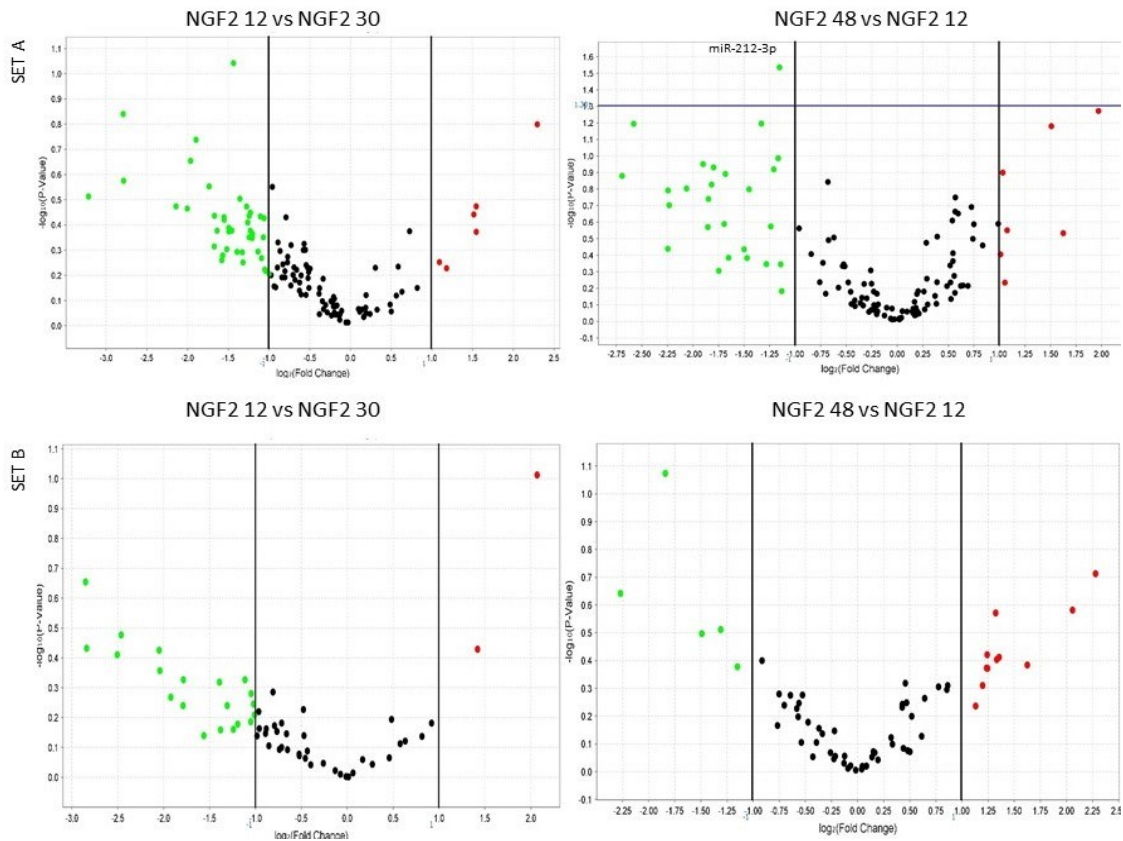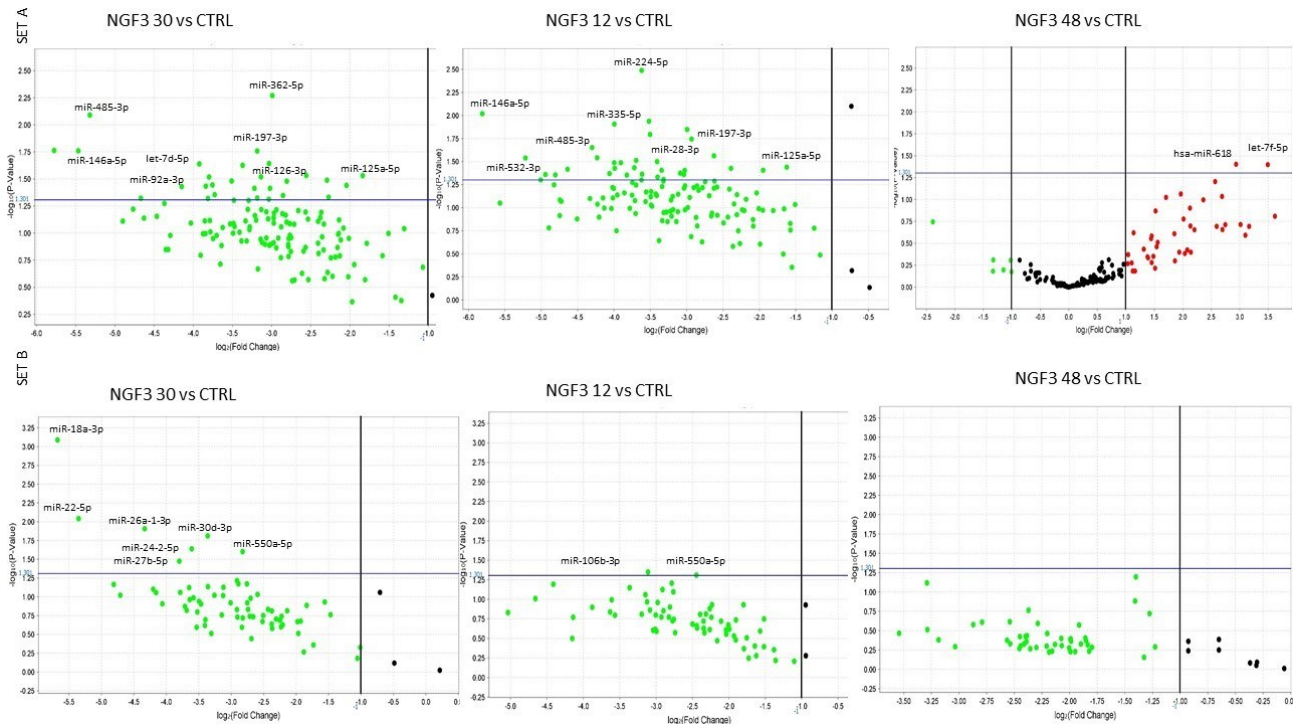
miRNA miRbase ID	NGF30	p-value	NGF12	p-value	NGF48	p-value	NGF12vs30	p-value	NGF48vs12	p-value
hsa-miR-362-5p	0,126	0,005	0,123	n.s.(0,058)	0,995	n.s.	0,96	n.s.	8,125	n.s.
hsa-miR-485-3p	0,025	0,008	0,051	0,022	0,55	n.s.	2,005	n.s.	10,866	0,051
hsa-miR-146a-5p	0,023	0,017	0,018	0,01	0,191	n.s.	0,781	n.s.	10,781	n.s.
hsa-miR-197-3p	0,11	0,017	0,131	0,018	0,493	n.s.	1,182	n.s.	3,781	n.s.
hsa-let-7e-5p	0,122	0,023	0,126	0,014	1,234	n.s.	1,014	n.s	9,87	n.s
hsa-let-7d-5p	0,066	0,023	0,076	0,037	1,097	n.s.	1,145	n.s	14,391	n.s
hsa-miR-28-3p	0,097	0,024	0,094	0,032	0,664	n.s.	0,955	n.s	14,391	n.s
hsa-miR-379-5p	0,072	0,03	0,063	0,033	0,826	n.s.	0,855	n.s	13,234	n.s
hsa-miR-182-5p	0,088	0,033	n.a.	n.s.	0,629	n.s.	n.a.	n.s.	n.s	n.s
hsa-miR-126-3p	0,114	0,03	0,087	0,012	0,697	n.s.	0,757	n.s.	8,023	n.s.
hsa-miR-194-5p	0,143	0,033	0,091	n.s.	2,872	n.s.	0,64	n.s.	25,568	n.s.
hsa-miR-370-3p	0,17	0,029	0,162	0,027	0,63	n.s.	0,913	n.s.	3,891	n.s.
hsa-miR-335-5p	0,204	0,032	0,063	0,012	1,365	n.s.	0,303	n.s.	21,844	n.s.
hsa-miR-320a-3p	0,242	0,036	0,259	0,039	0,824	n.s.	1,056	n.s.	3,195	n.s.
hsa-miR-125a-5p	0,28	0,029	0,325	0,036	1,173	n.s	1,142	n.s.	3,629	n.s.
hsa-miR-92a-3p	0,056	0,037	0,085	n.s.	1,018	n.s.	1,488	n.s.	12,03	n.s.
hsa-miR-99b-5p	0,07	0,037	0,074	n.s (0,053)	1,289	n.s.	1,053	n.s.	17,273	n.s.
hsa-miR-491-5p	0,074	0,036	0,138	n.s	1,122	n.s	1,806	n.s.	8,149	n.s.
hsa-miR-200c-3p	0,107	0,039	0,088	0,016	0,671	n.s.	0,816	n.s.	7,673	n.s.
hsa-miR-422a	0,123	0,039	0,149	n.s. (0,052)	1,357	n.s	1,194	n.s.	9,151	n.s.
hsa-let-7f-5p	0,138	0,045	0,194	n.s	11,26	0,04	1,361	n.s.	58,164	n.s
hsa-miR-374b-5p	0,207	0,047	0,191	0,037	1,357	n.s	0,913	n.s	7,1	n.s
hsa-miR-193a-5p	0,039	0,048	0,04	0,038	1,265	n.s.	1,007	n.s	35,865	n.s.
hsa-miR-15b-5p	0,09	0,05	0,067	0,032	1,467	n.s.	0,725	n.s	22,73	n.s.
hsa-miR-218-5p	0,102	0,05	0,095	0,047	0,399	n.s	0,915	n.s	4,242	n.s.
hsa-miR-28-5p	0,11	0,048	0,098	0,039	1,06	n.s	0,891	n.s	10,822	n.s
hsa-miR-210-3p	0,122	0,049	0,122	0,044	0,972	n.s.	0,98	n.s	8,018	n.s
hsa-miR-9-5p	0,076	0,044	0,082	0,043	1,059	n.s.	1,062	n.s	13,65	n.s
hsa-miR-22-5p	0,024	0,009	0,012	n.s	0,137	n.s	0,328	n.s	11,451	n.s
hsa-miR-18a-3p	0,02	0,001	0,115	n.s	0,144	n.s	4,816	n.s	1,277	n.s
hsa-miR-26a-1-3p	0,05	0,012	0,109	n.s	0,183	n.s	1,807	n.s	1,696	n.s
hsa-miR-27b-5p	0,072	0,033	0,133	n.s	0,193	n.s	1,56	n.s	1,469	n.s
hsa-miR-30d-3p	0,097	0,015	0,097	n.s	0,655	n.s	0,783	n.s	7,139	n.s
hsa-miR-24-2-5p	0,082	0,023	0,056	n.s	0,538	n.s	0,546	n.s	10,099	n.s
hsa-miR-550a-5p	0,141	0,025	0,183	0,049	0,413	n.s	1,066	n.s	2,253	n.s
hsa-miR-224	0,045	n.s	0,081	0,003	0,904	n.s	1,754	n.s	11,319	n.s
hsa-miR-495-3p	0,077	n.s	0,031	0,05	2,047	n.s	0,397	n.s	65,929	0,005
hsa-miR-532-3p	0,169	n.s	0,033	0,044	0,973	n.s	0,191	n.s	30,022	n.s
hsa-miR-25-3p	0,048	n.s. (0,053)	0,036	0,044	1,456	p-value	0,729	n.s	40,918	n.s
hsa-let-7g-5p	0,101	n.s	0,081	0,05	1,355	n.s	0,785	n.s	16,756	n.s
hsa-miR-31-5p	0,103	n.s	0,1	0,049	0,838	n.s	0,957	n.s	8,393	n.s
hsa-miR-192-5p	0,114	n.s	0,071	0,044	0,952	n.s	0,602	n.s	13,552	n.s
hsa-miR-135b-5p	0,108	n.s	0,06	0,043	0,86	n.s	0,551	n.s	14,417	n.s
hsa-miR-134-5p	0,158	n.s	0,118	0,042	0,763	n.s	0,73	n.s	6,509	n.s
hsa-miR-539-5p	0,153	n.s	0,053	0,029	0,669	n.s	0,344	n.s	12,605	n.s
hsa-miR-139-5p	0,127	n.s	0,077	0,031	1,208	n.s	0,597	n.s	15,67	0,05
hsa-miR-30b-5p	0,127	n.s	0,063	0,037	1,114	n.s	0.485	n.s	18,083	n.s
hsa-miR-339-5p	0,119	n.s	0,1	0,052	1,946	n.s	0,817	n.s	19,749	n.s
hsa-miR-95-3p	0,226	n.s	0,163	0,051	4,392	n.s	0,704	n.s	26.936	n.s
hsa-miR-618	n.a.	n.s	0,295	n.s	7,654	0,04	n.a.	n.s	25,992	n.s
hsa-miR-103a-3p	0,189	n.s	0,123	0,039	2,149	n.s	0,616	n.s	17,94	n.s
hsa-miR-106b-3p	0,038	n.s	0,116	0,045	0,676	n.s	3,045	n.s	5,954	n.s
hsa-miR-487b-3p	0,19	n.s	0,089	n.s	0,75	n.s	0,465	0,041	8,465	n.s
hsa-miR-486-5p	n.a.	n.s	n.a.	n.s	n.a.	n.s	2,569	0,047	0,292	n.s
hsa-miR-452-5p	0,374	n.s	0,715	n.s	6,706	n.s	1,913	n.s	7,938	0,019
hsa-miR-138-5p	0,199	n.s	0,188	n.s.	0,944	n.s.	0,933	n.s	5,039	0,021
hsa-miR-125a-3p	0,42	n.s	0,317	n.s.	2,198	n.s	0,729	n.s	6,93	0,042
hsa-miR-449a	0,611	n.s	0,446	n.s	4,038	n.s	0,722	n.s	9,029	0,042

Table 3- **Dynamic expression of miRNAs significantly dysregulated (n=58) at least in 1 comparison after NGF3 treatment.** Relative quantification (RQ) data obtained by comparing 30 min, 12 and 48 hours NGF-treated vs untreated cells (NGF30, NGF12, NGF48), NGF 12 hours vs 30 min (NGF12vs30) and NGF 48 vs 12 hours (NGF 48vs12). Green: RQ values expressing significant down-regulation, red: RQ values expressing significant up-regulation. n.s.: not significant, n.a.: not available.

5.1.4. Dysregulated miRNAs: overall expression levels' comparison among treatments

A total number of 88 unique dysregulated miRNAs in response to all the different bioformulations was detected. Distributions of significant miRNAs is represented by the Venn Diagram shown in Figure 11. In Table 4 significant miRNAs are filtered and listed on the basis of the following criteria: shared by all 3 bioformulations (n=3), by 2 out of 3 (n=37), only by NGF1 (n=12), NGF2 (n=16) and NGF3 (n=20). Overall, data show global miRNAs' down-regulation after NGFs' treatment compared to unstimulated cells, with lower number of significant dysregulated miRNAs detected after NGF1 with respect to NGF2 and NGF3 treatment. Of note, the latter two bioformulations show just slight differences in the amount of differentially expressed miRNAs. Furthermore, NGF2 and, more, NGF3 induce earlier miRNAs' down-regulation than NGF1. After 48 hrs, several NGF3- and, less pronounced, NGF1-induced miRNAs, mainly among the not significant, seem to move towards different levels of hyper-expression, whereas NGF2-induced miRNAs' hypo-expression is fully maintained (Fig. 8A-10A, Table 1-3). These results globally indicate different bioformulations' kinetics.

By taking into consideration the temporal progression of treatments (30 min vs ctrl; 12 hrs vs 30 min, 48 hrs vs 12 hrs), all bioformulations seem to induce first global miRNAs' down-regulation which, later, changes to different levels of over-expression, leaving to hypothesize a sort of compensatory mechanism to repristinate normal physiological conditions (Fig. 8B-10B, Table 1-3).
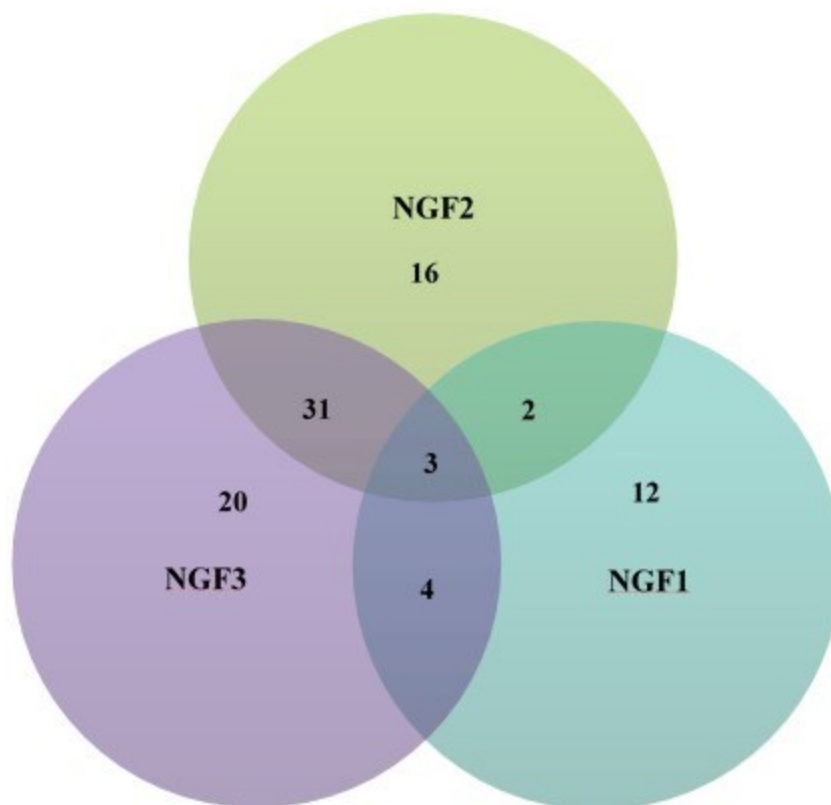
*Figure 11-**Venn diagram overall miRNAs.** Venn diagram of distribution of miRNAs (unique n=88) overall regulated by NGF bioformulations.

MiRNAs shared by all three bioformulations (n. 3)	MiRNAs shared by 2 out of 3 bioformulations (n. 37)	MiRNAs induced by NGF1 (n. 12)	MiRNAs induced by NGF2 (n.16)	MiRNAs induced by NGF3 (n.20)
hsa-miR-146a-5p	hsa-let-7d-5p	hsa-mir-151a-5p	hsa-miR-1225-3p	hsa-let-7g-5p
hsa-miR-362-5p	hsa-let-7e-5p	hsa-mir-425-3p	hsa-miR-137-3p	hsa-miR-125a-5p
hsa-miR-26a-1-3p	hsa-let-7f-5p	hsa-mir-1227-3p	hsa-miR-148b-3p	hsa-miR-134-5p
	hsa-miR-103a-3p	hsa-miR-200b-3p	hsa-miR-185-5p	hsa-miR-135b-5p
	hsa-miR-106b-3p	hsa-mir-222-5p	hsa-miR-204-5p	hsa-miR-138-5p
	hsa-miR-125a-3p	hsa-mir-27a-5p	hsa-miR-212-3p	hsa-miR-193a-5p
	hsa-miR-126-3p	hsa-mir-29b-3p	hsa-miR-301b-3p	hsa-miR-194-5p
	hsa-miR-139-5p	hsa-miR-337-5p	hsa-miR-328-3p	hsa-miR-22-5p
	hsa-miR-141-3p	hsa-mir-34a-3p	hsa-miR-378a-5p	hsa-miR-24-2-5p
	hsa-miR-15b-5p	hsa-mir-411-3p	hsa-miR-382-5p	hsa-miR-25-3p
	hsa-miR-182-5p	hsa-miR-671-3p	hsa-miR-489-3p	hsa-miR-30b-5p
	hsa-miR-18a-3p	hsa-let-7c-5p	hsa-miR-493-3p	hsa-miR-320a-3p
	hsa-miR-192-5p		hsa-miR-636	hsa-miR-374b-5p
	hsa-miR-197-3p		hsa-miR-708-5p	hsa-miR-452-5p
	hsa-miR-200c-3p		hsa-miR-758-3p	hsa-miR-485-3p
	hsa-miR-210-3p		hsa-miR-98-5p	hsa-miR-486-5p
	hsa-miR-218-5p			hsa-miR-487b-3p
	hsa-miR-224-5p			hsa-miR-495-3p
	hsa-miR-27b-5p			hsa-miR-532-3p
	hsa-miR-28-3p			hsa-miR-618
	hsa-miR-28-5p			
	hsa-miR-30d-3p			
	hsa-miR-31-5p			
	hsa-miR-324-5p			
	hsa-miR-335-5p			
	hsa-miR-339-5p			
	hsa-miR-370-3p			
	hsa-miR-379-5p			
	hsa-miR-422a			
	hsa-miR-491-5p			
	hsa-miR-539-5p			
	hsa-mir-550a-5p			
	hsa-miR-92a-3p			
	hsa-miR-95-3p			
	hsa-miR-9-5p			
	hsa-miR-99b-5p			
	hsa-miR-449a			

*Table 4-**Dysregulated miRs' list** Filtering and distributions of significantly dysregulated miRNAs (unique miRNAs total n. 88) with respect to NGF bioformulations. Colors as follows: pink: NGF2+NGF3; violet: NGF1+NGF2; blue: NGF1+NGF3

5.2. Induced KEGG pathways

5.2.1. Overall analysis: significant dysregulated miRNAs, target genes and pathways

A total number of 59, 75 and 77 significant pathways (P<0.05) were identified by DIANA Tarbase analysis (experimentally supported target genes' database) of significant 21 NGF1, 52 NGF2 and 58 NGF3 dysregulated miRNAs, whereas 49, 74 and 82 significant pathways were obtained by DIANA Micro-T analysis (predicted target genes' database), respectively. Interestingly, neurotrophin signalling pathway was included in every list. NGF-modulated neutrophin signalling pathway, as detected by Tarbase analysis, showed P values of 2.11e-05, 1.11e-05 and 8.65e-06, respectively associated to NGF1, NGF2, NGF3 (summarized in Table 8, Table S1a, S2a, S3a in Annex), whereas P values of 0.005864, 3.13e-05 and 2.34e-05 emerged by DIANA Micro-T analysis (summarized in Table 8, Table S1b, S2b, S3b in Annex). Total unique 91 and 96 pathways were identified by Tarbase and microT analysis, respectively. As expected, by linking the pathways identified with Tarbase for all 3 bioformulations (Table 5), most of the pathways identified (n=46) were shared by all three bioformulations, indicating comparable effects in terms of miRNAs/target gene induction. A relevant group of pathways (n=28) was shared by 2 out of 3 bioformulations (mainly NGF2 and NGF3), while nine, two and six were associated only with NGF1, NGF2 and NGF3 respectively. Among those more specifically related to each specific bioformulation, some can be interesting (e.g. ECM-receptor interaction, PI3K-Akt, axon guidance, Notch signalling pathway) and could be subjected to deeper analysis in the future. Regarding pathways identified with microT, 39 pathways were detected shared among all bioformulations, 31 shared by 2 of 3 (most between NGF2 and NGF3) while six, six and fourteen were associated only with NGF1, NGF2, NGF3, respectively (Table 6). Additional data about comparisons of pathways' lists identified by Tarbase and microT analyses (pathways' filtering and distributions, highlighting those shared by both Tarbase and microT analysis or not) are reported in Annex Tables S1c, S2c, S3c as well for each bioformulation.

Afterward, we mainly focused the analysis on target genes identified by DIANA Tarbase, as experimentally supported. As expected, and proportionally based on the number of dysregulated miRNAs, 1009 genes were induced by NGF1 (targeted 21 miRNAS), 2259 by NGF2 (targeted by 52 miRNAs) and 2337 by NGF3 (targeted by 58 miRNAs). After filtering, genes were distributed and represented in Table 7 (Annex) and Figure 12. A list of 2590 unique and experimentally supported genes was in addition filled out: 858 genes were shared by all the bioformulations, 1299 by 2 out of them (mainly NGF2 and NGF3, as expected), 76 were related to NGF1, 141 to NGF2, 216 to NGF3.

Pathways shared by all 3 bioformulations (n=46)	Pathways shared by 2 out of 3 bioformulations (n=28: n=24 NGF2 + NGF3; n=3 NGF1 + NGF2; n=1 NGF1 + NGF3)	Pathways NGF1 treatment-related (n=9)	Pathways NGF2 treatment-related (n.2)	Pathways NGF3 treatment-related (n.6)
Acute myeloid leukemia	2-Oxocarboxylic acid metabolism	Amoebiasis	Axon guidance	Base excision repair
Adherens junction	AMPK signaling pathway	Arrhythmogenic right ventricular cardiomyopathy (ARVC)	Carbon metabolism	Long-term potentiation
Bacterial invasion of epithelial cells	B cell receptor signaling pathway	Dorso-ventral axis formation		Notch signaling pathway
Bladder cancer	Basal cell carcinoma	ECM-receptor interaction		Phosphatidylinositol signaling system
Cell cycle	Circadian rhythm	Hepatitis C		RNA degradation
Central carbon metabolism in cancer	Citrate cycle (TCA cycle)	mRNA surveillance pathway		Terpenoid backbone biosynthesis
Chronic myeloid leukemia	Epithelial cell signaling in Helicobacter pylori infection	Pathogenic Escherichia coli infection		
Colorectal cancer	ErbB signaling pathway	PI3K-Akt signaling pathway		
Endocytosis	Estrogen signaling pathway	Sulfur metabolism		
Endometrial cancer	Fatty acid elongation			
Epstein-Barr virus infection	Fatty acid metabolism			
Fatty acid biosynthesis	Fc gamma R-mediated phagocytosis			
Focal adhesion	Glycosaminoglycan biosynthesis - chondroitin sulfate / dermatan sulfate			
FoxO signaling pathway	Glycosaminoglycan biosynthesis - heparan sulfate / heparin			
Glioma	HTLV-I infection			
Hepatitis B	Lysosome			
HIF-1 signaling pathway	MAPK signaling pathway			
Hippo signaling pathway	mTOR signaling pathway			
Insulin signaling pathway	N-Glycan biosynthesis			
Lysine degradation	One carbon pool by folate			
Melanoma	Other types of O-glycan biosynthesis			
Neurotrophin signaling pathway	Progesterone-mediated oocyte maturation			
NF-kappa B signaling pathway	Signaling pathways regulating pluripotency of stem cells			
Non-small cell lung cancer	Steroid biosynthesis			
Oocyte meiosis	TNF signaling pathway			
p53 signaling pathway	Vibrio cholerae infection			
Pancreatic cancer	Vitamin B6 metabolism			
Pathways in cancer	Wnt signaling pathway			
Prion diseases				
Prolactin signaling pathway				
Prostate cancer				
Protein processing in endoplasmic reticulum				
Proteoglycans in cancer				
Regulation of actin cytoskeleton				
Renal cell carcinoma				
RNA transport				
Shigellosis				
Small cell lung cancer				
Sphingolipid signaling pathway				
Spliceosome				
TGF-beta signaling pathway				
Thyroid cancer				
Thyroid hormone signaling pathway				
Transcriptional misregulation in cancer				
Ubiquitin mediated proteolysis				
Viral carcinogenesis				

*Table 5- **Pathways identified by Tarbase**. Relations and distributions of Tarbase (experimentally supported)-identified-pathways (unique total n=91) and bioformulations. Colors as follows: pink, NGF2+NGF3; violet, NGF1+NGF2; blue, NGF1+NGF3.

Pathways shared by all 3 bioformulations (n=39)	Pathways shared by 2 out of 3 bioformulations (n=31: n=27 NGF2+NGF3, n=2 NGF1+NGF3, n=2 NGF1+NGF2)	Pathways NGF1 treatment-related (n=6)	Pathways NGF2 treatment-related (n=6)	Pathways NGF3 treatment-related (n=14)
Adherens junction	Acute myeloid leukemia	Adipocytokine signaling pathway	Amphetamine addiction	Central carbon metabolism in cancer
Adrenergic signaling in cardiomyocytes	AMPK signaling pathway	Amoebiasis	Dorso-ventral axis formation	Endometrial cancer
Axon guidance	Basal cell carcinoma	Chagas disease (American trypanosomiasis)	Gastric acid secretion	Glutamatergic synapse
Bacterial invasion of epithelial cells	cAMP signaling pathway	Circadian rhythm	Glutamatergic synapse	Hepatitis B
Biotin metabolism	Cholinergic synapse	Glycosaminoglycan biosynthesis - chondroitin sulfate / dermatan sulfate	Hypertrophic cardiomyopathy (HCM)	Inositol phosphate metabolism
cGMP-PKG signaling pathway	Chronic myeloid leukemia	Glycosphingolipid biosynthesis - lacto and neolacto series	Thyroid hormone synthesis	Insulin signaling pathway
Choline metabolism in cancer	Circadian entrainment			mRNA surveillance pathway
ErbB signaling pathway	Cocaine addiction			N-Glycan biosynthesis
Estrogen signaling pathway	Colorectal cancer			Progesterone-mediated oocyte maturation
Focal adhesion	Dilated cardiomyopathy			Protein processing in endoplasmic reticulum
FoxO signaling pathway	Dopaminergic synapse			T cell receptor signaling pathway
Glioma	ECM-receptor interaction			Type II diabetes mellitus
Glycosaminoglycan biosynthesis - heparan sulfate / heparin	Endocytosis			Vascular smooth muscle contraction
Glycosaminoglycan biosynthesis - keratan sulfate	Fatty acid biosynthesis			Viral carcinogenesis
Hippo signaling pathway	GABAergic synapse			
Long-term depression	Gap junction			
Lysine degradation	GnRH signaling pathway			
MAPK signaling pathway	Hedgehog signaling pathway			
Melanoma	HIF-1 signaling pathway			
mTOR signaling pathway	Insulin secretion			
Neurotrophin signaling pathway	Melanogenesis			
Non-small cell lung cancer	Morphine addiction			
p53 signaling pathway	Mucin type O-Glycan biosynthesis			
Pancreatic cancer	Notch signaling pathway			
Pathways in cancer	Oxytocin signaling pathway			
Phosphatidylinositol signaling system	Platelet activation			
PI3K-Akt signaling pathway	Retrograde endocannabinoid signaling			
Prion diseases	Signaling pathways regulating pluripotency of stem cells			
Prolactin signaling pathway	Small cell lung cancer			
Prostate cancer	Ubiquitin mediated proteolysis			
Proteoglycans in cancer	Vasopressin-regulated water reabsorption			
Rap1 signaling pathway				
Ras signaling pathway				
Regulation of actin cytoskeleton				
Renal cell carcinoma				
Sphingolipid signaling pathway				
TGF-beta signaling pathway				
Thyroid hormone signaling pathway				
Wnt signaling pathway				

*Table 6- **Pathways identified by microT-CDS.** Relations and distribution of microT-CDS (predicted)-identified-pathways (unique total n=96) and bioformulations. Colors as follows: pink, NGF2+NGF3; violet, NGF1+NGF2; blue, NGF1+NGF3.
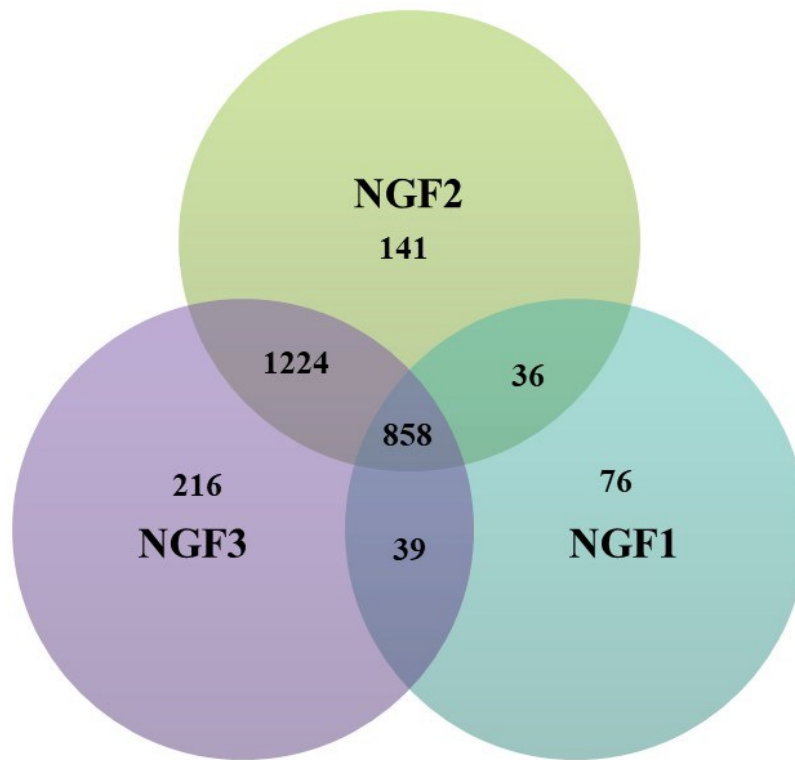
Figure 12- **Venn diagram target genes.** Venn diagram of distribution of experimentally supported (Tarbase) target genes (unique n=2590) overall induced by NGF bioformulations.

5.2.2. *Restricted pathways analysis: miRNAs' sub-groups more directly connected to NGF1, NGF2 and NGF3 treatments*

As shown in Table 4, 12, 16 and 20 dysregulated miRNAs have been identified directly related to treatments with NGF1, NGF2 and NGF3 respectively. Therefore, we performed an analysis both by Tarbase and by microT, limited to these 3 subgroups of miRNAs to identify the induced pathways. The results of the comparison and individual analyses can be found in the appendix section (Table S4a-b, S5a-b, S6a-b in Annex). Also, in this case, neurotrophin signalling pathway has emerged in every list with P value of 0.000656, 0.002553 and 0.01126206 associated to NGF1, NGF2, NGF3 respectively, by DIANA Tarbase analysis, whereas P value of 0.011516, 0.009063 and 0.011262 emerged by DIANA Micro-T analysis.

In conclusion, neurotrophin signalling was included within all the pathways' lists, irrespective of bioformulation (NGF1, NGF2, NGF3), database (Tarbase, microT) and significant dysregulated miRNAs (complete list or filtered specific sub-groups) used for data analysis.

5.3. Focus on neurotrophin signalling pathway: miRNAs' and target genes' analysis

5.3.1. Overall analysis of significant miRNAs and target genes involved in neurotrophin signalling pathway

As above-mentioned, a total number of 21, 52 and 58 miRNAs were significantly dysregulated after NGF1, NGF2 and NGF3, respectively. Among them, 18/21 (86%), 41/52 (79%) and 50/58 (86%) were directly associated to neurotrophin signalling pathway by targeting 60, 99 and 101 genes, as summarized in Table 8 (original data from Tables S1, S2, S3 in Annex). With this regard, by reporting Tarbase analysis results in percentage terms (to be referred to 100 putative target genes), less NGF1-regulated miRNAs (n=30) would be hypothetically involved in significantly modulating neurotrophin signalling pathway genes in comparison to NGF2 miRNAs (n=41) and NGF3 miRNAs (n=50). Similar results were obtained by micro-T analysis: percentage of miRNAs associated to neurotrophin signalling pathway: NGF1 16/21 (76%), NGF2 46/52 (88%), NGF3 52/58 (90%). In terms of percentage, miRNAs involved in hypothetically regulating 100 neurotrophin pathway genes are as follows: NGF1 n=32, NGF2 n=55, NGF3 n=58. With reference to neurotrophin pathway, here induced by all the bioformulations, our results might suggest a possible more specific effect of NGF1.

Bioformulation	TARBASE			microT-CDS		
	#genes	#miRNAs	p-value	#genes	#miRNAs	p-value
NGF1	60	18	2.11e-05	50	16	0.005864
NGF2	99	41	1.11e-05	84	46	3.13e-05
NGF3	101	50	8.65e-06	90	52	2.34e-05

Table 8 - **Neurotrophin signalling pathway**: numbers of miRNAs/target genes involved in and related P-values.

In Tables 9-11 are listed NGF1-, NGF2- and NGF3-induced microRNAs in neurotrophin pathway as well as related target genes, obtained from Tarbase (A) and microT (B) analysis, respectively. Often, a given gene was targeted by multiple miRNAs. Overall, 73 (Table 12A) and 77 (Table 12B) unique miRNAs were identified in Neurotrophin signalling pathway by Tarbase and microT analysis, respectively. The complete list of unique experimentally supported (Tarbase) target genes (n=102) in Neurotrophin pathway is shown in Table 13. As expected, most of genes were shared by all the bioformulations (n=59) and a relevant part (n=40) by two of them, mainly NGF2 and NGF3. As globally shown in the representations (Figures 13, 14 and 15), all the bioformulations do not seem to display relevant differences in terms of miRNAs' target genes involved in neurotrophin signalling. Of note, the genes here highlighted play a role in relevant signal transduction pathways (e.g. MAPK, PI3K, p53, NFkB) able to regulate fundamental cross-talks and cell processes, such as survival, apoptosis, differentiation, actin cytoskeleton regulation. However, by considering the ratio between

NGF1-regulated miRNAs and target genes compared to NGF2 and NGF3, as previously discussed (ref. Table 8), NGF1 might be considered more effective in inducing this pathway.

In conclusion, it might be hypothesized that, based on ratios and number of miRNAs and related target genes, NGF1 would be more effective and specific in inducing neurotrophin signalling pathway.

9A

miR-34a-3p	miR-222-5p	miR-151a-5p	miR-29b-3p	miR-26a-1-3p	miR-30d-3p	miR-449a	miR-550a-5p	miR-141-3p	miR-27a-5p	miR-200b-3p	miR-146a-5p	miR-324-5p	miR-425-3p	miR-362-5p	miR-411-3p	miR-27b-5p	miR-671-3p
YWHAE	CALM3	ARHGDIA	ABL1	PTPN11	GRB2	MAPKAPK2	MAPKAPK2	ABL1	ABL1	BCL2	ABL1	AKT1	NGFRAP1	GSK3B	GSK3B	JUN	GRB2
CALM1	CRKL	GRB2	AKT1		MAPKAPK2	NFKB1	PLCG1	BAX	AKT1	CRK	AKT2	ARHGDIA	PLCG2	RAP1B	RAC1	NRAS	
BCL2	KIDINS220	MAPK1	BAX		PTPN11	PIK3CA	RAF1	BCL2	CALM2	CRKL	GSK3B	MAP3K1	RAP1A	TP53			
RELA	MAPK1	RAPGEF1	BCL2		YWHAE	PTPN11	RPS6KA3	CALM2	CALM3	FRS2	IRAK1	NTRK3					
	SORT1	RIPK2	CALM3			RPS6KA3		CDC42	GRB2	JUN	IRAK2	SOS1					
	SOS2		CDC42					CRK	MAPK3	JUN	JUN						
	YWHAE		FOXO3					CRKL	PLCG1	KIDINS220	MAP3K5						
			FRS2					FOXO3	RHOA	KRAS	TRAF6						
			GSK3B					GRB2	SH2B3	PLCG1							
			JUN					IRS1	SHC1	RAP1B							
			KIDINS220					MAP3K1		RHOA							
			MAPK8					MAPK14		RPS6KA3							
			NRAS					NFKBIA		RPS6KA5							
			PIK3R1					PIK3R1		SHC1							
			PIK3R3					PSEN1									
			RELA					RAC1									
			SOS1					SHC1									
			TP53														
			YWHAE														

9B

miR-200b-3p	miR-27b-5p	miR-30d-3p	miR-29b-3p	miR-141-3p	miR-146a-5p	let-7c-5p	miR-449a	miR-27a-5p	miR-34a-3p	miR-411-3p	miR-26a-1-3p	miR-362-5p	miR-151a-5p	miR-222-5p	miR-550a-5p
NTF3	FASLG	SOS1	CAMK4	MAP3K3	CAMK2D	NRAS	CAMK4	CALM2	CAMK2D	CAMK4	PTPN11	AKT3	NTRK2	MAP3K5	MAPK10
RIPK2	RPS6KA3	AKT3	CALM3	FRS2	BRAF	NTRK3	IRAK3		MAPK8			CAMK2B			
CAMK4		MAP3K5	AKT2	KIDINS220	NRAS	MAP3K1	PIK3CB		PIK3CG						
CRKL			KIDINS220	IRS1	SORT1	MAPK8	BCL2								
SORT1			PIK3R1	CDC42	TRAF6	NGF	ARHGDIB								
FRS2			FOXO3	GAB1	IRAK1		PLCG1								
MAP2K5			PIK3R2				IRS1								
MAP3K1							MAP2K1								
BDNF															
IKBKB															
PLCG1															
JUN															
TP73															
SOS1															
PTPN11															
RPS6KA3															
GAB1															
SHC4															
AKT3															
PIK3CA															
RAP1B															

*Table 9 A-B- **Neurotrophin signalling pathway and NGF1 treatment**. Significantly dysregulated miRNAs (green: down-regulated, red: up-regulated) and related target genes, from Diana **TarBase (A)** and predicted genes from **microT-CDS (B).**

10A

miR-197-3p	miR-125a-3p	miR-126-3p	miR-422a	let-7e-5p		miR-212-3p	miR-28-5p	let-7d-5p	miR-9-5p	let-7f-5p		miR-200c-3p	miR-15b-5p		miR-103a-3p	
CALM1	PRKCD	CRK	CRKL	CAMK2D	RPS6KA5	GSK3B	CAMK2G	BRAF	NFKB1	CAMK2D	KRAS	NTRK2	RAPGEF1	MAPK9	BRAF	TP53
PRKCD	RHOA	PIK3R2	BCL2	NRAS	RIPK2	SOS2	CRKL	SH2B3	CALML5	BRAF	RPS6KA5	CRK	CRKL	MAPK8	GSK3B	AKT2
IRAK1	MAPK3	PIK3CD	MAPK1	CRKL	PLCG1	CRKL	YWHAE	NRAS	CALM3	RIPK2	TP53	SHC1	YWHAE	ARHGDIA	NFKB1	MAPK9
MAPK1	PIK3CA	AKT1		YWHAE	MAPK8	MAP3K3	CALM3	YWHAE	CALM1	NRAS	PLCG1	FRS2	CALM1	RAC1	RAPGEF1	JUN
ATF4	MAPK1	IRS1		CALM1	ARHGDIA	CRK	SORT1	MAP2K7	SHC1	CRKL	MAPK8	BCL2	CDC42	SH2B3	NRAS	ARHGDIA
		PIK3CA		CRK	RAC1	FRS2	FRS2	MAP3K1	MAP3K3	CALM1	RPS6KA3	KRAS	RHOA	NRAS	MAP3K3	PIK3CG
		MAPK1		MAP2K7	RPS6KA3	KIDINS220	MAPK1	PLCG1	MAP3K1	MAP3K1	CALM1	RPS6KA5	MAP2K1	MAP3K3	IRS1	IRS1
				FRS2	PRDM4	MAPK1		MAPK8	TP53	CRK	SH2B1	PLCG1	RPS6KA5	PIK3CB	CDC42	CDC42
				MAP3K1	MAPK1	MAPK1		RAC1	IRS1	FRS2	PRDM4	JUN	PRDM4	PIK3R2	RPS6KA3	RPS6KA3
								MAPK1	PSEN1	MAPK1	MAPK1	KIDINS220	GRB2	PIK3R5	PRDM4	PRDM4
									MAPK1		ATF4	RPS6KA3		MAPK14	IRAK1	IRAK1
									RAP1B			GAB1		MAGED1	ABL1	ABL1
									MAPKAPK2			RAP1B		RPS6KA5		

miR-18a-3p	miR-148b-3p	miR-141-3p	miR-708-5p	miR-218-5p	miR-92a-3p	miR-335-5p		miR-182-5p		miR-192-5p	miR-204-5p	miR-139-5p	miR-106b-3p	miR-31-5p
CRKL	NFKB1	CRKL	CRKL	SH2B3	BRAF	NTRK2	CALML6	GSK3B	AKT1	SH2B3	GSK3B	CAMK2D	KIDINS220	NFKB1
CALM1	ZNF274	CRK	YWHAE	NRAS	GSK3B	NTF3	IKBKB	NFKB1	ARHGDIA	CAMK4	NTRK2	NFKB1	RELA	YWHAE
RHOA	CRKL	SHC1	CALM3	CRKL	NRAS	SOS2	NFKBIA	NRAS	PIK3R1	CRK	PIK3CB	YWHAE		CALM1
FOXO3	CALM1	MAPK14	SORT1	MAP2K7	CRKL	RPS6KA6	MATK	YWHAE	SOS1	BCL2	BCL2	RAF1		NGFRAP1
	BAX	FRS2	FRS2	SORT1	CRK	CALML5	SHC4	CALM1	IRS1	MAPK9	RPS6KA5	RPS6KA5		CALM2
FRS2	BAX	BAX		BAX	PIK3CB	PLCG2	PIK3CA	NFKBIB	RAC1	SH2B1	PLCG1	PLCG1		RPS6KA5
KRAS	MAP3K1	TP53		RHOA	KRAS	SHC1	RPS6KA2	SHC1	CDC42	PRDM4	IRAK1	JUN		MAPK9
PLCG1	CALM2	PIK3R1		MAPK9	MAP2K5	MAPK14		PIK3CB	AKT3	IRAK1	MAP3K5	TRAF6		MAPK8
PIK3R3	NFKBIA	RPS6KA3		MAPK8	RPS6KA1	IRAK2		MAPK7	FOXO3	IRAK4		HRAS		RAC1
SOS1	PIK3R1	AKT3		SHC3	NGFR			BAX	PDPK1	ATF4		RPS6KA3		PRDM4
PIK3CG	IRS1	FOXO3		CALM2	RPS6KA2			FRS2	PRDM4			AKT3		MAPKAPK2
PSEN1	RAC1	ABL1						BCL2	RELA			PIK3CA		
RPS6KA3	CDC42	MAP3K5						MAP3K1	MAPKAPK2			ATF4		
GAB1	PSEN1							TP53	ATF4					
FOXO3	FOXO3							MAPK8						
MAPKAPK2	GRB2													
	ABL1													

miR-224-5p	miR-185-5p	miR-324-5p	miR-339-5p	miR-99b-5p	miR-28-3p	miR-146a-5p	miR-362-5p	miR-382-5p	miR-26a-1-3p	miR-137	miR-491-5p	miR-539-5p	miR-493-3p	miR-378a-5p
GSK3B	CAMK2D	NTRK3	GSK3B	RHOA	SOS2	GSK3B	GSK3B	BDNF	PTPN11	BRAF	GSK3B	MAPK14	JUN	CAMK2G
NRAS	GSK3B	MAP3K1	NTRK3	CALM2	FRS2	AKT2	TP53	AKT1		YWHAE	AKT2		ATF4	CALM1
CALM3	YWHAE	AKT1	BDNF	RAC1	RAC1	JUN	RAP1B			CALM3				KIDINS220
CALM1	SORT1	ARHGDIA	SOS1			TRAF6				AKT2				
SORT1	MAPK14	SOS1	SH2B1			IRAK2				CDC42				
PIK3R3	NTRK3		PRDM4			IRAK1				IRAK1				
MAPK8	RHOA		IRAK1			ABL1								
MAPK12	PTPN11					MAP3K5								
	CDC42													

10B

miR-212-3p	miR-758-3p	miR-339-5p	miR-9-5p	miR-204-5p	miR-103a-3p	miR-200c-3p	miR-200c-3p	miR-182-5p	miR-328-3p	miR-98-5p	let7e-5p	let7d-5p	let-7f-5p	miR-18a-3p	miR-148b-3p
RIPK2	CAMK4	NTRK2	NFKB1	CAMK2D	BRAF	NTF3	JUN	BRAF	RIPK2	NRAS	NRAS	NRAS	NRAS	SOS1	ZNF274
MAP3K3	PIK3R1	SHC1	SH2B3	RIPK2	MAP3K3	RIPK2	TP73	RIPK2	PIK3R2	NTRK3	NTRK3	CALM1	NTRK3		SOS2
CRK	RPS6KA3	PIK3CB	MAP3K3	SHC1	PIK3CB	CAMK4	SOS1	YWHAE	RPS6KA1	MAP3K1	MAP3K1	MAP3K1	MAP3K1		NRAS
FRS2	PIK3CA	SORT1	SHC1	SORT1	SORT1	CRKL	PTPN11	SORT1		MAPK8	FASLG	MAPK8	MAPK8		PIK3R3
KRAS	MAP2K1	SOS1	PIK3CB	SOS1	RAF1	SORT1	FRS2	FRS2		NGF	TP53	NGF	NGF		SOS1
SOS1	MAPK1		SORT1		BDNF	FRS2	RPS6KA3	BCL2		RPS6KA3					
AKT3	RAP1B		RAF1		NTRK1	MAP2K5	GAB1	PLCG1							
PIK3CA			SHC2		PIK3R1	SHC4	MAP3K1	ARHGDIA							
FOXO3			MAP3K1		RPS6KA3	BDNF	AKT3	IRS1							
MAPK1			PIK3R3		AKT3	IKBKB	PIK3CA	RAC1							
			KIDINS220		PRDM4	PLCG1	RAP1B	SHC4							
			SOS1			PRDM4		PIK3CA							
			RAP1B					FOXO3							
			MAPKAPK2					PRDM4							
								GRB2							

miR-539-5p	miR-15b-5p	miR-301b-3p	miR-192-5p	miR-185-5p	miR-370-3p	miR-493-3p	miR-224-5p	miR-137	miR-92a-3p	miR-1225-3p	miR-141-3p	miR-106b-3p	miR-489-3p	miR-28-5p
BRAF	BRAF	SOS2	CRK	CAMK2D	RAPGEF1	RAF1	GSK3B	BRAF	BRAF	MAP3K3	MAP3K3	IRAK2	NFKBIA	NTRK2
CAMK4	SOS2	CALM2	KIDINS220	MAPK14	RAF1	KRAS	IRAK3	GSK3B	GSK3B	MAP3K1	FRS2		MAP2K1	RPS6KA1
CALM1	CRK	MAP3K5		CDC42	PIK3CA	AKT2	PIK3CB	CRKL	PIK3CB	KIDINS220	KIDINS220			RAP1B
RAP1A	FRS2			RELA		RAC1	MAPK14	CALM3	RAP1A	SH2B1	IRS1			
MAPK14	RAF1						MAPK8	FRS2	FRS2		CDC42			
FRS2	BCL2						PIK3CG	MAP3K1	FASLG		GAB1			
PLCG2	IKBKB							BDNF	CAMK2A					
PSEN1	MAPK8							CAMK2A	PIK3R3					
AKT3	PIK3R1							AKT2	CDC42					
PIK3CA	RPS6KA3													
	AKT3													
	MAP2K1													
	IRAK2													
	PRDM4													

miR-708-5p	miR-146a-5p	miR-31-5p	miR-379-5p	miR-125a-3p	miR-382-5p	miR-362-5p	miR-636	miR-139-5p	miR-28-3p	miR-422a	miR-335-5p	miR-378a-5p	miR-26a-1-3p	miR-197-3p	miR-126-3p
NTRK2	CAMK2D	YWHAE	MAP3K1	RHOA	SHC4	AKT3	AKT3	AKT3	MAPK8	IRAK3	IRAK3	NFKBIB	PTPN11	MAPK7	IRS1
RPS6KA1	BRAF	MAP3K1				CAMK2B			FOXO3		CALM1				
RAP1B	NRAS	SHC4									RAP1A				
	SORT1														
	TRAF6														
	IRAK1														

Table 10 A-B- **Neurotrophin signalling pathway and NGF2 treatment**. Significantly dysregulated miRNAs (green: down-regulated, red: up-regulated) and related target genes, from Diana **TarBase (A)** and predicted genes from **microT-CDS (B).**

11A

miR-182-5p	miR-182-5p	miR-320a	miR-15b-5p	miR-218-5p	miR-24-2-5p	miR-139-5p	let-7e-5p	miR-200c-3p	let-7f-5p	let-7g-5p	miR-31-5p	miR-103a-3p	miR-103a-3p	miR-22-5p	let-7d-5p	miR-92a-3p
GSK3B	AKT1	NRAS	RAPGEF1	SH2B3	SH2B3	CAMK2D	CAMK2D	NTRK2	CAMK2D	CAMK2D	NFKB1	BRAF	RPS6KA5	NRAS	BRAF	BRAF
NFKB1	ARHGDIA	CRKL	CRKL	NRAS	MAP2K2	NFKB1	RIPK2	CRKL	BRAF	BRAF	YWHAE	GSK3B	TP53	MAP3K3	SH2B3	GSK3B
NRAS	PIK3R1	CALM3	YWHAE	CRKL	CALM1	YWHAE	NRAS	SHC1	RIPK2	RIPK2	CALM1	NFKB1	AKT2	CRK	NRAS	NRAS
YWHAE	SOS1	CALM1	CALM1	MAP2K7	PIK3CD	RAF1	CRKL	FRS2	NRAS	NRAS	NGFRAP1	RAPGEF1	MAPK9	MAPK14	YWHAE	CRKL
CALM1	IRS1	RAP1A	CRK	SORT1	AKT3	RPS6KA5	CALM1	BCL2	CRKL	CRKL	CALM2	SH2B3	JUN	NTRK3	MAP2K7	CRK
NFKBIB	RAC1	JUN	FRS2	BAX		PLCG1	BCL2	RHOA	YWHAE	YWHAE	RPS6KA5	NRAS	MAPK8	BDNF	MAP3K1	PIK3CB
SHC1	CDC42	PIK3R3	BCL2	RHOA		JUN	CRK	KRAS	CALM3	CALM3	MAPK8	MAPK8	PIK3CG	JUN	PLCG1	KRAS
PIK3CB	AKT3	KIDINS220	MAGED1	TP53		TRAF6	MAP2K7	RPS6KA5	CALM1	CALM1	RAC1	MAP3K3	IRS1	MAPK8	JUN	MAPK9
MAPK7	FOXO3	RAC1	RPS6KA5	PIK3R1		HRAS	FRS2	PLCG1	CRK	CRK	PRDM4	PIK3CB	CDC42	PIK3R1	MAPK8	JUN
BAX	PDPK1	AKT3	IKBKB	RPS6KA3		RPS6KA3	MAP3K1	JUN	FRS2	FRS2	MAPKAPK2	PIK3R2	RPS6KA3	CDC42	RAC1	MAPK8
FRS2	PRDM4	MAPK1	MAPK9	AKT3		AKT3	TP53	KIDINS220	MAP3K1	MAP3K1		PIK3R5		PRDM4	MAPK1	
BCL2	RELA	MAPK8	FOXO3			PIK3CA	PLCG1	RPS6KA3	KRAS	RPS6KA5				IRAK1		
MAP3K1	IRAK1	ARHGDIA	ABL1			ATF4	RAC1	GAB1	RPS6KA5	TP53				MAPK1		
TP53	MAPKAPK2	RAC1	MAP3K5				PSEN1	RAP1B	TP53	PLCG1				GRB2		
MAPK8	ATF4	CDC42					RPS6KA3		PLCG1	MAPK8				RPS6KA2		
		RPS6KA3					PRDM4		MAPK8	ARHGDIA						
		AKT3					MAPK1		ARHGDIA	RAC1						
		PIK3CA							RAC1	RPS6KA3						
		MAP2K1							RPS6KA3	SH2B1						
		PRDM4							SH2B1	PRDM4						
		GRB2							PRDM4	MAPK1						
									MAPK1	ATF4						
									ATF4							

miR-224-5p	miR-30b-5p	miR-618	miR-335-5p	miR-335-5p	miR-18a-3p	miR-126-3p	miR-125a-5p	miR-374b-5p	miR-192-5p	miR-452-5p	miR-485-3p	miR-9-5p	miR-138-5p	miR-99b-5p	miR-125a-3p	miR-25-3p	miR-28-3p
GSK3B	CAMK2D	JUN	NTRK2	CALML6	CRKL	CRK	NRAS	MAP3K3	SH2B3	GSK3B	NTRK3	NFKB1	SH2B3	RHOA	PRKCD	BRAF	SOS2
NRAS	SH2B3	MAPK8	NTF3	IKBKB	CALM1	CRK	CRK	CAMK4	CRK	CRK	IRS1	CALML5	MAP2K7	CALM2	RHOA	NRAS	FRS2
CALM3	MAP3K1	TRAF6	SOS2	NFKBIA	RHOA	PIK3CD	CRK	FRS2	CRK		GRB2	CALM3	BCL2	RAC1	MAPK3	NRAS	RAC1
CALM1	JUN		SH2B3	RPS6KA6	FOXO3	AKT1	SORT1	BCL2	BCL2			CALM1	AKT2	PIK3CA	PIK3CA	PIK3CB	
SORT1	MAPK8		CALML5	MATK		IRS1	TP53	MAP3K1	MAPK9			MAP3K3	PLCG1	MAPK1	MAPK1	MAP2K5	
PIK3R3	PIK3R1		CRK	PLCG2		PIK3CA	JUN	KRAS	SH2B1			SHC1	IRS1		MAPKAPK2	KRAS	
MAPK8	RAC1		SHC1	SHC4		MAPK1	KIDINS220	KIDINS220	IRAK1			MAP2K7	NGF			SOS1	
MAPK12	RPS6KA3		MAPK14	PIK3CA			SH2B1	GAB1	IRAK4			MAP3K1				PRDM4	
	PIK3CA		MAP2K5	FOXO3			PRDM4	PDPK1	ATF4			TP53				ATF4	
			RPS6KA1	IRAK2			IRAK1	PRDM4				IRS1					
			SHC3	NGFR			MAPKAPK2	MAPK1				PSEN1					
			CALM2	RPS6KA2								MAPK1					
												RAP1B					
												MAPKAPK2					

miR-194-5p	miR-539-5p	miR-486-5p	miR-422a	miR-28-5p	miR-197-3p	miR-339-5p	miR-30d-3p	miR-146a-5p	miR-491-5p	miR-532-3p	miR-135b-5p	miR-362-5p	miR-449a	miR-550a-5p	miR-27b-5p	miR-106b-3p	miR-26a-1-3p
YWHAE	MAPK14	NRAS	CRKL	CAMK2G	CALM1	GSK3B	YWHAE	GSK3B	GSK3B	GSK3B	CAMK2D	GSK3B	NFKB1	RAF1	NRAS	KIDINS220	PTPN11
JUN		MAPK14	BCL2	CRKL	PRKCD	NTRK3	PTPN11	AKT2	AKT2	SHC1	NFKBIB	TP53	PTPN11	PLCG1	JUN	RELA	
RAC1		BCL2	MAPK1	YWHAE	IRAK1	BDNF	GRB2	JUN		BAX	AKT1	RAP1B	RPS6KA3	RPS6KA3	RELA		
		PLCG1		CALM3	MAPK1	SOS1	MAPKAPK2	TRAF6		NGFRAP1			PIK3CA	MAPKAPK2			
				SORT1	ATF4	SH2B1		IRAK2		AKT2			MAPKAPK2				
				FRS2		PRDM4		IRAK1									
				IKBKB		IRAK1		ABL1									
				MAPK1				MAP3K5									

11B

miR-335-5p	miR-320a	miR-125a-5p	miR-92a-3p	miR-374b-5	miR-22-5p	miR-539-5p	miR-200c-3p		miR-26a-1-3	miR-15b-5p	miR-532-3p	miR-449a	miR-30b-5p	miR-362-5p	miR-495-3p		miR-103a-3p	miR-486-5p
IRAK3	SOS2	PIK3CB	BRAF	BRAF	PIK3CB	BRAF	NTF3	JUN	PTPN11	BRAF	NTRK1	CAMK4	CAMK2D	AKT3	CAMK2D	CALM2	BRAF	IRAK3
CALM1	CRKL	MAP2K7	GSK3B	GSK3B	RAP1A	CAMK4	RIPK2	TP73		SOS2	MAP2K1	IRAK3	SH3B3	CAMK2B	BRAF	CAMK2A	MAP3K3	PIK3R1
RAP1A	YWHAE	RAP1A	PIK3CB	NTF3	RAF1	CALM1	CAMK4	SOS1		CRK		PIK3CB	CAMK4		GSK3B	MAPK9	PIK3CB	MAPK1
	IRAK3	RPS6KA1	RAP1A	CRK	SOS1	RAP1A	CRKL	PTPN11		FRS2		CAMK4	KRAS		CAMK2G	TRAF6	SORT1	
	RPS6KA1	RAP1A	FRS2	SOS1	MAP2K1	MAPK14	SORT1	IRS1		RAF1		BCL2	PIK3CD		CAMK4	PIK3R1	RAF1	
	KRAS	FRS2	RAP1A	FRS2		FRS2	FRS2	RPS6KA3		BCL2		ARHGDIB	MAPK8		NRAS	SOS1	BDNF	
	RAC1	TRAF6	CAMK2A	PTPN11		PLCG2	MAP2K5	GAB1		IKBKB		PLCG1	KIDINS220		CRKL	IRS1	NTRK1	
	RPS6KA3	CAMK2A	PTPN11			MAP3K1	SHC4	AKT3		MAPK8		IRS1	SOS1		IRAK3	RAC1	MAPK8	
	AKT3	PIK3R3	GAB1			AKT3	BDNF	PIK3CA		PIK3R1		KIDINS220			CRK	CDC42	RPS6KA3	
	PIK3CA	MAPK12	PDPK1			PIK3CA	IKBKB	RAP1B		RPS6KA3		SOS1			PIK3CB	RPS6KA3	AKT3	
	MAPK1	IRAK1	RAP1B				PLCG1			AKT3		IRS1			SORT1	PIK3CA	PRDM4	
		CDC42								MAP2K1		FOXO3			BCL2	FOXO3		
		PIK3CA								IRAK2		RAP1B			MAP3K1	MAPK10		
		RAP1B								PRDM4		ABL1			BDNF			
												MAP3K5						
												RPS6KA2						

miR-224-5p	let-7e-5p	let-7d-5p	miR-379-5p	let-7f-5p	miR-9-5p	let-7g-5p	miR-31-5p	miR-618	miR-28-3p	miR-182-5p	miR-134-5p	miR-146a-5p	miR-485-3p	miR-28-5p	miR-25-3p	miR-370-3p
GSK3B	NRAS	NRAS	MAP3K1	NRAS	NFKB1	NRAS	YWHAE	MAP3K1	MAPK8	BRAF	BRAF	CAMK2D	RHOA	NTRK2	BRAF	RAPGEF1
IRAK3	NTRK3	CALM1		NTRK3	SH2B3	NTRK3	MAP3K1		FOXO3	RIPK2	CAMK4	BRAF	RPS6KA5	RPS6KA1	PIK3CB	RAF1
PIK3CB	MAP3K1	MAP3K1		MAP3K1	MAP3K3	MAP3K1	SHC4			YWHAE	KRAS	NRAS	RAC1	RAP1B	FRS2	PIK3CA
MAPK14	FASLG	MAPK8		MAPK8	SHC1	MAPK8				SORT1	BDNF	SORT1	RAP1B		FASLG	
MAPK8	TP53	NGF		NGF	PIK3CB	NGF				FRS2	PIK3CA	TRAF6			CAMK2A	
PIK3CG	MAPK8				SORT1					BCL2		IRAK1			PIK3R3	
	NGF				RAF1					PLCG1					PIK3CA	
	RPS6KA3				SHC2					ARHGDIA					RAP1B	
					MAP3K1					IRS1						
					PIK3R3					RAC1						
					KIDINS220					SHC4						
					SOS1					PIK3CA						
					RAP1B					FOXO3						
					MAPKAPK2					PRDM4						
										GRB2						

miR-192-5p	miR-135b-5p	miR-452-5p	miR-125a-3p	miR-194-5p	miR-24-2-5p	miR-30d-3p	miR-139-5p	miR-138-5p	miR-18a-3p	miR-339-5p	miR-126-3p	miR-197-3p	miR-550a-5p	miR-27b-5p	miR-106b-3p	miR-193a-5p	miR-422a
CRK	GSK3B	CAMK2G	RHOA	CAMK2G	MAPK8	SOS1	AKT3	SH2B3	SOS1	NTRK2	IRS1	MAPK7	MAPK10	FASLG	IRAK2	NTRK2	IRAK3
KIDINS220	CAMK4	YWHAE		AKT2		AKT3		SORT1		SHC1				RPS6KA3		CAMK2G	
	PIK3R2	RPS6KA3		TRAF6		MAP3K5		RELA		PIK3CB							
	PIK3CD			RAC1						SORT1							
	MAPK10									SOS1							
	PIK3R2																

Table 11 A-B- **Neurotrophin signalling pathway and NGF3 treatment**. Significantly dysregulated miRNAs (green: down-regulated, red: up-regulated) and related target genes, from Diana **TarBase (A)** and predicted genes from **microT-CDS (B).**

miRNAs shared by all 3 bioformulation (n=3)	miRNAs shared by 2 out of 3 bioformulation (n=30)	miRNAs induced by NGF1 (n=11)	mirRNAs induced by NGF2 (n=10)	miRNAs induced by NGF3 (n=19)
hsa-miR-146a-5p	hsa-let-7d-5p	hsa-miR-30d-3p	hsa-miR-185-5p	hsa-miR-197-3p
hsa-miR-26a-1-3p	hsa-let-7e-5p	hsa-miR-449a	hsa-miR-137	hsa-let-7g-5p
hsa-miR-362-5p	hsa-let-7f-5p	hsa-miR-151a-5p	hsa-miR-148b-3p	hsa-miR-125a-5p
	hsa-miR-103a-3p	hsa-miR-222-5p	hsa-miR-197-3p	hsa-miR-135b-5p
	hsa-miR-106b-3p	hsa-miR-27a-5p	hsa-miR-204-5p	hsa-miR-138-5p
	hsa-miR-125a-3p	hsa-miR-29b-3p	hsa-miR-212-3p	hsa-miR-194-5p
	hsa-miR-126-3p	hsa-mir-34a-3p	hsa-miR-378a-5p	hsa-miR-22-5p
	hsa-miR-139-5p	hsa-miR-411-3p	hsa-miR-382-5p	hsa-miR-24-2-5p
	hsa-miR-141-3p	hsa-miR-425-3p	hsa-miR-493-3p	hsa-miR-25-3p
	hsa-miR-15b-5p	hsa-miR-671-3p	hsa-miR-708-5p	hsa-miR-30b-5p
	hsa-miR-182-5p	hsa-miR-200b-3p		hsa-miR-30d-3p
	hsa-miR-18a-3p			hsa-miR-320a
	hsa-miR-192-5p			hsa-miR-374b-5p
	hsa-miR-218-5p			hsa-miR-449a
	hsa-miR-224-5p			hsa-miR-452-5p
	hsa-miR-27b-5p			hsa-miR-485-3p
	hsa-miR-28-3p			hsa-miR-486-5p
	hsa-miR-28-5p			hsa-miR-532-3p
	hsa-miR-31-5p			hsa-miR-618
	hsa-miR-324-5p			
	hsa-miR-335-5p			
	hsa-miR-339-5p			
	hsa-miR-422a			
	hsa-miR-491-5p			
	hsa-miR-539-5p			
	hsa-miR-550a-5p			
	hsa-miR-92a-3p			
	hsa-miR-9-5p			
	hsa-miR-99b-5p			
	hsa-miR-200c-3p			

Table 12 A - **Distributions of significantly dysregulated miRNAs** (unique miRNAs total n=73) **in Neurotrophin signalling pathway,** as detected by Tarbase (experimentally supported) analysis (ref Table 9-11A). Colors as follows: pink, NGF2+NGF3; violet, NGF1+NGF2; blue: NGF1+NGF3

miRNAs shared by all 3 bioformulation (n.2)	miRNAs shared by 2 out of 3 bioformulation (n.32)	miRNAs induced by NGF1 (n.8)	mirRNAs induced by NGF2 (n.16)	miRNAs induced by NGF3 (n.19)
hsa-miR-146a-5p	hsa-let-7d-5p	hsa-let-7c-5p	hsa-miR-1225-3p	hsa-let-7g-5p
hsa-miR-362-5p	hsa-let-7e-5p	hsa-miR-151a-5p	hsa-miR-137	hsa-miR-125a-5p
	hsa-let-7f-5p	hsa-miR-200b-3p	hsa-miR-148b-3p	hsa-miR-134-5p
	hsa-miR-103a-3p	hsa-miR-222-5p	hsa-miR-185-5p	hsa-miR-135b-5p
	hsa-miR-106b-3p	hsa-miR-27a-5p	hsa-miR-204-5p	hsa-miR-138-5p
	hsa-miR-125a-3p	hsa-miR-29b-3p	hsa-miR-212-3p	hsa-miR-193a-5p
	hsa-miR-126-3p	hsa-miR-34a-3p	hsa-miR-301b-3p	hsa-miR-194-5p
	hsa-miR-139-5p	hsa-miR-411-3p	hsa-miR-328-3p	hsa-miR-22-5p
	hsa-miR-141-3p		hsa-miR-378a-5p	hsa-miR-24-2-5p
	hsa-miR-15b-5p		hsa-miR-382-5p	hsa-miR-25-3p
	hsa-miR-182-5p		hsa-miR-489-3p	hsa-miR-30b-5p
	hsa-miR-18a-3p		hsa-miR-493-3p	hsa-miR-320a
	hsa-miR-192-5p		hsa-miR-636	hsa-miR-374b-5
	hsa-miR-197-3p		hsa-miR-708-5p	hsa-miR-452-5p
	hsa-miR-200c-3p		hsa-miR-758-3p	hsa-miR-485-3p
	hsa-miR-224-5p		hsa-miR-98-5p	hsa-miR-486-5p
	hsa-miR-26a-1-3p			hsa-miR-495-3p
	hsa-miR-27b-5p			hsa-miR-532-3p
	hsa-miR-28-3p			hsa-miR-618
	hsa-miR-28-5p			
	hsa-miR-30d-3p			
	hsa-miR-31-5p			
	hsa-miR-335-5p			
	hsa-miR-339-5p			
	hsa-miR-370-3p			
	hsa-miR-379-5p			
	hsa-miR-422a			
	hsa-miR-449a			
	hsa-miR-539-5p			
	hsa-miR-550a-5p			
	hsa-miR-92a-3p			
	hsa-miR-9-5p			

Table 12 B - **Distributions of significantly dysregulated miRNAs** (unique miRNAs total n=77) **in Neurotrophin signalling pathway,** as detected by microT (predicted) analysis (ref Table 9-11B). Colors as follows: pink, NGF2+NGF3; violet, NGF1+NGF2; blue: NGF1+NGF3

Shared by all three bioformulations (n=59)		Shared by 2 out of 3 bioformulations (n=40)		only by NGF1 (n=0)	only by NGF2 (n=1)	only by NGF3 (n=2)
AKT1	MAPKAPK2	ATF4	MATK		ZNF274	MAP2K2
ABL1	NFKB1	AKT3	NFKBIB			NGF
AKT2	NFKBIA	BDNF	NGFR			
ARHGDIA	NGFRAP1	BRAF	NTF3			
BAX	NRAS	CALML5	NTRK2			
BCL2	NTRK3	CALML6	PDPK1			
CALM1	PIK3CA	CAMK2D	PIK3CB			
CALM2	PIK3R1	CAMK2G	PIK3CD			
CALM3	PIK3R3	CAMK4	PIK3CG			
CDC42	PLCG1	HRAS	PIK3R2			
CRK	PLCG2	IKBKB	PIK3R5			
CRKL	PSEN1	IRAK4	PRDM4			
FOXO3	PTPN11	MAGED1	PRKCD			
FRS2	RAC1	MAP2K1	RAP1A			
GAB1	RAF1	MAP2K5	RPS6KA1			
GRB2	RAP1B	MAP2K7	RPS6KA2			
GSK3B	RAPGEF1	MAP3K3	RPS6KA6			
IRAK1	RELA	MAPK12	SH2B1			
IRAK2	RHOA	MAPK7	SHC3			
IRS1	RIPK2	MAPK9	SHC4			
JUN	RPS6KA3					
KIDINS220	RPS6KA5					
KRAS	SH2B3					
MAP3K1	SHC1					
MAP3K5	SORT1					
MAPK1	SOS1					
MAPK14	SOS2					
MAPK3	TP53					
MAPK8	TRAF6					
	YWHAE					

Table 13 - **Distributions of genes, belonging to Neurotrophin Signalling Pathway targeted by dysregulated miRNAs.** List of genes (unique total n=102) belonging to Neurotrophin Signalling Pathway and targeted by dysregulated miRNAs (n=21 NGF1, n=52 NGF2, n=58 NGF)3 (ref Table 9A, 10A,11A), as detected by Tarbase (experimentally supported) analysis. Colors as follows: pink, NGF2+NGF3; blue: NGF1+NGF3
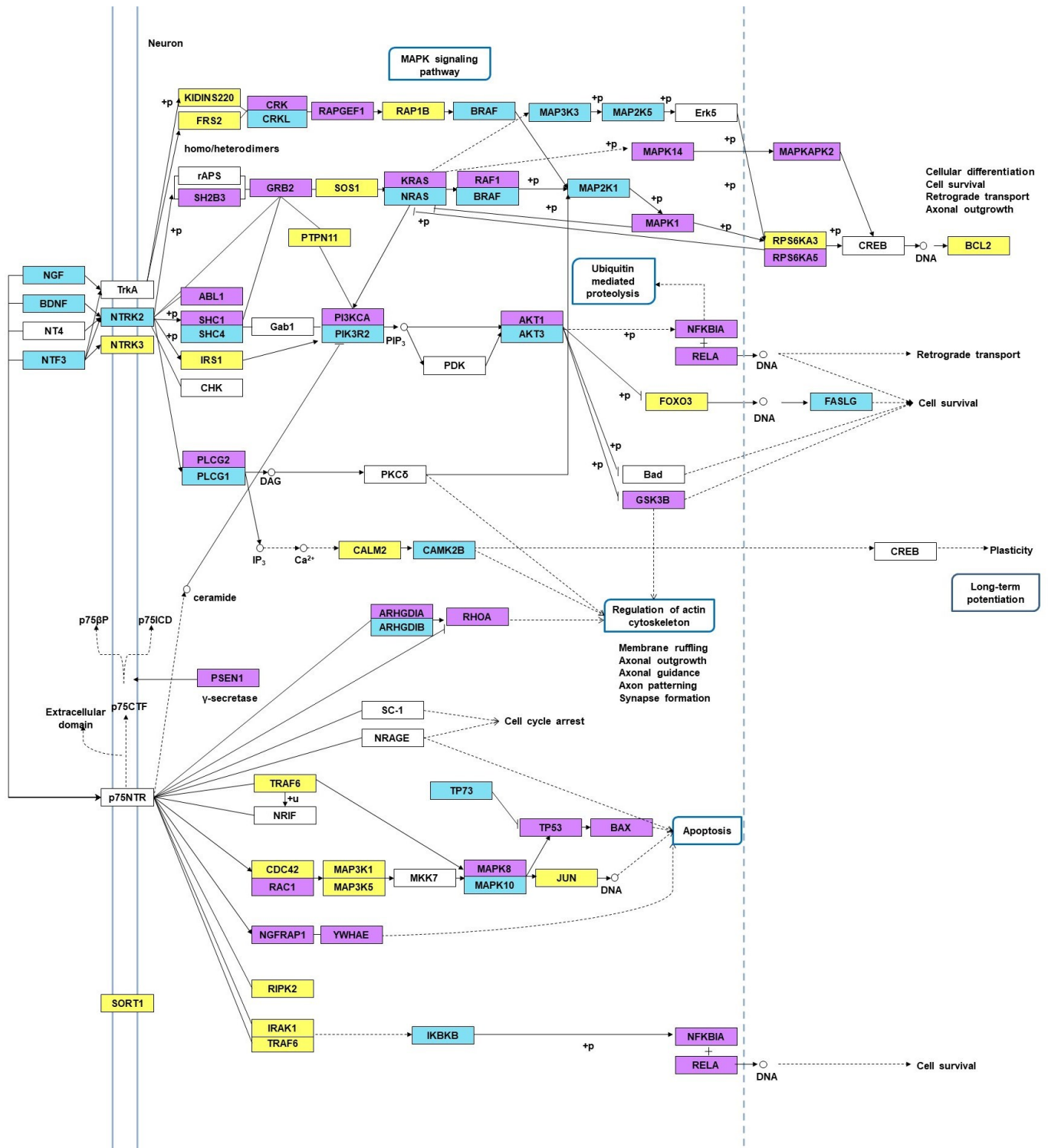
***Figure 13-* NGF1 treatment. Neurotrophin signaling pathway, from DIANA tools/KEGG and modified.** Colors of boxes as follows: blue: predicted target genes from Diana micro-T analysis; violet: validated target genes from Diana TarBase analysis; yellow: target genes identified by both Diana micro-T and TarBase analysis; white: genes not identified as target of significant miRs here described. Modified from KEGG pathway
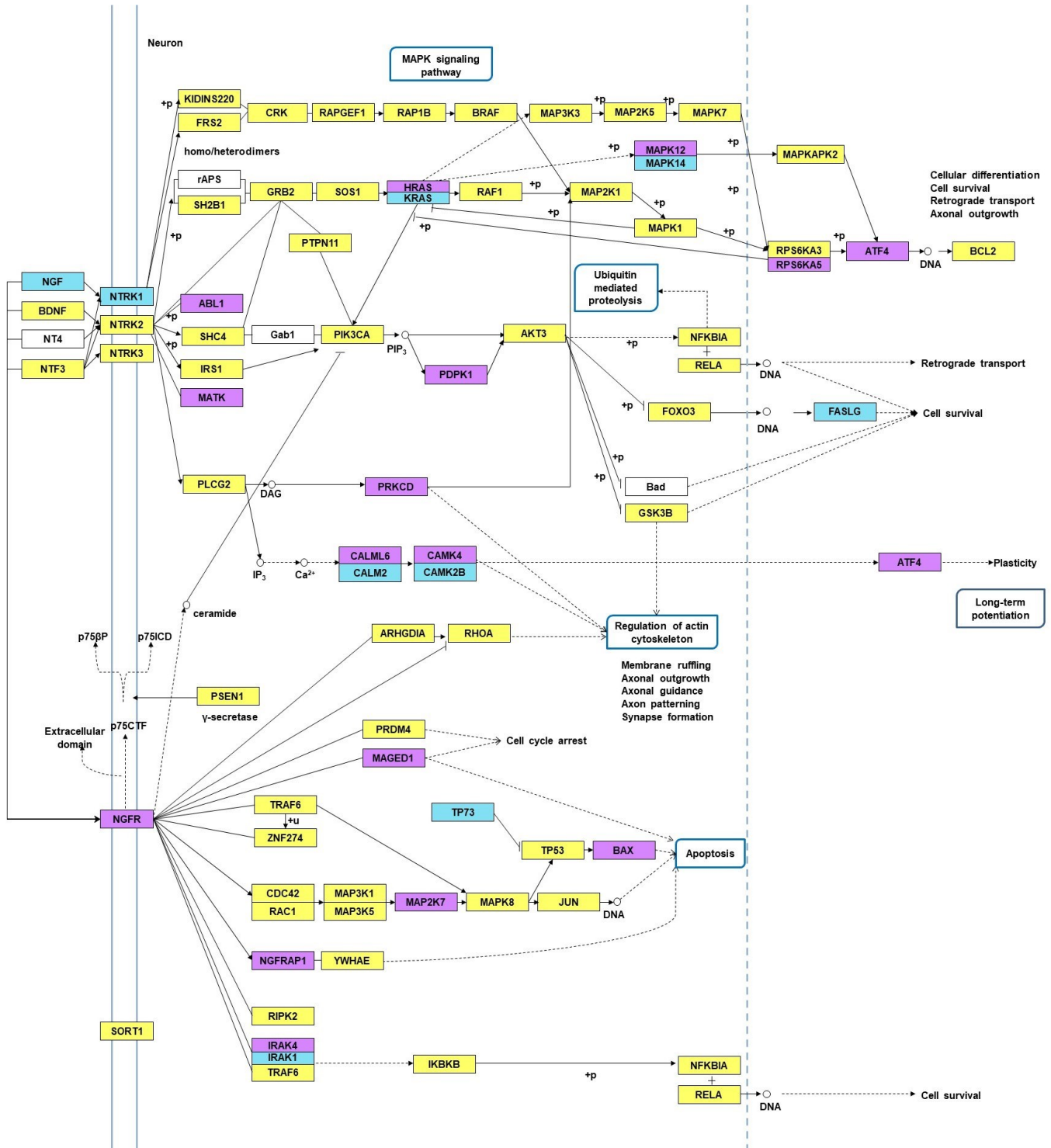
***Figure 14-* NGF2 treatment. Neurotrophin signalling pathway, from DIANA tools/KEGG and modified.** Colors of boxes as follows: blue: predicted target genes from Diana micro-T analysis; violet: validated target genes from Diana TarBase analysis; yellow: target genes identified by both Diana micro-T and TarBase analysis; white: genes not identified as target of significant miRs here described. Modified from KEGG pathway.
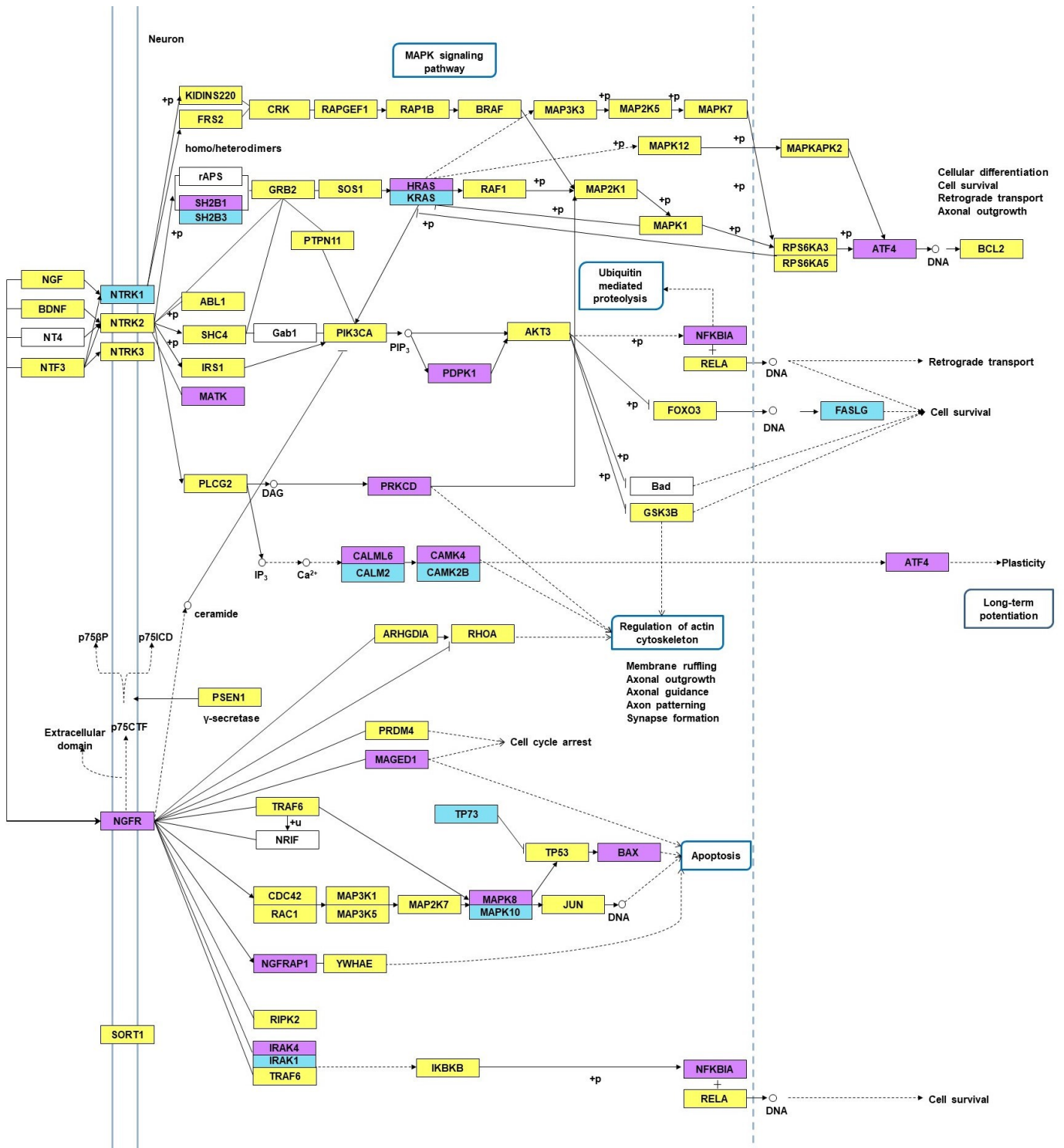
***Figure 15*-NGF3 treatment. Neurotrophin signalling pathway, from DIANA tools/KEGG and modified**. Colors of boxes as follows: blue: predicted target genes from Diana micro-T analysis; violet: validated target genes from Diana TarBase analysis; yellow: target genes identified by both Diana micro-T and TarBase analysis; white: genes not identified as target of significant miRs here described. Modified from KEGG pathway.

5.3.2. Neurotrophin pathway target genes: overall enrichment and functional analysis

Target genes involved in neurotrophin pathway were further subjected to analysis by Genemania, a bioinformatics tool that extends a user's gene list with genes which are functionally similar, or have shared properties with the initial query genes, and displays an interactive functional association network, illustrating the relationships among the genes and different data sets. For this purpose, based on Tarbase analysis, our 60, 99 and 101 genes targeted by significant NGF1-, NGF2- and NGF3-induced miRNAs, respectively (as summarized in Table 8), were entered in three different query gene lists. A total of 80, 119 and 121 interacting genes were identified, including the above-mentioned 60, 99 and 101 genes, respectively (represented in Figures 16, 17, 18) at the level of well-defined functional networks. Several groups of genes were associated to functions specifically related to neuron development, survival, apoptosis. As expected, regarding function enrichment, results obtained from all the bioformulations displayed at the top the neurotrophin signalling pathway and neurotrophin TRK receptor signalling pathways. As shown in Table 14, higher significance levels (expressed as lower FDRs) are reported for NGF3 compared to NGF2 and NGF1, but, if we look at the number of genes identified in those networks, 51 NGF1, 71 NGF2 and 72 NGF3 genes were found as functionally involved in neurotrophin signalling pathway, and 50 NGF1, 70 NGF2, 71 NGF3 were associated to neurotrophin TRK receptor signalling pathways (represented in Figures 16-18).

Bioformulation	NSP			NTRSP		
	FDR	#genes in network	# genes in genome	FDR	#genes in network	# genes in genome
NGF1	2.79E-71	51	277	1.11E-69	50	274
NGF2	1.88E-98	71	277	5.30E-97	70	274
NGF3	8.09E-100	72	277	2.25E-98	71	274

Table 14- **Genemania enrichment analysis**: functional interactions of genes in neurotrophin pathway, targeted by NGF1, NGF2, NGF3-induced miRNAs. Genes in query n=60 NGF1, n=99 NGF2, n=101 NGF3. False Discovery Rate (FDR) and number of genes in neurotrophin signalling pathway (NSP) and neurotrophin Trk receptor signalling pathways (NTRSP) are shown in table.

Consequently, if expressed in percentage terms with respect to total numbers of genes effectively in network (n=51, n=71, n=72 for neurotrophin pathway; n=50, n=70, n=71 for TRK receptor pathway) by considering the 60, 99 and 101 genes in query, 85% NGF1, 71% NGF2, 72% NGF3 genes were identified in neurotrophin signalling pathway network, and 83% NGF1, 70% NGF2, 70% NGF3 genes were correlated to neurotrophin TRK receptor signalling pathways network. Overall, in the face of less dysregulated miRNAs and targeted genes, NGF1 seems to induce comparable, even little higher, effects in terms of predicted neurotrophin functional networks, and associated genes, compared to NGF2 and NGF3.

Data confirm that all the bioformulations induce genes functionally involved in pathways highly relevant for this study. Regarding NGF1, results seem to underline that, despite less dysregulated miRNAs and related targeted genes, the induced response in predicted functional networks might be comparable, or maybe little higher, to that of NGF2 and NGF3.
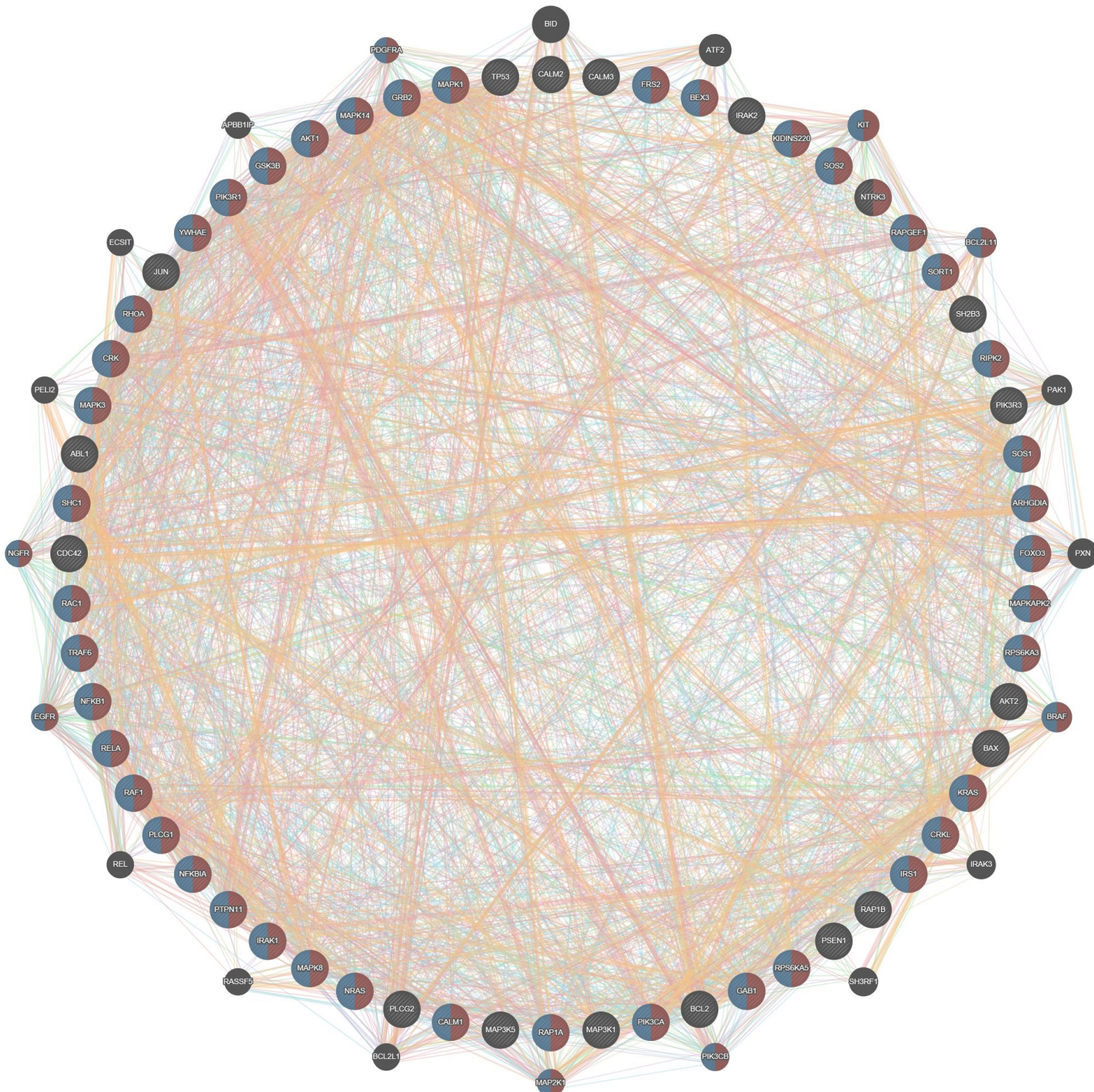
Figure 16- Genemania gene function enrichment NGF1. Representation of NGF1 genes in query (n=60), with stripes) functionally interacting with others (total n=80). Colors as follows: brown, genes involved in neurotrophin signalling function (n=51); blue: genes involved in neurotrophin TRK receptor signalling functions (n=50); black: genes involved in other functions.
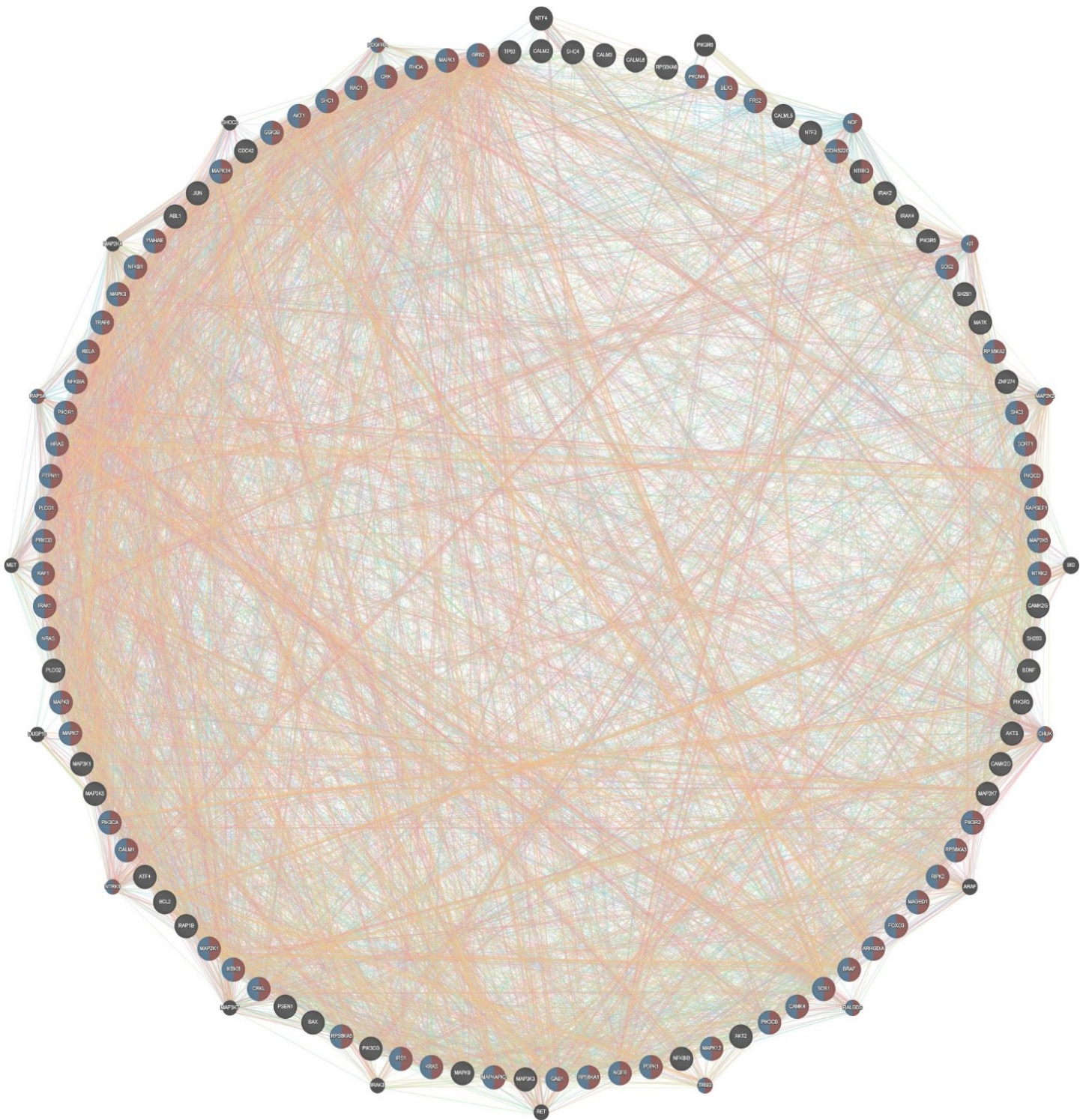
***Figure 17*-Genemania gene function enrichment NGF2.** Representation of NGF2 genes in query (n=99), with stripes) functionally interacting with other (total n=119). Colors as follows: brown, genes involved in neurotrophin signalling function (n=71); blue: genes involved in neurotrophin TRK receptor signaling functions (n=70); black: genes involved in other functions.
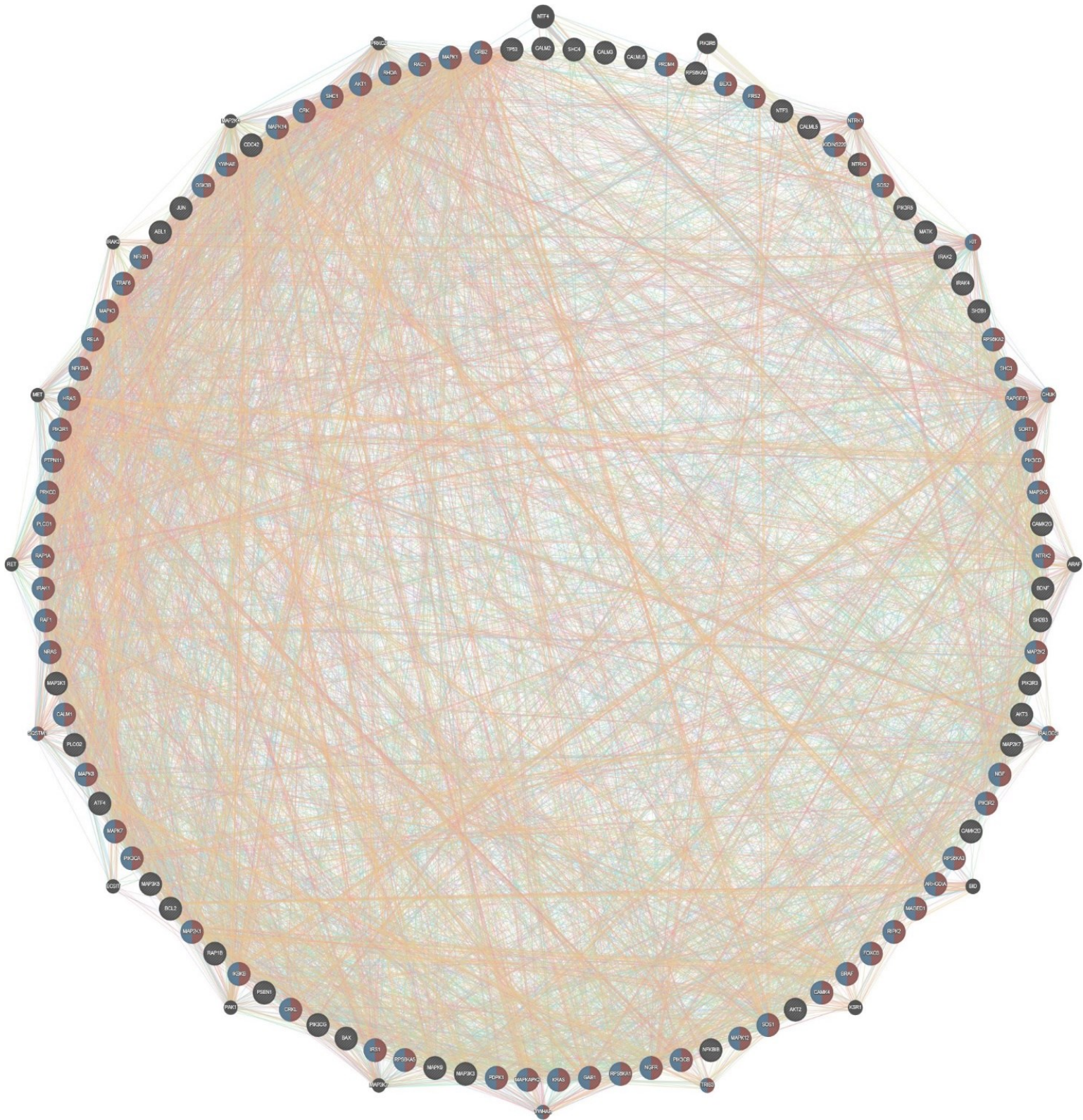
Figure 18- Genemania gene function enrichment NGF3. Representation of NGF3 genes in query (n=101), with stripes) functionally interacting with others (total n=121). Colors as follows: brown, genes involved in neurotrophin signalling function (n=72); blue: genes involved in neurotrophin TRK receptor signaling functions (n=71); black: genes involved in other functions.

5.3.3. Significant miRNAs and target genes for each single bioformulation: restricted analysis

Furthermore, among the overall dysregulated miRNAs (unique n=88, refer to Table 4), we restrict the analysis to the 3 sub-groups of those correlated only to each single bioformulation, in order to assess their putative role in neurotrophin pathway induction. To this aim, we individually analysed by Diana Tools miRPath the sets of 12, 16 and 20 miRNAs, more specifically related to NGF1, NFG2 and NGF3, respectively (Table 4). As shown in Table 15 (data from Tables S4, S5-S6 in Supplement), 9/12 (75%) NGF1 miRNAs, 9/16 (56%) NGF2 miRNAs, 16/20 (80%) NGF3 miRNAs were able to target 44, 45, 61 genes. In accordance to that previously reported, by taking into consideration Tarbase analysis results in percentage terms (to be related to 100 putative target genes), a similar number of NGF1-related miRNAs (n=20) can be hypothetically involved in targeting neurotrophin pathway genes in comparison to NGF2 miRNAs (n=20) and NGF3 miRNAs (n=26).

Bioformulation	TARBASE			microT-CDS		
	#genes	#miRNAs	p-value	#genes	#miRNAs	p-value
NGF1	44	9	0.0006	36	8	0.011
NGF2	45	9	0.002	50	16	0.009
NGF3	61	16	0.01	65	19	0.003

Table 15- **Neurotrophin signalling pathway: numbers of miRNAs/target genes involved in and related P-values.** Analysis restricted to miRNAs directly correlated to each bioformulation (n=12 NGF1, n=16 NGF2, n=20 NGF3).

Slightly different results were obtained by micro-T analysis [Percentage of miRNAs associated to neurotrophin signalling pathway: NGF1 8/16 (50%), NGF2 16/16 (100%), NGF3 (90%). miRNAs, in percentage terms, able to hypothetically regulate 100 neurotrophin genes: NGF1 (n=22), NGF2 (n=32), NGF3 miRNAs (n=29)]. However, neurotrophin pathway induced by miRNAs' sub-groups associated to NGF1 was characterized by more significant P-value by Tarbase analysis.

Altogether, 79 experimentally supported Tarbase unique genes belonging to the neurotrophin signalling pathway were targeted by the above-mentioned miRNAs' sub-groups (12 NGF1, 16 NGF2, 20 NGF3). After analysis by Diana Tarbase, 9 out of 12 (75%) NGF1-related miRNAs were identified which were able to regulate 44 target genes; 9 out of 16 (56%) NGF2-related miRNAs regulated 45 genes and finally 16 out of 20 (80%) NGF3-related miRNAs targeted 61 genes. By considering target genes, 23 of them were common to all bioformulations, 25 to 2 out of 3, 7 genes were attributable only to NGF1, 8 only to NGF2, 16 only to NGF3 (Table 16). These data were represented in Figure 19 by a Venn diagram.

Target genes shared by all 3 bioformulations (n=23)	Target genes shared by 2 out of 3 bioformulations (n.=25)	Target genes regulated only by NGF1 (n=7)	Target genes regulated only by NGF2 (n=8)	Target genes regulated only by NGF3 (n=16)
AKT1	**ARHGDIA**	ABL1	CAMK2G	AKT3
BAX	**AKT2**	CALM2	MAP3K5	IRS1
BCL2	**ATF4**	MAPK3	NFKB1	MAP2K2
CALM1	**BDNF**	PLCG2	NTRK2	MAP2K5
CALM3	**BRAF**	RAP1B	PIK3CG	MAP2K7
CDC42	**CAMK2D**	RAPGEF1	PSEN1	MAP3K1
CRK	**FOXO3**	RELA	PTPN11	MAPK9
CRKL	**GRB2**		ZNF274	NFKBIB
FRS2	**IRAK1**			NGF
GAB1	**MAP3K3**			PDPK1
GSK3B	**MAPK14**			PIK3CA
JUN	**MAPK8**			PIK3CD
KIDINS220	**MAPKAPK2**			PRDM4
KRAS	**NGFRAP1**			RPS6KA2
MAPK1	**NRAS**			SH2B1
PIK3R1	**NTRK3**			TRAF6
PIK3R3	**PIK3CB**			
PLCG1	**RAC1**			
RPS6KA3	**RAP1A**			
RPS6KA5	**RHOA**			
SORT1	**RIPK2**			
SOS1	**SH2B3**			
YWHAE	**SHC1**			
	SOS2			
	TP53			

Table 16- **Distributions of genes, belonging to Neurotrophin Signalling Pathway targeted by dysregulated miRNAs induced by each single bioformulation.** List of genes (total n=79) belonging to Neurotrophin Signalling Pathway and targeted by dysregulated miRNAs (n=12 NGF1, n=16 NGF2, n=20 NGF3) induced by each single bioformulation (NGF1 OR NGF2 OR NGF3, ref Table 4), as detected by Tarbase (experimentally supported) analysis. Colors as follows: pink, NGF2+NGF3; violet, NGF1+NGF2; blue: NGF1+NGF3
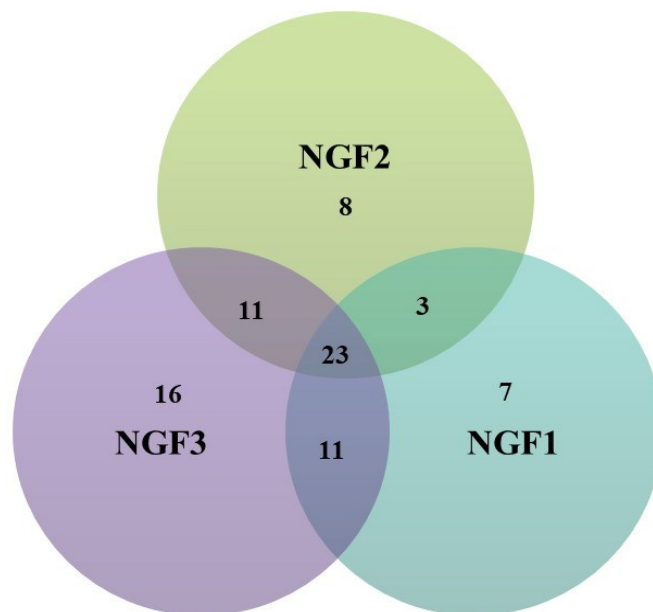
***Figure 19-* Venn diagram of genes targeted by dysregulated miRs induced by each bioformulation.** Genes (total n. 79, Table 16) belonging to Neurotrophin signalling pathway and targeted by bioformulation-restricted significant miRNAs (ref Table 4)

5.3.4. *Neurotrophin pathway target genes: restricted enrichment and functional analysis*

Restricted analysis was also performed on the above-mentioned groups of 44, 45, 61 neurotrophin signalling genes, targeted by 12, 16, 20 miRNAs more strictly correlated to NGF1, NGF2 and NGF3. A total of 64, 65 and 81 genes in network, including the 44, 45 and 61 genes in query, respectively, were identified and genes' interactions were represented in Figures 20,21 and 22. Also, in this case, the neurotrophin signalling pathway and neurotrophin TRK receptor signalling pathways were at the top of the functions' lists. FRD values are more significant for NGF3, with higher number of genes involved in those networks (n=51, n=50) compared to NGF1 (genes in network n=40) and NGF2 (genes in network n=39, n=40) which show comparable p-values. In this case, if we take into consideration the number of gene in network with respect to that of related miRNAs, NGF1 seems to be more effective with respect the other bioformulations. Global data are summarized in Table 17.

By restricting the functional enrichment analysis to target genes more strictly correlated to each bioformulation, data seem to confirm a more focused activity of NGF1 in neurotrophin signalling pathway and neurotrophin TRK receptor signalling pathways functions.

Bioformulation	NSP			NTRSP		
	FDR	#genes in network	# genes in genome	FDR	#genes in network	# genes in genome
NGF1	1.06E-54	40	277	1.06E-54	40	274
NGF2	5.44E-54	40	277	2.16E-52	39	274
NGF3	7.45E-71	51	277	2.87E-69	50	274

Table 17- Genemania enrichment analysis: functional interactions of genes in neurotrophin pathway, related only to NGF1 or NGF2 or NGF3. Genes in query: n=44 NGF1, n=45 NGF2, n=61 NGF3. False Discovery Rate (FDR) and number of genes in neurotrophin signalling pathway (NSP) and neurotrophin Trk receptor signalling pathways (NTRSP) are shown in table.
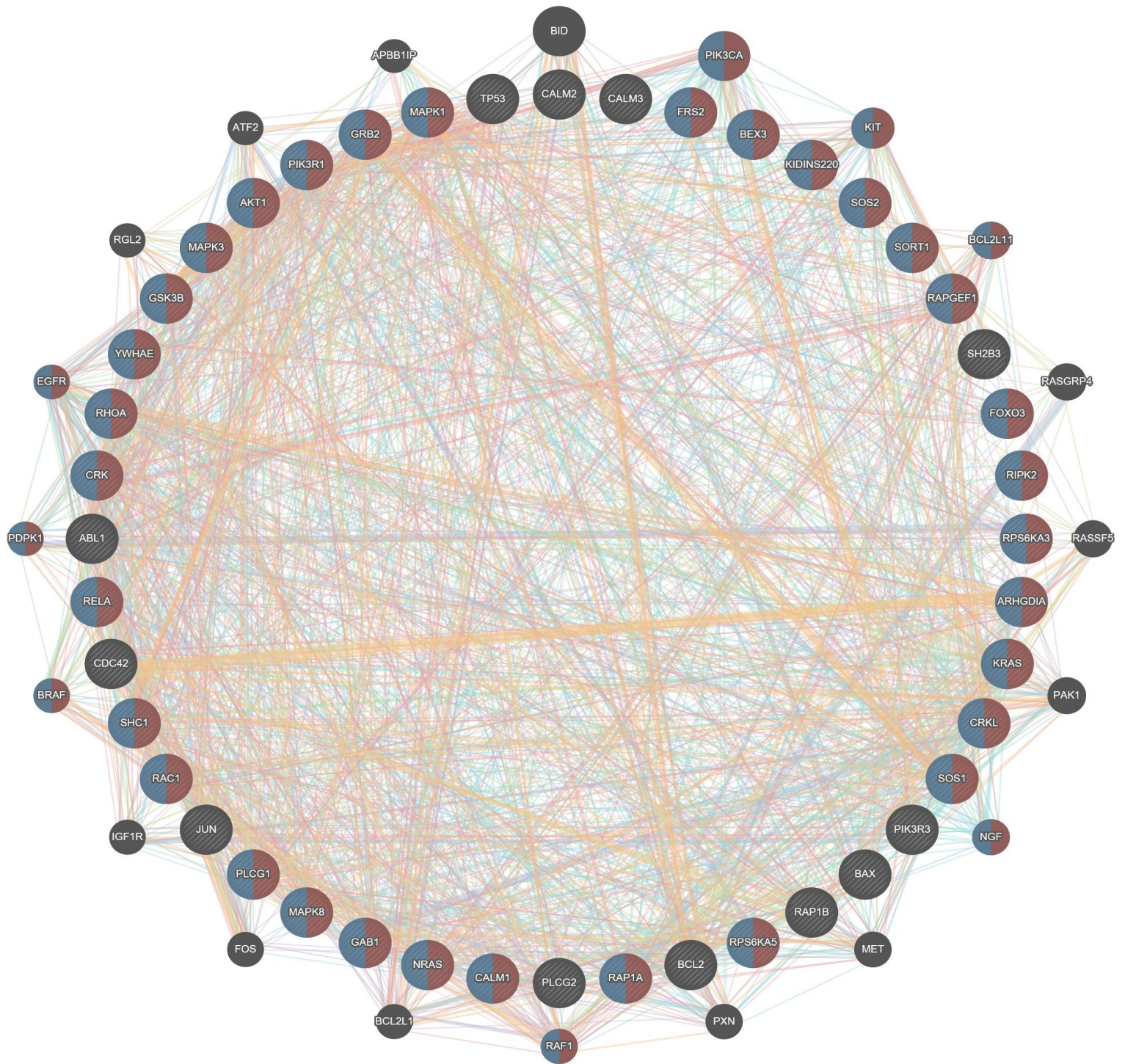
***Figure 20*-Genemania gene function enrichment NGF1**. Representation of NGF1 genes in query (n=44), with stripes functionally interacting with other (total n=64). Colors as follows: brown, genes involved in neurotrophin signaling function (n=40); blue: genes involved in neurotrophin TRK receptor signaling functions (n=40); black: genes involved in other functions.
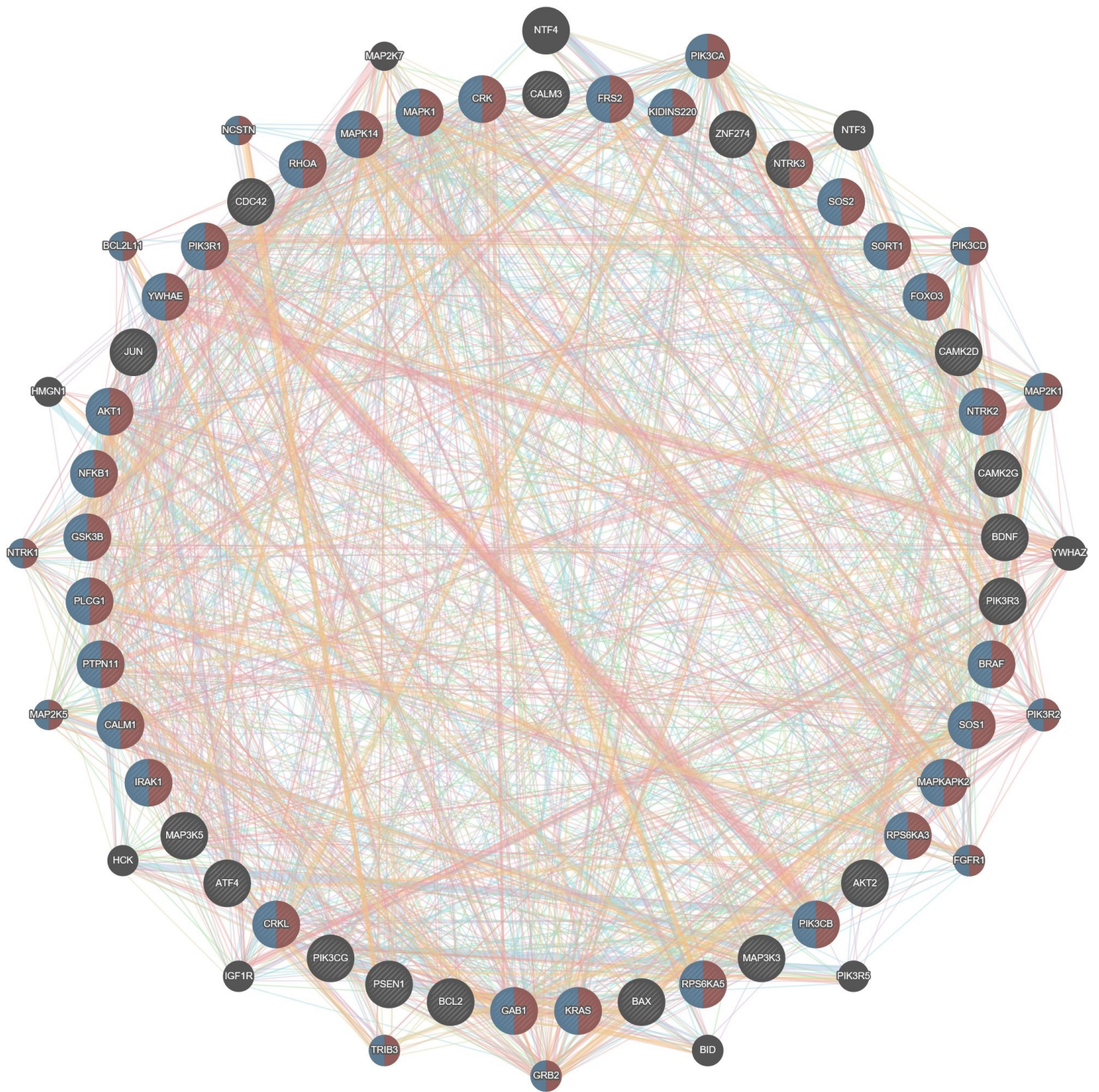
Figure 21- **Genemania gene function enrichment NGF2**. Representation of NGF2 genes in query (n=45), with oblique lines) functionally interacting with others (total n=65). Colors as follows: brown, genes involved in neurotrophin signaling function (n=40); blue: genes involved in neurotrophin TRK receptor signaling functions (n=39); black: genes involved in other functions.
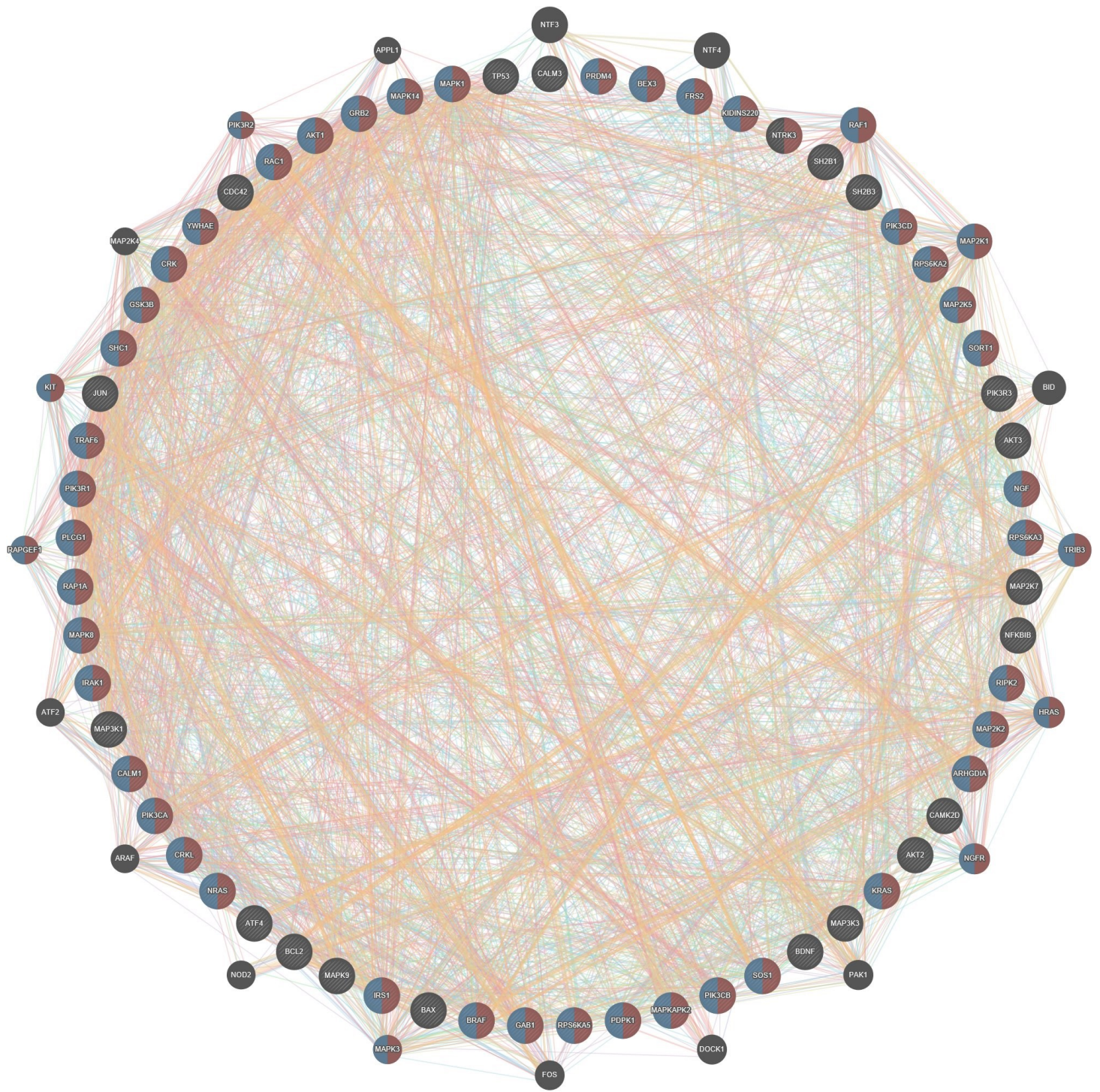
Figure 22- **Genemania gene function enrichment NGF3**. Representation of NGF3 genes in query (n=61), with oblique lines) functionally interacting with other (total n=81). Colors as follows: brown, genes involved in neurotrophin signaling function (n=51); blue: genes involved in neurotrophin TRK receptor signaling functions (n=50); black: genes involved in other functions.

5.4. Protein expression levels of target gene AKT

To validate *in silico* results, we evaluated expression levels of total AKT. As reported in Table 9-11, AKT1, AKT2 and AKT3 were identified as target genes of miR-29b-3p, miR-27a-5p, miR-146a-5p and miR-324-5p (NGF1), miR-126-3p, miR-15b-5p, miR-103a-3p, miR-218-5p, miR-182-5p, miR-139-5p, miR-324-5p, miR-146a-5p, miR-382-5p, miR-491-5p and miR-137-3p (NGF2), miR-182-5p, miR-320a-3p, miR-15b-5p, miR-218-5p, miR-24-2-5p, miR-139-5p, miR-103a-3p, miR-22-5p, miR-126-3p, miR-138-5p, miR-146a-5p, miR-491-5p, miR-532-3p and miR-135b-5p (NGF3). As shown in Tables 1-3, the above mentioned miRs are globally mostly hypo-expressed after 12 and 48 hours with respect to unstimulated cells, whereas after 30 minutes miRs had higher RQ value than later time points, close to iso-expression. Of note, at the same time, miRs are globally hyper-expressed after 48 hours when compared to that observed after 12 hours (Tables 1-3). If we consider the immunoblotting results, shown in Figure 23, total AKT expression levels reflect and are fully coherent with miRNAs' expression levels, being comparable to the control after 30 min, but hyper-expressed after 12 and, less marked, 48 hours. Therefore, AKT modulation after 12 and 48 hours seems to be more significant than control and 30 minutes. Small exception for AKT over-expression emerged after NGF3-treatment at 48 hours, where higher protein expression can be observed in comparison to that expected. However, this effect might be attributable to kinetics conditions, to protein accumulation or to half-life increase within the cell microenvironment. This analysis provides a preliminary validation and demonstration of *in silico* results strength.
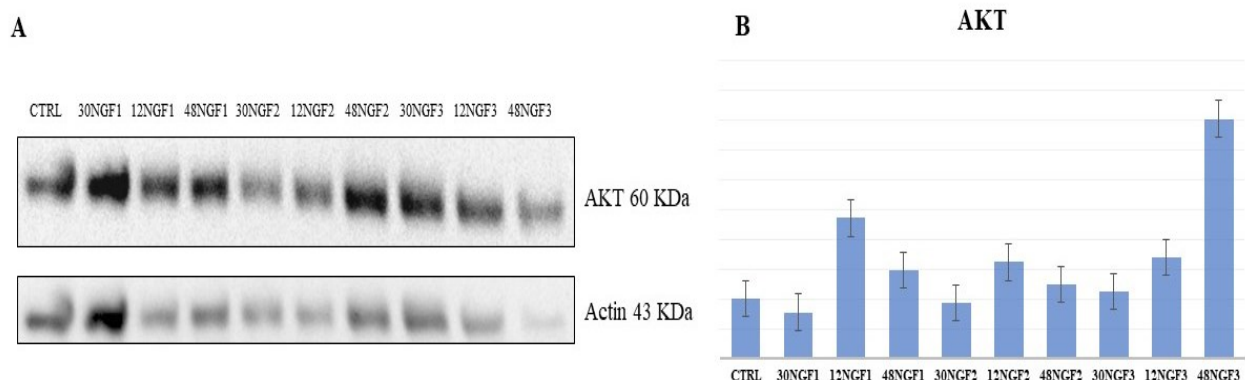
Figure 23-**AKT expression after NGF**. (A) Representative western blot analysis of AKT; (B) Densitometric analysis. Total AKT1, 2 and 3 proteins were detected: as shown, the level of their expression is in line with that of miRNAs regulating them.

5.5. NGF improves proliferation in HCEC *in vitro*

To confirm the effects of NGF to induce epithelial wound healing, we performed an in vitro scratch assay on Human Corneal Epithelial cells (HCEC). After scratch-induced and treatment with NGF1, cells were observed under a microscope and photographed in two different time points: at 0 and 24 hours. We showed that NGF1 accelerated the closure of the epithelium and proliferation was faster in the NGF-treated cells after 24 hours compared with injured cells without treatment (Figure 24). In fact, there is a significant difference between this two groups (**p < 0.01). The competence of NGF to promote corneal epithelial wound healing has been well documented (Lambiase et al., 2000; Micera et al., 2006; Bonini et al., 2000).
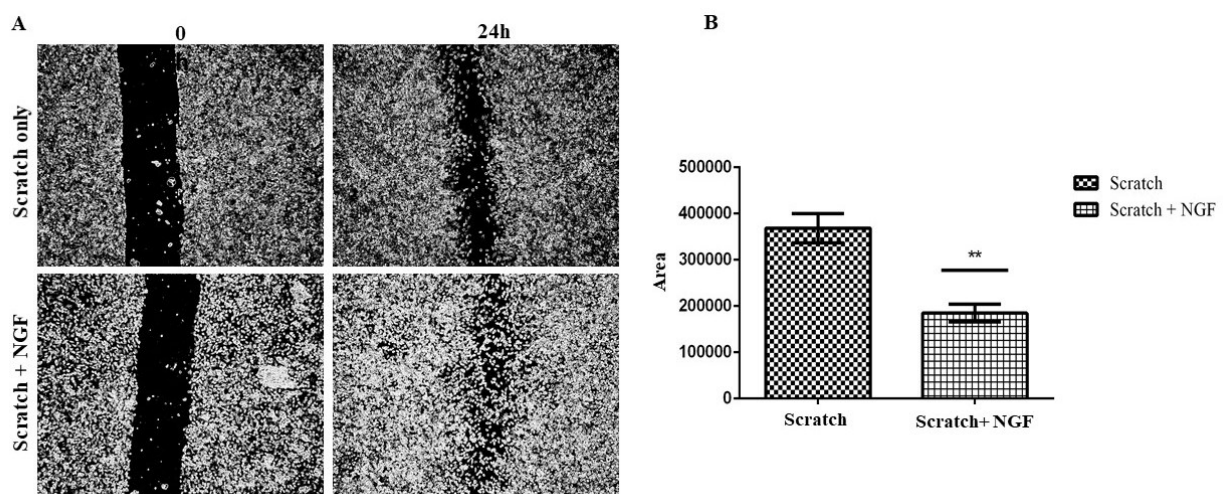
Figure 24- **Scratch wound healing assay. (A)** Effect of NGF on proliferation and migration in HCEC was demonstrated with a scratch model, by measuring epithelium closure using wound healing measurement, a tool of ImageJ. **(B)** Significant difference (**p < 0.01) between HCEC-treated and injured HCEC without treatment: NGF improved proliferation and speeds up wound healing.

DISCUSSION

NGF plays a pivotal role in maintaining the homeostasis of the ocular surface (corneal and conjunctival epithelium, fibroblasts and endothelium), and is able to also reach the retina and optic nerve, thus activating the primary structures of the visual system. Human corneal epithelium produces and releases NGF, and expresses the high-affinity receptor TrkA, playing an important role in the integrity and function of the ocular surface, stimulating the proliferation and survival of both epithelial and nerve fibers. In addition, NGF is also released in aqueous humor and tears and is produced by conjunctival cells (epithelial, goblet, immune cells and fibroblasts) (Lambiase et al., 2011a). Through *in vitro*, *ex vivo* and *in vivo* experiments on both animals and humans, it was demonstrated that NGF plays a key role in pathophysiology and the administration of exogenous NGF is able to accelerate corneal epithelium healing in both rats and animals (Lambiase et al., 2000; Lambiase et al., 2011b; Lambiase et al., 1998; Bonini et al., 2000). These studies have highlighted the therapeutic value of NGF in corneal diseases such as neurotrophic keratitis, peripheral ulcerative keratopathy, dry eye. Furthermore, it also acts on corneal infections from herpes virus. (Lambiase et al., 2011a, Lambiase et al., 2012). However, molecular mechanisms inducing biological response to NGF at the corneal level are still unknown.

MicroRNAs are a class of small RNA molecules, of 22 nucleotides, not coding, that regulate negatively, at the epigenetic level, post-transcriptional gene expression. MiRs deregulation, both in terms of activity and expression, is associated with different physiological and pathological processes. This, together with their peculiarity of being expressed not only in cells but also in body fluids such as blood, tears and urine, makes microRNAs of potential diagnostic, prognostic and predictive biomarkers as well as possible therapeutic targets. Several miRNAs have been described in corneal physiology, disease, and potential therapy (Rassi et al., 2017; Mukwaya et al., 2019).

In this study miRNAs' expression modulation in corneal cells after treatment with three different NGF bioformulations (NGF1, NGF2 and NGF3) was evaluated. A remarkable part of the human miRNome by using DIANA tools, an on-line bioinformatics tool able to identify both experimentally supported (Tarbase database) and predicted (microT-CDS database) miRNA target genes and pathways, was analysed as well. In the previous section results from both databases were shown, but data obtained from DIANA Tarbase analysis will be primarily discussed, thus providing more robust information about experimentally supported target genes and pathways.

Different amounts of dysregulated significant miRNAs were detected in response to each bioformulation: 21, 52 and 58 miRNAs were differentially, mainly hypo-expressed, after treatment with NGF1, NGF2 and NGF3, respectively. Globally, different kinetics were revealed, as both NGF2 and NGF3 induced earlier miRNAs' down-regulation with respect to NGF1. On the other hand, by

comparing miRNAs' expression levels after 48 hours with respect to 12 hours (in particular NGF1 e NGF3), several miRNAs showed different levels of hyper-expression, leaving to hypothesize a sort of a possible long-term compensatory mechanism for repristinating normal physiological conditions. Overall, a total number of 88 unique miRNAs were significantly modulated: 3 were induced and shared by all the bioformulations, whereas 37 were in common between two of them, mostly NGF2 and NGF3, indicating that both might drive epithelial corneal cell responses which are, at least in part, overlapping. The remaining 12 out of 21 (57%), 16 out of 52 (30%) and 20 out of 58 (34%) miRNAs were correlated only to NGF1 or NGF2 or NGF3, respectively.

After *in silico* analysis by using Tarbase database, miRNAs-induced pathways with significant p-value were identified for each bioformulation. Overall, a total number of 91 unique pathways were identified: as expected, most of them (n=46) were shared by all the bioformulations, a relevant part (n=28) was shared by 2 out of 3 bioformulations, mainly NGF2 and NGF3, a minor part, which might deserve interest for further studies, was related to each single bioformulation.

Our study has highlighted several common pathways between bioformulations that play a role in fundamental controlling cell processes, such as development, proliferation, differentiation, survival and apoptosis, also in corneal cells, injury and disease, such as adherens junctions, Hippo, HIF-1, NF-kB, p53, TGF-β (Mantelli et al., 2013; Lee et al., 2018; Vadlapatla et al., 2013; Azizi et al., 2011; Lan et al., 2012; Tandon et al., 2010). A pathway of potential interest, that of the N-glycan biosynthesis (Rodriguez Benavente et al., 2018), was also displayed in sharing by NGF1 and NGF2. Interestingly, ECM-receptor interaction and PI3K signalling pathways were ascribed only to NGF1. The first one was described in important corneal features and functions, such as transparency and wound healing (Hassel and Birk, 2010), the second one was analysed in a recent work by Li et al. (2020) who demonstrated that PTEN inhibition made easier diabetic corneal regeneration by reactivation of AKT signalling that improved a significant enhancement of cell migration and wound healing. On the other hand, the axon guidance pathway, ascribed only to NGF2, was shown as crucial for axonal targeting in the eye: indeed, axon guidance proteins were highly expressed in cornea in the steady state and quickly up-regulated after injury (Zhang et al., 2018; Guaiquil et al., 2019). In addition, Notch and phosphaditylinositol signalling were detected as associated only to NGF3. Notch pathway was described in corneal wound healing (Ma et al., 2007; Ma et al., 2011), whereas the phosphaditylinositol signalling, related to PI3K-AKT pathway, is involved in Fleck corneal dystrophy (FCD), a rare corneal dystrophy characterized by multiple asymptomatic, non-progressive symmetric minute flecks disseminated throughout the corneal stroma, associated to PIP5K3 gene mutations (ref. KEGG hsa04070 pathway). A more in-depth study of several among these pathways could be performed to further study the NGF biological effects.

More than 2000 miRNAs' target genes involved in the above-mentioned pathways were identified as well: 858 were shared by all the bioformulations, 1299 by 2 of them, mainly NGF2 and NGF3, 76 were related only to NGF1, 141 to NGF2, 216 to NGF3. This extensive and advantageous gene list can be in depth analysed in order to identify targets suitable for further molecular analyses and validations, especially for each single bioformulation, with the aim to possibly identify target genes and functions specifically related to them.

Interestingly, neurotrophin signalling pathway was induced by all three bioformulations; thus, after this first-level analysis, we focused our attention on miRNAs and target genes specifically involved in this pathway. One-hundred and two unique experimentally validated target genes were identified: a half were shared by all the bioformulations, the remaining were, mainly, in common between NGF2 and NGF3. All the bioformulations' stimuli led to the involvement of the same cell functions, such as cell differentiation and survival, retrograde transport, axonal outgrowth, guidance and patterning, synapse formation, plasticity. Relevant pathways, such as MAPK, ubiquitin mediated proteolysis, regulation of actin cytoskeleton and apoptosis were interested as well. Overall, as expected, NGF1, NGF2 and NGF3 did not show relevant dissimilarities in terms of efficacy to overall induce neurotrophin pathway; however, NGF1-induced miRNAs and, correspondingly, target genes were less than those induced by NGF2 and NGF3. In this context, some interesting differences could deserve interest. Indeed, by taking into consideration the ratio between dysregulated miRNAs and related target genes for each single bioformulation, NGF1 seemed to be more effective than NGF2 and NGF3 since, proportionally, it appeared able to regulate more target genes despite inducing less miRNAs. The latter observation, purely based on proportionality criteria, was further confirmed by *in silico* Genemania enrichment and functional analysis. This tool provided data about the miRNAs' target genes, others functionally correlated with them, and related functions as well. With this regard, neurotrophin signalling pathway and neurotrophin Trk receptor signalling pathways were at the top of the list of detected functions, which comprised also other functions (e.g. development, differentiation, apoptosis) there specifically related to neurons.

The NGF1 feature of inducing, in absolute terms, less miRNAs and genes, even if the latter were, proportionally, more with respect to that regulated by NGF2 and NGF3, could be of interest if the concept of homeostasis is taken into consideration. Indeed, after an external stimulus (such as a treatment), cells respond, lose homeostasis control, and then tend to balance the induced changes in order to repristinate a normal physiological condition. In this scenario, regarding the comparisons among bioformulations here analysed, NGF1, of proven therapeutic efficacy for some eye disease, would induce overall less, but maybe more specific, responses which could make easier cells to restore physiological equilibrium.

Furthermore, after restricting the analysis to miRNAs induced only by each single bioformulation, a list of target genes in neurotrophin signalling pathway was obtained. Also, in this case, by globally considering miRNAs and related target genes, NGF1-induced effects seemed more specific, as confirmed by Genemania enrichment analysis.

We submitted all the significant dysregulated miRNAs to PubMed search by using "miR-ID and cornea" as keywords and several studies were found and reported below. Some of them analysed miR-146a-5p, one of three microRNAs here detected and shared by all the NGF bioformulations. Mir-146 is involved in inflammatory and immune response, by considering that NF-κB has been shown to induce its transcription and that miR-146 regulates the expression of IRAK1 and TRAF6 (Taganov et al., 2006). By regulating the signalling of these genes as well as MyD88 and TLR4, miR-146 modulates inflammation through a negative feedback mechanism. MiR-146a-5p hyper-expression was described in two studies and was correlated with delayed corneal wound healing, most probably due to the inhibition of activated p38 MAPK and EGFR, known as mediator of epithelial wound closure (Funari et al., 2013; Winkler et al., 2014). MiR-146a was also found hyper-expressed in PMBC and sera from patients with Sjögren''s syndrome, a condition characterized by dry eye, and in Sjögren'-prone mice (Zilahi et al., 2011; Pauley et al., 2011; Alevizos et al., 2011; Shi et al., 2014; Sun et al., 2017; Jiang et al., 2018). Of note, these results are coherent with NGF-induced miR-146a down-regulation, as detected in our in vitro models, also providing an evidence about a putative mechanism of these neurotrophins in corneal cells and possible disorders' treatment.

Four miRNAs dysregulated in our study in response to NGF2 and/or NGF3, miR-185-5p, miR-138-5p, miR-194-5p and miR-28-5p, were described as down-regulated in thinner keratoconic corneal epithelia by Wang et al. (2018). In addition, still on miRNAs modulated by both NGF2 and NGF3, significant down-regulation of miR-126-3p and miR-15b-5p, known as neovascularization markers, was also observed after anti-VEGF bevacizumab or TKi sunitinib administration in a murine model of corneal neovascularization induced by silver nitrate (Cakmak et al., 2018). With this regard, anti-VEGF is considered as a treatment counteracting VEGF, often markedly increased in inflamed cornea epithelial and in vascular endothelial cells (Giannaccare et al., 2020). MiR-31, which is responsive to both NGF2 and NGF3 and plays a key role in the human cornea epithelium, negatively regulates a factor that inhibits hypoxia-inducible factor 1 (FIH-1), involved in anaerobic energy production and in Notch signalling. Peng et al. (2012) used human corneal epithelial keratinocytes and antagomir as an experimental model to reduce miR-31 levels, which caused an increase in FIH-1, resulting in a decrease in cell glycogen. In addition, overexpression of FIH-1 decreased signalling AKT, activated Gsk-3 and inactivated glycogen synthetase. This has shown that the corneal epithelium is able to regulate its energy requirements. Therefore miR-31 can have a protection role of the corneal

epithelium from hypoxic stress since by regulating negatively FIH-1 and leading to an increase in glycogen in the corneal epithelium, it is able to withstand periods of hypoxia.

Other information was reported for some of the significant miRs more strictly correlated to a single bioformulation. MiR-204, more abundant in the cornea (Drewry et al., 2016), is here included in the NGF2-only-regulated miRs' list. It plays a key role in wound healing since its down-regulation, as a damage response, promotes the proliferation and migration of corneal epithelial cells. To demonstrate this, experiments were conducted in which epithelial corneal cells were transfected with miR-204, which inhibited cell proliferation in phase G1. This miR also acts as a suppressor of the epithelial mesenchymal transition (EMT), as its down-regulation acts on cellular integration by accelerating it (An et al., 2015). Gao et al. (2015) detected miR-204 up-regulation in diabetic cornea and, conversely, demonstrated that down-regulation, associated to its target gene SIRT1 increase, may mitigate the detrimental corneal wound healing effects of high glucose and lead to restoration of the cell cycle. The authors demonstrated that miR-204 level decrease can promote human corneal epithelial cell migration and proliferation by targeting genes mainly involved in controlling those processes.

About NGF1-only regulated miRs, Mukwaya et al. (2016) demonstrated miR-27a over-expression during corneal neovascularization, hypothesizing a possible role of this miR in regulating angiogenesis in the cornea through Sema6a (inhibited semaphorinA angiogenesis). MiR-27a correlation with this semaphorin has been demonstrated by *in vitro* and *in vivo* experiments in which miR-27a, expressed by endothelial cells, regulated the expression of Sema6a, which controls the repulsion of endothelial cells, promoting angiogenesis (Urbich et al., 2012). In our study miR-27a was initially iso-expressed at 30 minutes compared to untreated control (RQ=0.863) reaching the hypo-expression already after 12 hours treatment and (RQ=0.226). Noteworthy, significant down-regulation can be observed after 48 hours (RQ=0.052). This could confirm the hypothesis that miR-27a could be a potential therapeutic target useful to suppress corneal neovascularization.

Lastly, decreased levels of miR-29b, included in the NGF1-only-modulated miRNAs, were reported in patients with Fuchs endothelial corneal dystrophy (FECD), characterized by progressive loss of corneal endothelial cells, thickening of Descement's membrane and deposition of extracellular matrix in the form of guttae (Toyono et al, 2016). Mir-29b is a member of the miR-29 family which regulates the production of extracellular matrix (ECM) proteins. The authors demonstrated that miR-29b over-expression decreased ECM protein production in immortalized Fuchs human corneal endothelial cell line, thus suggesting that, in FECD patients, miR-29 restoration therapy might be a new treatment strategy. Similarly, miR-29b was found down-regulated in pterygium, a pathological condition characterized by inflammation, fibrosis, proliferation, angiogenesis, and ECM breakdown in conjunctiva and in cornea too (He et al., 2019). In the ARVO 2019 meeting some interesting data

were presented about the possible use of miR-29b to reduce corneal fibrosis in a pre-clinical model (Gallant-Behm et al., 2019). The authors treated alkali-induced corneal damage in mouse with remlarsen, a miR-29b mimic, and demonstrated strong fibrosis reduction by inhibition of ECM, EMT and collagen mRNA expression.

In our analysis, miR-29b, together with let-7c-5p and miR-449a, was, even though without reaching significant P level, hyper-expressed after 30 min of NGF1 treatment with respect to unstimulated cells (RQ=4.4), indicating an early positive induction by this bioformulation, with consequent reduction of miR-29b target genes. Afterward, miR-29b expression level decreased after 12 hours (RQ=0.5) to reach iso-expression (RQ=0.9) after 48 hours. We reported significant miR-29b down-regulation (RQ=0.1) in the comparison between treatments at 30 minutes and 12 hours, which reflects the above-mentioned decreased levels at 12 hours compared to control cells. Overall, those data could be correlated to NGF1-induced putative miR-29b regulation of ECM proteins involved in corneal injury repair which, on the hand, can cause scar and fibrosis, but, on the other hand, are essential in wound healing (Maquart and Monboisse, 2014). For this reason, they should be subjected to subtle regulation in order to maintain a balance between different induced effects, thing that might be attributable to miR-29b levels change.

Overall, existing literature data here reported are globally consistent with our results in terms of miRNAs expression levels in response to corneal behaviour, treatments, or pathological conditions.

The only study that shed light on the expression of altered miRs following treatment with NGF in HCEC was done by Wu et al. (2017). Following treatment with a lower concentration of NGF, compared to that used in our study, and at an incubation time of only 1 hour, a profiling of differential miRNAs expressed was done by different tools (Affymetrix GeneChip miRNA Array). Twenty-seven up-regulated miRNAs and fifty down-regulated miRNAs have been identified. Among them, there are also miRs emerged from our analysis: miR-204, miR-337-5p, miR-30b and miR-370 which also in this study were down-regulated results as in ours, while miR-146a, miR-103 and miR-495, were up-regulated, instead in our analysis were down-regulated. After Go Analysis, they focused only on down-regulated miRs and, in particular, investigated miR-494, that in our study was down-regulated even though without reaching significant P level. Our data for NGF1 and NGF2 treatments, in reference to miR-494, are consistent with this study as it appeared that the expression level of this microRNA gradually decreased. Regarding the obtained results after NGF1 treatment, miR-494 was iso-expressed after 30 minutes with respect to unstimulated cells (RQ=1.423) and then reached a hypo-expression after 12 hours and 48 hours (RQ=0.498, RQ=0.351 respectively). After NGF2 treatment immediately emerged a hypo-expression already after 30 minutes compared to control cells (RQ=0.24) and the miR-494 expression level gradually decreased after 12 hours (RQ=0.199) and 48

hours (RQ= 0.122). On the other hand, miR-494 expression level after NGF3 treatment was different with respect to treatments mentioned above, in which an initial hypo-expression emerged after 30 minutes compared to the control (RQ=0.13) as well as after 12 hours (RQ=0.11) and then reached iso-expression (RQ=1.39) after 48 hours. Noteworthy, in the comparison between treatments at 12 hours and 48 hours, miR-494 was hyper-expressed (RQ=12.78). MiR-494 affected NGF function in promoting proliferation as it decreases the cyclin D1 expression, causing G1 phase arrest.

Regarding target genes, belonging to neurotrophin pathway, it was been seen that most of them targeted by more than 1 dysregulated miRNA. In addition, these genes are part of relevant molecular circuitries (i.e. MAPK, PI3K/AKT, NF-κB) that regulate important cell functions, such as differentiation, survival or apoptosis. Interestingly, these genes represent the majority of those reported in the KEGG scheme describing the neurotrophin signalling pathway, indicating a very strong impact of dysregulated miRNAs here identified on the potential modulation of specific NGF-induced cell response. Very few data about the regulation of those target genes by NGF in corneal cells can be recovered in literature. Regarding AKT (target genes validated with western blot experiment in our study), it was demonstrated that plays an important role in regulating corneal biology. Hong et al., (2012) showed correlation cyclin D, PI3K/AKT, MAPK/Erk pathways' activation (AKT and MAPK are target gene in our analysis) with epithelial corneal cells proliferation: in this study, NGF regulated proliferation of HCEC by activation of cyclin D via activation of AKT and ERK pathways. The NGF effect was demonstrated on inflammation and apoptosis in a diabetic high-glucose corneal model. NGF reduced these processes by reduction of ROS activation and cleaved-caspase 3, Bax, NF-κB-p65 (other target genes identified in our studies), IL-1β and TNF-α down-regulation (Park et al., 2016). On the other hand, a limited number of studies defined some of the target genes in connection with biological processes in corneal epithelial cells. GTPase RhoA, Rac1 and Cdc42 proteins, identified in this analysis, were described in maintaining corneal functions and barrier homeostasis: Zhu et al, (2014) observed expansion of HCECs monolayers due to RhoA-ROCK-non-canonical BMP (bone morphogenic protein)-NF-kB pathway activation, following p120 catenin and Kaiso proteins knocking-down; Cui et al. (2018) demonstrated *in vivo* that the exposition to airborne particulate can induce delayed corneal epithelium wound closure by suppressing RhoA activity; Ortega et al. (2016) showed that the activation of RhoA and Rac1 in response to a stimulus disrupting endothelial cell–cell junctions preserves corneal endothelial barrier function; Rac1 was described as an important factor for corneal cell adhesion, motility promotion by fibronectin and wound healing (Kimura et al., 2006); Cdc42, was able to promote wound repair and significantly improve the migration of human corneal epithelial cells in monolayer scratch assay (Pothula et al., 2013).

Taken together, literature data seem to be globally consistent with the results presented in this study: in fact, the above-mentioned genes are targeted by miRNAs which are mainly hypo-expressed after NGF incubation, leaving to hypothesize expression increase of their protein products, and evidencing the NGF biological activity on corneal cells.

In conclusion, this *in silico* research makes available interesting and novel insights, in terms of miRNAs/target genes identification, suitable to shed light on some of unknown epigenetics mechanisms induced by NGF in corneal epithelial cells. Absolutely, data here provided need further experimental validation, even though the analysis of AKT protein expression in response to NGF treatments can be considered a preliminary demonstration of the strength of *in silico* results. The emerging role of microRNAs in putatively modulating and directing the response of corneal epithelial cells to NGF here evidenced is of potential high impact. MicroRNAs are RNase-protected and very stable molecules, even in difficult conditions or extended storage. For this reason, they are considered as suitable biomarkers for diagnosis, and, when dysregulated, therapy targets to rehabilitate normal physiological conditions. Innovative therapeutic strategies are based on the use of synthetic miRNA inhibitors or mimics molecules, which, when appropriately delivered, can inhibit or restore normal expression levels and functions of hyper-expressed or down-regulated miRs, respectively (Tessitore et al., 2016). In this scenario, the characterization of miRNAs dysregulation in corneal biological processes or disease pathogenesis/progression can be of translational value, being this body part easily attainable by targeted therapies, since the eye is among the few organs where gene silencing can be successfully achieved. This innovative therapy is under evaluation for some eye disorders in several, mainly preclinical, trials. Simple local administration of naked siRNAs, a class of double stranded RNA fully complementary to mRNA and able to silence genes by endonucleolytic cleavage, demonstrated reduced systemic side effects and toxicity (Lam et al., 2015). On the contrary, although their potential therapeutic role is under evaluation for more in-depth-studied and high-impact diseases, such as cancer or cardiovascular diseases (Chakraborty et al., 2017; Chakraborty et al., 2018), little is still known about the possibility to use miRNAs for the treatment of anterior and/or posterior eye's segment disorders. Arguably, this requires more exhaustive understanding about their specific role in this organ and related diseases. In this scenario, by improving the knowledge in the field, also miRNAs might represent in the future a suitable method for the treatment of ocular disorders.

CONCLUSION

In this study we analysed the effects on epithelial corneal cells after treatment with three different NGF bioformulations (NGF1, NGF2, NGF3). The attention was focused on miRNAs expression levels modulation and, subsequently, an *in silico* analysis which led us to obtain an extensive list of novel putative target genes and pathways was performed. In addition, this study allowed to define the miRNAs expression in non-pathological corneal cells and, helping to better understand possible miRs' expression changes in eye diseases. This would make it possible to use miRs as a biomarkers and therapeutic target. Even though this analysis needs further validation *in vitro* and *in vivo*, at the biological level, currently ongoing, results demonstrated that all the NGF bioformulations here tested induced genes functionally involved in pathways whose functions are highly relevant, in particular that of the neurotrophin signalling. With this regard, by comparing the bioformulations, NGF1 regulated less than a half of miRNAs induced by NGF2 or NGF3. Of course, the absolute number of genes targeted by the latter two bioformulations was much higher, but, in comparison to the number of miRNAs modulated by every single bioformulation, NGF1 seemed able to regulate more genes. Furthermore, despite this, no relevant differences between NGF1, of proven therapeutic efficacy, and NGF2/NGF3 appeared in terms of efficacy in inducing neurotrophin pathway, as all the bioformulations drove through survival and proliferations signals. In conclusion, data led to hypothesize that NGF1 activity might be more specific than that of NGF2 and NGF3.

REFERENCES

1. Abu-Amero KK, Helwa I, Al-Muammar A, Strickland S, Hauser MA, Allingham RR, Liu Y. Screening of the Seed Region of MIR184 in Keratoconus Patients from Saudi Arabia. Biomed Res Int. 2015; 2015:604508.

2. Achberger S, Aldrich W, Tubbs R, Crabb JW, Singh AD, Triozzi PL: Circulating immune cell and microRNA in patients with uveal melanoma developing metastatic disease. Mol Immunol 2104; 58: 182–186.

3. Adijanto J, Castorino JJ, Wang ZX, Maminishkis A, Grunwald GB, Philp NJ. Microphthalmia-associated transcription factor (MITF) promotes differentiation of human retinal pigment epithelium (RPE) by regulating microRNAs-204/211 expression. J Biol Chem. 2012 Jun 8;287(24):20491-503.

4. Alevizos I, Alexander S, Turner RJ, Illei GG. MicroRNA expression profiles as biomarkers of minor salivary gland inflammation and dysfunction in Sjögren's syndrome. Arthritis Rheum. 2011 Feb;63(2):535-44.

5. Aloe L, Bracci-Laudiero L, Bonini S, Manni L. The expanding role of nerve growth factor: from neurotrophic activity to immunologic diseases. Allergy. 1997 Sep;52(9):883-94.

6. Aloe L, Rocco ML, Balzamino BO, Micera A. Nerve Growth Factor: A Focus on Neuroscience and Therapy. Curr Neuropharmacol. 2015;13(3):294-303.

7. Aloe L, Rocco ML, Bianchi P, Manni L. Nerve growth factor: from the early discoveries to the potential clinical use. J Transl Med. 2012;10:239.

8. An J, Chen X, Chen W, Liang R, Reinach PS, Yan D, Tu L. MicroRNA Expression Profile and the Role of miR-204 in Corneal Wound Healing. Invest Ophthalmol Vis Sci. 2015 Jun;56(6):3673-83.

9. Apfel SC. Nerve growth factor for the treatment of diabetic neuropathy: what went wrong, what went right, and what does the future hold? Int Rev Neurobiol. 2002;50:393-413.

10. Aroli M, Peluso I, Marigo V, Banfi S. Identification and characterization of microRNAs expressed in the mouse eye. Invest Ophthalmol Vis Sci. 2007 Feb;48(2):509-15.

11. Arora A, McKay GJ, Simpson DA. Prediction and verification of miRNA expression in human and rat retinas. Invest Ophthalmol Vis Sci. 2007 Sep;48(9):3962-7.

12. Askou AL, Alsing S, Holmgaard A, Bek T, Corydon TJ. Dissecting microRNA dysregulation in age-related macular degeneration: new targets for eye gene therapy. Acta Ophthalmol. 2018 Feb;96(1):9-23.

13. Azizi B, Ziaei A, Fuchsluger T, Schmedt T, Chen Y, Jurkunas UV. p53-regulated increase in oxidative-stress--induced apoptosis in Fuchs endothelial corneal dystrophy: a native tissue model. Invest Ophthalmol Vis Sci. 2011 Dec 2;52(13):9291-7.

14. Bai Y, Dergham P, Nedev H, Xu J, Galan A, Rivera JC, ZhiHua S, Mehta HM, Woo SB, Sarunic MV, Neet KE, Saragovi HU. Chronic and acute models of retinal neurodegeneration TrkA activity are neuroprotective whereas p75NTR activity is neurotoxic through a paracrine mechanism. J Biol Chem. 2010 Dec 10;285(50):39392-400.

15. Bartel DP. MicroRNAs: genomics, biogenesis, mechanism, and function. Cell. 2004 Jan 23; 116(2): 281-97.

16. Bazzoni F, Rossato M, Fabbri M, Gaudiosi D, Mirolo M, Mori L, Tamassia N, Mantovani A, Cassatella MA, Locati M. Induction and regulatory function of miR-9 in human monocytes and neutrophils exposed to proinflammatory signals. Proc Natl Acad Sci U S A. 2009 Mar 31;106(13):5282-7.

17. Berber P, Grassmann F, Kiel C, Weber BH. An Eye on Age-Related Macular Degeneration: The Role of MicroRNAs in Disease Pathology. Mol Diagn Ther. 2017 Feb;21(1):31-43.

18. Bernabei R, Landi F, Bonini S, Onder G, Lambiase A, Pola R, et al. Effect of topical application of nerve-growth factor on pressure ulcers. Lancet. 1999;354(9175):307.

19. Blanco-Mezquita T, Martinez-Garcia C, Proença R, Zieske JD, Bonini S, Lambiase A, Merayo-Lloves J. Nerve growth factor promotes corneal epithelial migration by enhancing expression of matrix metalloprotease-9. Invest Ophthalmol Vis Sci. 2013 Jun 4;54(6):3880-90.

20. Bonini S, Lambiase A, Rama P, Caprioglio G, Aloe L. Topical treatment with nerve growth factor for neurotrophic keratitis. Ophthalmology. 2000;107:1347-51.

21. Bonini S, Lambiase A, Rama P, Filatori I, Allegretti M, Chao W, et al. Phase I Trial of Recombinant Human Nerve Growth Factor for Neurotrophic Keratitis. Ophthalmology. 2018;125:1468-1471.

22. Bonini S, Lambiase A, Rama P, Sinigaglia F, Allegretti M, Chao W, et al. Phase II Randomized, Double-Masked, Vehicle-Controlled Trial of Recombinant Human Nerve Growth Factor for Neurotrophic Keratitis. Ophthalmology. 2018;125:1332-1343.

23. Boyd SR, Tan D, Bunce C, Gittos A, Neale MH, Hungerford JL, Charnock-Jones S, Cree IA. Vascular endothelial growth factor is elevated in ocular fluids of eyes harbouring uveal melanoma: identification of a potential therapeutic window. Br J Ophthalmol 2002; 86:448-52.

24. Budni J, Bellettini-Santos T, Mina F, Garcez ML, Zugno AI. The involvement of BDNF, NGF and GDNF in aging and Alzheimer's disease. Aging Dis. 2015 Oct 1;6(5):331-41.

25. Cakmak H, Gokmen E, Bozkurt G, Kocaturk T, Ergin K. Effects of sunitinib and bevacizumab on VEGF and miRNA levels on corneal neovascularization. Cutan Ocul Toxicol. 2018 Jun;37(2):191-195.

26. Calin GA, Dumitru CD, Shimizu M, Bichi R, Zupo S, Noch E, et al. Frequent deletions and down-regulation of micro- RNA genes miR15 and miR16 at 13q14 in chronic lymphocytic leukemia. Proc Natl Acad Sci U S A 2002;99:15524–9.

27. Calin GA, Sevignani C, Dumitru CD, Hyslop T, Noch E, Yendamuri S, Shimizu M, Rattan S, Bullrich F, Negrini M, Croce CM. Human microRNA genes are frequently located at fragile sites and genomic regions involved in cancers. Proc Natl Acad Sci U S A. 2004 Mar 2;101(9):2999-3004.

28. Calza L, Giardino L, Giuliani A, Aloe L, Levi-Montalcini R. Nerve growth factor control of neuronal expression of angiogenetic and vasoactive factors. Proc Natl Acad Sci U S A. 2001 Mar 27;98(7):4160-5.

29. Cambier S, Gline S, Mu D, Collins R, Araya J, Dolganov G, Einheber S, Boudreau N, Nishimura SL. Integrin alpha(v)beta8-mediated activation of transforming growth factor-beta by perivascular astrocytes: an angiogenic control switch. Am J Pathol. 2005 Jun;166(6):1883-94.

30. Carmignoto G, Maffei L, Candeo P, Canella R, Comelli C. Effect of NGF on the survival of rat retinal ganglion cells following optic nerve section. J Neurosci. 1989 Apr;9(4):1263-72.

31. Chakraborty C, Sharma AR, Sharma G, Doss CGP, Lee SS. Therapeutic miRNA and siRNA: Moving from Bench to Clinic as Next Generation Medicine. Mol Ther Nucleic Acids. 2017 Sep 15; 8:132-143.

32. Chakraborty C, Sharma AR, Sharma G, Sarkar BK, Lee SS. The novel strategies for next-generation cancer treatment: miRNA combined with chemotherapeutic agents for the treatment of cancer. Oncotarget. 2018 Jan 23;9(11):10164-10174.

33. Chang R, Yi S, Tan X, Huang Y, Wang Q, Su G, Zhou C, Cao Q, Yuan G, Kijlstra A, Yang P. MicroRNA-20a-5p suppresses IL-17 production by targeting OSM and CCL1 in patients with Vogt-Koyanagi-Harada disease. Br J Ophthalmol. 2018 Feb;102(2):282-290.

34. Chao MV. Neurotrophins and their receptors: a convergence point for many signalling pathways. Nat Rev Neurosci. 2003 Apr;4(4):299-309.

35. Chen X, Wang J, Shen H, Lu J, Li C, Hu DN, Dong XD, Yan D, Tu L. Epigenetics, microRNAs, and carcinogenesis: functional role of microRNA-137 in uveal melanoma. Invest Ophthalmol Vis Sci. 2011 Mar 2;52(3):1193-9.

36. Chiaretti A, Piastra M, Caresta E, Nanni L, Aloe L. Improving ischaemic skin revascularisation by nerve growth factor in a child with crush syndrome. Arch Dis Child. 2002 Nov;87(5):446-8.

37. Coassin M, Lambiase A, Costa N, De Gregorio A, Sgrulletta R, Sacchetti M, Aloe L, Bonini S. Efficacy of topical nerve growth factor treatment in dogs affected by dry eye. Graefes Arch Clin Exp Ophthalmol. 2005 Feb;243(2):151-5.

38. Cohen S, Levi-Montalcini R, Hamburger V. A nerve growth-stimulating factor isolated from sarcom as 37 and 180. Proc Natl Acad Sci U S A. 1954 Oct;40(10):1014-8.

39. Cohen S. Purification and metabolic effects of a nerve growth-promoting protein from snake venom. J Biol Chem. 1959 May;234(5):1129-37.

40. Collinson JM, Quinn JC, Hill RE, West JD. The roles of Pax6 in the cornea, retina, and olfactory epithelium of the developing mouse embryo. Dev Biol. 2003 Mar 15;255(2):303-12.

41. Conte I, Carrella S, Avellino R, Karali M, Marco-Ferreres R, Bovolenta P, Banfi S. miR-204 is required for lens and retinal development via Meis2 targeting. Proc Natl Acad Sci U S A. 2010 Aug 31;107(35):15491-6.

42. Creemers EE, Tijsen AJ, Pinto YM. Circulating microRNAs: novel biomarkers and extracellular communicators in cardiovascular disease? Circ Res. 2012 Feb 3;110(3):483-95.

43. Cui YH, Hu ZX, Gao ZX, Song XL, Feng QY, Yang G, Li ZJ, Pan HW. Airborne particulate matter impairs corneal epithelial cells migration via disturbing FAK/RhoA signaling pathway and cytoskeleton organization. Nanotoxicology. 2018 May;12(4):312-324.

44. Cui YH, Li HY, Gao ZX, Liang N, Ma SS, Meng FJ, Li ZJ, Pan HW. Regulation of Apoptosis by miR-122 in Pterygium via Targeting Bcl-w. Invest Ophthalmol Vis Sci.2016 Jul 1;57(8):3723-30.

45. Dalgard CL, Gonzalez M, deNiro JE, O'Brien JM. Differential microRNA-34a expression and tumor suppressor function in retinoblastoma cells. Invest Ophthalmol Vis Sci. 2009 Oct;50(10):4542-51.

46. Damiani D, Alexander JJ, O'Rourke JR, McManus M, Jadhav AP, Cepko CL, Hauswirth WW, Harfe BD, Strettoi E. Dicer inactivation leads to progressive functional and structural degeneration of the mouse retina. J Neurosci. 2008 May 7;28(19):4878-87.

47. Diederichs S, Haber DA. Dual role for argonautes in microRNA processing and posttranscriptional regulation of microRNA expression. Cell. 2007 Dec 14;131(6):1097-108.

48. Drewry M, Helwa I, Allingham RR, Hauser MA, Liu Y miRNA Profile in Three Different Normal Human Ocular Tissues by miRNA-Seq. Invest Ophthalmol Vis Sci. 2016 Jul 1;57(8):3731-9

49. Dunmire JJ, Lagouros E, Bouhenni RA, Jones M, Edward DP. MicroRNA in aqueous humor from patients with cataract. Exp Eye Res. 2013 Mar; 108:68-71.

50. Engelsvold DH, Utheim TP, Olstad OK, Gonzalez P, Eidet JR, Lyberg T, Trøseid AM, Dartt DA, Raeder S. miRNA and mRNA expression profiling identifies members of the miR-200 family as potential regulators of epithelial-mesenchymal transition in pterygium. Exp Eye Res. 2013 Oct; 115:189-98.

51. Ertekin S, Yıldırım O, Dinç E, Ayaz L, Fidancı SB, Tamer L. Evaluation of circulating miRNAs in wet age-related macular degeneration. Mol Vis. 2014 Jul 29; 20:1057-66. eCollection 2014.

52. Falsini B, Iarossi G, Chiaretti A, Ruggiero A, Manni L, Galli-Resta L, Corbo G, Abed E. NGF eye-drops topical administration in patients with retinitis pigmentosa, a pilot study. J Transl Med. 2016 Jan 9; 14:8.

53. Freund-Michel V, Frossard N. The nerve growth factor and its receptors in airway inflammatory diseases. Pharmacol Ther. 2008 Jan;117(1):52-76.

54. Fu Y, Hou B, Weng C, Liu W, Dai J, Zhao C, Yin ZQ. Functional ectopic neuritogenesis by retinal rod bipolar cells is regulated by miR-125b-5p during retinal remodeling in RCS rats. Sci Rep. 2017 Apr 21;7(1):1011.

55. Fuchshofer R, Tamm ER. The role of TGF-β in the pathogenesis of primary open-angle glaucoma. Cell Tissue Res. 2012 Jan;347(1):279-90.

56. Funari VA, Winkler M, Brown J, Dimitrijevich SD, Ljubimov AV, Saghizadeh M. Differentially expressed wound healing-related microRNAs in the human diabetic cornea. PLoS One. 2013;8:e84425. doi: 10.1371/journal.pone.0084425.

57. Gallant-Behm CL, Propp S, Jackson AL. The miR-29b mimic remlarsen inhibits fibrosis of a corneal ulcer by preventing EMT and reducing profibrotic gene expression. Poster 5316-C0249 http://www.miragen.com/publications/2019/04/ARVO-2019-The-miR-29b-mimic-remlarsen-inhibits-fibrosis-of-a-corneal-ulcer-by-preventing-EMT-and-reducing-profibrotic-gene-expression.pdf

58. Gao J, Wang Y, Zhao X, Chen P, Xie L. MicroRNA-204-5p-Mediated Regulation of SIRT1 Contributes to the Delay of Epithelial Cell Cycle Traversal in Diabetic Corneas. Invest Ophthalmol Vis Sci. 2015 Jan 22;56(3):1493-504.

59. Giannaccare G, Pellegrini M, Bovone C, Spena R, Senni C, Scorcia V, Busin M. Anti-VEGF Treatment in Corneal Diseases. Curr Drug Targets. 2020 Mar 19.

60. Guaiquil VH, Dimailing G, Zhou Q. Expression of axon guidance proteins in the trigeminal ganglia and cornea and their recovery after cornea subbasal nerve injury. Investigative Ophthalmology & Visual Science July 2019, Vol.60, 3217, ARVO meeting abstract, 2019

61. Hamada N, Fujita Y, Kojima T, Kitamoto A, Akao Y, Nozawa Y, Ito M. MicroRNA expression profiling of NGF-treated PC12 cells revealed a critical role for miR-221 in neuronal differentiation. Neurochem Int. 2012 Jun;60(8):743-50.

62. Hassell JR, Birk DE. The molecular basis of corneal transparency. Exp Eye Res. 2010 Sep;91(3):326-35.

63. He L, Hannon GJ. MicroRNAs: small RNAs with a big role in gene regulation. Nat Rev Genet. 2004 Jul;5(7):522-31.

64. He L, He X, Lim LP, de Stanchina E, Xuan Z, Liang Y, Xue W, Zender L, Magnus J, Ridzon D, Jackson AL, Linsley PS, Chen C, Lowe SW, Cleary MA, Hannon GJ. A microRNA component of the p53 tumour suppressor network. Nature. 2007 Jun 28;447(7148):1130-4.

65. He S, Sun H, Huang Y, Dong S, Qiao C, Zhang S, Wang C, Zheng F, Yan M, Yang G. Identification and Interaction Analysis of Significant Genes and MicroRNAs in Pterygium. Biomed Res Int. 2019 Jun 25; 2019:2767512.

66. He XL, Garcia KC. Structure of nerve growth factor complexed with the shared neurotrophin receptor p75. Science. 2004 May 7;304(5672):870-5.

67. Hébert SS, Horré K, Nicolaï L, Papadopoulou AS, Mandemakers W, Silahtaroglu AN, Kauppinen S, Delacourte A, De Strooper B. Loss of microRNA cluster miR-29a/b-1 in sporadic Alzheimer's disease correlates with increased BACE1/beta-secretase expression. Proc Natl Acad Sci U S A. 2008 Apr 29;105(17):6415-20.

68. Hirata H, Hibasami H, Yoshida T, Ogawa M, Matsumoto M, Morita A, Uchida A. Nerve growth factor signaling of p75 induces differentiation and ceramide-mediated apoptosis in Schwann cells cultured from degenerating nerves. Glia. 2001 Dec;36(3):245-58.

69. Hong J, Qian T, Le Q, Sun X, Wu J, Chen J, Yu X, Xu J. NGF promotes cell cycle progression by regulating D-type cyclins via PI3K/Akt and MAPK/Erk activation in human corneal epithelial cells. Mol Vis. 2012; 18:758-64.

70. Hughes AE, Bradley DT, Campbell M, Lechner J, Dash DP, Simpson DA, Willoughby CE. Mutation altering the miR-184 seed region causes familial keratoconus with cataract. Am J Hum Genet. 2011 Nov 11;89(5):628-33.

71. Ibanez-Ventoso, C., Vora, M. & Driscoll, M. Sequence relationships among C. elegans, D. melanogaster and human microRNAs highlight the extensive conservation of microRNAs in biology. PLoS One. 2008 Jul 30;3(7):e2818.

72. Iliopoulos D, Hirsch HA, Struhl K. An epigenetic switch involving NF-kappaB, Lin28, Let-7 MicroRNA, and IL6 links inflammation to cell transformation. Cell. 2009 Nov 13;139(4):693-706.

73. Jayaram H, Cepurna WO, Johnson EC, Morrison JC. MicroRNA Expression in the Glaucomatous Retina. Invest Ophthalmol Vis Sci. 2015 Dec;56(13):7971-82.

74. Jiang CR, Li HL. The value of MiR-146a and MiR-4484 expressions in the diagnosis of anti-SSA antibody positive Sjogren syndrome and the correlations with prognosis. Eur Rev Med Pharmacol Sci. 2018 Aug;22(15):4800-4805.

75. Kaneko Y, Wu GS, Saraswathy S, Vasconcelos-Santos DV, Rao NA. Immunopathologic processes in sympathetic ophthalmia as signified by microRNA profiling. Invest Ophthalmol Vis Sci. 2012 Jun 28;53(7):4197-204.

76. Karagkouni D, Paraskevopoulou MD, Chatzopoulos S, Vlachos IS, Tastsoglou S, Kanellos I, Papadimitriou D, et al. DIANA-TarBase v8: a decade-long collection of experimentally supported miRNA-gene interactions. Nucleic Acids Res. 2018 Jan 4;46(D1): D239-D245.

77. Kimura K, Kawamoto K, Teranishi S, Nishida T. Role of Rac1 in fibronectin-induced adhesion and motility of human corneal epithelial cells. Invest Ophthalmol Vis Sci. 2006; 47:4323-9.

78. Kovacs B, Lumayag S, Cowan C, Xu S. MicroRNAs in early diabetic retinopathy in streptozotocin-induced diabetic rats. Invest Ophthalmol Vis Sci. 2011 Jun 21;52(7):4402-9.

79. Kozomara A, Griffiths-Jones S (2011) miRBase: integrating microRNA annotation and deep-sequencing data. Nucleic Acids Res 39(Database issue): D152–D157. doi: 10.1093/ nar/gkq1027

80. La Torre A, Georgi S, Reh TA. Conserved microRNA pathway regulates developmental timing of retinal neurogenesis. Proc Natl Acad Sci U S A. 2013 Jun 25;110(26): E2362-70.

81. Lagos-Quintana M, Rauhut R, Meyer J, Borkhardt A, Tuschl T. New microRNAs from mouse and human. RNA. 2003 Feb;9(2):175-9.

82. Lam JK, Chow MY, Zhang Y, Leung SW. siRNA Versus miRNA as Therapeutics for Gene Silencing. Mol Ther Nucleic Acids. 2015;4:e252. doi: 10.1038/mtna.2015.23.

83. Lambiase A, Aloe L, Centofanti M, Parisi V, Báo SN, Mantelli F, Colafrancesco V, Manni GL, Bucci MG, Bonini S, Levi-Montalcini R. Experimental and clinical evidence of neuroprotection by nerve growth factor eye drops: Implications for glaucoma. Proc Natl Acad Sci U S A. 2009 Aug 11;106(32):13469-74.

84. Lambiase A, Aloe L. Nerve growth factor delays retinal degeneration in C3H mice. Graefes Arch Clin Exp Ophthalmol. 1996 Aug;234 Suppl 1:S96-100.

85. Lambiase A, Bonini S, Manni L, Ghinelli E, Tirassa P, Rama P, Aloe L. Intraocular production and release of nerve growth factor after iridectomy. Invest Ophthalmol Vis Sci. 2002 Jul;43(7):2334-40.

86. Lambiase A, Manni L, Bonini S, Rama P, Micera A, Aloe L. Nerve growth factor promotes corneal healing: structural, biochemical, and molecular analyses of rat and human corneas. Invest Ophthalmol Vis Sci. 2000 Apr;41(5):1063-9.

87. Lambiase A, Mantelli F, Sacchetti M, Rossi S, Aloe L, Bonini S. Clinical applications of NGF in ocular diseases. Arch Ital Biol. 2011a; 149:283-92.

88. Lambiase A, Micera A, Sacchetti M, Cortes M, Mantelli F, Bonini S. Alterations of tear neuromediators in dry eye disease. Arch Ophthalmol. 2011b Aug;129(8):981-6.

89. Lambiase A, Rama P, Bonini S, Caprioglio G, Aloe L. Topical treatment with nerve growth factor for corneal neurotrophic ulcers. N Engl J Med. 1998 Apr 23;338(17):1174-80.

90. Lambiase A, Sacchetti M, Bonini S. Nerve growth factor therapy for corneal disease. Curr Opin Ophthalmol. 2012;23:296-302.

91. Lan W, Chen S, Tong L. MicroRNA-215 Regulates Fibroblast Function: Insights from a Human Fibrotic Disease. Cell Cycle. 2015;14(12):1973-84.

92. Lan W, Petznick A, Heryati S, Rifada M, Tong L. Nuclear Factor-κB: central regulator in ocular surface inflammation and diseases. Ocul Surf. 2012 Jul;10(3):137-4

93. Lau N.C.,Lim L.P., E.G. Weinstein, D.P. Bartel, An abundant class of tiny RNAs with probable regulatory roles in Caenorhabditis elegans. Science, 294,2001, 858–862.

94. Lau PW, Guiley KZ, De N, Potter CS, Carragher B, MacRae IJ. The molecular architecture of human Dicer. Nat Struct Mol Biol. 2012 Mar 18;19(4):436-40.

95. Lee HK, Lee KS, Kim HC, Lee SH, Kim EK. Nerve growth factor concentration and implications in photorefractive keratectomy vs laser in situ keratomileusis. Am J Ophthalmol. 2005 Jun;139(6):965-71.

96. Lee M, Goraya N, Kim S, Cho SH. Hippo-yap signaling in ocular development and disease. Dev Dyn. 2018 Jun;247(6):794-806. doi: 10.1002/dvdy.24628.

97. Lee RC, Feinbaum RL, Ambros V. The C. elegans heterochronic gene lin-4 encodes small RNAs with antisense complementarity to lin-14. Cell. 1993 Dec 3;75(5):843-54.

98. Lee SK, Teng Y, Wong HK, Ng TK, Huang L, Lei P, Choy KW, Liu Y, Zhang M, Lam DS, Yam GH, Pang CP. MicroRNA-145 regulates human corneal epithelial differentiation. PLoS One. 2011;6(6):e21249.

99. Lee Y, Jeon K, Lee JT, Kim S, Kim VN. MicroRNA maturation: stepwise processing and subcellular localization. EMBO J. 2002 Sep 2;21(17):4663-70.

100. Levi-Montalcini R. The nerve growth factor: thirty-five years later. Biosci Rep. 1987 Sep;7(9):681-99.

101. Li G, Luna C, Qiu J, Epstein DL, Gonzalez P. Targeting of integrin beta1 and kinesin 2alpha by microRNA 183. J Biol Chem. 2009 Feb 19;285(8):5461-71.

102. Li J, Qi X, Wang X, Li W, Li Y, Zhou Q. PTEN inhibition facilitates diabetic corneal epithelial regeneration by reactivating Akt signaling pathway. Trans Vis Sci Tech. 2020;9(3):5.

103. Li W, Sun X, Wang Z, Li R, Li L. The effect of nerve growth factor on differentiation of corneal limbal epithelial cells to conjunctival goblet cells in vitro. Mol Vis. 2010 Dec 15;16:2739-44.

104. Li X, Zhou H, Tang W, Guo Q, Zhang Y. Transient downregulation of microRNA-206 protects alkali burn injury in mouse cornea by regulating connexin 43. Int J Clin Exp Pathol. 2015 Mar 1;8(3):2719-27.

105. Li Y, Kowdley KV. MicroRNAs in common human diseases. Genomics Proteomics Bioinformatics. 2012 Oct;10(5):246-53.

106. Li Z, Rana TM. Therapeutic Targeting of microRNAs: Current Status and Future Challenges. Nat Rev Drug Discov 2014 Aug;13(8):622-38.

107. Lin D, Halilovic A, Yue P, Bellner L, Wang K, Wang L, Zhang C. Inhibition of miR-205 impairs the wound-healing process in human corneal epithelial cells by targeting KIR4.1 (KCNJ10). Invest Ophthalmol Vis Sci. 2013 Sep 11;54(9):6167-78.

108. Lindberg RL, Hoffmann F, Mehling M, Kuhle J, Kappos L. Altered expression of miR-17-5p in CD4+ lymphocytes of relapsing-remitting multiple sclerosis patients. Eur J Immunol. 2010 Mar;40(3):888-98.

109. Liu B, Wu X, Liu B, Wang C, Liu Y, Zhou Q, Xu K. MiR-26a enhances metastasis potential of lung cancer cells via AKT pathway by targeting PTEN. Biochim Biophys Acta. 2012 Nov;1822(11):1692-704.

110. Lukiw WJ, Surjyadipta B, Dua P, Alexandrov PN. Common micro RNAs (miRNAs) target complement factor H (CFH) regulation in Alzheimer's disease (AD) and in age-related macular degeneration (AMD). Int J Biochem Mol Biol. 2012;3(1):105-16.

111. Luna C, Li G, Huang J, Qiu J, Wu J, Yuan F, Epstein DL, Gonzalez P. Regulation of trabecular meshwork cell contraction and intraocular pressure by miR-200c. PLoS One 2012; 7:e51688.

112. Luna C, Li G, Qiu J, Epstein DL, Gonzalez P. Role of miR-29b on the regulation of the extracellular matrix in human trabecular meshwork cells under chronic oxidative stress. Mol Vis. 2009 Nov 28;15:2488-97.

113. Luna G, Li G, Qiu J, Epstein DL, Gonzalez P. MicroRNA-24 regulates the processing of latent TGFβ1 during cyclic mechanical stress in human trabecular meshwork cells through direct targeting of FURIN. J Cell Physiol 2011;226: 1407–1414.

114. Ma A, Boulton M, Zhao B, Connon C, Cai J, Albon J. A role for notch signaling in human corneal epithelial cell differentiation and proliferation. Invest Ophthalmol Vis Sci. 2007 Aug;48(8):3576-85.

115. Ma A, Zhao B, Boulton M, Albon J. A role for Notch signaling in corneal wound healing. Wound Repair Regen. 2011 Jan-Feb;19(1):98-106.

116. Mantelli F, Mauris J, Argüeso P. The ocular surface epithelial barrier and other mechanisms of mucosal protection: from allergy to infectious diseases. Curr Opin Allergy Clin Immunol. 2013 Oct;13(5):563-8.

117. Maquart FX, Monboisse JC. Extracellular matrix and wound healing. Pathol Biol (Paris). 2014 Apr;62(2):91-5.

118. McDonald NQ, Chao MV. Structural Determinants of Neurotrophin Action. J Biol Chem. 1995 Aug 25;270(34):19669-72.

119. McGill GG, Haq R, Nishimura EK, Fisher DE. c-Met expression is regulated by Mitf in the melanocyte lineage. J Biol Chem. 2006 Apr 14;281(15):10365-73. Epub 2006 Feb 2. PubMed PMID: 16455654.

120. Ménard C, Rezende FA, Miloudi K, Wilson A, Tétreault N, Hardy P, SanGiovanni JP, De Guire V, Sapieha P. MicroRNA signatures in vitreous humour and plasma of patients with exudative AMD. Oncotarget. 2016 Apr 12;7(15):19171-84.

121. Micera A, Lambiase A, Aloe L, Bonini S, Levi-Schaffer F, Bonini S. Nerve growth factor involvement in the visual system: implications in allergic and neurodegenerative diseases. Cytokine Growth Factor Rev. 2004 Dec;15(6):411-7.

122. Micera A, Lambiase A, Puxeddu I, Aloe L, Stampachiacchiere B, Levi-Schaffer F, Bonini S, Bonini S. Nerve growth factor effect on human primary fibroblastic-keratocytes: possible mechanism during corneal healing. Exp Eye Res. 2006 Oct;83(4):747-57.

123. Micera A, Vigneti E, Pickholtz D, Reich R, Pappo O, Bonini S, Maquart FX, Aloe L, Levi-Schaffer F. Nerve growth factor displays stimulatory effects on human skin and lung fibroblasts, demonstrating a direct role for this factor in tissue repair. Proc Natl Acad Sci U S A. 2001 May 22;98(11):6162-7.

124. Montalban E, Mattugini N, Ciarapica R, Provenzano C, Savino M, Scagnoli F, Prosperini G, Carissimi C, Fulci V, Matrone C, Calissano P, Nasi S. MiR-21 is an Ngf-modulated microRNA that supports Ngf signaling and regulates neuronal degeneration in PC12 cells. Neuromolecular Med. 2014 Jun;16(2):415-30.

125. Morrison JC, Moore CG, Deppmeier LM, Gold BG, Meshul CK, Johnson EC. A rat model of chronic pressure-induced optic nerve damage. Exp Eye Res. 1997 Jan;64(1):85-96.

126. Mortuza R, Feng B, Chakrabarti S. miR-195 regulates SIRT1-mediated changes in diabetic retinopathy. Diabetologia. 2014 May;57(5):1037-46.

127. Mukwaya A, Jensen L, Peebo B, Lagali N. MicroRNAs in the cornea: Role and implications for treatment of corneal neovascularization. Ocul Surf. 2019 Jul;17(3):400-411.

128. Mukwaya A, Lindvall JM,Xeroudaki M, Peebo B, Ali Z,Lennikov A, Jensen L, Lagali N. A Microarray Whole-Genome Gene Expression Dataset in a Rat Model of Inflammatory Corneal Angiogenesis. Sci Data. 2016 Nov 22;3:160103.

129. Murad N, Kokkinaki M, Gunawardena N, Gunawan MS, Hathout Y, Janczura KJ, et al. MiR-184 regulates ezrin, LAMP-1 expression, affects phagocytosis in human retinal pigment epithelium and is downregulated in age-related macular degeneration. FEBS J. 2014;281:5251–64.

130. Nunes DN, Dias-Neto E, Cardó-Vila M, Edwards JK, Dobroff AS, Giordano RJ, Mandelin J, Brentani HP, Hasselgren C, Yao VJ, Marchiò S, Pereira CA, Passetti F, Calin GA, Sidman RL, Arap

W, Pasqualini R. Synchronous down-modulation of miR-17 family members is an early causative event in the retinal angiogenic switch. Proc Natl Acad Sci U S A. 2015 Mar 24;112(12):3770-5.

131. Nykjaer A, Willnow TE, Petersen CM. p75NTR--live or let die. Curr Opin Neurobiol. 2005 Feb;15(1):49-57.

132. O'Neill LA. Outfoxing Foxo1 with miR-182. Nat Immunol. 2010 Nov;11(11):983-4.

133. Ortega MC, Santander-García D, Marcos-Ramiro B, Barroso S, Cox S, Jiménez-Alfaro I, et al. Activation of Rac1 and RhoA Preserve Corneal Endothelial Barrier Function. Invest Ophthalmol Vis Sci. 2016;57:6210-6222.

134. Papa S, Zazzeroni F, Pham CG, Bubici C, Franzoso G. Linking JNK signaling to NF-kappaB: a key to survival. J Cell Sci. 2004 Oct 15;117(Pt 22):5197-208.

135. Paraskevopoulou MD, Georgakilas G, Kostoulas N, Vlachos IS, Vergoulis T, Reczko M, Filippidis C, Dalamagas T, Hatzigeorgiou AG. DIANA-microT web server v5.0: service integration into miRNA functional analysis workflows. Nucleic Acids Res. 2013 Jul;41(Web Server issue):W169-73.

136. Park JH, Kang SS, Kim JY, Tchah H. Nerve Growth Factor Attenuates Apoptosis and Inflammation in the Diabetic Cornea. Invest Ophthalmol Vis Sci. 2016;57:6767-6775.

137. Pasquinelli AE, Reinhart BJ, Slack F, Martindale MQ, Kuroda MI, Maller B, Hayward DC, Ball EE, Degnan B, Müller P, Spring J, Srinivasan A, Fishman M, Finnerty J, Corbo J, Levine M, Leahy P, Davidson E, Ruvkun G. Conservation of the sequence and temporal expression of let-7 heterochronic regulatory RNA. Nature. 2000 Nov 2;408(6808):86-9.

138. Pattarawarapan M, Burgess K. Molecular basis of neurotrophin-receptor interactions. J Med Chem. 2003 Dec 4;46(25):5277-91.

139. Pauley KM, Stewart CM, Gauna AE, Dupre LC, Kuklani R, Chan AL, et al. Altered miR-146a expression in Sjögren's syndrome and its functional role in innate immunity. Eur J Immunol. 2011;41:2029-39.

140. Peng H, Kaplan N, Hamanaka RB, Katsnelson J, Blatt H, Yang W, Hao L, Bryar PJ, Johnson RS, Getsios S, Chandel NS, Lavker RM. microRNA-31/factor-inhibiting hypoxia-inducible factor 1 nexus regulates keratinocyte differentiation. Proc Natl Acad Sci U S A. 2012 Aug 28;109(35):14030-4.

141. Platania CBM, Maisto R, Trotta MC, D'Amico M, Rossi S, Gesualdo C, D'Amico G, Balta C, Herman H, Hermenean A, Ferraraccio F, Panarese I, Drago F, Bucolo C. Retinal and circulating miRNA expression patterns in diabetic retinopathy: An in silico and in vivo approach. Br J Pharmacol. 2019 Jul;176(13):2179-2194.

142. Pogue AI, Li YY, Cui J-G, Zhao Y, Kruck TPA, Percy ME, et al. Characterization of an NF-kappaB-regulated, miRNA- 146a-mediated down-regulation of complement factor H (CFH) in metal-sulfate-stressed human brain cells. J Inorg Biochem. 2009;103:1591–5.

143. Pothula S, Bazan HE, Chandrasekher G. Regulation of Cdc42 expression and signaling is critical for promoting corneal epithelial wound healing. Invest Ophthalmol Vis Sci. 2013;54:5343-52.

144. Purves D, Augustine GJ, Fitzpatrick D, et al. Neuroscience. 2nd edition. Editors. Sunderland (MA): Sinauer Associates; 2001. https://www.ncbi.nlm.nih.gov/books/NBK10885/

145. Raghunath A, Perumal E. Micro-RNAs and their roles in eye disorders. Ophthalmic Res. 2015;53(4):169-86.

146. Ragusa M, Caltabiano R, Russo A, Puzzo L, Avitabile T, Longo A, Toro MD, Di Pietro C, Purrello M, Reibaldi M. MicroRNAs in vitreus humor from patients with ocular diseases. Mol Vis. 2013;19:430-40.

147. Rassi DM, De Paiva CS, Dias LC, Módulo CM, Adriano L, Fantucci MZ, et al. Review: MicroRNAS in ocular surface and dry eye diseases. Ocul Surf. 2017;15:660-669.

148. Rodriguez Benavente MC, Argüeso P. Glycosylation pathways at the ocular surface. Biochem Soc Trans. 2018 Apr 17;46(2):343-350.

149. Rupaimoole R, Slack FJ. MicroRNA therapeutics: towards a new era for the management of cancer and other diseases. Nat Rev Drug Discov. 2017 Mar;16(3):203-222.

150. Ryan DG, Oliveira-Fernandes M, Lavker RM. MicroRNAs of the mammalian eye display distinct and overlapping tissue specificity. Mol Vis. 2006 Oct 17;12:1175-84.

151. Santovito D, De Nardis V, Marcantonio P, Mandolini C, Paganelli C, Vitale E, Buttitta F, Bucci M, Mezzetti A, Consoli A, Cipollone F. Plasma exosome microRNA profiling unravels a new potential modulator of adiponectin pathway in diabetes: effect of glycemic control. J Clin Endocrinol Metab. 2014 Sep;99(9):E1681-5.

152. Shaham O, Gueta K, Mor E, Oren-Giladi P, Grinberg D, Xie Q, Cvekl A, Shomron N, Davis N, Keydar-Prizant M, Raviv S, Pasmanik-Chor M, Bell RE, Levy C, Avellino R, Banfi S, Conte I, Ashery-Padan R. Pax6 regulates gene expression in the vertebrate lens through miR-204. PLoS Genet. 2013;9(3):e1003357.

153. Shalom-Feuerstein R, Serror L, De La Forest Divonne S, Petit I, Aberdam ECamargo L, Damour O, Vigouroux C, Solomon A, Gaggioli C, Itskovitz-Eldor J, Ahmad S, Aberdam D. Pluripotent stem cell model reveals essential roles for miR-450b-5p and miR-184 in embryonic corneal lineage specification. Stem Cells. 2012 May;30(5):898-909.

154. Shen J, Yang X, Xie B, Chen Y, Swaim M, Hackett SF, Campochiaro PA. MicroRNAs regulate ocular neovascularization. Mol Ther. 2008 Jul;16(7):1208-16.

155. Shi H, Zheng LY, Zhang P, Yu CQ. miR-146a and miR-155 expression in PBMCs from patients with Sjögren's syndrome. J Oral Pathol Med. 2014 Nov;43(10):792-7.

156. Sposato V, Parisi V, Manni L, Antonucci MT, Di Fausto V, Sornelli F, Aloe L. Glaucoma alters the expression of NGF and NGF receptors in visual cortex and geniculate nucleus of rats: effect of eye NGF application. Vision Res. 2009 Jan;49(1):54-63.

157. Sridhar MS. Anatomy of cornea and ocular surface. Indian J Ophthalmol. 2018 Feb;66(2):190-194.

158. Sun HY, Lv AK, Yao H. Relationship of miRNA-146a to primary Sjögren's syndrome and to systemic lupus erythematosus: a meta-analysis. Rheumatol Int. 2017 Aug;37(8):1311-1316.

159. Sundermeier TR, Palczewski K. The impact of microRNA gene regulation on the survival and function of mature cell types in the eye. FASEB J. 2016 Jan;30(1):23-33.

160. Taganov KD, Boldin MP, Chang K-J, Baltimore D. NF-kB dependent induction of microRNA miR-146, an inhibitor targeted to signaling proteins of innate immune responses. Proc Natl Acad Sci U S A 2006; 103:12481–6.

161. Tandon A, Tovey JC, Sharma A, Gupta R, Mohan RR. Role of transforming growth factor Beta in corneal function, biology and pathology. Curr Mol Med. 2010 Aug;10(6):565-78.

162. Taniuchi M, Clark HB, Johnson EM Jr. Induction of nerve growth factor receptor in Schwann cells after axotomy. Proc Natl Acad Sci U S A. 1986 Jun;83(11):4094-8.

163. Tessitore A, Cicciarelli G, Mastroiaco V, Vecchio FD, Capece D, Verzella D, Fischietti M, Vecchiotti D, Zazzeroni F, Alesse E. Therapeutic Use of MicroRNAs in Cancer. Anticancer Agents Med Chem. 2016;16(1):7-19.

164. Toyono T, Usui T, Villarreal G Jr, Kallay L, Matthaei M, Vianna LM, Zhu AY,et al. MicroRNA-29b Overexpression Decreases Extracellular Matrix mRNA and Protein Production in Human Corneal Endothelial Cells. Cornea. 2016 Nov;35(11):1466-1470.

165. Tuveri M, Generini S, Matucci-Cerinic M, Aloe L. NGF, a useful tool in the treatment of chronic vasculitic ulcers in rheumatoid arthritis. Lancet. 2000;356:1739-40.

166. Urbich C, Kaluza D, Frömel T,Knau A, Bennewitz K, Boon RA, Bonauer A, et al. MicroRNA-27a/b Controls Endothelial Cell Repulsion and Angiogenesis by Targeting Semaphorin 6A. Blood. 2012 Feb 9;119(6):1607-16.

167. Vadlapatla RK, Vadlapudi AD, Mitra AK. Hypoxia-inducible factor-1 (HIF-1): a potential target for intervention in ocular neovascular diseases. Curr Drug Targets. 2013 Jul;14(8):919-35.

168. Velez-Montoya R, Oliver SC, Olson JL, Fine SL, Quiroz-Mercado H, Mandava N. Current knowledge and trends in age-related macular degeneration: genetics, epidemiology, and prevention. Retina. 2014 Mar;34(3):423-41.

169. Villarreal G Jr, Oh DJ, Kang MH, Rhee DJ. Coordinated regulation of extracellular matrix synthesis by the microRNA-29 family in the trabecular meshwork. Invest Ophthalmol Vis Sci. 2011 May 1;52(6):3391-7.

170. Vlachos IS, Zagganas K, Paraskevopoulou MD, Georgakilas G, Karagkouni D, Vergoulis T, et al. DIANA-miRPath v3.0: deciphering microRNA function with experimental support. Nucleic Acids Res. 2015;43:W460-6.

171. Wang FE, Zhang C, Maminishkis A, Dong L, Zhi C, Li R, Zhao J, Majerciak V, Gaur AB, Chen S, Miller SS. MicroRNA-204/211 alters epithelial physiology. FASEB J. 2010 May;24(5):1552-71.

172. Wang J, Wang X, Wu G, Hou D, Hu Q: MiR-365b-3p, down-regulated in retinoblastoma, regulates cell cycle progression and apoptosis of human retinoblastoma cells by targeting PAX6. FEBS Lett 2013a; 587: 1779–1786.

173. Wang S, Li K. MicroRNA-96 regulates RGC-5 cell growth through caspase-dependent apoptosis. Int J Clin Exp Med. 2014 Oct 15;7(10):3694-702.

174. Wang T, Li F, Geng W, Ruan Q, Shi W. MicroRNA-122 ameliorates corneal allograft rejection through the downregulation of its target CPEB1. Cell Death Discov. 2017 May 15;3:17021.

175. Wang Y, Li W, Zang X, Chen N, Liu T, Tsonis PA, Huang Y. MicroRNA-204-5p regulates epithelial-to-mesenchymal transition during human posterior capsule opacification by targeting SMAD4. Invest Ophthalmol Vis Sci. 2013b Jan 14;54(1):323-32.

176. Wang YM, Ng TK, Choy KW, Wong HK, Chu WK, Pang CP, Jhanji V. Histological and microRNA Signatures of Corneal Epithelium in Keratoconus. J Refract Surg. 2018 Mar 1;34(3):201-211.

177. Warde-Farley D, Donaldson SL, Comes O, Zuberi K, Badrawi R, Chao P, Franz M, et al. The GeneMANIA prediction server: biological network integration for gene prioritization and predicting gene function. Nucleic Acids Res. 2010 Jul;38(Web Server issue):W214-20.

178. Wiesmann C, de Vos AM. Nerve growth factor: structure and function. Cell Mol Life Sci. 2001 May;58(5-6):748-59.

179. Wightman B, T.R.Burglin,J. Gatto,P. Arasu,Ruvkun G, Negative regulatory sequences in the lin-14 3′-untranslated region are necessary to generate a temporal switch during Caenorhabditis elegans development. Genes Dev.,5,1991,1813– 1824.

180. Winkler MA, Dib C, Ljubimov AV, Saghizadeh M. Targeting miR-146a to treat delayed wound healing in human diabetic organ-cultured corneas. PLoS One. 2014;9:e114692

181. Wu CW, Cheng YW, Hsu NY, Yeh KT, Tsai YY, Chiang CC, Wang WR, Tung JN. MiRNA-221 negatively regulated downstream p27Kip1 gene expression involvement in pterygium pathogenesis. Mol Vis. 2014 Jul 21;20:1048-56.

182. Wu D, Qian T, Hong J, Li G, Shi W, Xu J. MicroRNA-494 inhibits nerve growth factor-induced cell proliferation by targeting cyclin D1 in human corneal epithelial cells. Mol Med Rep. 2017 Oct;16(4):4133-4142.

183. Xiao B, Liu Z, Li B-S, Tang B, Li W, Guo G, et al. Induction of microRNA-155 during Helicobacter pylori infection and its negative regulatory role in the inflammatory response. J Infect Dis 2009;200: 916–25.

184. Xie X, Lu J, Kulbokas EJ, Golub TR, Mootha V, Lindblad-Toh K, Lander ES, Kellis M. Systematic discovery of regulatory motifs in human promoters and 3' UTRs by comparison of several mammals. Nature. 2005 Mar 17;434(7031):338-45.

185. Xu S. microRNA expression in the eyes and their significance in relation to functions. Prog Retin Eye Res. 2009 Mar;28(2):87-116.

186. Yan D, Dong XD, Chen X, Yao S, Wang L, Wang J, Wang C, Hu DN, Qu J, Tu L. Role of microRNA-182 in posterior uveal melanoma: regulation of tumor development through MITF, BCL2 and cyclin D2. PLoS One. 2012;7(7):e40967.

187. Yan D, Zhou X, Chen X, Hu DN, Dong XD, Wang J, Lu F, Tu L, Qu J. MicroRNA-34a inhibits uveal melanoma cell proliferation and migration through downregulation of c-Met. Invest Ophthalmol Vis Sci. 2009 Apr;50(4):1559-65.

188. Yang J, Wang N, Luo X. Intraocular miR-211 exacerbates pressure-induced cell death in retinal ganglion cells via direct repression of FRS2 signaling. Biochem Biophys Res Commun. 2018 Sep 18;503(4):2984-2992.

189. Yi R, Qin Y, Macara IG, Cullen BR. Exportin-5 mediates the nuclear export of pre-microRNAs and short hairpin RNAs. Genes Dev. 2003 Dec 15;17(24):3011-6.

190. You L, Kruse FE, Völcker HE. Neurotrophic factors in the human cornea. Invest Ophthalmol Vis Sci. 2000 Mar;41(3):692-702.

191. Yu J, Peng H, Ruan Q, Fatima A, Getsios S, Lavker RM. MicroRNA-205 promotes keratinocyte migration via the lipid phosphatase SHIP2. FASEB J. 2010 Oct;24(10):3950-9.

192. Zampetaki A, Kiechl S, Drozdov I, Willeit P, Mayr U, Prokopi M, Mayr A, Weger S, Oberhollenzer F, Bonora E, Shah A, Willeit J, Mayr M. Plasma microRNA profiling reveals loss of endothelial miR-126 and other microRNAs in type 2 diabetes. Circ Res. 2010 Sep 17;107(6):810-7.

193. Zhang M, Zhou Q, Luo Y, Nguyen T, Rosenblatt MI, Guaiquil VH. Semaphorin3A induces nerve regeneration in the adult cornea-a switch from its repulsive role in development. PLoS One. 2018 Jan 25;13(1):e0191962.

194. Zhao JJ, Yang J, Lin J, Yao N, Zhu Y, Zheng J, Xu J, Cheng JQ, Lin JY, Ma X. Identification of miRNAs associated with tumorigenesis of retinoblastoma by miRNA microarray analysis. Childs Nerv Syst. 2009 Jan;25(1):13-20.

195. Zhou Q, Xiao X, Wang C, Zhang X, Li F, Zhou Y, Kijlstra A, Yang P. Decreased microRNA-155 expression in ocular Behcet's disease but not in Vogt Koyanagi Harada syndrome. Invest Ophthalmol Vis Sci. 2012 Aug 17;53(9):5665-74.

196. Zhu Q, Sun W, Okano K, Chen Y, Zhang N, Maeda T, Palczewski K. Sponge transgenic mouse model reveals important roles for the microRNA-183 (miR 183)/96/182 cluster in postmitotic photoreceptors of the retina. J Biol Chem. 2011 Sep 9;286(36):31749-60.

197. Zhu YT, Han B, Li F, Chen SY, Tighe S, Zhang S, Tseng SC. Knockdown of both p120 catenin and Kaiso promotes expansion of human corneal endothelial monolayers via RhoA-ROCK-noncanonical BMP-NFκB pathway. Invest Ophthalmol Vis Sci. 2014;55:1509-18

198. Zilahi E, Tarr T, Papp G, Griger Z, Sipka S, Zeher M. Increased microRNA-146a/b, TRAF6 gene and decreased IRAK1 gene expressions in the peripheral mononuclear cells of patients with Sjögren's syndrome. Immunol Lett. 2012;141:165-8.

199. Zuzic M, Rojo Arias JE, Wohl SG, Busskamp V. Retinal miRNA Functions in Health and Disease. Genes (Basel). 2019 May 17;10(5).

ANNEX

Table S1a- **KEGG pathways Tarbase NGF1**. KEGG pathways (n=59) identified by considering significant dysregulated miRNAs (n=21) after NGF1 treatment, as detected by Diana-Tarbase (experimentally supported) analysis.

KEGG pathway	p-value	#genes	#miRNAs
ECM-receptor interaction	1.94E-31	39	15
Adherens junction	1.37E-11	47	16
Proteoglycans in cancer	1.75E-09	85	19
Prion diseases	3.82E-09	12	15
Viral carcinogenesis	5.99E-09	91	17
Focal adhesion	1.90E-07	102	18
Protein processing in endoplasmic reticulum	2.99E-07	87	18
Pathways in cancer	1.04E-06	163	19
Fatty acid biosynthesis	1.76E-06	4	5
Chronic myeloid leukemia	3.63E-06	42	17
Cell cycle	5.44E-06	62	17
Glioma	5.44E-06	34	18
Renal cell carcinoma	5.44E-06	38	19
Hepatitis B	5.79E-06	66	17
Oocyte meiosis	6.01E-06	55	18
Bacterial invasion of epithelial cells	6.63E-06	41	16
Ubiquitin mediated proteolysis	7.71E-06	70	17
Prostate cancer	1.30E-05	47	17
Neurotrophin signaling pathway	2.11E-05	60	18
Small cell lung cancer	3.09E-05	46	17
PI3K-Akt signaling pathway	4.53E-05	141	18
Transcriptional misregulation in cancer	7.92E-05	70	19
Hippo signaling pathway	9.95E-05	59	18
Central carbon metabolism in cancer	0.000127	34	16
p53 signaling pathway	0.000134	37	17
Shigellosis	0.000227	33	14
Colorectal cancer	0.000227	33	16
Lysine degradation	0.000344	20	14
FoxO signaling pathway	0.000344	62	17
Endocytosis	0.000446	84	17
Acute myeloid leukemia	0.000496	29	17
Endometrial cancer	0.000515	27	16
Pancreatic cancer	0.000515	34	17
TGF-beta signaling pathway	0.000952	36	17
Epstein-Barr virus infection	0.001042	87	17
Sulfur metabolism	0.004825	5	5
Fatty acid elongation	0.005702	6	6
Non-small cell lung cancer	0.005702	27	17
Bladder cancer	0.005702	22	18
NF-kappa B signaling pathway	0.006256	32	17
Arrhythmogenic right ventricular cardiomyopathy (ARVC)	0.006413	26	16
HIF-1 signaling pathway	0.006698	47	18
Spliceosome	0.007512	56	18
Amoebiasis	0.011039	41	14
Sphingolipid signaling pathway	0.011162	49	18
Regulation of actin cytoskeleton	0.019688	79	16
AMPK signaling pathway	0.019688	53	17
Thyroid hormone signaling pathway	0.019688	52	19
Circadian rhythm	0.023121	16	13
mRNA surveillance pathway	0.024669	40	16
RNA transport	0.024669	64	18
Pathogenic Escherichia coli infection	0.024739	26	13
Dorso-ventral axis formation	0.024739	15	15
Insulin signaling pathway	0.024739	57	16
Hepatitis C	0.024739	53	17
N-Glycan biosynthesis	0.037600	19	14
Prolactin signaling pathway	0.039423	32	17
Thyroid cancer	0.048754	14	16
Melanoma	0.049562	29	17

Table S1b- KEGG pathways microT NGF1. KEGG pathways (n=49) identified by considering significant dysregulated miRNAs (n=21) after NGF1 treatment, as detected by Diana-MicroT-CDS (predicted) analysis.

KEGG pathway	p-value	#genes	#miRNAs
ECM-receptor interaction	1.74E-15	34	15
Prion diseases	1.12E-08	9	9
ErbB signaling pathway	1.12E-08	46	13
Glioma	3.13E-06	32	13
Focal adhesion	3.13E-06	92	16
Proteoglycans in cancer	3.13E-06	84	19
Renal cell carcinoma	3.35E-06	36	12
Glycosaminoglycan biosynthesis - heparan sulfate / heparin	5.01E-06	14	8
Choline metabolism in cancer	1.32E-05	51	14
FoxO signaling pathway	0.000104	58	14
PI3K-Akt signaling pathway	0.000104	127	20
Amoebiasis	0.000116	43	14
Adherens junction	0.000182	37	14
Lysine degradation	0.000186	19	10
mTOR signaling pathway	0.000192	33	14
Thyroid hormone signaling pathway	0.000211	49	18
Ras signaling pathway	0.000345	85	17
Rap1 signaling pathway	0.000661	84	16
Axon guidance	0.000768	51	15
Glycosaminoglycan biosynthesis - keratan sulfate	0.001064	8	6
Pathways in cancer	0.001065	142	18
Adrenergic signaling in cardiomyocytes	0.001896	54	18
p53 signaling pathway	0.004244	31	14
TGF-beta signaling pathway	0.004617	33	16
Glycosaminoglycan biosynthesis - chondroitin sulfate / dermatan sulfate	0.004672	8	6
Small cell lung cancer	0.005864	38	12
Neurotrophin signaling pathway	0.005864	50	16
Hippo signaling pathway	0.006055	49	15
HIF-1 signaling pathway	0.006421	45	14
Glycosphingolipid biosynthesis - lacto and neolacto series	0.006829	11	8
AMPK signaling pathway	0.007480	49	18
Prostate cancer	0.008563	38	13
Prolactin signaling pathway	0.008642	27	12
Circadian rhythm	0.008642	17	15
cGMP-PKG signaling pathway	0.100938	62	17
Regulation of actin cytoskeleton	0.012869	76	15
Phosphatidylinositol signaling system	0.014451	32	13
Biotin metabolism	0.014567	1	1
Long-term depression	0.014567	26	13
Sphingolipid signaling pathway	0.014740	44	16
Non-small cell lung cancer	0.019923	24	10
MAPK signaling pathway	0.021152	90	17
Pancreatic cancer	0.024846	26	10
Melanoma	0.024846	30	12
Estrogen signaling pathway	0.029488	35	15
Wnt signaling pathway	0.035309	55	16
Chagas disease (American trypanosomiasis)	0.038162	38	15
Bacterial invasion of epithelial cells	0.042141	28	13
Adipocytokine signaling pathway	0.043705	27	13

*Table S2a- **KEGG pathways Tarbase NGF2.** KEGG pathways (n=75) identified by considering significant dysregulated miRNAs (n=52) after NGF2 treatment, as detected by Diana-Tarbase (experimentally supported) analysis

KEGG pathway	p-value	#genes	#miRNAs
Proteoglycans in cancer	7.93E-17	168	42
Protein processing in endoplasmic reticulum	6.99E-10	142	41
Cell cycle	6.99E-10	105	42
Viral carcinogenesis	6.99E-10	162	42
Renal cell carcinoma	3.19E-09	61	42
Hippo signaling pathway	1.12E-07	121	40
Fatty acid metabolism	5.39E-07	37	28
Pathways in cancer	5.83E-07	296	43
Glioma	1.81E-06	55	39
Signaling pathways regulating pluripotency of stem cells	1.81E-06	112	41
Endocytosis	1.90E-06	164	42
Acute myeloid leukemia	2.24E-06	52	37
Chronic myeloid leukemia	2.39E-06	64	39
Colorectal cancer	7.91E-06	55	42
Neurotrophin signaling pathway	1.11E-05	99	41
Estrogen signaling pathway	1.64E-05	81	39
Ubiquitin mediated proteolysis	3.93E-05	110	43
Adherens junction	4.25E-05	63	40
Pancreatic cancer	5.54E-05	56	40
Thyroid hormone signaling pathway	7.58E-05	95	40
Hepatitis B	0.000113	111	41
TNF signaling pathway	0.000138	88	41
Fatty acid biosynthesis	0.000262	9	21
Lysine degradation	0.000281	40	32
Prostate cancer	0.000288	73	41
Steroid biosynthesis	0.000409	17	25
Non-small cell lung cancer	0.000647	46	39
mTOR signaling pathway	0.00066	52	37
TGF-beta signaling pathway	0.00066	63	40
Prion diseases	0.000746	24	33
N-Glycan biosynthesis	0.000931	40	32
Transcriptional misregulation in cancer	0.001262	130	42
Central carbon metabolism in cancer	0.003517	54	37
Endometrial cancer	0.003517	43	38
Wnt signaling pathway	0.003694	103	41
Lysosome	0.003696	89	37
FoxO signaling pathway	0.003696	102	42
Citrate cycle (TCA cycle)	0.004311	25	28
NF-kappa B signaling pathway	0.004311	64	38
Prolactin signaling pathway	0.004311	55	39
Thyroid cancer	0.004311	25	39
Insulin signaling pathway	0.004311	107	40
HTLV-I infection	0.004311	189	42
Fatty acid elongation	0.004973	17	26
Vitamin B6 metabolism	0.005487	6	11
p53 signaling pathway	0.007366	55	41
ErbB signaling pathway	0.007684	70	38
HIF-1 signaling pathway	0.007684	81	40
Oocyte meiosis	0.008215	84	37
Shigellosis	0.008215	50	37
Epstein-Barr virus infection	0.008215	148	41
Small cell lung cancer	0.008215	67	41
Focal adhesion	0.008215	151	42
Axon guidance	0.008711	93	39
Epithelial cell signaling in Helicobacter pylori infection	0.009013	54	39

Regulation of actin cytoskeleton	0.009606	152	41
Glycosaminoglycan biosynthesis - chondroitin sulfate / dermatan sulfate	0.009703	15	20
Bacterial invasion of epithelial cells	0.011275	58	40
Sphingolipid signaling pathway	0.011275	86	41
Other types of O-glycan biosynthesis	0.011856	22	25
Basal cell carcinoma	0.011856	44	33
Spliceosome	0.011856	100	42
AMPK signaling pathway	0.014004	94	42
Fc gamma R-mediated phagocytosis	0.019006	69	39
RNA transport	0.019006	123	42
Bladder cancer	0.022955	31	38
Glycosaminoglycan biosynthesis - heparan sulfate / heparin	0.023659	18	25
One carbon pool by folate	0.026028	16	23
Carbon metabolism	0.026028	75	37
Melanoma	0.026028	53	40
2-Oxocarboxylic acid metabolism	0.035051	12	17
MAPK signaling pathway	0.03583	177	42
B cell receptor signaling pathway	0.038206	55	37
Progesterone-mediated oocyte maturation	0.046894	66	42
Vibrio cholerae infection	0.048741	42	33

Table S2b- KEGG pathways microT NGF2. KEGG pathways (n=74) identified by considering significant dysregulated miRNAs (n=52) after NGF2 treatment, as detected by Diana-MicroT-CDS (predicted) analysis

KEGG pathway	p-value	#genes	#miRNAs
Proteoglycans in cancer	1.86E-07	134	46
Pathways in cancer	9.83E-07	249	50
Fatty acid biosynthesis	5.74E-06	7	17
Hippo signaling pathway	5.74E-06	97	40
Morphine addiction	5.74E-06	61	41
Long-term depression	1.31E-05	43	38
GABAergic synapse	1.46E-05	60	40
Axon guidance	1.72E-05	82	46
Oxytocin signaling pathway	1.72E-05	108	46
Estrogen signaling pathway	1.99E-05	68	43
Neurotrophin signaling pathway	3.13E-05	84	46
Adherens junction	3.31E-05	52	41
Endocytosis	4.27E-05	128	42
Thyroid hormone signaling pathway	4.27E-05	79	44
Mucin type O-Glycan biosynthesis	5.82E-05	19	22
Renal cell carcinoma	6.10E-05	50	41
Gap junction	6.85E-05	60	41
Prolactin signaling pathway	9.45E-05	50	40
Glioma	9.54E-05	45	38
Wnt signaling pathway	9.54E-05	93	42
Focal adhesion	9.54E-05	134	47
Adrenergic signaling in cardiomyocytes	0.000177	95	42
Glycosaminoglycan biosynthesis - heparan sulfate / heparin	0.0002	18	24
Glutamatergic synapse	0.000319	73	40
Melanogenesis	0.000391	69	40
Chronic myeloid leukemia	0.000391	51	40
ErbB signaling pathway	0.000391	63	42
Rap1 signaling pathway	0.000413	131	47
Choline metabolism in cancer	0.00066	70	44
Phosphatidylinositol signaling system	0.000681	55	35
Signaling pathways regulating pluripotency of stem cells	0.000718	88	41
TGF-beta signaling pathway	0.000878	51	37
Circadian entrainment	0.001211	65	42
Dilated cardiomyopathy	0.001474	62	36
Retrograde endocannabinoid signaling	0.002068	67	40
FoxO signaling pathway	0.002111	86	42
Cholinergic synapse	0.002111	73	42
Ras signaling pathway	0.002111	137	47
Prion diseases	0.002118	14	16
Thyroid hormone synthesis	0.002219	45	34
cAMP signaling pathway	0.002219	123	43
MAPK signaling pathway	0.002656	153	48
Bacterial invasion of epithelial cells	0.003973	50	42
Cocaine addiction	0.004203	30	28
Regulation of actin cytoskeleton	0.004398	132	46
Hedgehog signaling pathway	0.004669	37	31
Basal cell carcinoma	0.006623	39	34
p53 signaling pathway	0.006623	46	38
cGMP-PKG signaling pathway	0.008169	101	46
Colorectal cancer	0.008843	43	37
Hypertrophic cardiomyopathy (HCM)	0.009177	55	34
Sphingolipid signaling pathway	0.013904	72	42
Platelet activation	0.016253	78	45
ECM-receptor interaction	0.01666	51	36
Acute myeloid leukemia	0.020003	37	34

Ubiquitin mediated proteolysis	0.020003	82	43
PI3K-Akt signaling pathway	0.020003	193	48
Biotin metabolism	0.024575	2	4
Amphetamine addiction	0.024575	40	34
Pancreatic cancer	0.024989	40	34
Prostate cancer	0.025559	55	38
Gastric acid secretion	0.027101	49	40
Insulin secretion	0.032214	54	39
Dorso-ventral axis formation	0.033233	20	32
Melanoma	0.033233	45	35
GnRH signaling pathway	0.033233	57	39
Dopaminergic synapse	0.033233	80	43
Non-small cell lung cancer	0.033831	36	40
Vasopressin-regulated water reabsorption	0.036918	29	28
AMPK signaling pathway	0.036918	76	43
Glycosaminoglycan biosynthesis - keratan sulfate	0.042851	10	12
Notch signaling pathway	0.04362	32	29
mTOR signaling pathway	0.04362	40	39
Lysine degradation	0.044071	30	37

Table S3a- KEGG pathways Tarbase NGF3. KEGG pathways (n=77) identified by considering significant dysregulated miRNAs (n=58) after NGF3 treatment, as detected by Diana-Tarbase (experimentally supported) analysis

KEGG pathway	p-value	#genes	#miRNAs
Proteoglycans in cancer	7.24E-18	173	52
Viral carcinogenesis	3.47E-11	168	52
Cell cycle	3.94E-11	110	51
Hippo signaling pathway	6.06E-09	126	50
Protein processing in endoplasmic reticulum	1.19E-08	142	51
Renal cell carcinoma	1.74E-08	62	51
Chronic myeloid leukemia	1.87E-08	68	49
Pathways in cancer	4.34E-08	307	52
Endocytosis	5.88E-08	169	51
Glioma	9.95E-08	57	49
Acute myeloid leukemia	1.35E-06	53	47
ErbB signaling pathway	1.46E-06	75	48
Ubiquitin mediated proteolysis	2.70E-06	116	52
Neurotrophin signaling pathway	8.65E-06	101	50
Spliceosome	8.65E-06	108	51
Estrogen signaling pathway	1.07E-05	82	49
Prostate cancer	1.67E-05	77	51
Signaling pathways regulating pluripotency of stem cells	3.01E-05	111	50
Pancreatic cancer	6.24E-05	57	49
Adherens junction	7.16E-05	64	49
Colorectal cancer	8.67E-05	54	51
Glycosaminoglycan biosynthesis - chondroitin sulfate / dermatan sulfate	0.00014	16	23
Lysine degradation	0.00018	41	42
Thyroid hormone signaling pathway	0.000183	96	50
Non-small cell lung cancer	0.000185	48	49
Endometrial cancer	0.000231	46	48
Hepatitis B	0.000313	112	51
Fatty acid metabolism	0.000316	35	40
Sphingolipid signaling pathway	0.000483	92	51
Thyroid cancer	0.000549	26	45
TNF signaling pathway	0.00056	88	49
FoxO signaling pathway	0.0006	107	52
HTLV-I infection	0.0006	198	52
Prion diseases	0.000657	25	38
Steroid biosynthesis	0.000678	17	27
Oocyte meiosis	0.000801	88	49
TGF-beta signaling pathway	0.000801	64	49
Focal adhesion	0.000801	159	52
Bacterial invasion of epithelial cells	0.000847	63	51
Fatty acid biosynthesis	0.001595	8	27
Small cell lung cancer	0.002291	70	51
Citrate cycle (TCA cycle)	0.002301	26	33
Wnt signaling pathway	0.002301	105	50
Insulin signaling pathway	0.002301	110	50
RNA transport	0.002859	129	52
mTOR signaling pathway	0.00346	51	45
NF-kappa B signaling pathway	0.003856	65	47
Regulation of actin cytoskeleton	0.004023	158	51
Prolactin signaling pathway	0.005187	57	49
Other types of O-glycan biosynthesis	0.005222	24	33
Bladder cancer	0.005222	33	47
Vitamin B6 metabolism	0.006949	6	11
p53 signaling pathway	0.006949	56	50
Central carbon metabolism in cancer	0.007334	55	46
Melanoma	0.007753	56	48

Shigellosis	0.008241	51	48
Terpenoid backbone biosynthesis	0.008332	19	30
HIF-1 signaling pathway	0.009834	82	48
Epstein-Barr virus infection	0.009834	151	50
Progesterone-mediated oocyte maturation	0.009834	70	51
Basal cell carcinoma	0.009958	45	40
Notch signaling pathway	0.014158	40	46
Phosphatidylinositol signaling system	0.017875	62	49
2-Oxocarboxylic acid metabolism	0.019136	13	23
Circadian rhythm	0.019136	27	41
Fc gamma R-mediated phagocytosis	0.024525	70	48
Long-term potentiation	0.027473	53	45
Transcriptional misregulation in cancer	0.035585	131	52
Epithelial cell signaling in Helicobacter pylori infection	0.03701	53	50
Lysosome	0.039058	87	47
Base excision repair	0.040109	24	36
Glycosaminoglycan biosynthesis - heparan sulfate / heparin	0.041236	18	30
One carbon pool by folate	0.041236	16	36
Vibrio cholerae infection	0.041236	43	44
B cell receptor signaling pathway	0.041236	56	48
MAPK signaling pathway	0.041236	182	52
RNA degradation	0.041766	61	49

Table S3b- KEGG pathways microT NGF3. KEGG pathways (n=82) identified by considering significant dysregulated miRNAs (n=58) after NGF3 treatment, as detected by Diana-MicroT-CDS (predicted) analysis

KEGG pathway	p-value	#genes	#miRNAs
Proteoglycans in cancer	9.77E-13	148	51
Morphine addiction	3.75E-10	66	45
Pathways in cancer	2.16E-09	273	55
ErbB signaling pathway	1.45E-08	73	48
Renal cell carcinoma	7.71E-08	56	47
Axon guidance	2.41E-07	92	50
Circadian entrainment	1.06E-06	71	47
Fatty acid biosynthesis	1.10E-06	9	19
Thyroid hormone signaling pathway	2.82E-06	87	48
Ras signaling pathway	2.82E-06	156	53
Rap1 signaling pathway	2.82E-06	148	53
Prolactin signaling pathway	3.40E-06	55	42
Signaling pathways regulating pluripotency of stem cells	4.46E-06	100	47
Hippo signaling pathway	1.02E-05	106	47
GABAergic synapse	1.03E-05	63	43
Phosphatidylinositol signaling system	1.33E-05	59	40
Estrogen signaling pathway	1.38E-05	69	46
FoxO signaling pathway	1.64E-05	98	47
Endocytosis	1.66E-05	138	50
Oxytocin signaling pathway	1.74E-05	112	50
Pancreatic cancer	2.21E-05	51	42
Glioma	2.34E-05	48	45
Neurotrophin signaling pathway	2.34E-05	90	52
Cholinergic synapse	2.82E-05	81	46
Focal adhesion	2.82E-05	143	52
Retrograde endocannabinoid signaling	2.94E-05	72	47
MAPK signaling pathway	4.57E-05	171	53
Gap junction	7.08E-05	63	45
Choline metabolism in cancer	0.000106	76	48
Wnt signaling pathway	0.000145	97	47
Adherens junction	0.000199	55	47
Prostate cancer	0.000287	65	47
Glycosaminoglycan biosynthesis - heparan sulfate / heparin	0.000384	19	29
Chronic myeloid leukemia	0.000668	53	44
Adrenergic signaling in cardiomyocytes	0.000668	99	48
Melanoma	0.000997	52	42
PI3K-Akt signaling pathway	0.001002	214	53
Long-term depression	0.00104	41	42
Glutamatergic synapse	0.001113	75	46
Regulation of actin cytoskeleton	0.001113	143	51
Sphingolipid signaling pathway	0.001181	79	47
Viral carcinogenesis	0.001269	114	46
cAMP signaling pathway	0.001533	131	49
Glycosaminoglycan biosynthesis - keratan sulfate	0.001538	11	14
N-Glycan biosynthesis	0.001606	32	35
Insulin secretion	0.001606	61	45
cGMP-PKG signaling pathway	0.00201	109	50
Acute myeloid leukemia	0.002103	42	39
Colorectal cancer	0.002815	46	43
Protein processing in endoplasmic reticulum	0.003225	109	47
Hedgehog signaling pathway	0.003596	39	30
Platelet activation	0.003664	84	49
Melanogenesis	0.003728	69	43
TGF-beta signaling pathway	0.003984	56	43
p53 signaling pathway	0.004296	49	43

Mucin type O-Glycan biosynthesis	0.00492	18	24
Lysine degradation	0.00501	31	43
T cell receptor signaling pathway	0.00501	71	44
mTOR signaling pathway	0.006035	45	43
Non-small cell lung cancer	0.006035	39	43
Vasopressin-regulated water reabsorption	0.006201	33	30
Insulin signaling pathway	0.006201	93	50
Ubiquitin mediated proteolysis	0.007558	88	46
Dopaminergic synapse	0.00838	87	49
Prion diseases	0.010945	14	18
Endometrial cancer	0.016204	36	39
mRNA surveillance pathway	0.019805	60	44
GnRH signaling pathway	0.022291	61	45
Cocaine addiction	0.024574	30	31
Bacterial invasion of epithelial cells	0.024574	52	47
Basal cell carcinoma	0.024826	39	35
Inositol phosphate metabolism	0.027182	43	37
Dilated cardiomyopathy	0.029691	60	40
Notch signaling pathway	0.034525	34	31
Type II diabetes mellitus	0.035594	33	40
Hepatitis B	0.035594	88	50
Biotin metabolism	0.036719	2	6
Progesterone-mediated oocyte maturation	0.039912	59	45
Vascular smooth muscle contraction	0.041683	73	48
Small cell lung cancer	0.04422	56	44
HIF-1 signaling pathway	0.046493	68	42
Central carbon metabolism in cancer	0.04764	45	41

Table S1c- Comparison between **NGF1**-induced Tarbase and microT-CDS pathways

Shared Tarbase-MicroT pathways (n.29)	Tarbase pathways (n.30)	MicroT-CDS pathways (n.20)
Adherens junction	Acute myeloid leukemia	Adipocytokine signaling pathway
Amoebiasis	Arrhythmogenic right ventricular cardiomyopathy (ARVC)	Adrenergic signaling in cardiomyocytes
AMPK signaling pathway	Bladder cancer	Axon guidance
Bacterial invasion of epithelial cells	Cell cycle	Biotin metabolism
Circadian rhythm	Central carbon metabolism in cancer	cGMP-PKG signaling pathway
ECM-receptor interaction	Chronic myeloid leukemia	Chagas disease (American trypanosomiasis)
Focal adhesion	Colorectal cancer	Choline metabolism in cancer
FoxO signaling pathway	Dorso-ventral axis formation	ErbB signaling pathway
Glioma	Endocytosis	Estrogen signaling pathway
HIF-1 signaling pathway	Endometrial cancer	Glycosaminoglycan biosynthesis - chondroitin sulfate / dermatan sulfate
Hippo signaling pathway	Epstein-Barr virus infection	Glycosaminoglycan biosynthesis - heparan sulfate / heparin
Lysine degradation	Fatty acid biosynthesis	Glycosaminoglycan biosynthesis - keratan sulfate
Melanoma	Fatty acid elongation	Glycosphingolipid biosynthesis - lacto and neolacto series
Neurotrophin signaling pathway	Hepatitis B	Long-term depression
Non-small cell lung cancer	Hepatitis C	MAPK signaling pathway
p53 signaling pathway	Insulin signaling pathway	mTOR signaling pathway
Pancreatic cancer	mRNA surveillance pathway	Phosphatidylinositol signaling system
Pathways in cancer	NF-kappa B signaling pathway	Rap1 signaling pathway
PI3K-Akt signaling pathway	N-Glycan biosynthesis	Ras signaling pathway
Prion diseases	Oocyte meiosis	Wnt signaling pathway
Prolactin signaling pathway	Pathogenic Escherichia coli infection	
Prostate cancer	Protein processing in endoplasmic reticulum	
Proteoglycans in cancer	RNA transport	
Regulation of actin cytoskeleton	Shigellosis	
Renal cell carcinoma	Spliceosome	
Small cell lung cancer	Sulfur metabolism	
Sphingolipid signaling pathway	Thyroid cancer	
TGF-beta signaling pathway	Transcriptional misregulation in cancer	
Thyroid hormone signaling pathway	Ubiquitin mediated proteolysis	
	Viral carcinogenesis	

Table S2c- Comparison between **NGF2**-induced Tarbase an microT-CDS pathways

Shared Tarbase-MicroT pathways (n.38)	Tarbase pathways (n.36)	MicroT-CDS pathways (n.35)
Acute myeloid leukemia	2-Oxocarboxylic acid metabolism	Adrenergic signaling in cardiomyocytes
Adherens junction	B cell receptor signaling pathway	Amphetamine addiction
AMPK signaling pathway	Carbon metabolism	Biotin metabolism
Axon guidance	Cell cycle	cGMP-PKG signaling pathway
Bacterial invasion of epithelial cells	Central carbon metabolism in cancer	Choline metabolism in cancer
Basal cell carcinoma	Citrate cycle (TCA cycle)	Cholinergic synapse
Chronic myeloid leukemia	Endometrial cancer	Circadian entrainment
Colorectal cancer	Epithelial cell signaling in Helicobacter pylori infection	Cocaine addiction
Endocytosis	Epstein-Barr virus infection	Dilated cardiomyopathy
ErbB signaling pathway	Fatty acid elongation	Dopaminergic synapse
Estrogen signaling pathway	Fatty acid metabolism	Dorso-ventral axis formation
Fatty acid biosynthesis	Fc gamma R-mediated phagocytosis	ECM-receptor interaction
Focal adhesion	Glycosaminoglycan biosynthesis - chondroitin sulfate / dermatan sulfate	GABAergic synapse
FoxO signaling pathway	Hepatitis B	Gap junction
Glioma	HIF-1 signaling pathway	Gastric acid secretion
Glycosaminoglycan biosynthesis - heparan sulfate / heparin	HTLV-I infection	Glutamatergic synapse
Hippo signaling pathway	Insulin signaling pathway	Glycosaminoglycan biosynthesis - keratan sulfate
Lysine degradation	Lysosome	GnRH signaling pathway
MAPK signaling pathway	NF-kappa B signaling pathway	Hedgehog signaling pathway
Melanoma	N-Glycan biosynthesis	Hypertrophic cardiomyopathy (HCM)
mTOR signaling pathway	One carbon pool by folate	Insulin secretion
Neurotrophin signaling pathway	Oocyte meiosis	Long-term depression
Non-small cell lung cancer	Other types of O-glycan biosynthesis	Melanogenesis
p53 signaling pathway	Progesterone-mediated oocyte maturation	Morphine addiction
Pancreatic cancer	Protein processing in endoplasmic reticulum	Mucin type O-Glycan biosynthesis
Pathways in cancer	RNA transport	Notch signaling pathway
Prion diseases	Shigellosis	Oxytocin signaling pathway
Prolactin signaling pathway	Small cell lung cancer	Phosphatidylinositol signaling system
Prostate cancer	Spliceosome	PI3K-Akt signaling pathway
Proteoglycans in cancer	Steroid biosynthesis	Platelet activation
Regulation of actin cytoskeleton	Thyroid cancer	Rap1 signaling pathway
Renal cell carcinoma	TNF signaling pathway	Ras signaling pathway
Signaling pathways regulating pluripotency of stem cells	Transcriptional misregulation in cancer	Retrograde endocannabinoid signaling
Sphingolipid signaling pathway	Vibrio cholerae infection	Thyroid hormone synthesis
TGF-beta signaling pathway	Viral carcinogenesis	Vasopressin-regulated water reabsorption
Thyroid hormone signaling pathway	Vitamin B6 metabolism	
Ubiquitin mediated proteolysis		
Wnt signaling pathway		

Shared Tarbase-MicroT pathways (n.47)	Tarbase pathways (n.30)	MicroT-CDS pathways (n.35)
Acute myeloid leukemia	2-Oxocarboxylic acid metabolism	Adrenergic signaling in cardiomyocytes
Adherens junction	B cell receptor signaling pathway	Axon guidance
Bacterial invasion of epithelial cells	Base excision repair	Biotin metabolism
Basal cell carcinoma	Bladder cancer	cAMP signaling pathway
Central carbon metabolism in cancer	Cell cycle	cGMP-PKG signaling pathway
Chronic myeloid leukemia	Circadian rhythm	Choline metabolism in cancer
Colorectal cancer	Citrate cycle (TCA cycle)	Cholinergic synapse
Endocytosis	Epithelial cell signaling in Helicobacter pylori infection	Circadian entrainment
Endometrial cancer	Epstein-Barr virus infection	Cocaine addiction
ErbB signaling pathway	Fatty acid metabolism	Dilated cardiomyopathy
Estrogen signaling pathway	Fc gamma R-mediated phagocytosis	Dopaminergic synapse
Fatty acid biosynthesis	Glycosaminoglycan biosynthesis - chondroitin sulfate / dermatan sulfate	GABAergic synapse
Focal adhesion	HTLV-I infection	Gap junction
FoxO signaling pathway	Long-term potentiation	Glutamatergic synapse
Glioma	Lysosome	Glycosaminoglycan biosynthesis - keratan sulfate
Glycosaminoglycan biosynthesis - heparan sulfate / heparin	NF-kappa B signaling pathway	GnRH signaling pathway
Hepatitis B	One carbon pool by folate	Hedgehog signaling pathway
HIF-1 signaling pathway	Oocyte meiosis	Inositol phosphate metabolism
Hippo signaling pathway	Other types of O-glycan biosynthesis	Insulin secretion
Insulin signaling pathway	RNA degradation	Long-term depression
Lysine degradation	RNA transport	Melanogenesis
MAPK signaling pathway	Shigellosis	Morphine addiction
Melanoma	Spliceosome	mRNA surveillance pathway
mTOR signaling pathway	Steroid biosynthesis	Mucin type O-Glycan biosynthesis
Neurotrophin signaling pathway	Terpenoid backbone biosynthesis	N-Glycan biosynthesis
Non-small cell lung cancer	Thyroid cancer	Oxytocin signaling pathway
Notch signaling pathway	TNF signaling pathway	PI3K-Akt signaling pathway
p53 signaling pathway	Transcriptional misregulation in cancer	Platelet activation
Pancreatic cancer	Vibrio cholerae infection	Rap1 signaling pathway
Pathways in cancer	Vitamin B6 metabolism	Ras signaling pathway
Phosphatidylinositol signaling system		Retrograde endocannabinoid signaling
Prion diseases		T cell receptor signaling pathway
Progesterone-mediated oocyte maturation		Type II diabetes mellitus
Prolactin signaling pathway		Vascular smooth muscle contraction
Prostate cancer		Vasopressin-regulated water reabsorption
Protein processing in endoplasmic reticulum		
Proteoglycans in cancer		
Regulation of actin cytoskeleton		
Renal cell carcinoma		
Signaling pathways regulating pluripotency of stem cells		
Small cell lung cancer		
Sphingolipid signaling pathway		
TGF-beta signaling pathway		
Thyroid hormone signaling pathway		
Ubiquitin mediated proteolysis		
Viral carcinogenesis		
Wnt signaling pathway		

Table S4a- KEGG pathways Tarbase. KEGG pathways (n.54) identified by considering significant miRNAs (n=12, ref Table 4) which appear specifically modulated **only by NGF1** treatment, as detected by Diana-Tarbase (experimentally supported) analysis

KEGG pathway	p-value	#genes	#miRNAs
ECM-receptor interaction	4.91E-24	26	9
Adherens junction	3.85E-12	38	8
Proteoglycans in cancer	1.04E-10	64	10
Pathways in cancer	3.16E-10	128	10
Fatty acid biosynthesis	1.59E-09	2	2
Glioma	5.91E-09	30	9
Viral carcinogenesis	1.02E-07	64	8
Focal adhesion	4.16E-07	77	9
Prostate cancer	9.91E-07	39	8
Hippo signaling pathway	1.14E-06	47	9
Chronic myeloid leukemia	1.46E-06	33	8
Lysine degradation	1.31E-05	16	7
Renal cell carcinoma	1.31E-05	30	10
Colorectal cancer	2.38E-05	28	7
Endometrial cancer	4.37E-05	23	7
Ubiquitin mediated proteolysis	6.35E-05	51	8
PI3K-Akt signaling pathway	7.46E-05	102	9
Transcriptional misregulation in cancer	0.000121	52	10
Small cell lung cancer	0.000211	34	8
Hepatitis B	0.000244	48	8
FoxO signaling pathway	0.000266	48	8
MicroRNAs in cancer	0.000328	84	10
Acute myeloid leukemia	0.000426	22	8
Neurotrophin signaling pathway	0.000656	44	9
Thyroid cancer	0.000671	14	7
Pancreatic cancer	0.000938	27	8
Oocyte meiosis	0.000949	38	9
Non-small cell lung cancer	0.001111	23	8
Bacterial invasion of epithelial cells	0.001189	27	8
TGF-beta signaling pathway	0.001374	26	9
Ras signaling pathway	0.001955	64	9
Bladder cancer	0.002871	18	9
Insulin signaling pathway	0.002917	46	8
Wnt signaling pathway	0.003217	43	8
Sulfur metabolism	0.004099	3	2
Central carbon metabolism in cancer	0.004798	23	8
Melanoma	0.005346	24	8
Cell cycle	0.005995	43	8
p53 signaling pathway	0.005995	25	8
ErbB signaling pathway	0.007153	30	8
Endocytosis	0.007175	54	9
Thyroid hormone signaling pathway	0.007452	39	10
Valine, leucine and isoleucine biosynthesis	0.008149	2	3
Protein processing in endoplasmic reticulum	0.008600	51	9
Shigellosis	0.009460	22	7
Signaling pathways regulating pluripotency of stem cells	0.015913	40	8
Amoebiasis	0.016181	29	8
Dorso-ventral axis formation	0.020577	12	7
mTOR signaling pathway	0.020577	22	8
Axon guidance	0.022027	34	8
Epstein-Barr virus infection	0.025792	59	9
Steroid biosynthesis	0.025793	5	3
Fatty acid elongation	0.035548	3	3
Prolactin signaling pathway	0.040620	23	8

***Table S4b-* KEGG pathways microT.** KEGG pathways (n.34) identified by considering significant dysregulated miRNAs (n=12, ref Table 4) specifically induced **only by NGF1** treatment, as detected by Diana-MicroT-CDS (predicted) analysis

KEGG pathway	p-value	#genes	#miRNAs
ECM-receptor interaction	1.17E-40	28	9
Focal adhesion	4.48E-07	70	9
Proteoglycans in cancer	4.48E-07	59	10
Amoebiasis	9.59E-07	33	7
Lysine degradation	2.06E-06	15	5
PI3K-Akt signaling pathway	3.33E-06	96	11
Glioma	2.14E-05	23	6
ErbB signaling pathway	0.000135	30	6
FoxO signaling pathway	0.000135	42	6
Signaling pathways regulating pluripotency of stem cells	0.000135	43	8
mTOR signaling pathway	0.000289	25	6
Renal cell carcinoma	0.000460	24	5
Small cell lung cancer	0.000460	31	7
Glycosaminoglycan biosynthesis - heparan sulfate / heparin	0.000617	9	3
Hippo signaling pathway	0.000701	38	8
Biotin metabolism	0.001185	1	1
Protein digestion and absorption	0.001949	30	6
TGF-beta signaling pathway	0.002067	22	8
Thyroid hormone signaling pathway	0.002331	33	9
AMPK signaling pathway	0.002491	35	10
Choline metabolism in cancer	0.005714	32	6
Ras signaling pathway	0.007953	55	8
Platelet activation	0.009775	35	5
p53 signaling pathway	0.009821	23	7
Prolactin signaling pathway	0.011516	18	6
Wnt signaling pathway	0.011516	39	8
Neurotrophin signaling pathway	0.011516	36	8
Prostate cancer	0.022313	27	6
Chronic myeloid leukemia	0.030837	22	4
Pathways in cancer	0.030837	90	9
Circadian rhythm	0.030954	12	9
Phosphatidylinositol signaling system	0.036122	18	7
Pancreatic cancer	0.039516	17	4
HIF-1 signaling pathway	0.042390	29	6

***Table S5a*- KEGG pathways Tarbase.** KEGG pathways (n.47) identified by considering significant miRNAs (n=16, ref Table 4) which appear specifically modulated **only by NGF2** treatment, as detected by Diana-Tarbase (experimentally supported) analysis

KEGG pathway	p-value	#genes	#miRNAs
Prion diseases	3.37E-12	11	7
Hippo signaling pathway	3.60E-10	56	9
Proteoglycans in cancer	2.26E-09	77	9
Fatty acid biosynthesis	2.67E-09	4	2
Oocyte meiosis	1.37E-05	44	7
Cell cycle	2.91E-05	51	9
Colorectal cancer	3.90E-05	29	9
Adherens junction	4.19E-05	32	8
Glioma	4.51E-05	28	8
Protein processing in endoplasmic reticulum	6.26E-05	61	9
Estrogen signaling pathway	0.000112	40	9
Non-small cell lung cancer	0.000218	24	9
Thyroid hormone signaling pathway	0.000277	44	9
Prostate cancer	0.000277	39	9
ECM-receptor interaction	0.000325	26	9
Signaling pathways regulating pluripotency of stem cells	0.000325	50	9
Chronic myeloid leukemia	0.000325	33	9
TGF-beta signaling pathway	0.00034	29	9
Pathways in cancer	0.000699	117	10
Viral carcinogenesis	0.000775	61	9
Neurotrophin signaling pathway	0.002553	45	9
Pancreatic cancer	0.00296	27	9
HIF-1 signaling pathway	0.009239	40	9
mTOR signaling pathway	0.009239	25	9
Endometrial cancer	0.009592	21	8
Steroid biosynthesis	0.009818	6	5
Focal adhesion	0.01022	68	9
Progesterone-mediated oocyte maturation	0.01291	34	9
Ubiquitin mediated proteolysis	0.01291	49	10
Renal cell carcinoma	0.013204	26	9
Sulfur metabolism	0.014807	4	3
Hepatitis B	0.014807	47	9
Acute myeloid leukemia	0.02119	22	7
Regulation of actin cytoskeleton	0.021719	64	9
AMPK signaling pathway	0.022779	44	9
Prolactin signaling pathway	0.023592	24	8
mRNA surveillance pathway	0.023592	33	9
Transcriptional misregulation in cancer	0.024922	47	9
Bacterial invasion of epithelial cells	0.026525	26	8
Thyroid cancer	0.026525	12	10
RNA degradation	0.026729	30	9
PI3K-Akt signaling pathway	0.028665	97	9
Endocytosis	0.031535	63	10
Bladder cancer	0.03301	17	9
Small cell lung cancer	0.03615	30	9
RNA transport	0.043139	51	9
Central carbon metabolism in cancer	0.045083	24	8

***Table S5b-* KEGG pathways microT**. KEGG pathways (n.52) identified by considering significant dysregulated miRNAs (n=16, ref Table 4) specifically induced **only by NGF2** treatment, as detected by Diana-MicroT-CDS (predicted) analysis

KEGG pathway	p-value	#genes	#miRNAs
Prion diseases	3.97E-06	7	7
Axon guidance	3.97E-06	56	16
ECM-receptor interaction	5.44E-06	37	13
Renal cell carcinoma	7.00E-06	38	16
Adherens junction	2.51E-05	34	14
ErbB signaling pathway	3.13E-05	48	15
Signaling pathways regulating pluripotency of stem cells	4.36E-05	63	15
Proteoglycans in cancer	0.000106	78	16
TGF-beta signaling pathway	0.00012	37	13
Glioma	0.00019	31	13
Focal adhesion	0.000681	88	16
Estrogen signaling pathway	0.001281	45	16
Pathways in cancer	0.001281	151	16
Chronic myeloid leukemia	0.001802	36	15
FoxO signaling pathway	0.002055	60	16
Prolactin signaling pathway	0.002512	34	16
Oxytocin signaling pathway	0.002512	66	16
Thyroid hormone signaling pathway	0.004469	48	16
Thyroid hormone synthesis	0.004889	27	13
Pancreatic cancer	0.00524	29	13
Wnt signaling pathway	0.00524	55	15
Rap1 signaling pathway	0.00524	82	16
Dilated cardiomyopathy	0.005322	41	14
Long-term depression	0.007737	27	14
Lysine degradation	0.00792	19	13
Glutamatergic synapse	0.00792	43	14
cAMP signaling pathway	0.00792	80	16
Dorso-ventral axis formation	0.009063	16	14
Adrenergic signaling in cardiomyocytes	0.009063	58	15
MAPK signaling pathway	0.009063	95	16
Neurotrophin signaling pathway	0.009063	50	16
Melanogenesis	0.009063	45	16
Ras signaling pathway	0.010007	82	16
Acute myeloid leukemia	0.011356	26	13
GnRH signaling pathway	0.011502	40	14
Glycosphingolipid biosynthesis - ganglio series	0.011617	7	8
Ubiquitin mediated proteolysis	0.013611	57	16
Hippo signaling pathway	0.016869	59	14
Hypertrophic cardiomyopathy (HCM)	0.018414	36	13
Gap junction	0.02182	34	15
Regulation of actin cytoskeleton	0.02182	84	16
Morphine addiction	0.022323	35	14
PI3K-Akt signaling pathway	0.026698	122	16
Colorectal cancer	0.031508	28	13
mTOR signaling pathway	0.031508	28	14
Retrograde endocannabinoid signaling	0.03222	40	13
cGMP-PKG signaling pathway	0.032543	64	16
Melanoma	0.039076	31	13
Thyroid cancer	0.041876	12	10
Prostate cancer	0.04445	35	13
Long-term potentiation	0.049475	29	16

***Table S6a*- KEGG pathways Tarbase** KEGG pathways (n.60) identified by considering significant miRNAs (n=20, ref Table 4) which appear specifically **modulated only by NGF3** treatment, as detected by Diana-Tarbase (experimentally supported) analysis

KEGG pathway	p-value	#genes	#miRNAs
Proteoglycans in cancer	7.17E-14	116	17
Protein processing in endoplasmic reticulum	1.66E-13	111	17
Hippo signaling pathway	1.29E-11	84	17
Viral carcinogenesis	6.05E-11	114	17
Adherens junction	6.61E-11	51	15
Cell cycle	6.61E-11	81	16
Fatty acid biosynthesis	8.52E-11	7	8
Lysine degradation	1.81E-09	30	15
Prion diseases	5.26E-08	16	10
p53 signaling pathway	1.05E-07	49	17
Oocyte meiosis	2.70E-07	67	17
RNA transport	6.23E-06	94	17
Colorectal cancer	8.03E-06	39	16
Ubiquitin mediated proteolysis	1.55E-05	80	17
Renal cell carcinoma	2.65E-05	41	16
ErbB signaling pathway	5.97E-05	51	17
FoxO signaling pathway	5.97E-05	77	17
Pathways in cancer	8.28E-05	191	17
Estrogen signaling pathway	8.40E-05	53	17
Sphingolipid signaling pathway	0.000111	62	17
Hepatitis B	0.000121	77	17
Chronic myeloid leukemia	0.000142	44	17
TGF-beta signaling pathway	0.00025	42	16
Focal adhesion	0.00025	108	17
Thyroid hormone signaling pathway	0.000414	68	17
Endometrial cancer	0.000577	32	16
N-Glycan biosynthesis	0.000611	29	14
Small cell lung cancer	0.000673	50	17
Insulin signaling pathway	0.000769	76	17
Endocytosis	0.000875	99	17
Non-small cell lung cancer	0.001252	31	17
HTLV-I infection	0.001403	128	17
Epstein-Barr virus infection	0.001474	107	16
2-Oxocarboxylic acid metabolism	0.001524	9	8
Wnt signaling pathway	0.001789	72	16
mRNA surveillance pathway	0.001905	52	16
Glioma	0.002405	35	16
Pancreatic cancer	0.002876	38	16
Progesterone-mediated oocyte maturation	0.003444	49	16
Signaling pathways regulating pluripotency of stem cells	0.003749	69	16
mTOR signaling pathway	0.006419	36	16
Prostate cancer	0.006419	49	17
ECM-receptor interaction	0.006683	38	17
Regulation of actin cytoskeleton	0.006683	100	17
Central carbon metabolism in cancer	0.007416	35	15
Bacterial invasion of epithelial cells	0.007416	41	17
Phosphatidylinositol signaling system	0.011262	45	16
Neurotrophin signaling pathway	0.011262	61	16
Prolactin signaling pathway	0.011262	37	16
Terpenoid backbone biosynthesis	0.012078	13	10
Bladder cancer	0.020052	23	16
Spliceosome	0.020108	68	17
Inositol phosphate metabolism	0.022399	34	16
Other types of O-glycan biosynthesis	0.02335	13	10

Sphingolipid metabolism	0.026218	22	11
Sulfur relay system	0.03385	6	4
Melanoma	0.039937	34	15
AMPK signaling pathway	0.039987	65	16
Apoptosis	0.043029	42	16
Shigellosis	0.043517	34	16

***Table S6b*- KEGG pathways microT.** KEGG pathways (n.75) identified by considering significant dysregulated miRNAs (n=20, ref Table 4) specifically induced **only by NGF3** treatment, as detected by Diana-MicroT-CDS (predicted) analysis

KEGG pathway	p-value	#genes	#miRNAs
Proteoglycans in cancer	2.51E-12	115	19
Pathways in cancer	3.58E-08	208	19
Signaling pathways regulating pluripotency of stem cells	1.01E-07	82	18
Renal cell carcinoma	1.43E-07	47	20
Axon guidance	5.51E-06	71	18
ErbB signaling pathway	5.51E-06	57	20
FoxO signaling pathway	8.87E-06	78	18
PI3K-Akt signaling pathway	8.87E-06	175	19
Pancreatic cancer	8.87E-06	43	19
Thyroid hormone signaling pathway	1.11E-05	66	18
Focal adhesion	1.27E-05	115	20
Prion diseases	1.47E-05	12	8
Morphine addiction	2.49E-05	47	17
Ras signaling pathway	3.08E-05	117	20
Hippo signaling pathway	3.86E-05	80	18
Wnt signaling pathway	3.91E-05	76	18
Rap1 signaling pathway	4.49E-05	113	20
TGF-beta signaling pathway	9.51E-05	47	17
Melanoma	9.51E-05	45	18
GABAergic synapse	0.000129	43	16
Acute myeloid leukemia	0.000215	36	17
MAPK signaling pathway	0.000215	131	19
Regulation of actin cytoskeleton	0.000298	112	19
Sphingolipid signaling pathway	0.000364	64	19
Glioma	0.000371	37	19
N-Glycan biosynthesis	0.000492	25	14
Choline metabolism in cancer	0.000742	60	18
Non-small cell lung cancer	0.000797	33	18
Circadian entrainment	0.000818	50	18
Adrenergic signaling in cardiomyocytes	0.000934	75	18
Cholinergic synapse	0.001003	61	18
Chronic myeloid leukemia	0.001003	43	18
Ubiquitin mediated proteolysis	0.001073	72	17
Phosphatidylinositol signaling system	0.001114	44	17
Retrograde endocannabinoid signaling	0.001114	56	19
Prostate cancer	0.001142	51	19
T cell receptor signaling pathway	0.001208	59	19
Prolactin signaling pathway	0.00134	40	16
mTOR signaling pathway	0.00156	38	16
Colorectal cancer	0.00214	37	17
Circadian rhythm	0.002203	21	16
Estrogen signaling pathway	0.003037	46	16
Neurotrophin signaling pathway	0.003383	65	19
Lysine degradation	0.004163	22	18
Protein processing in endoplasmic reticulum	0.004163	83	18
Oxytocin signaling pathway	0.005311	79	19
Adherens junction	0.006079	41	18
Platelet activation	0.006302	63	19
Endometrial cancer	0.008351	30	16
AMPK signaling pathway	0.009242	66	19
Dopaminergic synapse	0.010877	68	19
p53 signaling pathway	0.011893	38	16
Nicotine addiction	0.013416	21	16
Glycosaminoglycan biosynthesis - keratan sulfate	0.014442	8	5

mRNA surveillance pathway	0.014442	49	19
Arrhythmogenic right ventricular cardiomyopathy (ARVC)	0.014531	38	16
B cell receptor signaling pathway	0.014531	39	17
Transcriptional misregulation in cancer	0.014531	89	18
RNA transport	0.014531	81	19
cAMP signaling pathway	0.014531	96	19
Small cell lung cancer	0.019644	45	18
Glutamatergic synapse	0.021309	54	18
Mucin type O-Glycan biosynthesis	0.028428	14	10
Hepatitis B	0.028428	69	19
Thyroid cancer	0.031473	16	14
Amphetamine addiction	0.031622	32	15
Long-term potentiation	0.031622	36	17
Viral carcinogenesis	0.031622	84	18
TNF signaling pathway	0.031622	58	19
cGMP-PKG signaling pathway	0.034629	79	18
Inositol phosphate metabolism	0.042462	31	17
Type II diabetes mellitus	0.043588	25	16
Gap junction	0.043588	42	18
Insulin signaling pathway	0.043588	68	18
Endocytosis	0.043588	98	19

Table 10- **Filtering and distribution of genes (unique n=2591) targeted by miRNAs induced by bioformulations.** Data from Tarbase (experimentally supported) elaboration. Colors as follows: pink, NGF2+NGF3, violet, NGF1+NGF2, blue: NGF1+NGF3

shared by all three bioformulations (n=858)				shared by 2 out of 3 bioformulations (n=1299)						only by NGF1 (n=76)	only by NGF2 (n=141)	only by NGF3 (n=217)
ABCC1	EIF2S3	MOB1A	SAR1A	AAAS	CHMP2A	FGF4	LAMTOR5	PIK3CG	SGPP2	ANAPC4	ABLIM1	ACAP1
ABL1	EIF3F	MOB1B	SAR1B	ABCA2	CHMP4A	FGF7	LAPTM4A	PIK3R2	SH2B1	BPNT1	ACACB	ACAP2
ACACA	EIF3J	MSH2	SCD	ABCB9	CHMP7	FGF8	LAPTM4B	PIK3R5	SH3GL2	CASP8	ACOT4	ACAP3
ACAT2	EIF4A2	MSH6	SDC2	ABI2	CHPF	FGF9	LAPTM5	PIP4K2C	SH3GLB2	CD47	ACOT7	ADCY3
ACIN1	EIF4A3	MSN	SEC23A	ABL2	CHPF2	FH	LBP	PIP5K1A	SH3KBP1	CDH2	ACSS2	ALDH1B1
ACSL3	EIF4B	MVB12B	SEC23B	ACAA1	CHRM2	FIGF	LCK	PIP5K1B	SHC3	CLDN1	ADH5	APEX1
ACSL4	EIF4E2	MYC	SEC24A	ACAA2	CHRM3	FKBP4	LDB1	PIP5KL1	SHC4	COMMD3-BMI1	ADPGK	APEX2
ACTB	EIF4EBP2	MYCN	SEC24B	ACADM	CHST12	FKBP5	LDLR	PKM	SHH	CPSF6	ALDH6A1	APH1A
ACTN1	EIF4G1	MYL12A	SEC24C	ACADSB	CHST14	FLNA	LEF1	PLA2G15	SHISA5	CPSF7	ALDOC	APH1B
ACTN4	EIF4G2	MYL12B	SEC31A	ACADVL	CHST15	FLNC	LEFTY1	PLA2G4F	SHMT1	CSF3	ALG1	ARF5
ACVR1B	EIF4G3	NCBP1	SEC61A1	ACAT1	CHST3	FLOT1	LFNG	PLAT	SHMT2	CSTF1	ALG10	ARNTL
ACVR1C	EIF5	NCKAP1	SEC61B	ACER2	CHSY1	FLT3	LGMN	PLAU	SIL1	CSTF2T	ALG10B	ATP6V0E2
ACVR2A	ELK4	NCOA1	SEC62	ACLY	CHSY3	FMR1	LIF	PLAUR	SIN3A	CYCS	ALG12	B3GALT4
ACVR2B	ELMO2	NCOA2	SEH1L	ACO1	CHUK	FOLR2	LIFR	PLCB3	SIRT6	DAG1	ALG3	BBC3
ADCY9	ELOVL5	NCOA3	SEL1L	ACO2	CISH	FOS	LIMD1	PLCB4	SIX1	DHX16	ALG8	BHLHE40
ADRB1	ENO1	NCOA4	SEPT11	ACOX1	CKS1B	FOSL1	LIPA	PLCD1	SKIL	DNM3	ANGPT1	BHLHE41
ADRBK1	EP300	NCOR1	SEPT2	ACOX3	CLN3	FOXG1	LLGL1	PLCD3	SLC11A2	DSC2	AP4E1	BTG1
AFF1	EPAS1	NCOR2	SEPT8	ACP1	CLN5	FOXO4	LLGL2	PLCE1	SLC12A2	DSG2	ARHGEF11	BTG2
AGAP1	EPN1	NDC1	SERPINE1	ACP2	CLNS1A	FRMD1	LMAN2	PLD2	SLC16A10	DSP	ASPSCR1	BTG3
AJUBA	ERC1	NEDD4	SESN1	ACSL1	CLOCK	FTCD	LPAR2	PLK1	SLC17A5	EDNRB	ATP6V0D1	C1D
AKT1	ERO1L	NEDD4L	SESN2	ACSL5	CLTA	FUCA1	LPAR3	PLK3	SLC25A31	EFNA4	CAMKK2	C8orf44-SGK3
AKT1S1	ETS1	NF2	SESN3	ACTG1	CLTB	FUT4	LRP5	PLK4	SLC25A5	EMD	CCL4	CACNA1A
AKT2	ETV1	NFE2L2	SETD1A	ACVR1	COL21A1	FUT8	LRP6	PLOD1	SLC25A6	ETF1	CD36	CBLB
ALDOA	FARP2	NFKB1	SETD1B	ADAM10	COL5A3	FUT9	LSM3	PLOD2	SLC2A4	FMN2	CPS1	CD58
AMOT	FASN	NFKBIA	SETD2	ADAM17	COL6A5	FZD1	LSM4	PLOD3	SLC45A3	GSPT1	CRTC1	CDC16

ANAPC13	FBXW11	NFKBIZ	SETD8	ADCY1	COL6A6	FZD10	LSM7	PLRG1	SLC9A1	HBS1L	DAD1	CDC45
ANAPC7	FBXW7	NGFRAP1	SETDB1	ADCY6	COLGALT1	FZD2	LSS	PML	SMAD3	IFIT1	DERL2	CDIPT
AP2B1	FGFR1	NHP2L1	SF3B1	ADCY7	COLGALT2	FZD3	LUM	PNPO	SMAP1	IFNAR2	DOLPP1	CDKN2B
APC	FGFR3	NLK	SF3B2	ADIPOR1	CPT1A	FZD7	LYL1	POFUT1	SMAP2	IL4R	DPM2	CDS1
AR	FLCN	NMD3	SF3B3	ADIPOR2	CPT1B	FZD8	LYN	POFUT2	SMARCAD1	LAMA2	DPM3	CDS2
ARAP1	FLI1	NOTCH1	SGK1	ADRB2	CPT2	FZR1	M6PR	POLD1	SMC3	MAGOHB	DPYSL2	CERS1
ARF3	FLNB	NOTCH2	SGK3	ADRBK2	CRB2	GAA	MAD2L1	POLD3	SMNDC1	MAN1B1	DPYSL5	CHST10
ARF6	FLOT2	NR4A1	SGMS2	AGAP3	CREB1	GAB2	MAD2L2	POLD4	SMO	MCL1	DUSP9	CLTCL1
ARFGAP3	FLT1	NRAS	SGOL1	AKT3	CREB3L1	GABBR1	MAGED1	POLE3	SMPD1	MSI2	EEF2K	CNOT1
ARFGEF2	FN1	NSD1	SGPL1	ALDH1L2	CREB3L2	GADD45A	MAGI2	POLR1C	SMPD2	NCL	EFNA2	CNOT10
ARHGAP35	FOXO1	NSMAF	SH2B3	ALDH2	CREBBP	GART	MALT1	POLR1D	SNAI2	NFATC4	EFNA3	CNOT2
ARHGAP5	FOXO3	NTRK3	SH3GL1	ALDH3A2	CRTC3	GBA	MAN1A1	POLR2C	SNF8	NUDT21	EFNB1	CNOT3
ARHGDIA	FRMD6	NUP153	SH3GLB1	ALDH9A1	CRY2	GCK	MAN1A2	POLR2F	SNRNP40	OAS3	EFNB2	CNOT4
ARHGEF12	FRS2	NUP155	SHC1	ALG13	CS	GDF5	MAN2A2	POLR2G	SNRPA	OCLN	EHD3	CNOT6
ARHGEF4	FST	NUP160	SIAH1	ALG2	CSF1	GEMIN2	MAN2B1	POLR2K	SNRPB	PABPN1	ELAVL1	CNOT6L
ARNT	FUS	NUP205	SIRT1	ALG9	CSGALNACT1	GEMIN4	MANBA	POLR2L	SNRPB2	PAPOLA	ELOVL1	CNOT7
ARPC1B	FXR1	NUP50	SIX4	ALYREF	CSK	GEMIN5	MAP2K1	POLR3B	SNRPD2	PAPSS1	ELOVL7	CNOT8
ARPC2	FYN	NUP62	SKP1	AMFR	CSNK1A1	GEMIN8	MAP2K3	POLR3H	SNRPD3	PAPSS2	EPHA1	COL4A3
ARPC5	FZD4	NUP98	SKP2	AMHR2	CSNK1D	GGA1	MAP2K4	POLR3K	SNRPF	PCF11	EPHA3	CSGALNACT2
ARPC5L	FZD5	NUPL1	SLC16A3	AMPH	CTBP1	GGA2	MAP2K5	POM121	SOAT1	PCK2	EPHA4	DAXX
ASAP1	FZD6	NUPL2	SLC1A5	AMT	CTNNB1	GGA3	MAP2K7	POMGNT1	SOAT2	PHLPP2	EPHA5	DCP1A
ASAP2	G6PD	NXF1	SLC2A1	ANAPC1	CTNNBIP1	GIT1	MAP3K11	POMT1	SOD1	PKN1	EPHA7	DCP1B
ASH1L	GAB1	ORC2	SLC7A5	ANAPC10	CTNNBL1	GLB1	MAP3K12	POMT2	SOST	PKN2	EPHB2	DCP2
ATF2	GABARAP	OS9	SLK	ANAPC2	CTSA	GLCE	MAP3K14	POP1	SOX2	PPARA	EPHB4	DDX6
ATF6	GABARAPL1	PABPC1	SLU7	ANAPC5	CTSB	GLI2	MAP3K2	POP4	SP100	PRKCB	ERCC8	DET1
ATG12	GANAB	PABPC3	SMAD2	ANGPT4	CTSC	GLI3	MAP3K3	POP7	SPDYA	PSME3	ESD	DGKB
ATM	GAPDH	PABPC4	SMAD4	ANK2	CTSD	GLS2	MAP3K4	PPAP2A	SPHK1	RALA	FES	DGKD
ATP1A1	GBF1	PAIP1	SMAD5	ANK3	CTSF	GNA11	MAP3K8	PPAP2B	SPHK2	RASGRF1	FGF5	DGKE
ATP1B1	GIT2	PAK2	SMAD7	AOX1	CTSL	GNAI1	MAP4K3	PPARGC1A	SPI1	RBM8A	FRAT2	DGKH
ATP1B3	GLI1	PARD6B	SMC1A	AP1B1	CTSW	GNAI3	MAP4K4	PPIH	SPN	RNASEL	FXYD2	DGKZ

ATP2A2	GLS	PARP1	SMURF1	AP1G1	CTSZ	GNAO1	MAPK12	PPIL2	SPTLC1	SCARB1	GEMIN7	DHDDS
ATXN3	GNA12	PARVA	SMURF2	AP1G2	CUL2	GNAS	MAPK7	PPM1A	SQLE	SERPINB6	GPI	DHX36
B4GALT1	GNA13	PBX1	SNAI1	AP1M1	CUL4A	GNB2	MAPK8IP2	PPM1B	SRC	SERPINB9	GRK5	DIS3
BAIAP2	GNAI2	PCBP1	SND1	AP1S1	CUL7	GNB4	MAPK8IP3	PPP1CA	SRF	SHFM1	H6PD	DIS3L
BAIAP3	GNAQ	PCNA	SNRNP200	AP1S2	CXCL1	GNG11	MAPK9	PPP1R12B	SRSF3	SMAD1	HDAC5	DLL1
BAK1	GNB1	PDCD6IP	SNRNP27	AP1S3	CXCL10	GNG2	MAPKAPK3	PPP1R12C	SRSF6	SMG1	HHEX	DLL3
BAX	GNG12	PDE3A	SNRNP70	AP2A1	CXCL3	GNG8	MAPKAPK5	PPP1R3C	SRSF8	SMG6	HIBCH	DTX1
BCL2	GNG5	PDGFC	SNRPC	AP2A2	CXCL5	GNGT1	MARCKS	PPP2CB	SS18	SPIRE1	HIST1H2BJ	DTX2
BCL2A1	GOLPH3	PDGFRA	SNRPD1	AP2M1	CXCL8	GNGT2	MARCKSL1	PPP2R2D	SSH1	SYMPK	HK2	DTX3
BCL2L11	GPC1	PDHA1	SOCS3	AP2S1	CXCR1	GNPTAB	MATK	PPP2R3A	SSR3	TBC1D1	IL1B	DTX3L
BDKRB2	GRB2	PDHB	SOCS4	AP3B1	CXCR2	GNS	MAX	PPP3CB	ST3GAL3	TCL1A	ITGAE	EDC3
BIRC3	GRIA3	PDIA6	SOCS5	AP3B2	CXCR4	GOLPH3L	MCAT	PPP3R2	ST6GAL1	TNFRSF1A	ITGB3	EIF1B
BIRC5	GSK3B	PER2	SOCS6	AP3D1	CYFIP1	GOT1	MCM2	PPP5C	ST6GAL2	TNR	JAM3	EIF2B4
BIRC6	GSTP1	PFKFB4	SOCS7	AP3M1	CYFIP2	GOT2	MCM5	PPT1	STAG1	TUBA1A	KCNJ3	ERBB2
BLOC1S5-TXNDC5	GTF2A1	PFKM	SOD2	AP3M2	CYP24A1	GPC3	MCM6	PRCC	STAM	TUBA1B	KCNJ6	ERBB3
BMI1	GTF2E1	PFKP	SORT1	AP3S1	CYP2R1	GPC4	MDH1	PRDM4	STAM2	TUBA1C	L1CAM	ERG
BMP2	H3F3B	PFN2	SOS1	AP3S2	CYP51A1	GPER1	MDH2	PRICKLE1	STAMBP	TUBB	LEPR	EXOSC10
BMPR1A	H3F3C	PGK1	SOS2	AP4B1	CYTH1	GPS2	MECOM	PRICKLE2	STAT2	TUBB2B	LHCGR	EXOSC3
BMPR2	HADHA	PGR	SP1	APAF1	CYTH2	GPT2	MED24	PRKACB	STAT3	TUBB4B	LRRC4	EXOSC5
BNIP3	HDAC3	PHYKPL	SPINT1	APPL1	CYTH3	GRK6	MED4	PRKAG1	STAT4	TUBB6	LSM8	EXOSC6
BRCA1	HDAC4	PIAS2	SPP1	AQR	DAAM1	GSN	MEIS1	PRKAG2	STAT6	WDR82	MAN2A1	EXOSC9
BRCA2	HDAC7	PIAS4	SPTLC2	ARAP3	DAAM2	GTF2A2	MEN1	PRKAR1B	STIP1		MAP2K6	FBXW8
BRK1	HERC1	PIK3CA	SREBF1	AREG	DAPK1	GTF2B	MFNG	PRKAR2B	STK11		ME1	FEN1
BTRC	HERC4	PIK3R1	SRRM1	ARF1	DAPK2	GTF2E2	MFSD8	PRKCA	STK36		MGAT1	FNTA
BUB1	HERPUD1	PIK3R3	SRSF1	ARFGAP1	DAPP1	GTF2H1	MGAT2	PRKCD	STMN1		MGAT5	FNTB
CAB39	HIF1A	PIKFYVE	SRSF10	ARFGAP2	DBF4	GTF2H3	MGAT3	PRKCG	STT3A		MLYCD	FXR2
CACNA2D1	HIST1H2BD	PIM1	SRSF2	ARFGEF1	DCC	GTF2H4	MGAT4A	PRKCI	STT3B		MUT	GGPS1
CALM1	HIST1H2BG	PIM2	SRSF4	ARHGEF1	DCN	GTSE1	MGAT4B	PRKCQ	SUCLA2		MYF5	GM2A
CALM2	HIST1H3B	PIP4K2A	SRSF5	ARHGEF7	DDIT3	GUSB	MGRN1	PRKCZ	SUCLG1		MYH6	GRIA1
CALM3	HIST1H3F	PIP4K2B	SRSF7	ARNT2	DDX20	GXYLT1	MITF	PRMT5	SUCLG2		NODAL	GRIN2C

CANX	HIST1H4B	PIP5K1C	SSH2	**ARPC3**	**DDX23**	**GYS1**	**MKNK1**	**PRPF18**	**SUV39H2**		NTN1	GRIN2D
CAPN2	HIST1H4C	PKMYT1	SSR1	**ARPC4**	**DDX42**	**H3F3A**	**MLF1**	**PRPF38A**	**SVIP**		NTN3	GRM5
CASC3	HIST1H4D	PLAA	SSR2	**ARRB1**	**DDX46**	**HADH**	**MLH1**	**PRPF38B**	**SYK**		NTN4	HES1
CASP3	HIST2H2BF	PLCG1	SSX2IP	**ARRB2**	**DDX58**	**HADHB**	**MLLT1**	**PRPF40B**	**TAB1**		NTNG1	HES5
CAV2	HK1	PLCG2	STAG2	**ARSA**	**DEGS1**	**HAND1**	**MLLT3**	**PRPF6**	**TAOK1**		NUP93	HIST1H4J
CBL	HLA-C	PLD1	STAT1	**ARSB**	**DHCR24**	**HBEGF**	**MMP1**	**PSAP**	**TAOK2**		PARD6G	HMGCS1
CCNA2	HLA-DPA1	PLK2	STAT5A	**ASAH1**	**DHCR7**	**HDAC1**	**MMP14**	**PSAT1**	**TAOK3**		PGAM1	HMGCS2
CCNB1	HLA-E	PMAIP1	STAT5B	**ASAP3**	**DHFR**	**HDAC11**	**MMP7**	**PSD**	**TBL1X**		PGD	HOMER3
CCND1	HMGA2	PNN	STEAP3	**ATF1**	**DHFRL1**	**HDAC2**	**MOGS**	**PSMC2**	**TBL1XR1**		PHAX	HSPA9
CCND2	HMGCR	POLR2A	STK3	**ATF3**	**DIO1**	**HDAC6**	**MPP5**	**PSMC3**	**TBPL1**		PHGDH	HSPD1
CCNE1	HMOX1	POLR2B	STK4	**ATF4**	**DKK1**	**HDAC8**	**MRPS18B**	**PSMC5**	**TBX3**		PLXNA1	ICMT
CCNE2	HNRNPA1	POLR2D	STRAP	**ATF6B**	**DKK2**	**HERC2**	**MS4A2**	**PSMD11**	**TCEB1**		PLXNA2	IDH3G
CCNG1	HNRNPA3	POLR2E	SUFU	**ATG5**	**DKK4**	**HERC3**	**MSH3**	**PSMD13**	**TCF3**		PLXNA3	IDI1
CCNG2	HNRNPC	POLR2H	SUMO1	**ATP1B2**	**DLAT**	**HESX1**	**MSMO1**	**PSMD2**	**TCF7**		PLXNB1	IL10
CCNT1	HNRNPK	POLR3A	SUMO3	**ATP6AP1**	**DLD**	**HEXA**	**MSX2**	**PSMD6**	**TCIRG1**		PLXNB2	IL18R1
CCNT2	HNRNPM	POLR3D	SUV420H1	**ATP6V0A1**	**DLG2**	**HGF**	**MTFMT**	**PSMD7**	**TEAD2**		PLXNC1	IMPA1
CCR7	HNRNPU	POLR3F	SUV420H2	**ATP6V0A2**	**DLG4**	**HGSNAT**	**MTHFD1**	**PTCH2**	**TEAD4**		POU5F1	INPP4A
CD2AP	HOXA10	POM121C	SYVN1	**ATP6V0B**	**DLST**	**HHIP**	**MTHFD1L**	**PTGER4**	**TECR**		PPP1R3A	INPP4B
CD44	HOXA9	PPARD	TAB2	**ATP6V0C**	**DLX5**	**HIST1H2BB**	**MTHFD2**	**PTK2B**	**TERT**		PRPS2	INPP5A
CD81	HSP90AA1	PPARG	TAB3	**ATP6V0D2**	**DNAJA2**	**HIST1H2BC**	**MTHFR**	**PTMA**	**TF**		PSMC1	INPP5E
CDC20	HSP90AB1	PPIL1	TACC3	**ATP6V0E1**	**DNAJA3**	**HIST1H2BF**	**MTHFS**	**PTPLB**	**TFAP4**		RAB8A	IPPK
CDC23	HSP90B1	PPM1D	TAF15	**ATP6V1A**	**DNAJB1**	**HIST1H2BH**	**MTOR**	**PTPN6**	**TFDP1**		RGS3	IQGAP3
CDC25A	HSPA1A	PPP1CB	TBC1D4	**ATP6V1B2**	**DNAJB12**	**HIST1H2BI**	**MTR**	**PTPN7**	**TFDP2**		ROBO1	ITGA9
CDC25B	HSPA1B	PPP1CC	TBK1	**ATP6V1C1**	**DNAJC1**	**HIST1H2BK**	**MYB**	**PTPRC**	**TFE3**		ROBO2	ITPK1
CDC27	HSPA4L	PPP1R12A	TBP	**ATP6V1C2**	**DNAJC5G**	**HIST1H2BL**	**MYBL1**	**PUF60**	**TGFA**		RPE	ITPKB
CDC40	HSPA5	PPP1R15A	TCERG1	**ATP6V1D**	**DNASE2B**	**HIST1H2BO**	**MYBL2**	**PVRL2**	**TGFB1**		RPIA	JAG2
CDC42	HSPA8	PPP1R3B	TCF7L1	**ATP6V1E1**	**DNM1**	**HIST1H3C**	**MYD88**	**PVRL3**	**TGFB3**		SEMA3A	KAT2B
CDC6	HSPBP1	PPP1R3D	TCF7L2	**ATP6V1F**	**DNM1L**	**HIST1H3D**	**MYH10**	**PYGB**	**TGFBR2**		SEMA3B	LIG1
CDH1	HSPG2	PPP2CA	TEAD1	**ATP6V1G1**	**DOLK**	**HIST1H3E**	**MYH14**	**PYGM**	**THBS3**		SEMA3C	LIMK2
CDK2	HSPH1	PPP2R1A	TFG	**ATP6V1H**	**DPAGT1**	**HIST1H3G**	**MYH9**	**RAB10**	**THOC2**		SEMA3G	LSM1

130

CDK4	HUWE1	PPP2R1B	TFRC	ATR	DPM1	HIST1H3H	MYL9	RAB11FIP3	THOC3		SEMA4B	LTB
CDK6	HYOU1	PPP2R2A	TGFB2	AURKA	DSE	HIST1H3J	MYLK	RAB11FIP4	THOC6		SEMA4C	MAD1L1
CDKN1A	ID3	PPP2R5A	TGFBR1	AXIN1	DUSP1	HIST1H4A	MYLK3	RAB11FIP5	THOC7		SEMA4D	MAF
CDKN1B	IFIH1	PPP2R5C	TGS1	AXIN2	DUSP10	HIST1H4E	MYLPF	RAB14	THRA		SEMA5A	MAML1
CEBPA	IFNAR1	PPP2R5D	THBS1	B3GALT6	DUSP16	HIST1H4F	MYO10	RAB2A	THRB		SEMA6A	MAML2
CEBPB	IFNGR2	PPP2R5E	THBS2	B3GALTL	DUSP2	HIST1H4H	NAGA	RAB5C	TIAM1		SEMA6B	MAML3
CERS2	IGF1R	PPP3CA	THOC5	B3GAT3	DUSP3	HIST1H4I	NANOG	RABEP1	TIMP1		SEMA6C	MAP2K2
CERS5	IGF2	PPP3R1	TLR2	B4GALT3	DUSP4	HIST2H2BE	NCAM2	RAD51	TIMP3		SEMA6D	MAPT
CERS6	IGFBP3	PPT2	TNC	BAG1	DUSP5	HIST2H4A	NCK1	RALGDS	TJP1		SEMA7A	MBD4
CFL1	IL10RB	PREB	TNFAIP3	BAG2	DUSP6	HIST3H2BB	NCK2	RANBP3	TJP2		SLIT2	MMP3
CFL2	IL2RB	PRKAA1	TNFRSF10B	BAG4	DUSP7	HIST4H4	NDST1	RAP1A	TLN1		SRGAP1	MPHOSPH6
CHEK2	IL6R	PRKAA2	TNFSF10	BAMBI	DUSP8	HLA-A	NDST2	RAPGEF2	TLR4		SRGAP2	MUTYH
CHMP1B	IL6ST	PRKAB2	TNFSF13B	BCAR1	DVL2	HLA-B	NDST3	RARB	TLX3		SRGAP3	MVD
CHMP2B	INSR	PRKACA	TP53	BCAS2	E2F1	HLA-DMA	NDST4	RASA1	TM7SF2		SSR4	MVK
CHMP3	IQGAP1	PRKAR1A	TRA2A	BCAT1	EBP	HLA-DQA1	NEUROG1	RASGRP1	TMPRSS2		SUMF1	MYL5
CHMP4B	IQSEC1	PRKAR2A	TRA2B	BCAT2	EDEM2	HLA-DRA	NF1	RASGRP3	TNFRSF11A		TALDO1	NCAM1
CKAP4	IRAK1	PRKCE	TRAF2	BCL10	EDN1	HLA-DRB5	NFATC2	RASGRP4	TNFRSF1B		TKT	NCBP2
CLTC	IRAK2	PRKCSH	TRAF4	BCL2L1	EDNRA	HNF4A	NFATC3	RASSF6	TP53AIP1		TKTL1	NCSTN
COL11A1	IRF1	PRKDC	TRAF6	BCL3	EEF2	HNRNPA1L2	NFKBIB	RBM17	TP53BP2		TKTL2	NEIL1
COL1A1	IRF3	PRKX	TRAM1	BCL6	EFNA1	HOMER1	NFYB	RBM22	TP53INP1		TPI1	NEIL2
COL1A2	IRF7	PRLR	TRIM25	BCR	EFNA5	HOMER2	NGFR	RBMX	TPM3		TPP1	NEIL3
COL3A1	IRS1	PRMT1	TRIM37	BDNF	EGLN3	HOXA11	NKX3-1	RBX1	TPR		TSPO	NFKB2
COL4A1	IRS2	PRNP	TRIP12	BIRC2	EGR3	HOXB1	NOD1	RCAN2	TRAF3		UNC5B	NGF
COL4A2	IRS4	PRPF19	TRNT1	BLNK	EHMT1	HOXD10	NOD2	RELN	TRAF5		UNC5C	NGLY1
COL4A5	ITCH	PRPF3	TSC1	BMP2K	EIF1AX	HPN	NOS3	REST	TRIM32		XAB2	NOG
COL5A1	ITGA11	PRPF4	TSG101	BMP4	EIF2AK3	HRAS	NOTCH3	RET	TRIP10		ZFYVE16	NR1D1
COL5A2	ITGA5	PRPF40A	TTK	BMP5	EIF2B1	HS3ST3A1	NPAS2	RFNG	TRRAP			NRG1
COL6A1	ITGA6	PRPF8	TUSC3	BMP6	EIF2B2	HS3ST3B1	NPC1	RFWD2	TSC2			NUDT16
COL6A2	ITGA7	PSD3	TWIST2	BMP7	EIF2B5	HS3ST5	NPC2	RGPD1	TWIST1			NUDT16L1
COL6A3	ITGA8	PSEN1	U2AF1	BMP8B	EIF3A	HS6ST2	NPLOC4	RGPD2	TYK2			NUMB

CPEB2	ITGAV	PSMC4	U2AF2	BRAF	EIF3B	HS6ST3	NRG4	RGPD3	TYMS			NUMBL
CPEB3	ITGB1	PSMD1	U2SURP	BTC	EIF3D	HSD17B12	NRP1	RGPD4	UBA2			NUP54
CPEB4	ITGB2	PSMD12	UBA1	BTK	EIF3E	HSD17B7	NSFL1C	RGPD8	UBA3			OCRL
CREB5	ITGB5	PSMD3	UBA6	BUB1B	EIF3G	HSPA1L	NTF3	RHEB	UBE2A			PAN2
CRK	ITGB8	PSMD4	UBE2C	BUB3	EIF3H	HSPA2	NTRK2	RHOBTB1	UBE2B			PAN3
CRKL	ITPR1	PTCH1	UBE2D2	BUD31	EIF3I	HSPB1	NUP210	RHOBTB2	UBE2D1			PAPD5
CRTC2	ITPR2	PTEN	UBE2I	C12orf5	EIF4A1	ICAM1	NUP214	RHOG	UBE2D3			PAPD7
CSNK1E	ITPR3	PTGER2	UBE2J1	C1QA	EIF4E	ID1	NUP35	RHOQ	UBE2D4			PARN
CSNK2A1	JAK1	PTGS2	UBE2K	C3	EIF4EBP1	ID2	NUP37	RICTOR	UBE2E1			PARP4
CSNK2A2	JMJD1C	PTK2	UBE2M	C8A	EIF5B	ID4	NUP107	RIF1	UBE2E2			PATL1
CTBP2	JUN	PTPN1	UBE2N	C8G	ELAC2	IDH1	NUP133	RNF41	UBE2G1			PCYOX1
CTGF	JUP	PTPN11	UBE2O	CAB39L	ELK1	IDH2	NUP188	RNF7	UBE2G2			PDGFD
CTNNA1	KDR	PTPRB	UBE2Q2	CACNA1B	ELOVL4	IDH3A	NUP43	RNPS1	UBE2H			PDSS1
CTNND1	KEAP1	PTPRF	UBE2R2	CACNA1C	ELOVL6	IDH3B	NUP85	ROCK1	UBE2L6			PDSS2
CTTN	KIDINS220	PTPRJ	UBE2S	CACNA1H	EML4	IDS	NUPR1	ROCK2	UBE2Q1			PER1
CUL1	KIT	PTPRM	UBE2W	CACNA2D3	ENAH	IDUA	NXF3	RORA	UBE2QL1			PI4K2B
CUL3	KLF3	PVRL1	UBE2Z	CACNA2D4	ENO2	IFITM1	NXT2	RORB	UBE3A			PI4KA
CUL4B	KMT2A	PVRL4	UBE3B	CACNB3	ENO3	IFNA21	OGDH	RPP25L	UBOX5			PI4KB
CUL5	KMT2C	PXN	UBE3C	CACNG1	ENTPD3	IGF2R	OGDHL	RPS6KA1	UBQLN2			PIK3C2A
CWC15	KMT2D	RAB11A	UBE4A	CACNG4	ENTPD4	IKBKB	OGT	RPS6KA2	UBQLN4			PIK3C2B
CXCL12	KPNB1	RAB11B	UBE4B	CACNG8	EOGT	IL15	ORC1	RPS6KA4	UGGT2			PIK3C3
CXCL2	KRAS	RAB11FIP1	UBQLN1	CALML5	EPHA2	IL1A	ORC4	RPS6KA6	ULK2			PLCB2
DAB2	LAMA4	RAB11FIP2	UBR4	CALML6	EPN2	IL1R1	ORC5	RPS6KB1	ULK3			PNPT1
DDB1	LAMA5	RAB22A	UBR5	CALR	EPS15	IL2RG	ORC6	RPS6KB2	UPF2			POLB
DDB2	LAMB1	RAB31	UBXN6	CAMK2D	ERBB4	IL6	OXSM	RPTOR	UPF3A			POLD2
DDIT4	LAMC1	RAB4A	UGGT1	CAMK2G	EREG	ILK	P4HB	RRAGA	USP39			POLE
DDOST	LAMC2	RAB5A	ULK1	CAMK4	ERN1	IMPAD1	PABPC1L	RRAGC	UST			POLL
DDX39B	LATS1	RAB5B	UPF1	CAMKMT	ERO1LB	INADL	PABPC4L	RRAGD	UTY			PPP1R1A
DDX3X	LATS2	RAB7A	USP7	CAPN1	ERP29	INHBA	PAK1	RRAS2	VANGL1			PPP2R3C
DDX5	LDHA	RAC1	VAC14	CARD11	ESPL1	INHBB	PAK3	RRM2B	VANGL2			PRPF31

DERL1	LDLRAP1	RAD21	VAV3	CASP7	ESR1	INHBE	PAK4	RUFY1	VAV2			PSENEN
DHX15	LIMK1	RAD23A	VCL	CASP9	ESR2	INPP5K	PAK6	RUNX1T1	VCAM1			PSMD14
DHX8	LMAN1	RAD23B	VEGFA	CAT	ESRRB	INPPL1	PARD3	RUVBL1	VCP			PTTG1
DIAPH1	LMO2	RAE1	VEGFC	CAV1	ESX1	IQGAP2	PARK2	RXRA	VDAC1			PYGL
DIAPH2	LMO7	RAF1	VHL	CCDC6	ETS2	IRAK4	PAX3	RXRB	VDAC2			RAPGEF3
DLG1	LPAR1	RAG1	VIM	CCL19	ETV5	ISL1	PAX5	S1PR1	VDAC3			RBMXL1
DLG3	LTBP1	RALB	VIMP	CCL2	ETV6	ISY1	PAX6	SAE1	VPS36			RCE1
DNAJA1	LTBR	RALBP1	VMP1	CCL20	EWSR1	ITGA1	PBX3	SAP18	VPS37B			RORC
DNAJB11	MAN1C1	RAN	VPS25	CCNA1	EXOC7	ITGA10	PC	SART1	VPS4A			RQCD1
DNAJC10	MAP3K1	RANBP1	VPS37A	CCNB2	EXT1	ITGA2	PCGF2	SAV1	VTA1			S1PR3
DNAJC3	MAP3K5	RANBP2	VPS37C	CCND3	EXT2	ITGA3	PCGF3	SC5D	VTN			SKIV2L
DNAJC5	MAP3K7	RANGAP1	VPS4B	CCR4	EXTL2	ITGA4	PCGF5	SCARB2	VWF			SKIV2L2
DNM2	MAPK1	RAP1B	WASF2	CCR5	EXTL3	ITGB4	PCGF6	SCD5	WASF1			SLC16A2
DOT1L	MAPK14	RAPGEF1	WASF3	CD14	EYA1	ITGB6	PDCD4	SCIN	WBP11			SLC9A1
DROSHA	MAPK3	RARA	WASL	CD164	EZR	JAG1	PDE3B	SCRIB	WIBG			SMUG1
DVL3	MAPK8	RASA2	WEE1	CD22	F11R	JAK2	PDGFA	SDC1	WIF1			SNRPE
E2F2	MAPKAPK2	RASSF5	WHSC1	CD38	F2	JAK3	PDGFB	SDC4	WNT10B			SNW1
E2F3	MARCH6	RB1	WHSC1L1	CD63	F2R	JARID2	PDGFRB	SDHA	WNT11			SOCS1
E2F4	MAVS	RBL1	WWTR1	CD79A	FADD	JUNB	PDIA3	SDHC	WNT2B			SOCS2
E2F5	MBTPS1	RBL2	XBP1	CD82	FADS1	JUND	PDIA4	SDHD	WNT3			SUV39H1
ECHS1	MBTPS2	RBM25	XIAP	CDC14A	FADS2	KAT2A	PDK1	SEC13	WNT3A			SYF2
EDEM1	MCM3	RBPJ	XPO1	CDC34	FANCL	KAT5	PDPK1	SEC24D	WNT4			SYNJ1
EDEM3	MCM4	RCAN1	XPOT	CDC5L	FAS	KAT6A	PDXK	SEC61A2	WNT5A			SYNJ2
EEA1	MCM7	RCHY1	YES1	CDC7	FBP2	KCNJ9	PDXP	SEC61G	WNT5B			TDG
EEF1A1	MDM2	RDX	YOD1	CDK1	FBXL3	KDELR1	PECR	SEC63	WNT6			TEAD3
EEF1A2	MDM4	REL	YWHAB	CDK14	FBXO25	KDELR2	PER3	SENP2	WNT7B			TEK
EFTUD2	MED1	RELA	YWHAE	CDK7	FBXO32	KDM6A	PERP	SEPT1	WNT8A			THOC1
EGFR	MED12	RHOA	YWHAG	CDK9	FBXO4	KLF2	PFKFB2	SEPT3	WNT9A			TMSB4X
EGLN1	MED12L	RIPK1	YWHAH	CDKN1C	FBXO5	KLF4	PFKFB3	SEPT6	WWP1			TNFSF14
EGLN2	MED13	RIPK2	YWHAQ	CDKN2A	FBXO6	KLHL13	PFKL	SEPT9	XPO5			TOB1

EGR1	MED13L	RNF185	YWHAZ	**CDKN2C**	**FDFT1**	**KLHL9**	**PFN1**	**SERPINB5**	**XYLT1**			TOB2
EHD1	MED14	RPN1	ZEB1	**CDKN2D**	**FDPS**	**KLK3**	**PGAM5**	**SETD7**	**XYLT2**			TTC37
EHD2	MED16	RPN2	ZFYVE9	**CEL**	**FER**	**KMT2B**	**PHF5A**	**SETDB2**	**YAP1**			UBE2E3
EHD4	MED17	RPP14	ZMAT3	**CERS4**	**FGD3**	**KMT2E**	**PHKA1**	**SF3A1**	**ZAK**			UNG
EI24	MEF2C	RPS6	ZYX	**CFLAR**	**FGF1**	**LAMA1**	**PHKA2**	**SF3A2**	**ZBTB17**			USP8
EIF1	MET	RPS6KA3		**CFTR**	**FGF10**	**LAMB2**	**PHKB**	**SF3A3**	**ZFHX3**			VPS45
EIF2AK1	MID1	RPS6KA5		**CGA**	**FGF11**	**LAMC3**	**PHKG2**	**SF3B4**	**ZFP36**			WNT2
EIF2AK2	MKNK2	RRBP1		**CHD4**	**FGF16**	**LAMP1**	**PHOSPHO2**	**SF3B5**	**ZFYVE20**			WWC1
EIF2AK4	MLLT4	RRM2		**CHD8**	**FGF17**	**LAMP2**	**PIAS1**	**SF3B6**	**ZMAT2**			XRCC1
EIF2S1	MMP2	RUNX1		**CHEK1**	**FGF2**	**LAMP3**	**PIAS3**	**SFRP1**	**ZMPSTE24**			XRN1
EIF2S2	MMP9	RUNX2		**CHERP**	**FGF23**	**LAMTOR3**	**PIDD1**	**SFRP2**				XRN2
							PIK3CB	**SGMS1**				ZCCHC7
							PIK3CD	**SGPP1**				